Electroencephalography (EEG) Profile and Sense of Body Ownership: A Study of Signal Processing, Proprioception and Tactile Illusion

Finding a link in neural correlates of human's perceptual and illusion

Sheyda Shahriari

A thesis submitted for the degree of Doctor of Philosophy

School of Engineering and Design Brunel University

Submission date: March 2018

Deceleration

I hereby declare that this Ph.D. thesis entitled "**Electroencephalography (EEG) Profile and Sense of Body Ownership: A Study of Signal Processing, Proprioception and Tactile Illusion"** I have submitted to the office of Engineering and Design department, Brunel university London, is entirely my original work prepared under the supervision of Prof. Ibrahim Esat. I have duly acknowledged all the sources of information which have been used in the thesis. The results of this dissertation have not been presented or submitted anywhere else for the award of any degree or for other purpose. I shall be solely responsible if any evidence is found against my declaration.

<div align="right">

………………….

Sheyda Shahriari

Brunel University London

</div>

Problem Description

Loss of limb function affects over 25 million globally, mainly due to cardiovascular and trauma causes. The loss or the genetic absence of an upper limb may seriously compromise the functional independence of a person in his/her daily living. Current prostheses are useful to overcome the restrictions that the lack of a limb implies and to provide the amputee with certain autonomy but due to the complex nature of the upper extremity, the acceptance of current devices is still below 50%. Many of these devices are often extremely expensive in the range from the $3000-$30000 or more and many afflicted persons in developing countries cannot afford to seek this type of treatment. In these areas often there is not adequate medical assistance, and trained personnel with a rehabilitation of upper limb loss is almost none existent with devices that are inherently the same as the devices used over a thousand years ago.

This project looks at assessing whether there is a potential to use classical conditioning for patients to transmit messages from and to the brain in the arm, meaning they get their sensory feedback from artificial limbs and feels lifelike. This work will in specific focus on investigating the ability to provide sensory tactile feedback from an artificial limb, replicating real biological sensation for prostheses uses, by means of illusion and whether or not it is possible to make this illusion permanent by repeatedly applying it to users.

Abstract

With the ability to feel through artificial limbs, users regain more function and increasingly see the prosthetics as parts of their own bodies. So, main focus of this project was dedicated to recuperating sensation by deception both in sighted and unsighted patients, started with illusionary experiments on healthy volunteers, brain signals were captured with medical EEG headsets during these tests to have a better understanding of how the brain works during body ownership illusions. EEG results suggest that gender difference exists in the perception of body transfer illusion. Visual input can be induced to trick the brain. Using the results, a new device has been designed (sound generator system-SGS) with the principal goal to find ways to include rich sensory feedback in prosthetic devices that would aid their incorporation of the user's body representation or schema.

Studying the brain is fascinating; SGS tested and was found to have an adequate level of dexterity over course of one-month multiple times. After each try, the results were more tolerable than before that proved the idea that brain can learn and understand anything and can be manipulated temporary or lasting due to influences. Different methods used to validate the results, EEG acquisition, mapping subject brain function with EEG and finally interviewing participant after each attempt.

Although the results of the illusion shows that when heat applies on rubber hand, subjects behave in similar manner as if their real hand was effected, but main question is still remains. How can the conditioning apply to daily life of amputees so that illusion become permanent?

This is a rapidly developing field with advancements in technology and greater interdisciplinary integration of medicine, mechatronics and control engineering with the future looking to have permanent, low power consumption, highly functional devices with a greater intuitive almost natural feel using a variety of body signals including EMG, ultrasound, and Electrocorticography.

Acknowledgment

I am using this opportunity to express my gratitude to everyone who supported me throughout my research. I am thankful for their aspiring guidance, invaluably constructive criticism and friendly advice during the project work. I am sincerely grateful to them for sharing their truthful and illuminating views on a number of issues related to the project.

I would like to express my special appreciation and thanks to my supervisor Professor Ibrahim Esat, you have been a tremendous mentor for me. I would like to thank you for encouraging my research and for allowing me to grow as a research scientist. Your advice on both research as well as on my career have been priceless.

I would also like to thank my summer assistant, Maya Rose Gumussoy, and all my colleagues at Brunel University, for all helps and support. I also want to thank you for letting my defense be an enjoyable moment, and for your brilliant comments and suggestions, thanks to you.

Special thanks goes to my family. Words cannot express how grateful I am to my mother, Fatemeh Rahimi, father, Bahram Shahriari, and my siblings, Shiva and Sahand, for all of the sacrifices that you have made on my behalf and for your endless love and mental support. Your prayer for me was what sustained me thus far. I would also like to thank all of my friends who supported me in experimenting, writing, and incented me to strive towards my goal.

Table of Contents

List of Figures

List of Tables

List of Publication

1. Shahriari, S. (2015), **Brain Illusion Technique to Obtain Sensation From Prosthetics**. Accepted and presented in Biomechanics of human motion (BioMot2015 Workshop), northern Cyprus.

2. Shahriari, S. (2015), **Body Transfer Illusion Experiment to Investigate Into Future Artificial Limbs**, Accepted, SDPS conference in Dallas Texas

3. Shahriari, S. (2016), **Prosthetic with Illusionary Sensation**, Accepted, ICBME conference in Singapore

4. Shahriari, S. (2016), **Investigate into Future of Prosthetic with Sensation**, 2nd world Congress on Automation and Robotics. Philadelphia, USA, 05(02), p.68

The following above-mentioned publications have evolved from my doctoral dissertation.

Abbreviations

AAR	Automatic Artefact Rejection
ADHD	Attention Deficit Hyperactivity Disorder
AMPA	α-Amino-3-hydroxy-5-methyl-4-isoxazol Propionic-Acid
ANT	Advanced Neuron Technology
AR	Autoregressive
ARM	Auto Regressive Method
BCI	Brain Computer Interface
BSS	Blind Source Separation
C	Cervical (for Nerve Origin)
CAM kinase	Calmodulin-dependent kinase
CNS	Central Nervous System
CR	Conditioned Response
CS	Conditioned Stimulus
CT	Computerized Tomography
DAC	Digital Analogue Convertor
DARPA	Defense Advanced Research Projects Agency
DC	Direct Current
DFT	Discrete Fourier Transform
DIP	Distal Interphalange
DSP	Digital Signal Processing
ECG	Electrocardiography
ECoG	Electrocorticographic
EEG	Electroencephalogram
EGG	Electrogastrography
EMG	Electromyography
EOG	Electrooptigraphy
EPR	Event Related Potential
ERD	Event Related Desynchronization
FFT	Fast Fourier Transform
FIR	Finite Impulse Response
fMRI	Functional Magnetic Resonance Imaging
HCI	Human Computer Interface
IC	Semiconductor sensor

ICA	Independent Component Analysis
IIR	Infinite Impulse Response
K+	Potassium ion (Positively charged)
LED	Light Emitting Diode
LTD	Long-Term Depression
LTP	Long-Term Potentiation
MBI	Mirror Box Illusion
MCP	Metacarpal Phalange
MEG	MagnetoEtoencephalography
MRI	Magnetic Resonance Imaging
MU	Motor Unit
Na+	Sodium ion (Positively charged)
NFB	NeuroFeedBack
NIH	National Institutes of Health
NIRS	Near-Infrared Spectroscopy
NMDA	N-methyl-D-aspartate receptor
NS	Neutral Stimulus
OCD	Obsessive Compulsive Disorder
OTG	On-The-Go
PAD	Peripheral Arterial Disease
PCA	Principle Component Analysis
PET	Positron Electron Tomography
PIP	Proximal Interphalange
PLS	Phantom Limb Syndrome
PNS	Peripheral Nervous System
PSD	Power Spectral Density
PWM	Pulse width Modulation
QEEG	Quantitative EEG
Revs	Revolutions
RHI	Rubber Hand Illusion
RL	Reinforcement Learning
Rpm	Revolutions per minute
SCP	Slow Cortical Potential
SCR	Skin Conductance Respomse
sEMG	Surface Electromyography
SGS	Sound Generator System

SNS	Somatosensory Nervous System
SPWV	Smooth Pseudo-Wigner-Ville
sRPNI	Sensory Regenerative Peripheral Nerve Interface
SSVEP	Steady-State Visual Evoked Potentials
STS	Superior Temporal Sulcus
T	Thoracic (for Nerve Origin)
TFD	Time Frequency Distributions
TMR	Targeted Muscle Reinnervation
TMS	Transcranial Magnetic Stimulation
UCR	Unconditioned Response
UCS	Unconditioned Stimulus
ULP	Upper Limb Prosthetic
USB	Universal Serial Bus
VTA	Ventral Tegmental Area
WT	Wavelet Transform

Introduction

A prosthetic is an artificial device that replaces a body part lost through trauma, disease, or congenital developmental abnormality, and is used to allow the body to work more efficiently or to replace the functions that are lost as a result of absence of the particular limb. Prosthetics can be created in an attempt to replace some or all of the structure or function of one or more limbs, or other structures including eye, hand, legs, teeth, and varying joints. Mechanical devices or tissues taken from living organisms like pig or cow, or laboratory tissue cultures can also replace the function of parts of organs, such as heart valves. Prosthetics can also be used to improve appearance, in the case of a false eye, as well as to replace function.

According to UK National Health Service (NHS), approximately 5-6,000 major limb amputations are carried out in England every year. Most amputations in the UK are carried out on people who have severely reduced blood circulation as a result of peripheral arterial disease (PAD) or the complications of diabetes. Amputation may consider for many other reasons such as, serious trauma to a limb, serious infections, skin or bone cancer, war or persistent pain that means the limb is of limited functional use (NHS.UK 2013). Upper limb amputations – such as the removal of an arm, hand or fingers, are often carried out in young people as result of a serious injury.

It may be likely to fit an artificial limb after amputation onto the remaining stump. Advanced artificial limbs proven that there is possibility to giving patients the feeling that prosthesis is no longer separated from the rest of the body. However, absence of touch and sensation in prosthesis delays this advantage. For this reason, much effort has been put to spend to bring sensation to prosthesis. In recent years, there has been remarkable progress in this field and new improvement has been presented in artificial limbs, such as surgically implanted cuff electrons or implants directly through brain. Both these methods will give the patient sensory feedback, but it can be very expensive and high-risk procedure not to mention they are not permanent solutions and after few months, these implants need to be remove.

Active prosthetic limbs -functional prostheses that are not purely cosmetic in purpose- can be largely characterised into two main groups: body-powered prostheses and externally powered myoelectric prostheses. In body-powered prostheses, which is a far older prosthetic technology (dating back to 1912), the individual controls the artificial limb through their own body movements. This is achieved through a cable and harness attached to the individual which conveys the forces generated by the body movements to the prostheses. Myoelectric prosthetic limbs are battery powered and operated via electronic motors. Electrode sensors detect EMG signals from muscle activity (incited by the individual), which are then electrically processed to control the prosthesis. Myoelectric prostheses offer many advantages over body-powered, such as greater dexterity and range of motion, more effortless control and better cosmetic acceptance. Despite this, the majority of myoelectric prostheses do not incorporate any sensory feedback mechanism to produce tactile sensations and rely solely on the user's vision for prosthesis control. Body-powered prostheses can provide limited sensory feedback from reaction forces delivered through the cable to the skin. Overall, however, providing an effective means of tactile-sensory feedback still remains one of the major challenges in prostheses development.

This work tries to open up new possibility for prosthesis to have sensory feedback by using brain illusion. Using recorded brain activities proves that can form direct communication between brain and artificial limbs. The Rubber Hand Illusion (RHI) and Mirror Box Illusion (MBI) are the two most famous examples of experiments in which illusionary body ownership is convinced by tactile stimulation of participant's hand. To identify the functional anatomy of these experiments, multichannel (64 channel) EEG was used. New device was designed based on the results of these experiments to determine the sensory illusion hypothesis.

This chapter introduces the Project by elaborating its why, how and what. It presents the project motivation and context. Finally, an overview of the thesis is state.

1.1 Project purpose: Why prosthesis needs sense of touch

In the past the main focus have been about developing device to make life easier for amputee patients, it needed to be easy to control, lighter, cheaper and in terms of cosmetic, closer to real limbs. Advanced prosthetic limbs share many attributes with the limbs they replace. However, new developments are no longer constrained to just cheaper designs; there is a shift of focus towards robotic touch. Existing prosthetic limbs do not provide amputees with cutaneous feedback. Sense of body awareness is linked to sense of touch, to have a
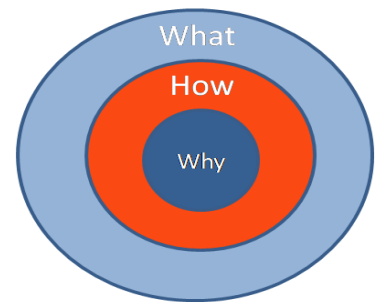
Figure 1: The golden Circle (Sinek, 2009)

better connection and better control of prosthetic, tactile feedback is essential (Marasco et al., 2011) . The purpose of this project is to investigate and explore the possibility that lies within the domain of artificial limbs, using classical conditioning to retrieve sense of touch without risk of surgery. This study aims to further praise the research carried out towards the developments of sensory feedback mechanism involving non-invasive approaches of delivering tactile feedback to amputees. The focus will involve investigating sensory substitution techniques, incorporating RHI as seen in prior studies.

This study will explore both psychological and physiological impact of different techniques to identify the optimal ways to induce sensory feedback from fully functioning prosthetic and what variables the feedback is most depending on. In completing this research, identifying more efficient and effective method of applying illusionary body ownership and delivery sensory feedback to amputees will be easy.

A concise breakdown of individual targets that this project aims to achieve listed as below:

- The main aim is to complement the research undertaken towards the development of sensory feedback mechanisms involving noninvasive methods of delivering tactile feedback to amputees.
- Finding alternative for vision in body recognition. Also to evaluate the rehabilitative tool for the management of PLP in blind limb amputees.

1.2 Project strategy: How sensory feedback device can level up robotic arms

Touch is one of the most essential elements of human development, and the border between body and outside world. It is a profound method of communication, a critical component of the health and growth of infants, and a powerful healing force and effects everything a man do (Bretherton, 1992 and Parke et al., 1994). Lack of this sense in amputee patient, not only affecting the way they controlling their Prosthesis, but it will change their everyday life experiences, physical and emotional.

The objectives of this project are as follow:

- Investigating sensory substitution techniques incorporating the Rubber Hand Illusion (RHI) methodology as seen in prior studies.
- Investigating if classical conditioning like Pavlovian method can 'teach' the brain to become accustomed to the integration of audio, visual and tactile stimulation over time and showing its effect on response recovery.
- Explore fundamental self-awareness question as how brain categorize location, movement, and force of the limb.
- Theoretical study of closed-looped sensory feedback control and mechanism.
- To determine if the subjects can be conditioned by auditory cues in absence of visual cues. Furthermore, to see the effect of visual cues on brain, and how the auditory cues is associating with sense of ownership attributed to RHI.

According to Dr. David Linden, "There are two distinct but parallel pathways in the brain for processing touch information". First is sensory pathway, which is processing the fact of the touch like pressure, location and temperature and the other route social and emotional information (Gregoire, 2015).

In September 2012, new robotic arm was introduced by Johns Hopkins University that were connected directly to a human brain and allows person to control it with his/her thoughts. The remarkable achievement of this project was providing volunteer with brain-controlled device and it used for paralyzed patient to help them with everyday living (Andrei, 2015). Few months later, this group attached the electrodes inside remaining limb to restore sensory feedbacks for amputee patients, they called it Luck Hand. By

finding connection between brain and robotic arm, not only controlling the arm for patient will be easier, it can help them to communicate better with outside world. Especially in a young patient, it can help their development and prevent them from psychological issues and social stigma.

1.3 Project results: What new device could become

Development of medical devices such as prosthetic limbs has been a key area of study for engineering applications. Extensive research and development of artificial limbs has been undertaken to replace their real-life counterparts for amputees. In doing so, engineers have taken on the task to try to close the gap in the distinction between these artificially created devices to their genuine biological equivalents. This project will in specific focus on investigating the ability to provide sensory tactile feedback from an artificial limb, replicating real biological sensations for prostheses uses.

In recent years, there have been great technological advances in creating mechanically/bioengineered prostheses, providing precise motor control and reliability. Considerations including the mechanisms used to generate movement, material choice and weight, fittings used for attachment to the stump and the ergonomics of the device are all thoroughly considered by engineers who develop prostheses. These all play a key role in producing successful prostheses implementation. However, an area that is somewhat less progressive in prostheses development is producing sensory feedback and authentic biological sensations for amputees. A journal on *Plastic and Reconstructive Surgery* has stated that though there have been great technical advances on the dexterity and fine precision of prostheses, the ability to provide sensory feedback has been somewhat overlooked and as a result lagging behind other substantial developments; "The lack of sensation is the key limitation to re-establishing the full functionality of the natural limb", (Nghiem et al., 2015). Adequate sensory feedback is vital in providing proprioceptive (bodily sense of position, equilibrium and motion) and exteroceptive awareness.

The whole promise for the project is to gain knowledge of the two domains, to design and develop circuits that stimulate sense of touch by accessing memories from brain and manipulating those memories. And to determine the possibility of reducing phantom

sensation in blind amputee via adding auditory input, by relaying on previous studies that show the presence of a prosthetic can be registered in the brain of blind limb amputees despite the loss of visual cues and that aids in the reduction of PLP.

The final design was intended to demonstrate the touch of temperature, this device designed and built based on rubber hand illusion and it can be perceived by patient as if this sense is coming from their own hand.

To be brief, the main impact of this work is as follow:
- Recovering thermal sensation using noninvasive methods for amputee patients.
- Create long lasting illusion using classical conditioning.
- Treating phantom sensation on blind patients using auditory illusion.

1.4 Organization of thesis

The thesis is structure as follow, the goals and objectives of the project have been introduces in this chapter.

Chapter 2 describes related work and background for this project and identifies the most important research questions and methods of approach. It also explains different terms relates to this project; how EEG technology works, and different brain activity patterns. It also describes how brain recognizes body.

Chapter 3 illuminates the evaluation of prosthetic from the first device created to most recent one with new technology, both on commercial and research side.

Chapter 4 introduces the main system design and equipment that was available for realizing and implementing it. Technology used to establish new design. The different components and their relations to each other are explained.

Chapter 5 briefly describe this implementing design in practical applications, defines how unlike another designs available today, this system can be easily set in and thus potentially usable for most patients.

Chapter 6 elaborates the theory behind the signal processing of this project and software used to analyzing the results.

Chapters 7 review the results of previous chapter, and validate them according to the project goal.

Chapter 8 reports result analysis in discussion.

Chapter 9 summarizes and concludes the project in perspective of big picture. It also makes suggestions for further work.

Chapter 2: Literature Survey

This chapter describes the background for this work, and finds the main research questions and methods to bring clarity and define the projects focus, based on lessons learned from earlier efforts and new anticipations. There is extensive literature in both the medical and engineering spheres related to the aspects of design, manufacture and performance of prosthetic limbs.

Background research was conducted into the structure of human arm, behavior of the human hand, the history of prosthetic design, new methods of recovering sensation, and the learning mechanisms of brain, the analysis of EEG signals, the actions and nerve supply of muscles, and comparison between commercially available prosthetics and the present proposal.

Literature reviewed includes books, journals, conference extracts, commercial websites and web encyclopedias, videos, patent applications, and existing reports. This chapter encases all basic aspects and concepts that review the current knowledge on this topic; it can be taken as a secondary source.

2.1 Structures and mobility of human arm

Figure 2: Human arm anatomy (Tortora and Derrickson, 2010)

The human is very complex and highly intricate in its interlinking of all the different physiological systems including the musculoskeletal system, the nervous system, the circulatory system etc. and it is for this reason that replicating any action inherit to the body by an artificial means is very difficult. In the upper limb the biological component systems that make up the bulk of the material is dictated by its function (as with

everything in the body), which include manipulation of the environment. The base structure to which everything is attached and acts, as the scaffold of the upper limb is the skeletal system.

Table 1: Muscle actions of the forearm (Cooljargon.com, 2016)

Movement	Target	Target motion direction	Prime mover	Origin	Insertion
Superficial anterior of forearm					
Bends wrist toward body; tilts hand to side away from body	Wrist; hand	Flexion; abduction	Flexor carpi radialis	Medial epicondyle of humerus	Base on second and third metacarpals
Assists in bending hand up toward shoulder	Wrist	Flexion	Palmaris longus	Medial epicondyle of humerus	Palmar aponeurosis; skin and fascia of palm
Assists in bending hand up toward shoulder; tilts hand to side away from body; stabilizes wrist	Wrist; hand	Flexion, abduction	Flexor carpi ulnaris	Medial epicondyle of humerus; olecranon process; posterior surface of ulna	Pisiform, hamate bones, and base of fifth metacarpal
Bends fingers to make a fist	Wrist; fingers 2-5	Flexion	Flexor digitorum superficialis	Medial epicondyle of humerus; coronoid process of ulna; shaft of radius	Middle phalanges of fingers 2-5
Deep anterior compartment of forearm					
Bends tip of thumb	Thumb	Flexion	Flexor pollicis longus	Anterior surface of rad interosseous membran	Distal phalanx of thumb
Bends fingers to make a fist; also bends wrist toward body	Wrist; fingers	Flexion	Flexor digitorum profundus	Coronoid process; anteromedial surface of ulna; interosseous membrane	Distal phalanx of fingers 2-5
Superficial posterior compartment of forearm					
Straightens wrist away from body; tilts hand to side away from body	Wrist	Extension; abduction	Extensor radialis longus	Lateral supracondylar ridge of humerus	Base of second metacarpal
Assists extensor radialis longus in extending and abducting wrist; also stabilizes hand during finger flexion	Wrist	Extension; abduction	Extensor carpi radialis brevis	Lateral epicondyle of humerus	Base of third metacarpal
Opens fingers and moves them sideways away from the body	Wrist; fingers	Extension; abduction	Extensor digitorum	Lateral epicondyle of humerus	Extensor expansion; distal phalanges of fingers
Extends little finger	Little finger	Extension	Extensor digiti minimi	Lateral epicondyle of humerus	Extensor expansion; distal phalanx of finger 5
Straightens wrists away from body; tilts hand to side toward body	Wrist	Extension; abduction	Extensor carpi ulnaris	Lateral epicondyle of humerus; posterior border of ulna	Base of fifth metacarpal
Deep posterior compartment of forearm					
Moves thumb sideways toward body; extends thumb; moves hand sideways toward body	Wrist; thumb	Thumb: abduction; extension; wrist: abduction	Abductor pollicis longus	Posterior surface of radius; interosseous membrane	Base of first metacarpal; trapezium
Extends thumb	Thumb	Extension	Extensor pollicis brevis	Dorsal shaft of radius and ulna; interosseous membrane	Base of distal phalanx of thumb
Extends thumb	Thumb	Extension	Extensor pollicis longus	Dorsal shaft of radius and ulna; interosseous membrane	Base of distal phalanx of thumb
Extends index finger; straightens wrist away from body	Wrist; index finger	Extension	Extensor indicis	Posterior surface of distal ulna; interosseous membrane	Tendon of extensor digitorum of index finger

The arm consists of three bones: Humerus (upper arm), radius and ulna (lower arm) and the hand consists of the scaphoid, trapezium, trapezoid, lunate, triquetrum, pisiform, hamate and capitate that constitute the wrist and base of the palm. The remaining bones are the longer hand bones of the metacarpals in the hand and the phalangeal (fingers) that are named according to the finger numbered 1-5 and location either proximal, inter or distal. The muscles control the forearm and hand. This extremely comprehensive system with over 30 muscles that give the upper limb and hands its extraordinary dexterity and function. These functions are illustrated in table 1 and the median, ulnar and radial nerves innervate these muscles.

2.2 Anatomy of the brain

The brain is a sophisticated structure that manages the entire body. As a component of the central nervous system (CNS), the brain sends, receives, processes, and directs sensory information through the body (Hubel, 1995). The brain is divided into left, and right hemispheres by a band of fibres named the corpus callosum (Woolsey et al., 2003). The brain consists of three major sections, with each section having precise functions. The major divisions of the brain are the forebrain (Prosencephalon), midbrain (Mesencephalon), and hindbrain (Rhombencephalon) as shown in Figure 3 (Nowinski, 2011). This project will be focusing on the forebrain only for the study purposes.
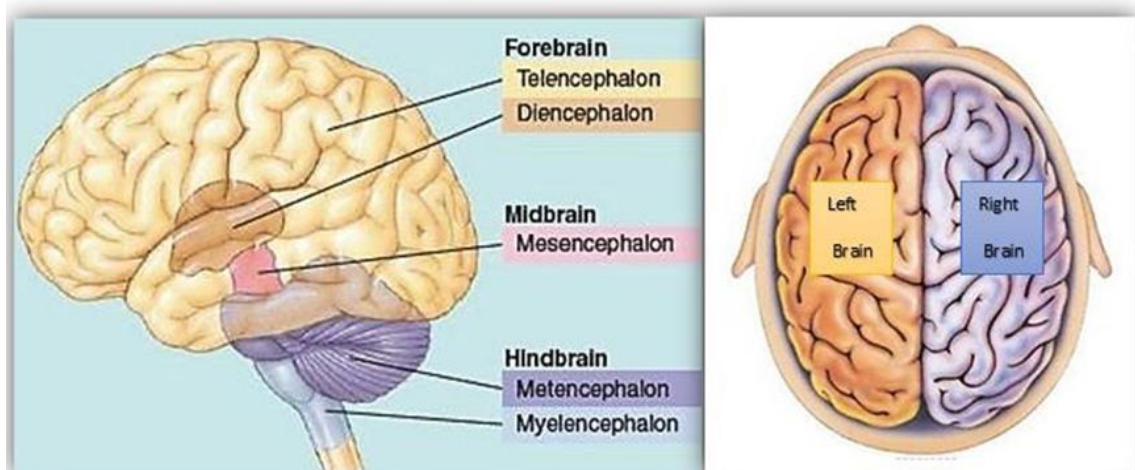
Figure 3: Anatomy of the brain

The brain is divided into left and right hemispheres. The brain is also anatomically divided into the forebrain, midbrain and hindbrain, each containing different structures (Biology, 2017)

Forebrain (Prosencephalon)

The forebrain is the part that is liable for multiple functions such as receiving and processing sensory input, thinking, recognising, understanding language, and regulating motor function. The forebrain is the biggest brain division. It contains the cerebrum, which weighs two-thirds of the brains mass as shown in Figure 4. The forebrain consists of two subsections named the telencephalon and diencephalon (Wheelock, 2013).
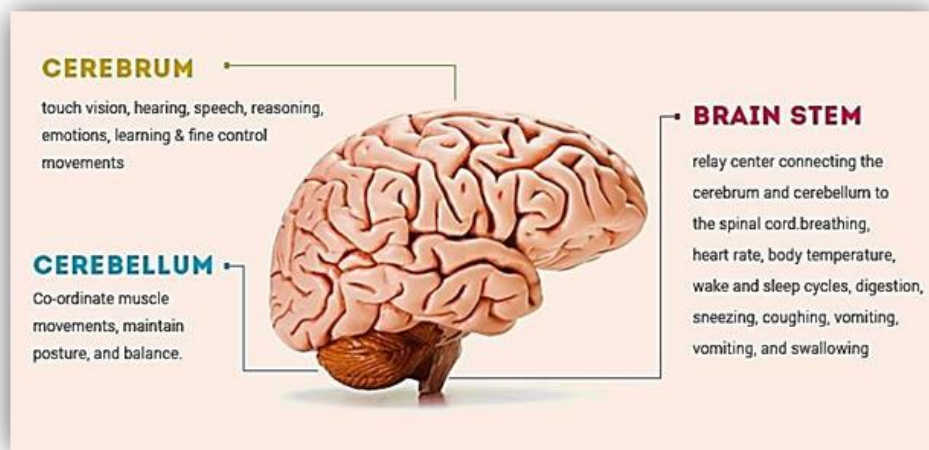
Figure 4: Structure of human brain

The figure shows the cerebrum, cerebellum and brainstem as a part of human brain. (Humanbrainfacts, 2016)

Telencephalon

A main section of the telencephalon is the cerebral cortex, which can be dissected into four lobes that are liable for processing, encoding and interpreting inputs from various sources and managing cognitive function. Sensory functions illustrated by the cerebral cortex related to the functions of hearing, touch, and vision. Cognitive functions related to thinking, perceiving, and language (Nowinski, 2011). These lobes are originated in both right and left hemispheres of the brain. The lobes are (1) Parietal Lobes located posteriorly to the frontal lobes and over the occipital lobes. They are responsible for delivering and encoding sensory information. The somatosensory cortex is located in the parietal lobes and is necessary for processing touch sensations. (2) Frontal Lobes are located at the front area of the cerebral cortex. They are responsible for movement, decision-making, problem solving, and planning (Hubel, 1995). (3) Occipital Lobes

Located underneath the parietal lobes, they are the primary part of visual processing. The visual inputs are directed to the parietal lobes and temporal lobes for more processing. (4) Temporal Lobes located under the frontal and parietal lobes. These lobes coordinate sensory inputs; also, they support auditory perception, memory creation, and language and speech production (Woolsey et al., 2003). The functions of human's brain lobes are illustrated in Figure 5.
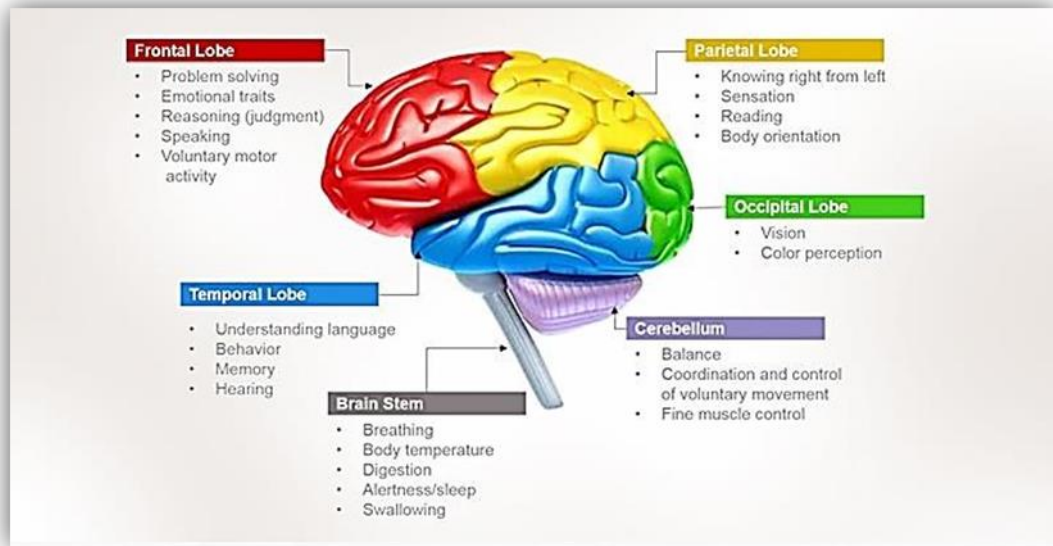
Figure 5: Lobes of the Cerebrum

The cerebrum consists of four major lobes: occipital, temporal, parietal and frontal. Different functional parameters are attributed to each lobe as depicted in the figure. (Humanbrainfacts.org, 2016)

Diencephalon

The diencephalon is the region of the brain that transmits sensory inputs and joins the parts of the endocrine system with the nervous system (Kandel et al., 2013). The diencephalon regulates some functions such as motor functions. As well as, plays a significant role in sensory awareness (Hubel, 1995). The diencephalon consists of Thalamus, which is a limbic system structure that joins parts of the cerebral cortex that are associated with sensory awareness and movement with other sections of the brain and spinal cord. Hypothalamus is responsible for controlling autonomic functions of the body. Pineal Gland is in charge melatonin hormone production. (Carter, 2014)

2.3 Sensory system

Touch

"You can't turn off touch. It never goes away, you can close your eyes and imagine what it is like to be blind, and you can stop up your ears and imagine what it is like to be deaf. But touch is so central and ever-present in our lives that we can't imagine losing it" says David Linden a neurobiologist at Johns Hopkins and author of the book" Touch: The Science of Hand, Heart, and Mind." (Stromberg, 2015).
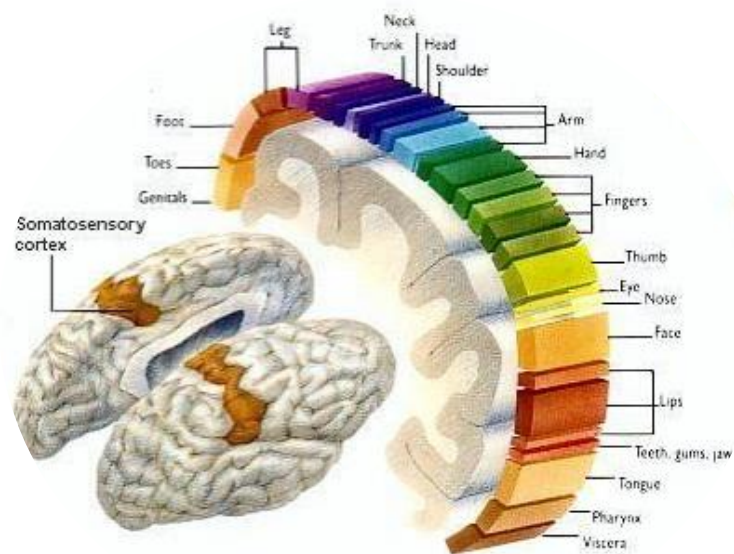
Figure 6: Human Figures scaled to match the proportions of how touch sensors is presented in brain
(Stromberg, 2015)

First sense developing in human is sense of touch and is the most difficult to fathom doing without. Somatosensory Nervous System is a complex system of nerve cells that responds to changes to the surface or internal state of the body. It plays a fundamental role in creation of body map in brain.

From 5 million, touch receptor in many part of body including skin, epithelial tissues, skeletal muscles, organs, cardiovascular system, bones and joint, 3000 are located in fingertips. These receptors come in four variations, for sensing vibration, for tiny amounts of slippage, for stretching the skin and that senses the finest kinds of textures. Most of the receptors thorough human body is for pain, 200 pain receptors (nociceptors) for every square centimeter of skin, while it is only 15 receptor for pressure, seven for temperature

(thermoreceptors) which is six for cold and only one for warmth are available for same area (Stromberg, 2015).

Touch or somatosensory perception is recognised by stimulation of neural receptors in the skin (Kandel et al., 2013). The sensation begins from pressure applied to these receptors, named mechanoreceptors. The skin has several receptors that sense different stages of the pressure applied from mild stroking to strong, also the time of application from a concise touch to continuous (Krantz, 2012). The sensory inputs from the receptors are conveyed through one of the three systems depending on the type of the receptor as shown in Figure 7 below: (1) dorsal-column-medial (lemniscal system) that is responsible for touch and proprioception, (2) anterolateral system responsible for pain and temperature, and (3) spinocerebellar system responsible for proprioception to the dorsal columns. After this point, the inputs are conveyed to the thalamus, which then transmits the inputs to the primary somatosensory cortex for further processing (Patestas & Gartner, 2016).
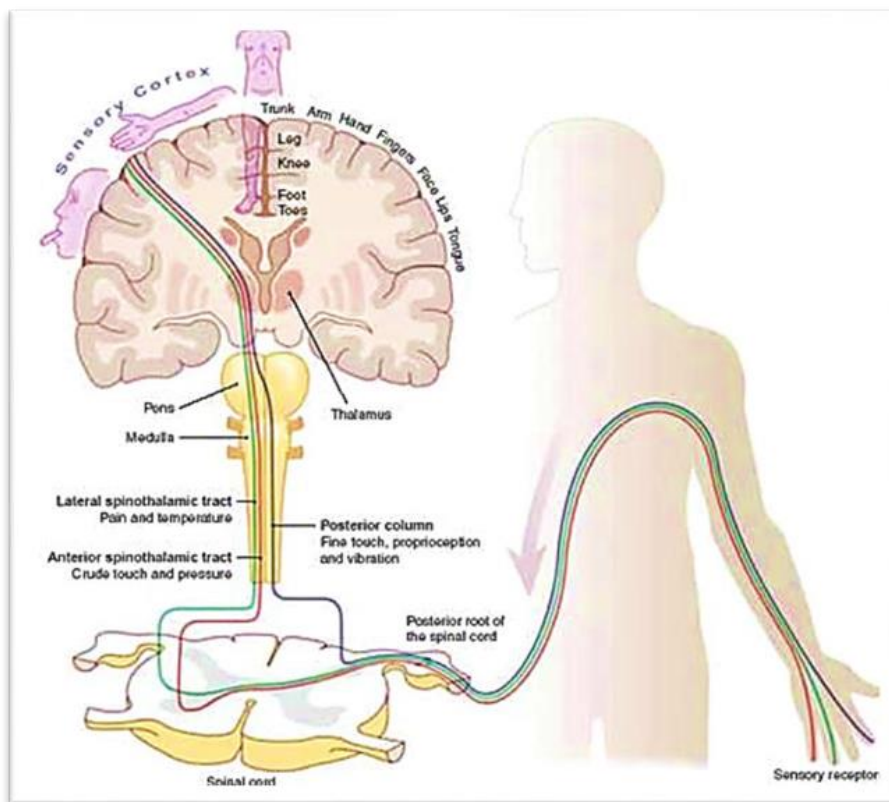
Figure 7: Sensory pathway

The sensory inputs from the receptors are conveyed through one of the three systems: (1) dorsalcolumn-medial (lemniscal system), (2) anterolateral system, (3) spinocerebellar system. (Clinicalgate, 2017)

Chouchkov divides skin receptors into two types, unencapsulated nerve ending and encapsulated nerve endings. Encapsulated receptors terminals are of two kinds, epidermal nerve endings and dermal nerve endings. Dermal nerve endings are enveloped by Schwann cell lamella and basal lamella. There are three types of encapsulated nerve endings; Pacinian corpuscles (lamella corpuscles), Meissner's corpuscles (tactile corpuscles) and Ruffini nerve endings (bulbous corpuscles). Pacinian corpuscles are sensitive to pressure and vibration. When pressure is exerted on an area of the skin that contains Pacinian corpuscles and bends, pressure is exerted on the central neuron in the corpuscle. The pressure leads to an outflow of Na+ from the plasma membrane, and if the pressure exceeds a certain threshold, an action potential is generated. Meissner's corpuscles are sensitive to light touch, due to being rapidly activated and deactivated, and vibration. Ruffini nerve endings are sensitive to skin stretching, sustained pressure and temperature. They respond to sustained pressure by showing little adaptation so they do not reduce in firing even as the pressure duration increases. They can detect angles changes up to a specificity of 2.75 degrees and also act as thermo receptors (Terjung and Darin-Smith, 2011).

Visual

Sight, or vision, is the ability of the eyes to perceive images of visible light. Light goes into the eye through the pupil and is concentrated through the lens onto the retina on the back of the eye (Hubel, 1995). There are two types of photoreceptors, called cones and rods, perceive this light and produce nerve impulses which are directed to the brain through the optic nerve (Lee et al., 1998). Once that visual input has been sent, it is then conveyed to different brain areas. The ending point of the optic nerve named the lateral geniculate nucleus, found in the thalamus near the centre of the brain. The visual input from there is then directed to the primary visual cortex that is in the occipital lobe. When that input is in the primary visual cortex, the brain starts to rebuild that image. Visual input is also directed to the secondary visual cortex for further processing (Tong, 2003).
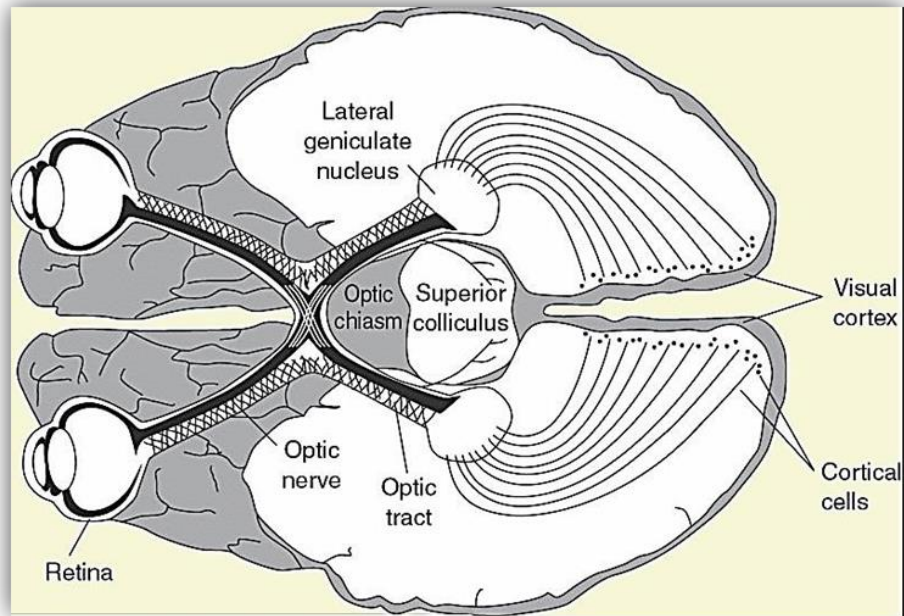
Figure 8: Visual pathway

Retinal signals move to the optic nerve (ON) and the lateral geniculate nucleus (LGN), to the visual cortex and cortical cells (Helm, 2017).

Auditory

Audition is the human feeling of hearing is credited to the sound-related framework, which utilises the ear to gather, increase, and transduce sound waves into electrical impulses that enable the cerebrum to realise and confine the sound (Scott & Johnsrude, 2003). Inside the ear, the mechanoreceptors consist of organs that perceive the sound's vibrations. Firstly, the Sound is moving through the ear canal and vibrates the drum as shown in Figure 9. Next, the vibrations are displaced to ossicles bones in the centre of the middle ear named consecutively the malleus, incus and stapes, which vibrate the liquid in the internal ear. This liquid filled organ, identified as the cochlea, covers little hair cells that yield to electrical signals when disfigured. The signals are moving through the auditory nerve straightforwardly to the cerebrum, which deciphers these signals to sound (Delano & Elgoyhen, 2016). People can regularly recognise sounds inside a scope of the frequency of 20 – 20,000 Hertz.
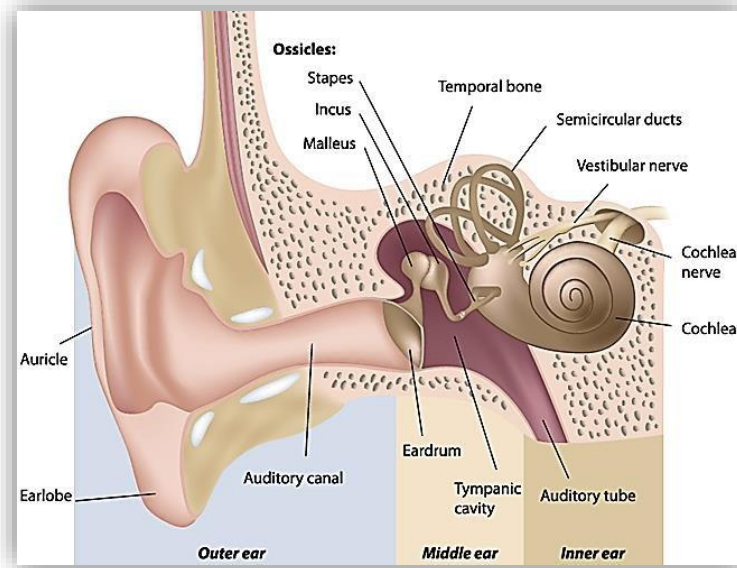
Figure 9: Ear anatomy

Anatomy of the ear that shows the hearing pathway (Pinterest, 2017)

2.3 Phantom syndrome

Phantom Limb Syndrome (PLS) is a condition in which sensations can be felt from limb that has been amputated. It is reported that 60-80% of people will experiencing phantom limb sensations after amputation (Sherman et al., 1984). The first indication of these clinical facts was by an Ambrose Paré in mid 16s who was involved in the practice of surgical amputation as well as the design of limb prostheses (Thurston, 2007). The term "phantom" may imply that the painful symptoms are illusory. Sensations can vary from pain, in form of burning, stabbing or crunching sensations, to pleasure and even movement such as waving, shaking hands or clenching of fists (Subedi & Grossberg, 2011). Sometimes, an amputee will experience a sensation called telescoping. This is the feeling that the phantom limb is gradually shortening over time. The symptoms of the syndrome occur immediately following amputation in 75% of cases or usually within at least a year of amputation (Neil, 2015). Wolff (2011) has defined Phantom Limb pain (PLP) as a pain resulted from the elimination or missing of sensory nerve by injuring the sensory nerve fibres after amputation or differentiation. Put it simply, PLS is caused by the brain still receiving messages from the nerves that once inhabited the missing limb (Flor, 2002). Until the brain readjusts and re-wires to account for the physiological change the sensation will be felt in 90% of cases.

The prevailing assumption for the reason of PLP was an annoyance in the nerve endings named "neuromas". After a limb is cut off, several nerve endings are concluded at the remaining limb. These nerve endings can be irritated and were believed to refer abnormal signs to the brain. These signs were thought to be understood by the brain as hurt (Vaso et al., 2014). Actions founded on this assumption were mostly disappointments. Where neurosurgeons would do another elimination, to shorten the stump, with the optimism of eliminating the irritated nerve endings and producing impermanent help from the PLP. However, then again, the PLP increased, because of the combined sensation of both the initial PLP, in addition to the new phantom stump (Ramchandran & Hirstein, 1998).

When looking more deeply into the cause and underlying mechanisms of PLS, brain reorganization and synaptic plasticity emerge as the key foundation. It is known from animal studies by National Institutes of Health (NIH), let by Tim Pons, that there is plasticity in the somatosensory cortex (Pons et al., 1991). Two months after monkeys had their middle finger amputated the area of cortex dedicated to the finger began to respond to tactile stimulation of the finger adjacent to the middle one (Merzenich et al, 1984). Not only can amputees experience spontaneous phantom limb Sensation they can also experience feeling in the phantom limb when other body areas are touched. For example, MEG studies showed that due to two different cortical reorganization sensory information from the facial nerves can be sent to two different cortical areas: the original face area and the area that preciously received information from the arm. These effects can even be modality specific, i.e. vibration on the face leads to perception of vibration on the phantom limb.

.
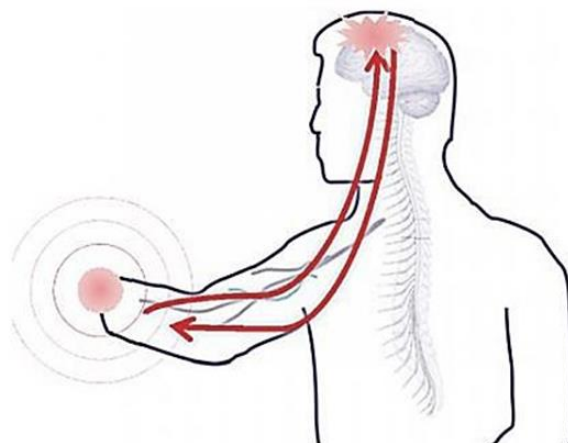
Figure 10: PLS is connected directly to the brain (Aalborg University, 2013)

The mechanism underlying the neural reorganization that leads to these kinds of experiences may be the classical Hebbian synaptic plasticity that involves the activation of NMDA receptors at neuron synapses. Another explanation for feeling in the limb when the face touched may be that the tactile and proprioceptive input from the face and tissues proximal to the stump takes over the brain area- so spontaneous discharges from these tissues would get misrepresented as arising from the missing limb (Figure 11) (Ramachandran & Hirstein, 1998).
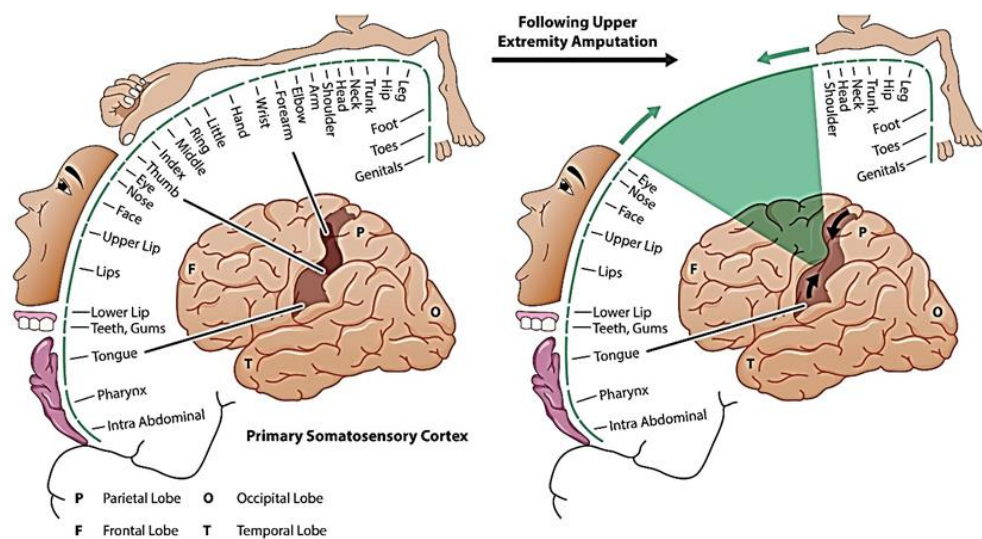
Figure 11: The effect of limb amputation on the somatosensory homunculus (Morgan, 2015)

Treatment of phantom limb pain after amputation is quite challenging, but not impossible. There are a number of tested treatments for PLS some more successful than others. Treatments can be classified as medical, non-medical and surgical where medical treatment is the most effective (Bosanqueta et al., 2015). A successful treatment is the well-known mirror box illusion treatment. It allows PLS patients to feel relief from the pain by superimposing their functioning limb onto their lost limb using the mirror and a space to hide the missing limb. Medicinal treatments include use of antidepressants, anticonvulsants, antipsychotics, opioids and others. Electrical nerve stimulation treatments also exist such as use of transcutaneous electrical nerve stimulation and transcranial magnetic stimulation (L. Nikolajsen, 2001). PLS can disappear over time using these treatments but in some rare cases it never vanished completely.

2.4 Learning mechanism
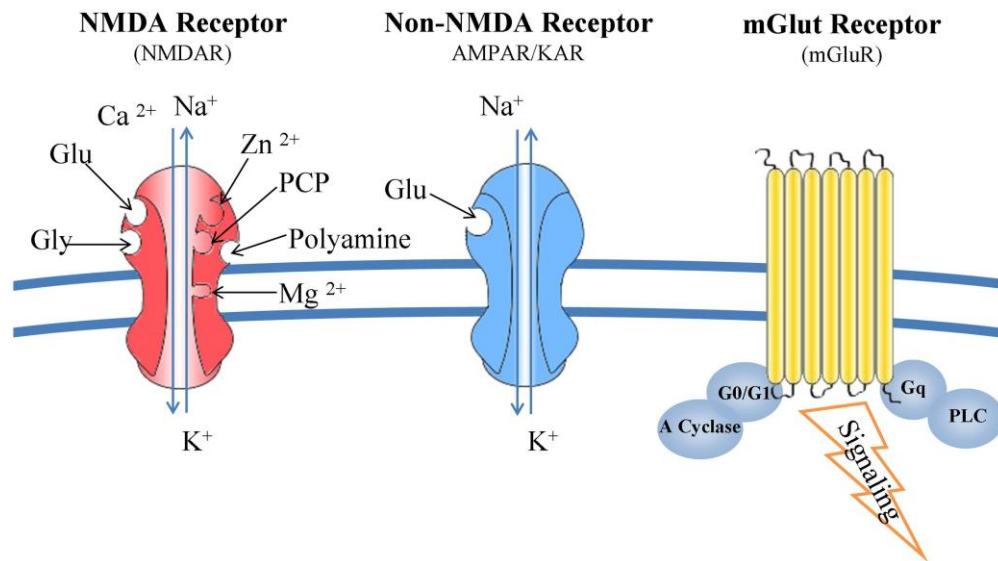
Figure 12: Glutamate receptors: structure and function (Kritis et al., 2015)

Classical conditioning, also known as reinforcement learning, is a learning mechanism. Reinforcement learning is dependent on assessing the reward value of stimuli in environment. Measuring the dopamine release triggered by the stimuli does this assessment. As more dopamine is released. The feeling of reward in the individual increases and the stimuli or behavior that led to this rewarding feeling gains incentive salience – the individual will strive towards replicating this feeling. Incentive salience is achieved through the action of NMDA receptors and calcium, predominantly in the hippocampus. The altering of neuronal networking due to the action of NMDA receptors is known as synaptic plasticity and is the neural basis for learning in humans.

Classical conditioning is best explained through example. Thorndike (1898) demonstrated the effect of conditioning using 'puzzle boxes'. Dogs, cats and chicks were put in a box and when they were hungry had to pull down a loop of wire, depress and leaver and step on a platform to obtain food. When the animals had perfectly associated the sequence of actions to the consequences, they were saying to be conditioned. Classical conditioning is therefore said to be learning process in which an innate response to an important stimulus, in this case the food, becomes linked to a previously neutral stimulus, in this case the sequence of actions, as consequence of repeatedly being exposed to the neutral stimulus and the important one at the same time (McLeod, 2007). A person learns the value of stimuli or action through experience and achieves this by testing and updating

predictions- known as delta rule updating. The basal ganglia in the midbrain plat a role in classical conditioning. Neurons in the basal ganglia project to the brain stem motor areas and the thalamocortical circuits making the basal ganglia capable of producing body movement based on expected reward. The basal ganglia plays role in guiding eye movement towards locations where rewards is available. There is a bias in excitability between the superior colliculi in a way that means saccade to the to-be-rewarded position occurs more quickly (Hikosaka et al, 2006). It therefore facilitates the actions that lead to reward- the process at the heart of classical conditioning.

From this, it is clear that learning and reward mechanisms are intertwined. This then points to the role of dopamine in learning, as it is the neurotransmitter that produces the rewarding feeling that is crucial to reinforcement learning. Certain behaviors lead to reward in the form of dopaminergic response, which leads to an experience of pleasure. This leads to conditioning learning where the environment cues associated with that behavior would be associated with the pleasure. Dopamine its role in the ventral tegmental area (VTA), within the mesolimbic dopamine pathway in the midbrain when rewarding stimuli is encountered the VTA fires and produce the dopaminergic response in the nucleus accumbens. How strongly that happens correlates with the feeling of euphoria and the reinforcement potential for that stimulus. The VTA projects to the nucleus accumbens via distinct pathway: the meso-ventral medial pathway (the shell) and the meso-ventral pathway (the core). The core is said to be more involved in learning than the shell as it responds to stimuli whether positive or negative (Bassareo and Di Chiara, 1999). Once conditioning has taken place, there will be a spike in dopaminergic responding when the cue that has been associated with reward appears. This is due to synaptic strength- so the increase (the spike) is due to development of synapses and the structure of the synapse changing in a way that it becomes more efficient.

Synaptic plasticity is the process that allows learning and classical conditioning to occur. Long-term potentiation (LTP) is a form of synaptic plasticity that involves long-lasting enhancement in the transmission of signals between two neurons, resulting from repeated simultaneous activation of the neurons. LTP is dependent on Hebb's rule being fulfilled. Hebb's rule is that LTP will only occur if a synapse is active at the same time as postsynaptic cell –if this is the case, the synapse will be strengthened. This process needs to involve repeated simultaneous activation which results in structural and chemical

changes in the synapse, that lead to heightened post-synaptic potentials. The NMDA receptor on the membrane of these neurons is key for learning and memory. Experimental evidence for the role of NMDA receptor in learning and memory comes from the finding that ketamine, an NMDA receptor antagonist, impairs explicit memory (Malhotra et al, 1996). Furthermore, Morris et al (1986) found that blocking the NMDA receptors blocks LTP. Rats were trained in a water maze after being administered an NMDA antagonist (AP5) or a placebo. Those who had been given the AP5 displayed disrupted learning and reduced LTP, so were unable to navigate the maze.

The action of the NMDA receptor is intertwined with the action of calcium- when an NMDA receptor fires there is intracellular cascades that potentiate the activities of calcium. The process is as follows: when there is stimulation, ions (glutamate) flow into the postsynaptic neuron through AMPA channels, but NMDA channels are blocked by magnesium. It is upon repeated stimulation, when the cell becomes depolarized, that the magnesium is removed and the ions can flow in through NMDA receptors. The flow of ions through the NMDA receptors activates it, which has knocked on effects for calcium, e.g. cascades begin. Calcium then has three effects, 1. It activates CAM kinase, which affects AMPA receptors by phosphorylating the ones already present, which increases their conductance to sodium ions. 2. It increases release of neurotransmitter from presynaptic cell via retrograde signals e.g. nitrous oxide. 3. It makes more AMPA receptors available. Due to more AMPA receptors the response to a stimulus of given strength will be stronger than it was before the NMDA receptors were activated – so the synapse is enhanced. This physiological change is one of the mechanisms underlying LTP. LTD is opposite of this and occur when there is a lack of depolarization and this allows synapse to stay efficient. Is stimulation is strong enough and continuous enough you can end up with another synapse. When AMPA receptors increases in number the synapse can grow and turn into two. LTP, triggered by reinforcement learning is therefore the mechanism that underlies learning.

To summarize, classical conditioning theory involves learning new behavior via the process of association (McLeod, 2008). The unconditioned stimulus (UCS) is the object or event that originally produces the natural response or unconditioned response (UCR). The neutral stimulus (NS) is a new stimulus that does not produce a response. Once the neutral stimulus has become associated with the unconditioned stimulus, it becomes a

conditioned stimulus (CS). The conditioned response (CR) is the response to the conditioned stimulus.
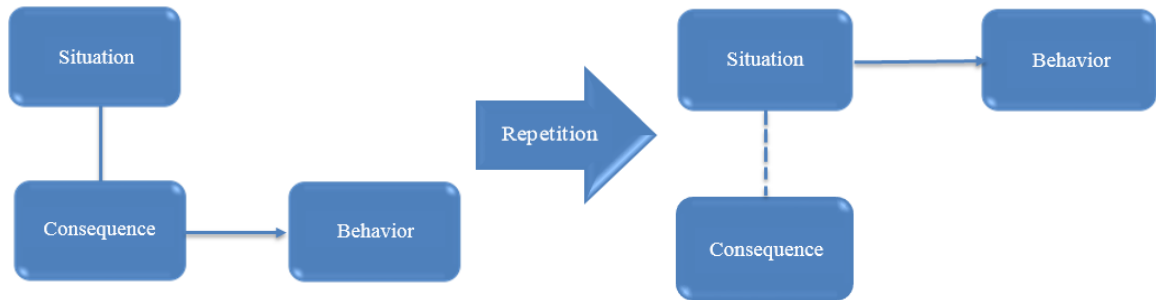
Figure 13: Classical conditioning flow chart

2.5 Brain manipulation

The brain can be manipulated temporarily by illusions, which can have effect in a wide variety of modalities. The brain can also be manipulated in more long lasting ways, due to environmental influences on brain maturation.
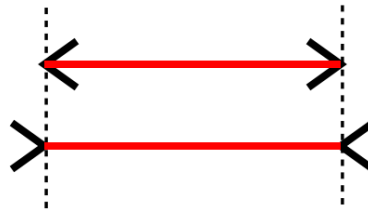
Figure 14: Muller-Lyre illusion

There exist many effective visual illusions that will manipulate the brain for a short period of time. There also exist auditory illusions, which again, manipulate the brain temporarily. The Muller-Lyre illusion is a visual illusion that manipulates the brain into believing one line is longer than another, when they are in fact the same length. The illusion works due to smaller lines at the end of each line that either protrudes outwards from the end of the line or inwards. The lines going inwards create the illusion that line is shorter. The ability of the shorter lines to interfere with the perception of length of the longer line is one of the features of geometric patterns that are known as the 'confusion effect' (Sekuler and Erlebacher, 1971). A different type of illusion that relies on the integration of visual and auditory stimuli is known as the McGurk effect. This is where an ambiguous phoneme sound is played with a video of a mouth movement simultaneously. The mouth movement will change half way through the video but the sound remains the same. For example an ambiguous phoneme that lies between the 'fah' and 'bah' sounds will be played. For half

of the video the mouth will move in a way that would imply the sound was 'fah'. For the second half of the video it will move in a way that would imply the sound was 'bah'. The illusion arises as the perception of the phoneme changes as the mouth movement does. This illusion shows the power of visual information to manipulate the perception of sound. The brain areas involved in creating the illusion have been investigated using fMRI. From this was found that there was a positive correlation between the strength of the McGurk effect and activation in the left occipito-temporal junction, an area, which is associated with processing visual motion. This suggests that auditory information modulates visual processing to affect perception (Jones and Callan, 2003). Another study used fMRI data to find the location of auditory-visual speech processing in the superior temporal sulcus (STS), as it is an area believed to be involved in creation of the McGurk effect. They then used transcranial magnetic stimulation (TMS) to disrupt this location within the STS and found that this led to less reports form participants of experiencing the McGurk effect. The authors concluded that this meant the STS was involved in the McGurk effect and the auditory-visual integration of speech (Beauchamp et al., 2010).

Another way the brain can be manipulated in the short term is shown through the phonemic restoration effect. This is where a missing phoneme from a word reported to be heard by a listener. Testing the effect involves playing a recording of a spoken word where one of the letters or phonemes is masked by a sound. In many cases, the listeners will claim to have heard the missing sound. It is thought that this is the mechanism that allows perception of words in loud environments – the context is sometimes able to provide enough information and manipulate the brain into hearing a sound that does not exist (Warren, 1970).

A more long-term manipulation of the brain from sound stimuli is the loss of phoneme detection that occurs in the infant years. Very young infants' English infants have been known to detect differences in phoneme sounds in Japanese. These same infants tested when they neared one year old could no longer differentiate the Japanese phonemes but could distinguish differences in their native language – English. The mechanism behind this process is most likely long-term depression (LTD) in synaptic plasticity. The neurones required to differentiate the foreign phonemes do not get used when the environment the infant is maturing in does not involve those sounds. This leads to LTD and the loss of function in those neurones. A similar process is involved in the perception

of faces. Very young infants find it as easy to distinguish monkey faces as human faces. This is an ability that is lost with age. This is again most likely due to LTD and the loss of the brain areas needed to distinguish monkey faces, as that is not a skill used or practiced by the infants. These processes are ways in which the brain can be manipulated by the environment, the effects of which will last many years or indefinitely.

Perceptual learning is the way in which the brain learns to distinguish stimuli it is more familiar with due to practice. This is the mechanism that underlies the brain being manipulated by the environment. Perceptual learning usually relies on the stimulus of concern being attended to. This concept can be applied to the perception of colour. Linguistic relativity plays a role in this. As children learn colour they will begin to learn the boundaries that are assigned to different spectrums of colour – something that depends on the word use specific to each language. This can affect the perceptual categorisation of different colours and consequently may subtly effect their perception of colour. This is a long-term manipulation of the brain in the visual modality.

2.7 Body ownership illusion

Body transfer illusion, "body proprietorship" or "body ownership" is referred to it in the literature reviews as the deception of owning a body part or a whole-body other than one's own (Kammers et al., 2006). It can be instigated tentatively by controlling the visual input of the individual and furthermore providing visual and sensory signs, which connect to the individual's body (Petkova & Ehrsson, 2008).

 In general, there are two ways involved in perception and sensation (Bottom-up processing) that means the sensory processing data as it is coming in. Whereas (Top-down processing), the perception was determined and motivated by perception (Bruce et al., 2003). For the illusion to happen, bottom-up processing, for example, the contribution of visual data, must prevail top-down the awareness that the specific body part does not be in the right place.

The rubber hand illusion (RHI) is the ability of an individual to experience a tactile sensation when an inanimate rubber hand is touched. It arises when one of their hands is hidden from view, for example under a cloth, and a rubber hand is placed in front of them

in a way that mimics the position of their real hand. The real hand and rubber hand are then stroked simultaneously for as long as it takes for the individual to begin to feel the strokes on the rubber hand in the same way as strokes on their real hand – at this point, the illusion has been achieved. The mirror hand illusion is similar in concept to the RHI in that they both involve a transition in the sense of ownership of a body part. It is most commonly used as a therapy for phantom limb pain or as a way of restoring action in limbs after stroke. In the mirror illusion, a mirror is placed in front of the individual at a perpendicular angle to them. Their injured limb in placed out of sight while their functioning limb is placed in front of the mirror. If the angle is correct, the patient will be able to look into the mirror and see what appears to be their injured limb looking fully functional. After a period of time, they may experience a relief from pain that is induced by the reflection of their arm being intact. In some cases touching the intact limb can give the visual and perceptual illusion of the injured limb being touched – a similar concept to the RHI.

Experiments involving the RHI can vary in terms of the way the participant is conditioned. One study varied if the visual and tactile stimuli were exhibited in synchrony or asynchrony. The study also varied the position of the rubber hand in relation to the real hand. For example, the rubber hand was said to be congruent with the real hand when they were held in the same orientation e.g. palm facing downwards (Tsakiris and Haggard, 2005). Experiments involving the RHI can also differ on the methods used to examine participants. Rohde, DiLuca and Ernst (2011) similarly varied if the stimuli were presented in synchrony or asynchrony, but also measured participants using a self-report questionnaire to gain an insight into subjective ratings. Perhaps more in depth and neurobiological approach was taken by Ehrsson, Spence and Passingham (2004). While also varying synchrony and orientation, they measured the brain activity during the illusion using functional magnetic resonance imaging (fMRI). This allowed them to observe specific brain areas involved in creating the experience of the illusion.

Tsakinis and Haggard concluded from their experiments that the RHI is the result of purely bottom-up mechanisms as the illusion was only found to occur when the rubber and real hands were incongruent positions and the visual and tactile stimuli were experienced in synchrony. They explained their findings using evidence from Graziano et al (2000). Graziano and colleagues found that there were neurones in area five of the

parietal lobe that responded to the RHI when the real and rubber hands had congruent positions. The findings from Rohde, DiLuca and Ernst's experiment was that the illusion correlated with proprioceptive drift (change of perceived finger location towards the rubber hand), and that the drift occurred in both the synchronous and asynchronous conditions. Interestingly, however, the feelings of ownership of the rubber hand only occurred in the synchronous conditions, highlighted by the questionnaires. From this, it is clear that the feelings of ownership and proprioceptive drift are dissociated so one cannot be used to infer the other. Furthermore, different mechanisms of multisensory integration are responsible for proprioceptive drift and sense of ownership. Their study also highlights the importance of questionnaires when gaining insight into the mechanisms at play in this illusion. The fMRI data provided by Ehrsson, Spence and Passingham showed three main neural mechanisms involved in creating the RHI. Firstly, multisensory integration (integrating the various forms of sensory information that the participant is being provided) occurs in the parietocerebellar regions. Specifically, the ventral premotor cortex plays a key role as it is anatomically connected to the visual and somatosensory areas and frontal motor areas. Secondly, the recalibration needed for proprioceptive drift to occur happens in the reaching circuits. Lastly, the self-attribution of the rubber hand, at the heart of the illusion, occurs in the bilateral premotor cortex, as shown by those feeling the illusion most strongly also showed the strongest BOLD response in that region.

Figure 15: the paradigm of rubber hand illusion (RHI) (Mind Tricks Gallery, 2018)

Many studies have aimed to describe the applications of the mirror hand illusion and provide explanations for the mechanisms involved. In a study outlining three case studies of patients with limb pain treated by the mirror illusion, an explanation for its effectiveness is proposed. In these cases, the illusion induced the perception of being touched in the injured limb. Rosén and Lundborg, (2005) claim that the illusion of being touched, which is mediated through the visual system, may be based on neurones in the somatosensory cortex, which are activated by tactile stimulation of the hand as well as visual observation of this tactile stimulation. This proposal is based on the idea that there are mirror neurones in the premotor cortex, which are activated, by hand actions and observation of these hand actions. Another explanation is, proposed by Giummarra et al (2010). They suggest a model in which observation of the hand movement in the mirror triggers body representations through activation of the posterior parietal cortex and temporoparietal junction. They claim activity in these regions heightens awareness of peripersonal space and increases tactile sensitivity which enhances the perception of illusory touch and embodiment. Another explanation for the illusion comes from a study using fMRI. The illusion was carried out as normal using a mirror and then repeated in the same way except the mirror was removed. From the fMRI data, two areas were found to only light up in the mirror present condition. These were the right superior temporal gyrus and the right superior occipital gyrus (Matthys et al, 2009).

2.8 Blind vs blindfolded

Studies have confirmed that the visual cortex in blind people has some deficiencies. Significantly, in congenitally blind individual, however in late blindness (after puberty) and blindfolded sighted individuals the situation is different (Petkova et al., 2012). Overall, when the brain receives no visual information, this leads not only to variations in the visual system but also to the physical and functional reorganisation of brain areas that help other sensory areas that arbitrate the integration of information across these sensory areas (Kupers et al., 2011).

Older studies for brain anatomy assumed that each area of the human brain was responsible only for specific tasks. Therefore, each area can process a precise type of information without a shift in its function. Whereas, in the last decade, scientists found

that the brain can modify form new and different neural connections performing in plasticity manner. For instance, the occipital cortex is assumed to be used primarily for visual processing. In the case of blind people, however, this area is inactive. An experiment that examines subjects who are congenitally blind and late-blind was conducted by Burton et al. (2001) to test if the brain can rewire and use the inactive neurons in the visual system for other sensory (Burton et al., 2001). By using functional magnetic resonance imaging (fMRI), the scientists measured cerebral blood flow while the subjects read Braille words. The fMRI shows that major activity sensed while the subjects read words happened in the visual cortex, notably, in the completely blind, the subjects had extra activity in the visual cortex than the late-blind subjects (Coxa & Savoya, 2002).

2.9 Telemetry biopotential data

In new medicine era, many imaging procedures for the human body are being employed. Where the electro-biological measurements involve the group of Electrocardiography (ECG) for heart activity, electromyography (EMG) for muscles contractions. Electroencephalography (EEG) and magnetoencephalography (MEG) for the brain activities, Electrogastrography (EGG) for stomach, and Electrooptigraphy (EOG) for eye movement (Taplan, 2002). The different electro-biological measurements are exhibited in Figure 16 below:
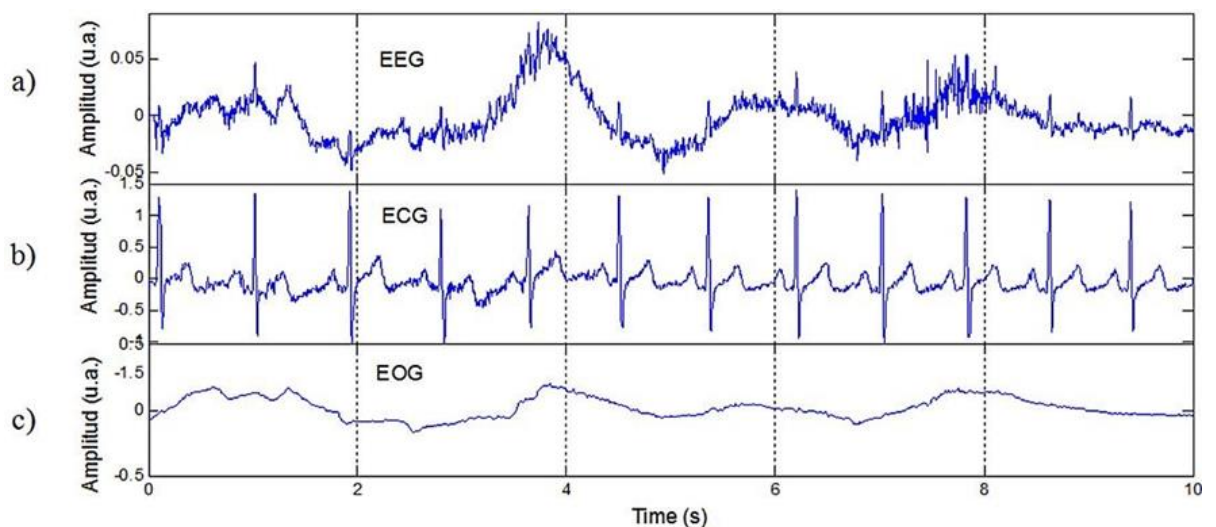
Figure 16: Different Electro-Biological Measurements Signals

(a) Electroencephalography (EEG), (b) Electrocardiography (ECG) and (C) Electromyography (EMG) (Correa & Leber, 2011)

Electroencephalogram
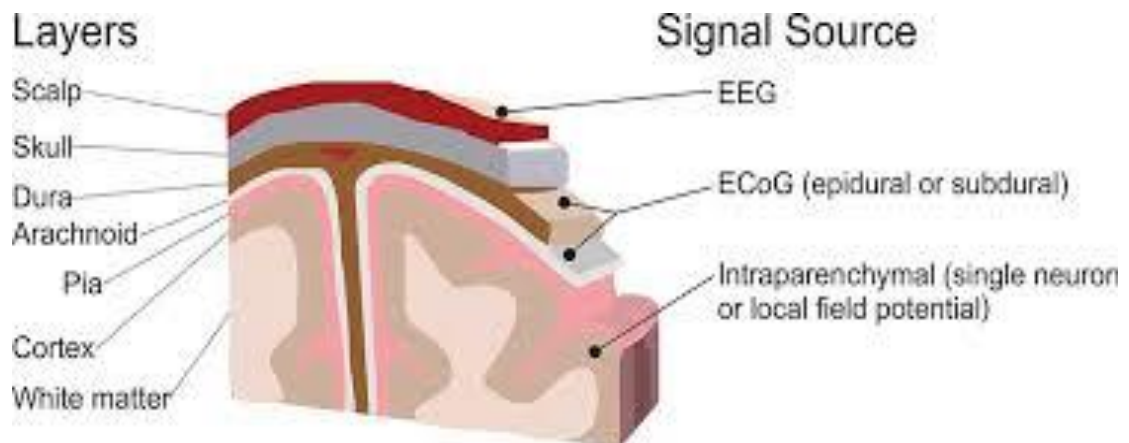
Electroencephalogram (EEG) is a test to measure and record electrical activity of the brain using electrodes attached to scalp, it was first discovered by German scientist Hans Berger 80 years ago.

Measuring brain signals can be categorize into two groups of invasive and non-invasive. An invasive approach like electrocorticographic (ECoG) requires physical implants of electrodes in humans or animals brain, and has advantage of providing measures single neurons or very local field potentials. While non-invasive approach, for instance, EEG or PET scan, provide useable measurements they are unable to provide image from inside the brain and to observe what happens (Kropotov, 2009).

Pair of conductive electrodes made of silver, for example, is used to record brain activity from the scalp. The difference in voltage between the electrodes is measured, and since the signal is weak (30-100µV) it has to be amplified. Current occurs when neurons communicate. The simplest event is called action potential, and it is a discharge caused by fast opening and closing of Na+ and K+ ion channels in the neuron membrane. If the membrane depolarize to some threshold, the neuron will "fire". The resulting trace of these discharges over time represents the brain activity. The EEG is one of the few techniques available that has such high temporal resolution and it can detect changes in electrical activity in the brain on a millisecond-level.

The most used application of EEG is to search for brain damage and various disorders like epilepsy or declaring brain dead. Studying EEG signals and how they linked to

different mental states, directed to number of alternative methods to manipulate these waves. For example, music with specific Hertz can help to become more relaxed, focused and smarter (Brain Entertainment). Investigation the relation between medication and EEG is another area that has been interested a lot of researcher. According to Braverman (1990) using antidepressants, morphine, heroin and marijuana, are addictive because they increase the alpha activity. Alcohol is quick remedy to become relaxed as it increases the amplitude of slow wave frequencies, decrease the fast wave, and has excess of occurring beta waves. Further, Braverman talks about "how brain waves symbolizes the various parts of our consciousness, and that if we get the knowledge and treatment to change them, we can get closer to get our very balanced brain waves, or happiness" in his article in two ways, event related potentials (ERP) or Neurofeedback training.

Electromyography

EMG is the electrical recording of muscle activity; also, diagnostic procedure to assess the health of muscles and the nerve cells that control them.it involves electrodes detecting changes in the muscle. The signal is detected by means of electrodes that are either transcutaneous on the surface, or implanted. In the model that is being designed, electrodes and sensors make electrical contact with the skin, with two of them at a target muscle, and the third closer to the relevant bone (Knipe, n.d.). As surface EMG is non-invasive, it is the most common, and important, technique for programming a prosthetic. Electrodes are made of stainless steel and sense the activities of the muscle. The activity of the muscle is low power, so isolation and differential amplifiers are required to increase the power and isolate the EMG from any other electromagnetic "phenomena" that may be sensed by the electrodes. The EMG is decoded to produce a voltage to correspond to subsequent muscle activity. The process therefore involves the muscle fiber responses stimulating the electrode sensors; the resulting signals are decoded and then processed. One disadvantage is that the strength of the signals depends on the voltage output and on the muscle contractions.

Following the amputation or removal of a limb, the neuromuscular system supplying motor function to the limb remains intact. This residual nerve and muscle supply can be utilized to provide input to the prosthesis (Camdir, 2015). However, different limbs have a different pattern of nerve supply and muscle control, so the origin and pattern of control of the prosthetic will depend on implementation and timing. Only relatively recently has

it been possible to harness EMG signals for functioning residual muscles to drive prosthetic limb function (Sudarsan and Sekaran, 2012).

2.10 Brain- Computer Interface

Brain- Computer Interface (BCI) is a method of communication, which uses neural activity generated by the brain and is independent of the brains normal neural outputs and pathways. It provides a new channel of output for the brain that requires voluntary adaptive control by the user. BCI differs from Human-Computer Interface (HCI), which is the interaction between humans, and electrical equipment such as keyboards, as it is more direct because involves an interaction between the device and the brain. BCI can be used to help individuals with mild-severe muscular handicaps or even mental handicaps, e.g. autism. The goal of the BCI system is for the user to interact with the device and this is achieved through functional components, control signals and feedback loops. The aim of this is to convert user intention into action.

The BCI relies on the measurement of brain waves in some form or another. This can be invasive or non-invasive. Invasive techniques have the advantage of providing high temporal and spatial resolution, but have the drawback of needing to penetrate the scalp. Non-invasive techniques for measuring the brain include Computerized Tomography (CT), Near-infrared spectroscopy (NIRS), Positron Electron Tomography (PET), Magnetic Resonance Imaging (MRI), functional MRI (fMRI), Magnetoencephalography (MEG) and Electroencephalography (EEG). EEG is used most frequently because of its superior temporal resolution and recently its spatial resolution is increasing. There are two classes of signals that are measured in BCI; spikes, which are action potentials of individual neurons and field potentials, which are measures of combined synaptic, neuronal and axonal activity of groups of neurons- this can be measured using EEG. BCI research focuses on signals from the Alpha band (8-13 Hz) and the Beta band (14-30 Hz). The components (signals) of interest in BCI can be divided into four categories: 1. Oscillatory EEG activity, 2. Event-related potentials (ERP), and 3. Slow cortical potentials (SCP) and 4. Neuronal potentials.

Oscillatory EEG activity is the synchronized firing of neurons, which create observable oscillations. ERP are time-locked responses to a specific event. SCP is caused by shifts

in the depolarization level of certain dendrites. Neuronal potentials are voltage spikes from individual neurons.
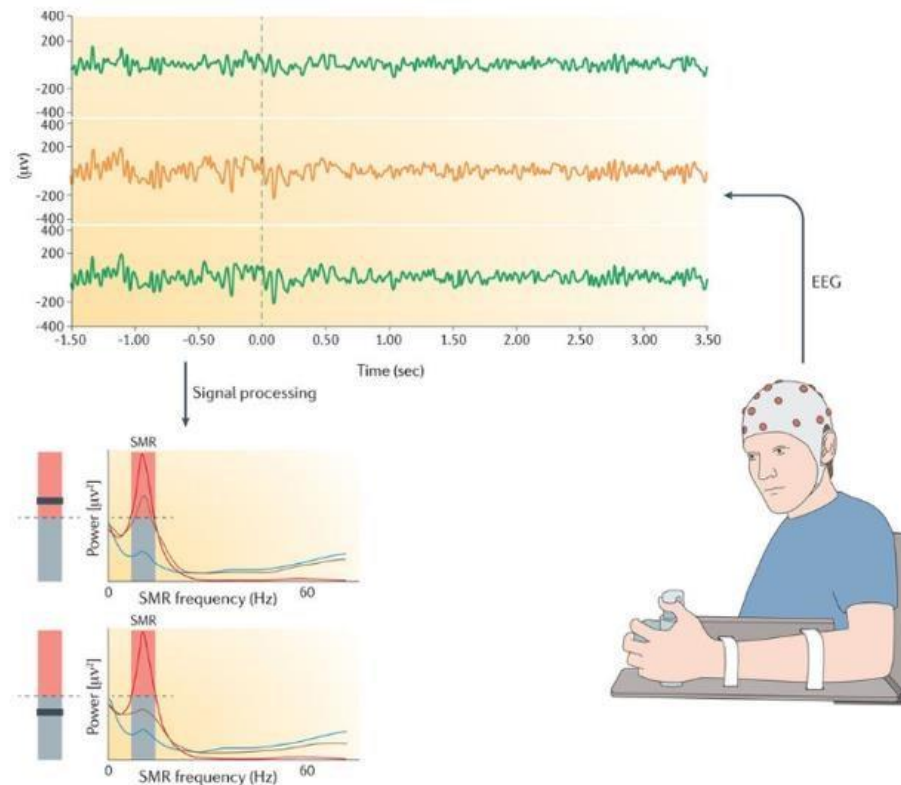
In order for BCI to occur, patients need to be able to control brain activity, a task that is difficult without training. Training is available that can be in the form of cognitive tasks e.g. motor imagery, or operant conditioning which helps the user gain automatic control of the device. The feedback provided by the system conditions the user to continue to produce and control the EEG components that achieved the desired outcome. Training can be effected factors such as concentration, distractions, frustration, emotional state, fatigue, motivation and intentions, so these need to be taken into consideration when training patients (Vallabhaneni et al., 2005).

BCI in prosthetics

One of the important applications of BCI is the control of neuroprosthetic device. EEG-based BCI has been found to be able to move the prosthetic limb of someone who is paralyzed. BCI devices can be controlled by at least one binary output signal of the BCI, which can be obtained by classifying EEG patterns during Imagination of left and right

hand movements. Unilateral hand movements result in contralateral event-related desynchronization (ERD) close to primary motor areas. Because of this EEG channels are assembled closed to primary hand areas as an array of electrodes overlying motor and somatosensory areas. An experiment based on these principles showed that an EEG-based BCI system allows control of prosthetic hand by imagination of left and right hand movement with a highest accuracy of 90%. The problem with this device is that it requires a lot of attention from the patient, a level that is not always achievable. In order for the ease if commanding movement to be closest to natural the spatial resolution of the measuring devices needs to increase. This could occur by implanting electrodes over the sensorimotor areas (Guger et al., 1999).

Steady-state visual evoked potentials (SSVEP) – based BCI has also been found to allow movement of prosthetic limb. A study used a four-class BCI based on SSVEP to control prosthetic hand- in an asynchronous mode it worked (Muller-Putz and Pfurtscheller, 2008). Schwartz et al (2006) summarize the processes involved in BCI in prosthetic and highlight the importance of somatosensory feedback. The first stage is recording the electrical activity within the cerebral cortex then the signals are translated into command signals, which drive the prosthetic limb. Somatosensory feedback is a vital component of motor planning, control and adaptation, so it is good to include this feedback in natural prosthetic systems.

2.11 EEG Signal Acquisition and Registration

As it mentioned before, EEG is the representation of brain electrical activity and studying these recorded signals can led to diagnoses of many neurological diseases. It is also used in many new methods to check the BCI devices. Although recording EEG signals is not difficult but analysis of this signals are not undemanding, there are many sources of artifacts, mainly from muscular activities like blinking, and power line electrical noises (Al-Fahoum and Al-Fraihat, 2014). To neglect these signals many methods was presented. Figure 19 shows the usual route of EEG signal processing.

Figure 19: Usual route of analyzing EEG signal

The acquisition of brain waves data can be gained by several techniques depending on the way the data is being extracted either, invasive, partially invasive or non-invasive. The different BCI techniques are illustrated in figure 20:
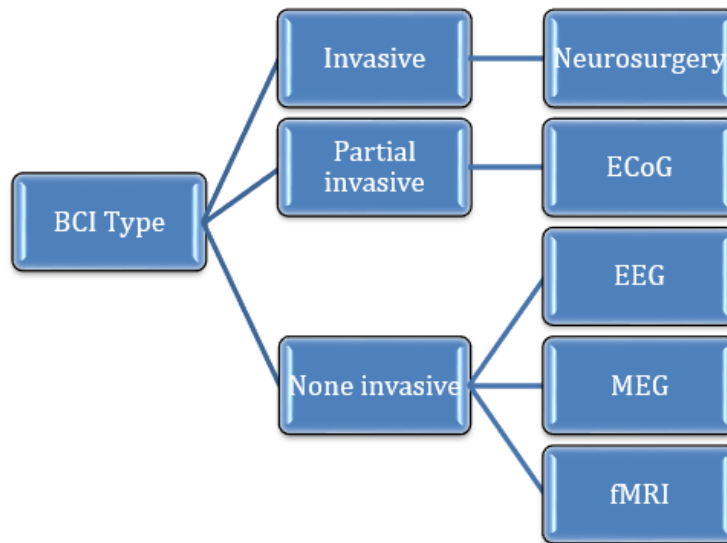
Figure 20: Different BCI techniques for data acquisition (Hassanien & Azar, 2015)

In this project, the BCI technique used in performing the RHI experiments is a non-invasive technique, which will be the main concern of discussion. The non-invasive technique has weak signal detection proprieties, yet it is the most secure and cheap sort BCI (Hassanien & Azar, 2015). BCI techniques usually use electrodes (sensors) to be placed on the scalp to detect and extract brain signals (Nunez, 1995).
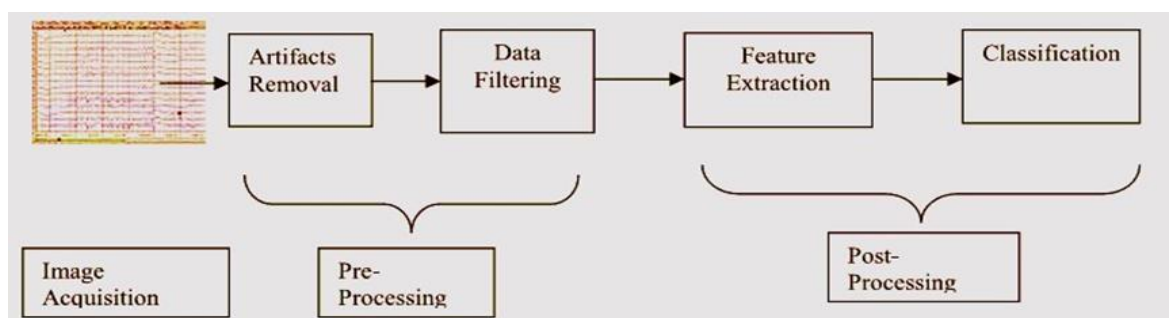
Figure 21: EEG signal processing (Kumar & Bhuvaneswarib, 2012)

EEG outline with commonly used EEG signal processing stages modules in most of the EEG study shown in Figure 21. In EEG signal registering stage, raw EEG signals are obtained right away from the brain by placing the electrodes on the scalp. Signal processing is divided into two broad stages: pre-processing and post-processing (Orfanidis, 2010). The two main steps of pre-processing are artefact removal and data filtration, while the post-processing stage involves feature extraction and classification as shown in Figure 21 (Başar, 1998; Singhi & Bansa, 2004). The stage of pre-processing that involves two equally important procedures, data filtration (Başar, 1998) and artefacts elimination (Singhi & Bansa, 2004). Signal filtration is a significant procedure in signal processing (Figure 22). Simply, it cleans the signal to produce an improved better signal (Strang, 1999). Recognition and elimination of artefact is a demanding stage in EEG signal analysis.
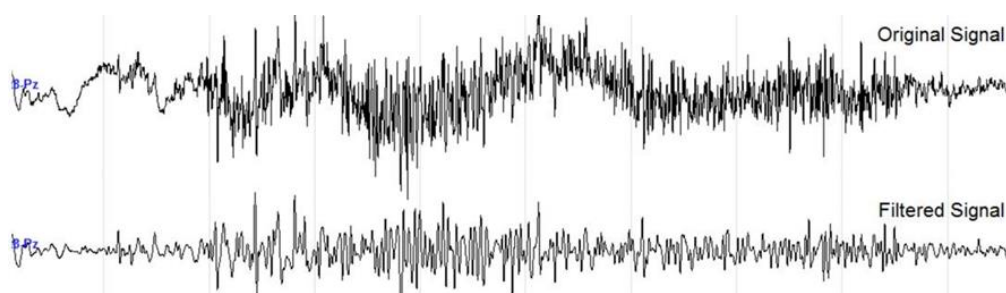
Figure 22: The difference between original and filtered EEG signals (Scolaro et al., 2013)

Artefacts are generated as a result of several causes, for example, poor electrodes placement positions, unclean scalp, and the impedance of electrodes. The improper interaction between the electrodes and the scalp also the sweat or wetness of the subjects under the electrodes could influence the electrode impedance which results in little frequency artefacts (Salenius et al., 1997). Furthermore, findings of physical artefacts, like the bioelectrical signals generated from different body parts (heartbeats and muscular action, eye squint and eyeball development) are also recorded in the EEG (Figure 23) (Reddy & Narava, 2013). Therefore, these forms of noise are undesirable and importantly has to be eliminated prior any additional signal processing, for accurate and appropriate

investigation and demonstration of EEG signal. Consequently, it is essential to use the appropriate filters to reduce artefacts in EEG signals (Correa et al., 2009).
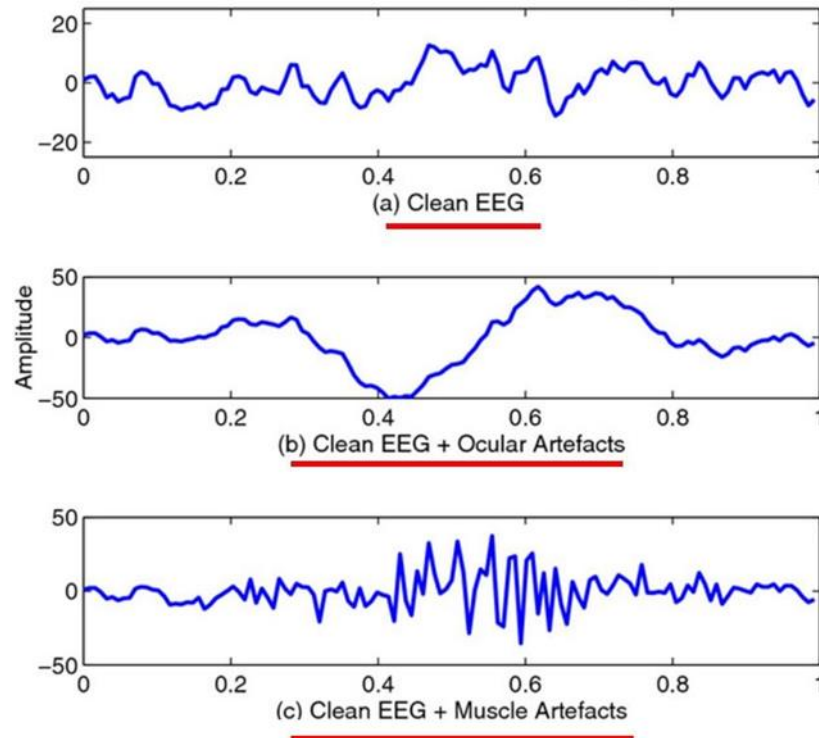
Figure 23: Examples of artefacts types of contaminated EEG signals

(a) Clean EEG signals (b) effect of eye blinks artefacts on clean EEG (c) effect of Muscle artefacts on clean EEG (Yong et al., 2012)

Feature extraction is the following stage in EEG signal analysis where many signal processing methods such as Fast Fourier Transform (FFT), Wavelet, and Principle Component Analysis (PCA) (Tong & Thankor, 2009). The best common computerised technique is FFT, which is essential to classify the brain wave signals to five frequency oscillations (Gamma, Beta, Alpha, Theta, and Delta) (Fonseca et al., 2006) as it will be elaborated more in the coming section. Lastly is an important stage that is Classification. In classification, extracted features are utilised to get the objective observations (Kaneko et al., 1996).

The Software used to conduct the signal processing is EEGLAB toolbox of MATLAB. EEGLAB is an intelligent MATLAB programme for processing consistent and event-related potential ERP, EEG, MEG and other electrophysiological information that incorporates Independent Component Analysis (ICA), time/recurrence investigation, artefact removal, and much more (Al-ani & Trad, 2010). EEGLAB by MATLAB offers extraction of epoch, baseline elimination; data resampling, artefacts elimination, and

offers a plot of scalp map, channels in time-frequency domain (Pfurtscheller et al., 2000). EEGLAB has the property of saving all the information corresponded to a specific recording such as channels positions, Epochs and sampling rate as a separate structure or document called EEG dataset (Pfurtscheller et al., 2000).

Electrodes positioning system
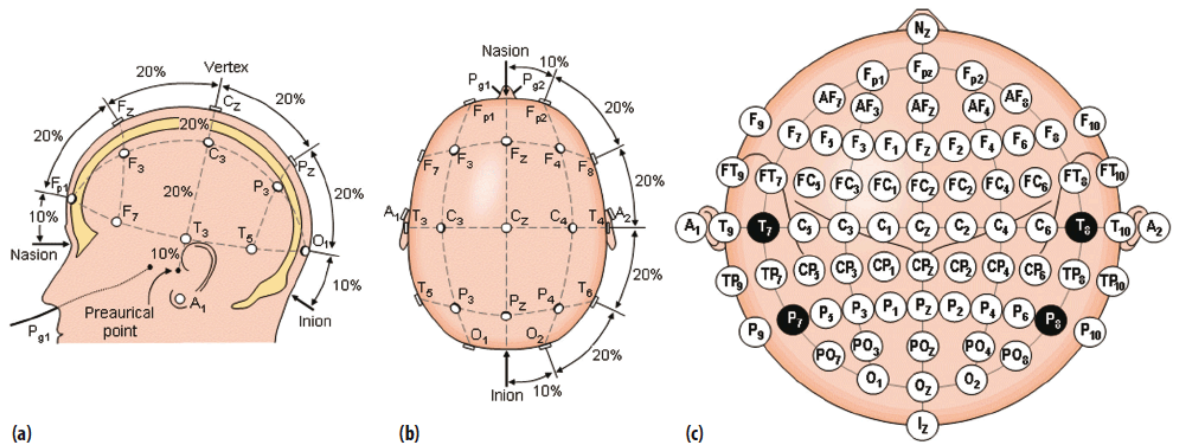
Figure 24: EEG landmark for 64 channels by 10/20 systems (Campisi, La Rocca and Scarano, 2012)

The American Encephalographic Society (1994) founded the global 10-20 system as a standard system to define the position of electrodes on the scalp (Oostenvelda & Praamstrac, 2001). The system is based on the connection between the position of an electrode and the related region of cerebral cortex. In addition, it many depends on four main positions on the head that are easily transferable between patients. First is the Nasion at the bridge of the nose, then the Inion a bone of protuberance on back of the head and then two pre-Auricular points just anterior to each ear. Figure 24 presents these points (Sleepdata.org, n.d.).

The numbers "10" and "20" relate to the space between contiguous electrodes either 10% or 20% of the overall distance of the skull from right to left or front to back (Nunez & Srinivasan, 2006). More specifically, the first measurement is from Nasion to Inion, front to back, this measurement then divided into 10% and 20% increments, this is how 10-20 systems gets its name. Next measurement made from one Preaurcular point to another, and this is again divided to 10% and 20% increments. Further marks are made around the head (Bisawarna, 2013).

Each location has a letter to recognize the corresponding lobe and number to recognize the hemisphere position as shown in Table 2. It is worth mentioning here that, letter C is used to indicate the central position rather than central lobe which does not exist, whereas z (zero) relates to an electrode placed on the midline as shown in Figure 24. Even numbers refer to electrode locations on the right hemisphere, and odd numbers relate to electrode locations on the left hemisphere (Trans Cranial Technologies, 2012).

Table 2: Electrodes and lobes labelling according to 10-20 system (Trans Cranial Technologies, 2012)

Electrode	Lobe
F	Frontal
T	Temporal
C	Central
P	Parietal
O	Occipital

Evidently, from brain anatomy, different brain parts might be connected to different functionality of the brain (Başar, 1998). Each scalp channel is placed adjacent to specific brain centre. For instance, F7 is placed close to rational thinking centre, Fz close to the centre of motivation and intentions, and F8 is adjacent to bases of emotive instincts. Cortex around where channels C3, C4, and Cz are placed in the cortex which deals with motor and sensory purposes.

Positions close to P3, P4, and Pz deals with proprioception and differentiation (Kabdebon et al., 2014; Teplan, 2002). Close to T3 and T4 the position of emotion processors, whereas at T5, T6 acting for memory purposes. Main visual parts can be found under channels O1 and O2 (Grill-Spector & Malach, 2004; Teplan, 2002). Nevertheless, the scalp channels might not reproduce the specific parts of the cortex, as the precise position of the electrodes is still problematic as a result of limitations affected by the inhomogeneous skull properties and dissimilar alignment of the cortex bases (Nunez, 1995).

EEG records are achieved from multiple electrodes. The value at Cz does not reveal the electrical activity at that place. There is no voltage at a single point. Alternatively, EEG

voltage displayed the current between the location (ex; Cz) and the electrode at the ground position (G) (Tatum et al., 2008). Consequently, the voltage recorded concerning Cz and G is calculated by (Cz − G). There is some electrical noise presented by the ground electrode because in the amplifier the ground electrode is always linked to the ground circuit. Accordingly, the calculated voltage between Cz and G has brain activity in addition to electrical noise (Teplan, 2002; iMotions, 2016). To get over this restriction, EEG systems present an electrode R acts as a reference. The amplifier records the current among Cz and the ground electrode (Cz − G) along with the current among the reference and ground electrodes (R − G). Hence, the amplifier now calculates the difference among Cz and the reference electrode as ([Cz − G] − [R − G]), which is equal to (Cz − G − R + G), that makes it simpler to Cz − R (as G negate). Thus, the production of the amplifier is the electrical current among the registered point (Cz) and the reference electrode. (Michel et al., 2004; iMotions, 2016).

How the EEG recorded
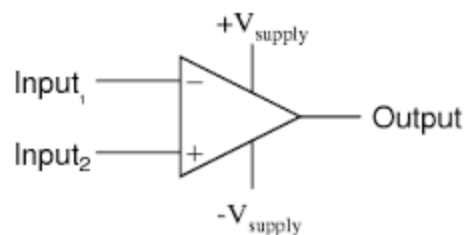
Figure 25: Differential amplifiers

EEG recorded using the technology of the differential amplifier; it takes two electrical inputs and displays the outputs as the difference between the two inputs. This is particularly useful at recording and displaying for very small electrical signals such as those in EEG (Keim, n.d.)

How EEG is displayed

EEG can be displayed in different ways that all known as montages. In other worlds, the term montage refers to the order and choices of channel displayed on EEG page (Kratouni, 2015). The most common montage is Bipolar Montage, in this way of display, there will be two electrodes per channel, so each channel will have reference electrode from one scalp location to a nearby scalp location in chains of electrodes going across the head from left to right or front to back. Another common montage called, Common Average Reference Montage (Referential), unlike bipolar montage, in referential

montages, all electrodes are referenced to a single common reference point that commonly consists of linked ears (Bobele, 1990).
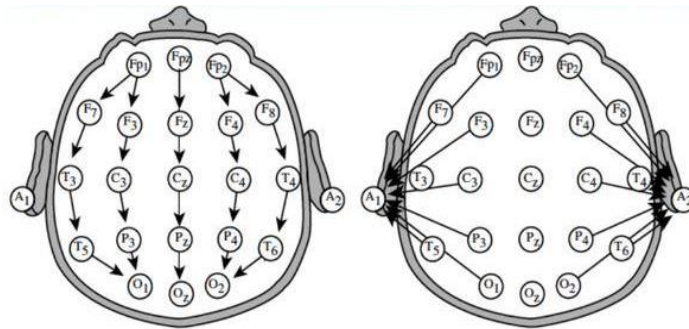
Figure 26: Arrangement of bipolar chain (left) and referential (right)

Finite-duration Impulse Response (FIR) Filtering

Finite-duration Impulse Response (FIR) and Infinite-duration Impulse Response (IIR) filters are major forms of digital filters used application in Digital Signal Processing (DSP) (Zahoor & Naseem, 2017). The FIR is finite because simply a feedback does not exist in the FIR. The absence of feedback assures that the FIR is still finite; on the other hand, IIR filters use feedback (Widmann & Schröger, 2012). Each filter has its pros and cons. The pros of FIR filters prevail over the cons. Accordingly, they are widely used. FIR filters can simply be designed to be a linear phase and straightforward to apply. They are used for multiple-rate operations either by decreasing the sampling rate or raising the sampling rate; both can be used as well (Singh & Priya, 2013). Using FIR filters permits some of the computations to be overlooked, therefore producing a significant computational efficacy. FIR filters need extra memory and computation to attain a specified filter response characteristic (Gaydecki, 2004).

Blind source separation (BSS) and Independent Component Analysis (ICA)

ICA, Principle component analysis (PCA) and BSS are algorithms based tools that are implemented in several operations in the field of neuroscience and specifically in signal processing (Peterson et al., 2005). The reason for using these types of algorithms is to modify and replicate the registered signals in order to be analysed. BSS is utilised to resolve matrix factorisation and signals decomposition by providing the ideal signal estimation (Clifford, 2008).

ICA is an effective tool in separating extracting noise and artefacts from the EEG signals. ICA can efficiently identify and eliminate a significant quantity of the artefacts and noise

such as blinking, neck twisting and muscular movements that cannot be eliminated by using FIR filter (Ungureanu et al., 2004). A constraint of using ICA is that it has to depend on an optical examination of the ICA components for more processing (Taigang et al., 2005). Mostly, the noise and artefacts can be eliminated and investigated by applying algorithms as PCA, ICA and BSS.

Fast Fourier Transform (FFT) method

The Discrete Fourier Transform (DFT) is utilised when dealing with discrete time domain data, and convert it to frequency analysis. The fast Fourier transforms FFT another version of DFT method in terms of reaching the same result, but with fewer computations and faster (Press et al., 1997). In other words, FFT is a DFT algorithm which decreases the number of times of calculations required for N points from $2N^2$ to $[2N \log_2 N]$, where log is logarithm with base 2 (Cooley & Tukey, 1965). Cooley and Tukey were the first who deliberated FFT; they build on Gauss factorisation step that they discovered on early 1800 (Abhishek & Vali, 2016). FFT algorithms mostly divided into two groups: time and frequency domain. The FFT algorithm by Cooley-Tukey has first reorganised the input components in opposite command, at that time, shapes the output transform in time. The main indication is to split up a transform of length N in two transforms of a distance N/2. On the other hand, FFT technique is not suitable for greater noise proportion in EEG signals. That is why Parametric Spectrum Estimation techniques such as Autoregressive (AR) are utilised to lessen spectral loss and provides improved frequency conclusion. Alternatively, the parametric technique is not appropriate for EEG non-stationary signals (Klem et al., 1999).

With respect to EEG signals, they can be modified by FFT from time to frequency domain and vice versa. FFT is appropriate for narrowband and stationary signals and the mathematical formula that the FFT is implementing to analyse EEG data (Wang et al., 2013).

In spite of the fact that FFT has the speediest approach in real time presentation in contrast with all other accessible approaches and is great apparatus for Signal processing preparing, it is more proper for narrowband signal, for example, sine wave (Wang et al., 2013). In any case, it is the slightest productive of every other approach as it cannot be utilised for investigation of short EEG signal as it does not have a great spectral

approximation, it additionally cannot examine the nonstationary signals. Besides, FFT is extremely sensitive to noise and does not have shorter period information registered (Blahut, 1985).

The formula for the mathematical way of this method is as below steps: (Al-Fahoum and Al-Fraihat, 2014).

$$X(\omega) = \int_{-\infty}^{\infty} x(t)e^{-i\omega t}\,dt$$

$$x(t) = \frac{1}{2\pi} \int_{-\infty}^{\infty} X(\omega)e^{i\omega t}\,d\omega$$

Fourier transforming the valued autocorrelation classification, which is found by nonparametric techniques, calculates the PSD. Welch's method is one of these techniques. The data sequence is applied to data windowing, creating improved periodograms.

$$x_i(n) = x(n + iD), \quad n = 0, 1, 2, \dots, M - 1$$
$$\text{while} \quad i = 0, 1, 2, \dots, L - 1;$$

Equation 2: Information sequence X_i (n)

Where "iD" is point of start of "ith" series then "L=2M" indicate data sector that are created.

$$\overset{\approx(i)}{P_{xx}}(f) = \frac{1}{MU}\left|\sum_{n=0}^{M-1} x_i(n)w(n)e^{-j2\pi fn}\right|^2$$

Equation 3: Output periodograms result

U gives normalization factor of power in window function (w (n)), and it calculate as:

$$U = \frac{1}{M}\sum_{n=0}^{M-1} w^2(n)$$

Equation 4: Calculating U in window function

Using average of these improved periodograms, Welch's power range can be calculated as below:

$$P_{xx}^{W} = \frac{1}{L} \sum_{i=0}^{L-1} \overset{\approx}{P}_{xx}^{(i)} (f)$$

2.12 Identifying different brain activity patterns
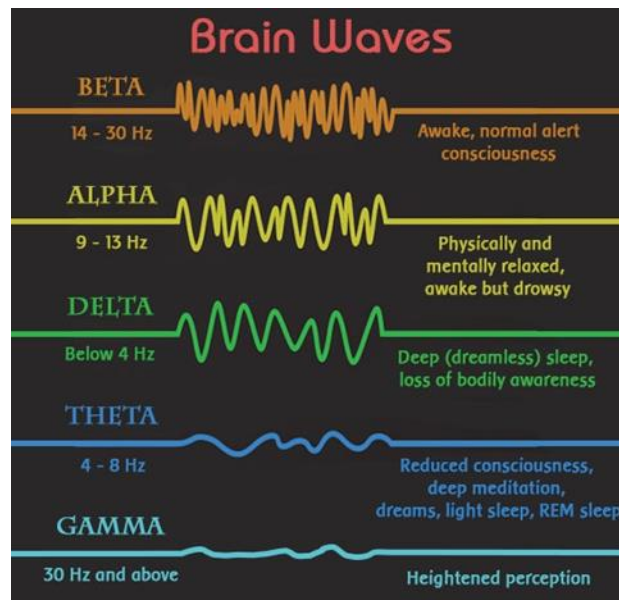
Figure 27: General human brain wave frequencies (Tri, n.d.)

brainwave, or (Neural oscillation), is synchronised or repetitive neural activity arise from masses of neurons communicating with each other producing electrical pulses in the central nervous system (Nunez, 1981) . Hans Berger, the German psychiatrist in 1929, created the electroencephalography (EEG) to measure the electrical activity in the brain (Tudor et al., 2005). He observed subjects performing the different task, like solving mathematical problems, while recording EEG, and found that different brain waves are associated with different stages of perception. Frequencies of the brain can be divided into five groups in order of high to low by Gamma waves, Beta waves, Alpha waves, Theta waves and Delta waves. Each of these waves serves a unique purpose to mental function (Andreassi, 2007; Idris et al. 2014).

The unit of frequency is Hertz that equals to cycle per second (Hz=cycle/sec). The brainwave Amplitude is measured in microvolts (µV). Slow wave's frequencies ranges of less than 8 Hz, while fast waves ranges of more than 13 Hz. Brain waves are classified

as a Low amplitude if it is less than 20 µV, medium amplitude ranges between 20 - 50 µV and high amplitude, if higher than 50 µV.

Gamma waves

When a person is highly alert and focused or when they carrying out very complex motor processes gamma waves are created. They are also found during hypnotic states. They have the highest frequency out of five frequencies with the range of 30Hz and higher, around 5-10 µV. It is understood that it reflects the mechanism of consciousness and appears during cognitive actions, processing information, learning, and memory. Gamma happens irregularly when the sensory stimuli, for instance, auditory snaps or strong flashes of strong light (Galambos et al., 1981).

Lowered or absence of gamma waves is disclose depression, learning disability and attention deficit hyperactivity disorder (ADHD), people with learning difficulty have a small number of gamma waves. The good level of gamma wave action allows people to think clearly, process information, use problem solving and logic easily while too many presents of gamma waves reveal stress, anxiety and panic attack type behavior. Gamma waves are important in matching and bringing together thoughts being processed in different parts of the brain. Beta and gamma waves together have been associated with attention, perception, and cognition (Rangaswamy et al., 2002)

Beta waves

The beta waves known as "high frequency low amplitude" are small and fast; they are range between 14 and 30Hz; 2 - 20 µV and found in the frontal and central region in adults (Chang et al., 2007). Beta wave distinguishing of an engage mind, which is alert, aware and well-focused and can be divided into two groups of β1 and β2 to get a more specific range. They are main wave most people experience during day for problem-solving, decision-making, having conversation, conscious thought and logical reasoning and normally present during a waking state and well defined in central and frontal areas (Zhang et al., 2008). Scanty of the beta wave plead as poor cognition, ADHD, depression and too prone to daydream and adequate of Beta range can show stress or anxious thoughts.

Alpha waves

Alpha waves, mentioned to as "idle state", ranging from 9 to 13 Hz; 20-60 µV, primarily occur in the posterior half of the head and are commonly found in the parieto-occipital area of the brain. It may occur as round, sinusoidal or occasionally as sharp waves and regarded as the most outstanding wave in brain activity. It typically specifies a peaceful consciousness without any consideration or attention (Chang et al., 2007).

Alpha form a bridge between subconscious and conscious mind. Relaxation and disengagement, like closing the eyes and thinking about something peaceful, meditating or practicing being mindful will increase alpha activity and can be reduced by opening one's eyes or any concentrated effort. They are usually found in frontal lobe and back of the head. The upper end of alpha range in person can present itself as the inability to focus on tasks and complete them while person with insufficient alpha waves can suffer from insomnia of OCD, highly stressed and anxiety ridden.

Theta waves
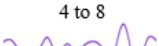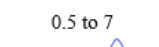
Theta waves, ranging from 4 to 8 Hz; 20 - 100 µV are second slowest waves, it is initiated from the thalamus. They are present most frequently in children up to their early teenage years. Theta waves associate with light sleep, heavy relaxation, daydreaming or drowsiness the very lowest waves of theta represent the fine line between being awake or in a sleep state. They are known as natural intuition, imaginative or creativity that controlled by subconscious as believe they make communication between conscious and subconscious minds easier (Mihail & Leon, 2013). Theta arises from emotional stress, especially frustration or disappointment (Zhang et al., 2005). Hyperactive nature and impulsive decision-making, suggest high number of theta waves and feeling anxious, stressful or having emotional deficits in terms of emotion indicate poor number of theta waves.

Delta waves

Delta waves, ranging from 0 to 4 Hz; 20 - 200 µV, are the slowest waves. They are dominant in young children and babies and in adult occurs when sleeping, hyper-relaxed or in a deep meditation (Hammond, 2006). Hence, the amount of Delta wave decreases with age in waking and sleeping state (Mihail & Leon, 2013). If these wave shows during waking moment, it implies physical defect in the brain. Certain frequencies, in the delta

range, interconnected with the body's healing and growth mechanisms. Deficient of delta waves present itself as tiredness after sleep while too much of them shows as inability to focus, ADHD and learning difficulties. Table 3 summarize the brain activity pattern.

Table 3: Brain wave frequency range and characteristics

	Frequency (Hz)	Brain Location	Description
Gamma	30 and up	• Somatosensory cortex both sides of brain and midline to front and back	• Indicative of sensory processing • Shown during short term memory activities
Beta	14 to 30	• Both left and right sides of the brain • Has symmetrical distribution of activity • Most evident frontally	• Indicative of an alert or focused working state, active, busy or anxious thinking or active concentration
Alpha	9 to 13	• Posterior regions of head both sides • Higher in amplitude on dominant side • Central Sites at rest	• Indicative of a relaxed/ reflecting state • Closing of eyes
Theta	4 to 8	• Various location	• Common frequency found in young children • Indicative of drowsiness or arousal in older children and adults • Idling • Has been found to spike when person is actively attempting to repress an action or response
Delta	0.5 to 7	• Frontal (adults) • Posterior (children)	• Occurs in sleeping adult and is frequent in babies • Indicative of continuous attention task [kirmizi-alsan et al 2006]

Further categories of brainwaves are: a) Kappa waves—created at 10 Hz and related with rational thinking; b) Lambda waves are happening at occipital region so it is related to visual sensation; c) Mu waves are documented at the vertex of the scalp in alpha frequency (9 - 11 Hz) but it is separate from alpha wave, it is most prominent when the body is physically at rest; d) Rho waves are positive temporary sharp waves at occipital area, and e) Spindle (sigma) waves are A sleep spindle is a burst of oscillatory brain wave detectible on an EEG that happens within stage 2 of sleeping. It consists of 12–14 Hz waves that happen for minimum 0.5 seconds (Rechtschaffen & Kales, 1968). Sleep spindles are produced in the reticular nucleus of the thalamus.

2.13 Neurofeedback (NFB)

Neurofeedback (NFB), also called neurotherapy or neurobiofeedback, is uses real-time displays of brain activity most commonly EEG, to teach self-regulation of brain function

feedback usually send to user by sound or video display and user can understand if there was adequate change in brain waves.

Neurofeedback training is the use of brain scanning technology, often EEG, to allow individuals to monitor their brain activity and even sensory feedback, and use this knowledge to train their brain. Sensory training that limits the extent of somatosensory reorganization can reduce phantom limb pain (Dhillon and Horch, 2005) also; it can help people with ADHD have better attention (Levesque et al., 2006).

"Can neurofeedback training enhance performance?" (Vernon, 2005) Neurofeedback (aka EEG bio feedback) requires an individual to alter some part of cortical activity - the goal is to allow people to know what specific states of cortical arousal feel like and how to activate those states voluntarily. Training is done by EEG being recorded and fed back to individual in the form of audio or visual information. For example a bar whose, width is determined by the frequency of the brain signal. Participant may have to increase the bar size, when they achieve this a tone may sound and a symbol representing a point appears. It works through associations (like classical conditioning) between cortical activity and specific states. But the results of this kind of training do not yet point to an unequivocal result.

Sensory feedback

Fine control of the hand in healthy humans requires the feedback of many of the sensations provided by the hand (proprioception, being able to sense the proper state like its joint angles (Antfolk et al., 2013)) and environment (exteroreception, being able to detect physical interactions with the environment (Antfolk et al., 2013)) as well as the ability to send information to the user in a quick and effective manner (Antfolk et al., 2013). Although a certain degree of grasp control is provided by visual and auditory feedback in prosthetics this is still an under developed area in most commercial devices and a big factor to the non-acceptance of ULP. Exteroreception includes environment (and object) information including texture, stiffness, weight, temperature, size, touch, pain, vibration and proprioception is the information fed back internally regarding the position and joint angles of the joints (digits/wrist). The main difficulty with replicating this is the complexity of this system in biological hands.

Feedback comes from somatic receptors subcutaneous/ cutaneous that include mechanoreceptors (plus muscle and skeletal mechanoreceptors) nociceptors and thermal receptors that encodes and transmits information about touch/force, proprioception, pain and temperature. This external information is what helps the user recognize and manipulate objects and avoid harm, reflex arcs and maneuvering around obstacles, and requires the use of closed-loop system using the feedback to make real-time adjustments to the hand movement ideally with minimal visual/ auditory input. This is possible in body powered devices to certain degree by the tension in the cables and the harness against the body meaning that myoelectric are more technologically advanced and at the same time less advanced than previous devices. The processes involved in sensing can be segmented into four distinct operations: sensing, transduction, decoding algorithm, encoding algorithm and actuating transduction (converting voltage to current). Humans can register tactile sensation in 14-28ms and this should be the upper limit achievable by an artificial device with faster processing being preferential (3-5ms) to allow for actuation time and a greater sense of embodiment of the device. Further to this continued stimulation without change leads to adaptation meaning that brain stops registering this sensation without great changes, to overcome this a discrete event stimulation could be adopted with different actions (touch/grip/lifting object etc.) send a stimulation signal to ensure that it is continuously registered by the user. A three-channel feedback system was proposed with visual/auditory – currently the main method of feedback using viewing, sound (touch – different fingers have different sounds/timbres, motor) and experience to regulate grip strength; device intrinsic – managing spillage with inbuilt sensors and an automatic subroutine (mimicking biological hand); somatic sensory – that transmits extero/proprioception information to the afferent PNS. The last aspect of the 3- channel system can deliver information either transcutaneous or directly to afferent nerves using implantable electrodes both requiring extensive training with the latter transmitting information as electrical current disregarding the form of sensory input (tactile, temperature etc.). Direct interface with the PNS has many advantages as it requires a less intense signal, in the order of one to two magnitudes lower (0.1-10nC) using cuff or longitudinal intra-fascicular electrodes that can restore all sensations (extero/proprioception) however current studies have resulted in an unnatural feeling that could be due to low selectivity and how the biological hand encodes the sensory information. The input information can come from a wide variety of sensors including (multimodal) tactile (Xu), force, temperature sensors and torque, strain gauges, some of

which is used to a certain extent in a few commercial devices already implementing device intrinsic feedback. Currently feedback is mainly delivered transcutaneous using either vibrotactile or electrotactile stimulation also known as sensory substitution where one modality is represented as another (i.e. stretching skin to relay information on position). The former method uses vibrations at different frequencies (10-500Hz) and amplitudes (0.07-14 m @ 200Hz) depending upon the electrode site and information being relayed with electrode arrays allowing for a certain degree of proprioception to be transmitted as well that can be embedded in the socket due to being small, unobtrusive and low-power consuming. This method also has a high compatibility with EMG and better acceptance than electrotactile as it improves user performance by increasing grip strength control and decreasing chance of errors during tasks. Electro tactile uses either current regulated that is not affected by impedance changes in tissue load or voltage regulated, that minimizes skin burns due to high current density, electrical stimulation of afferent nerves. However, this method interferes with EMG use if electrodes are too close and has been described as a tingle/itch to a sharp burning pain dependent upon simulation voltage, current waveform, and electrode size, material, location, hydration and thickness and contact force. Principal features of stimulation are amplitude (1-20mA), frequency (1Hz-5kHz), and waveform (mono/biphasic, rectangular/sinusoidal), and pulse frequency and duration with biphasic being more comfortable and consume less power than vibrotactile with no moving parts. Modality matched feedback is where sensory input is fed back as its respective input and exteroreception can be done theoretically using Pielter cells but proprioception has a higher complexity but Simpson put forward the idea of extended physiological proprioception where the human machine interfaces directly with the physiology of the body and different modalities have been developed by Weir et al. Gillespie et al., Goodwin et al.

Mechanotactile is a modality matched feedback where force sensed at the fingertip is delivered via pusher to the skin with its benefits of accuracy, precision, resolution, range and bandwidth but drawbacks include the slow speed, high energy consumption and miniaturization of the device (Liu, Yang, Jiang, & Fan, 2014; Belter, Segil, Dollar, & Weir, 2013 and Liu et al., 2016).
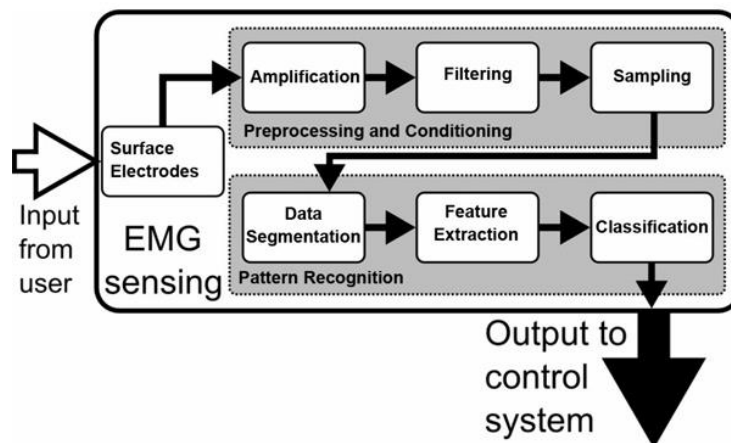
In a better word, two main ways of reproducing of sensory feedback are invasively or noninvasively. Sensory feedback is about joint position and grip force from an artificial arm could be provided to an amputee through stimulation of the severed peripheral nervous system or central nervous system. Also, motor command signals for controlling joint position and grip force could be obtained are recording motor neuron activity from these nerves (Dhillon, G. and Horch, K. 2005), on the other word rewiring the nerves that would connect to the limb (invasive way). Noninvasive sensory feedback feeds feedback to intact sensory systems to remaining limbs or structures. The sensation is provided away from the prosthetic, so the stimulus is felt somewhere other than directly on the prosthetic. In either case, the amputee must be trained to associate each stimulus with physical sensation (Antfolk et al., 2013).

It is important to have temporal delay lower than 300 ms to send information to nervous system, so it can make use of it in that moment. These short time frames for sending signals help the "brain develop a sense of embodiment (body ownership) of the prosthesis" (Shimade et al., 2009; Antfolk et al., 2013).

Chapter 3: Evolution of prosthetics

3.1 History

Prosthetics has been in use since approximately 900 BC (Clements, 2008) to replace missing body parts. The word is derived from the Greek word for "to apply, attach or add". They were initially made of wood or leather (Norton, 2007), although bronze limbs were also made as early as 300 BC. The first prosthetics, which incorporated the upper limb, were mentioned in 210 BC, but it took many centuries before they were used on a wider scale although Pliny the Elder wrote of a Roman scholar in the Second Punic War [218-210 BC] who had an iron prosthetic for his right hand.

The first use of an upper extremity prosthetic in its contemporary form was in 1536, when Ambrose Paré became responsible for the pioneering of the first prosthetics whose digits were individually controllable, using an array of levers and gears. Subsequent advances in prosthetics included the use of springs to help increase the realism of leg prosthetics. Prosthetics were regarded as cumbersome and uncomfortable until as late as the 20th century, as shown by this picture of a wood and leather prosthetic worn by a soldier who lost a limb in WW1, in Belgium, and on display in the Flanders Fields museum in Ypres (Figure 29) (Ott et al., 2002). Because of the enormous demand after the war when metals were expensive and difficult to obtain, the prosthetics were made of obtainable materials including legs of tables and chairs (Spector, 2014).
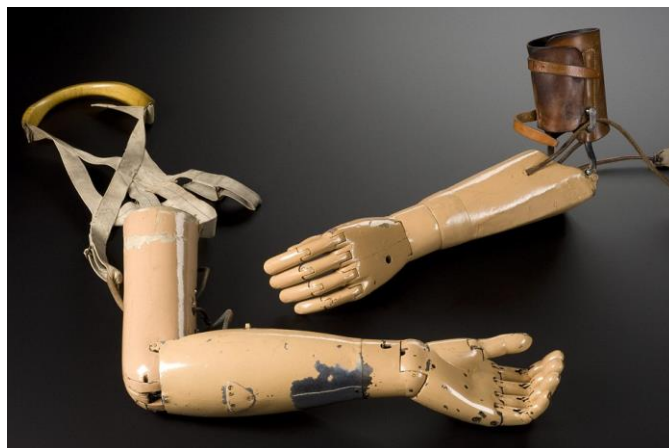
Figure 29: WWI era prosthetic

Lighter materials became more widely available and Duralumin was the first to be used as a prosthetic material in 1915. It was made of aluminum alloy which was much lighter

than wood, but its use was prohibitively expensive. Today the main materials used for prosthetics are plastic polymer laminates and reinforcement textiles (Uellendahl, 1998). These materials are highly durable and lightweight, and thermosets, which are particularly robust because they are able to form permanent bonds after single heating. However, most 3D printed materials are thermoplastics, which are not as robust, but are completely recyclable and reusable.

The potential need for upper limb prosthetics is very great. Today, there are over 20 million amputees (Szychowski et al., 2012). In 1996, the ratio of upper limb to lower limb amputations was 1:4 (in the USA at the time, 30% of amputations were in the upper limbs) (Davies et al., 1970) .The incidence of upper limb amputation due to trauma is increasing and the population of amputees in the USA alone is projected to double by 2050. However, the market for lower limb amputations decreased by 29% from 2000 to 2010 (Aofas.org, 2013) possibly due to better treatment of diabetes and improved treatment of infections and gangrene with antibiotics, both of which reduce the need for amputation. Elsewhere, particularly, but not exclusively, in LEDCs (Less Economically Developed Countries), the total has increased (ITV News, 2015) and by the end of the last decade, hospital costs associated with amputation were over $8 billion (£5.5 bn) in the USA (Amputee Coalition, 2016). It is a particular concern that only half the upper extremity amputees have actually been fitted with a prosthetic   (Florida Orthotics and Prosthetics Westcoast Brace & Limb, n.d.). There are 2 million hand amputees worldwide (Hu et al., 2013) the majority of whom, according to 'Open Prosthetics', an important firm for designing ready-made 3D-printed prosthetics, either have no arm, or have a hook, which is less expensive than a prosthetic, but much less efficient, with a very limited range of functional options available from it.

There is a particularly large demand for prosthetics in LEDCs in 2008, it was estimated 80% of arm amputees were in LEDCs, and 65% of these had their amputation to a wrist or below the elbow (LeBlanc, 2008). In the developing world, it is particularly important that an "easy to make" prosthetic can be used. In Sudan for example, over 50,000 people have arm amputations, often as a result of war, and many cannot afford complex prosthetics. EMG controlled methods are also becoming much cheaper and easier to use year on year. The most important recent case of prosthetic usage for an LEDC on a cheap, mass produced scale, is "*Not Impossible*" (Figure 30) set up by M. Ebeling et al in USA

and nominated for Design Museum's Design of the year 2015 (Ebeling and Kotek, 2014). It was the world's first 3D printing prosthetic lab, and Ebeling, after creating a successful prosthetic for a child with both arms amputated, developed a training program for local workers in additive manufacturing techniques, and set up 3D printing labs, which produce one arm per week. He describes it as being "an equivalent of the steam engine and printing press in terms of what it is going to do." This prosthetic limb is articulated, but not driven by EMG.

Figure 30: Project Daniel for upper limb prosthesis

Prosthetic upper limbs can be easy to model and produce in a simple form, but the complexities of producing efficient and effective function make development much more difficult. Techniques of manufacturing are becoming more specialized with the development of new materials that allow the prosthesis to be lighter and easier to use. Greater advances in engineering have meant that prosthetics can be more reliable and authentic but the enormously variable patterns of need amongst patients has meant that variable functions of the limb are necessary, and often have to be adjusted to the individual needs of the patient.

The brain's ability to send electricity to the muscles, making them contract was first discovered in 1664 by Croone (Open Bionics, 2016). EMG was discovered in 1771, when Galvani observed that electrical simulation results in force and contraction of the muscular tissue (Sudarsan and Sekaran, 2012), although similar voluntary muscle reactions had been recorded by Jan Swemmerdam stroking a frog a century earlier, to find out about the bioelectricity of its muscles (Camdir, 2015). Alessandro Volta invented devices to generate electricity and stimulate muscles (Medved, 2001) but electric

responses were not quantified until the 1920's when single motor unit potential was recorded, and EMG signals were tested in elephants by Forbes and his colleagues. The McGill University group in Canada, using a digital audio analogue correlation, created by Jasper in the early 1940's, popularized the first modern EMG machine. This was the Royal Canadian Army Medical Corps model, the world's first electromyography able to detect audio and visual records of electric activity using the electrodes (Kazamel et al., 2013). In addition, at that time, a widely accepted surface sensor was developed that was able to measure muscle activity associated with shoulder movement. Surface EMG was first used for diagnosis in 1948. Basmijian in 1963 demonstrated that the neuromuscular system could be trained using biofeedback techniques; this technique has been increasingly used. EMG used exclusively analogue signals on paper until 1973 and manual analysis was used for many years (Zachry, 2004). Subsequently, digital reading has been developed and the introduction of micro processing in 1983 allowed full computerization.

In 1998, needle studies from Chen et al (Boos and Aebi, 2008) showed the highest level of spontaneous activity at trigger points, which had previously been used in studies of feedback mechanics 20 years earlier. 85% of patients have active trigger point, which provide responses to a stimulus and have the highest levels of electrical activity (Ladegaard, 2002).

The first widely recorded use of an EMG driven prosthetic (Cram, 2003) occurred in World War 2, when a harness was designed to deliver movement to a mechanism on the back. When the use of Thalidomide sleeping pills saw 10,000 children born without limbs, only half of whom survived (Talbo, 2014),a skeleton was created to provide the replacement limbs. This skeleton was controlled by impulses sent by muscle sensors to hydraulically driven CO_2 canisters, which allowed its arms to move about. A disadvantage of the method (Figure 31), developed at the Princess Margret Rose hospital in Scotland, is that two CO_2 canisters need to be used every day, and can only be used by children older than 18 months. Survivors of acute polio have also used this system.
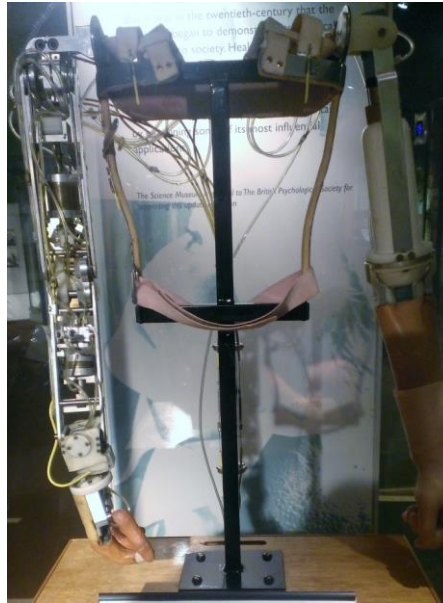
Figure 31: EMG driven prosthetic arm for thalidomide victims as seen in science museum

Much more recently, in 2014, Myography allowed a drummer who had his right hand amputated to be able to resume his career (Sciencemuseum.org.uk, n.d.), with the arm being controlled by programming which documented the movements he made before the loss of his limb, and it has been hoped that the methods used to drive it can be used for prosthetics in other high accuracy industries. More recently still 'Open Bionics' became the first British company to 3D print a prosthetic for a US soldier. The prosthetic has its electronics fitted into the palm of its hand, and residual muscles are covered with EMG sensors. It is described as merely being a "testing bed for new features" but it costs 1% of the cost of preceding prosthetic arms (Rutkin, 2014). 'Open Bionics' was awarded a Dyson prize for engineering innovation for its low cost, quick to manufacture designs (Open Bionics, 2015) have provided 3D printed prosthetics on a mass produced scale. The company has recently created branded prosthetics for children with designs based on popular films including 'Star Wars', 'Frozen' and 'Batman' with special effects pertaining to them. They have also been responsible for prosthetics worn by models (Kelion, 2015), which have above- the-elbow EMG electrodes to correspond to the movement, allowing the user to control it from her back.

3.2 Current commercial and Research Devices

Commercial
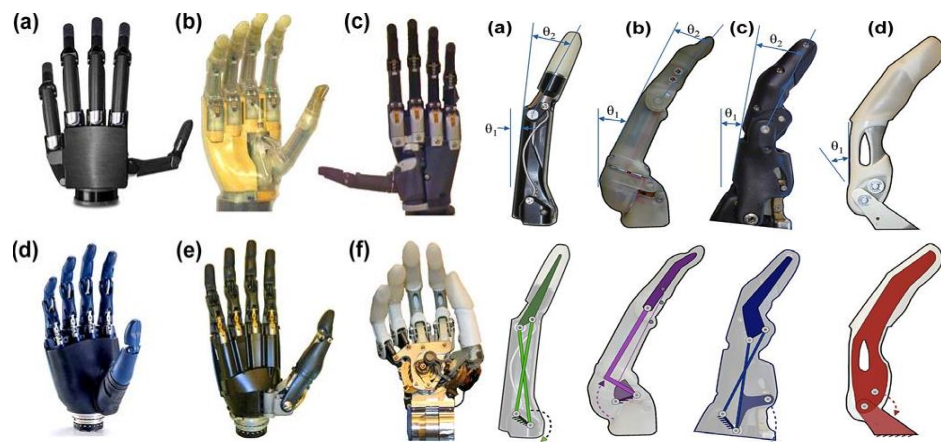
Figure 32: *Current Commercial devices on the left the Vincent*

(a), iLimb (b), iLimb Pluse (c), Bebionic (d), Bebionic V2 (e), Michelangelo hand (f) and on the right the finger segment coupling method of the four companies (Belter et al., 2013)

Current commercial devices as shown in figure 32 have many similarities in them inherit design due to the constraints of the device. Each company has slight modifications of their own coupling method of actuating the fingers though.

Table 4: Comparing joint actuation of existing prosthetics *(Belter et al., 2013)*

Hand	Developer	Weight (g)	Overall size (mm)	Number of joints	Degrees of freedom	Number of actuators	Actuation method	Joint coupling method	Adaptive grip
Sensorhand	Otto Bock	350-500	Glove sizes 7-8 ¼	2	1	1	DC motor	Fixed pinch	NO
Vincent hand	Vincent systems	-	-	11	6	6	DC motor-Worm Gear	Linkage spanning MCP to PIP	Yes
iLimb	Touch Bionics	450-615	180-182 long 75-80wide 35-41 thick	11	6	5	DC motor-Worm Gear	Tendon liking MCP to PIP	Yes
iLimb Plus	Touch Bionics	460-465	180-182 long 75-80wide 35-45 thick	11	6	5	DC motor-Worm Gear	Tendon liking MCP to PIP	Yes
Bebionic	RSL Steeper	496-539	198 long 90 wide 50 thick	11	6	5	DC Motor-Lead Screw	Linkage spanning MCP to PIP	Yes
Bebionic v2	RSL Steeper	496-539	190-200 long 84-92 wide 50 thick	11	6	5	DC Motor-Lead Screw	Linkage spanning MCP to PIP	Yes
Michelangelo	Otto Bock	~ 420	-	6	2	2	-	Cam design with links to all fingers	No

Hand	Grip Force (N)			Range of Motion						Grasp Type	
	Precision Grasp	Power Grasp	Lateral Pinch	MCP Joints	PIP Joints	DIP Joints	Thumb Flexion	Thumb Circumduction	Thumb Circumduction Axis	Finger/ Grasp Speed	Achievable
Sensorhand	NA	100	NA	0-70	NA	NA	0-70	NA	None	Up to mm/s at tip	Power
Vincent hand	-	-	-	0-90	0-100	NA	-	-	Parallel with wrist axis	-	Power, precision lateral, hook, finger-point
iLimb	10.8	-	17-19.6	0-90	0-90	~ 20	0-60	0-95	Parallel with wrist axis	200 mm/s	Power, precision lateral, hook, finger-point
iLimb Plus	-	136	-	0-90	0-90	~ 20	0-60	0-95	Parallel with wrist axis	1.2s (power grasp)	Power, precision lateral, hook, finger-point
Bebionic	34 (tripod)	75	15	0-90	10-90	~ 20	-	0-68	Parallel with wrist axis	1.9s (power grasp), 0.8 (tripod grasp), 1.5-1.7 s (key grasp)	Power, precision lateral, hook, finger-point
Bebionic v2	34 (tripod)	75	15	0-90	0-90	~ 20	-	0-68	Parallel with wrist axis	0.9s (power grasp), 0.4 (tripod grasp), 0.9s (key grasp)	Power, precision lateral, hook, finger-point
Michelangelo	70	NA	60	0-35	NA	NA	-	-	Compound axis	-	Opposition, lateral and neutral mode

Table 6: Finger flexion extension comparison *(Belter et al., 2013)*

Finger	Average speed ⁰/sec	Number of Trials	Standard Deviation
Vincent large (Ring, middle and index)	103.3	2	3.0
Vincent small (little)	87.9	2	5.1
iLimb large (mddle)	81.8	4	3.3
iLimb medium (index/ring)	95.3	2	3.4
iLimb small (little)	95.4	2	2.6
iLimb Plus (Thumb)	110.6	4	4.1
iLimb Plus large (index,middle)	60.5	4	1.8
iLimb Plus medium (ring)	74.3	4	2.8
iLimb Plus small (little)	82.2	4	4.0
Bebionic (Thumb)	36.6	16	7.7
Bebionic large (Ring, middle and index)	45.8	8	2.2
Bebionic small (little)	37.8	8	5.2
Bebionic v2 large (Ring, middle and index)	96.4	2	0.4
Michelangelo (index)	86.9	4	2.8

Table 7: Comparing the pinch grip force of existing prosthetic fingers *(Belter et al., 2013)*

Finger	Average speed °/sec	Number of Trials	Standard Deviation
Vincent large (Ring, middle and index)	4.82 or 8.44*	14 or 8*	0.8 or 1.3*
Vincent small (little)	3.00	2	0.1
iLimb large (mddle)	7.66	2	0.2
iLimb medium (index/ring)	5.39	4	0.1
iLimb small (little)	5.17	2	0.1
iLimb Pulse Medium (index)	4.15 or 6.54*	1	-
iLimb Pulse Large (middle)	3.09 or 6.24*	2 or 2*	0.7 or 0.4*
iLimb Pulse Medium (ring)	6.43 or 11.18*	2 or 2*	0 or 0.3*
iLimb Pulse small (little)	4.09 or 8.56*	2 or 2*	0.1 or 0*
Bebionic (index)	12.47	1	-
Bebionic (middle)	12.25	2	1.0
Bebionic (ring)	12.53	2	1.1
Bebionic Small (little)	16.11	2	0.2
Bebionic v2 Large (ring, middle, and index)	14.5	2	1.2

* Holding force after pulse mode.

Research

These devices often are focused upon a singular extremely specific aspect and thus will just be mentioned without any need for evaluation to illustrate the extent and variety of work currently being undertaken on upper limb prosthetic designs in comparison with the number of current commercial devices. Another increasing trend is to create open source designs that are for research purposes and not commercial with the hope that developments can happen at an increased rate with a better and wider communication and information-sharing network with many devices seeking to help amputees that cannot afford devices in developing countries.

Table 8: Comparisons of joint coupling on prosthetics developed by research *(Belter et al, 2013)*

Hand	Developer	Weight (g)	Overall size	Number of joints	Degrees of freedom	Number of actuators	Actuation method	Joint coupling method	Adaptive grip
TBM hand	University of Toronto	280	146mm long 65mm wide 25mm thick	15	6	1	DC motor with linear ball screw	Compliant springs	Yes
Remedi hand	University of Southampton	400	Similar to human hand	14	6	6	DC motor (Maxon)	Coupled MCP, DIP, PIP	No
RTR II	ARTS/Mitech laboratories (Pisa Italy)	350	-	9	9	2	DC motor	Tendon and free-spinning pulleys	Yes
MANUS - hand	Spain, Belgium, Israel	1200	-	9	3	2	Brushless DC motors	Fixed coupling of MCP, PIP and DIP	No
DLR/HIT I	DLR German Space Agency, Harbin Institute of Technology	2200	1.5 x human hand	17	13	13	Brushless DC motors with planetary drive	1:1 coupling of two distal flexion joints	No
DLR/HIT II	DLR German Space Agency	1500	Human hand size	20	15	15	Brushless DC motors with Harmonic drive	1:1 coupling of two distal flexion joints	No
UB hand 3	University of Bologna, Italy	-	Human hand size	18	15	16	HiTec Servos	PIP and DIP coupled in ring, little and thumb	No
UNB hand	University of New-Brunswick	-	7.5	10	5	3	DC motors (MicroMo 1724)	Fixed coupling of PIP to MCP	Yes
FluidHand III	Forschungszen-trum Karlsruhe GmbH (KIT)	400	Similar to human hand	8	8	1 pimp, 5 valves	Pressurized fluid	Distributed pressure	Yes
Smarthand	ARTS Laboratory, Pontedera Italy	520	12mm longer and 8mm thicker than 50% male	16	16	4	DC motor (faulhaber)	Tendon/spring based	Yes
Keio hand	Keio University, Yokohama, Japan	730	320mm length (with motor) 120 mm fingers	15	15	1	Ultrasonic Motor	Single tendon for each finger	Yes
Vanderbilt hand	Vanderbilt University	580	190mm long 330mm with motor 75mm thick	16	16	5	Brushed DC servomotors mounted in forearm	Single cable for each finger	Yes
LO/SH Southampton hand	University of Southampton	-	-	8	4	2	DC motors	Wiffle tree along finger	Yes

3.3 Invasive sensory feedback

Analysis of relevant literature shows there are various methods in which sensory feedback could be achieved, each having their own advantages and limitations. Invasive methods

such as targeted muscle reinnervation (TMR) and sensory regenerative peripheral nerve interface (sRPNI) use surgical implantation or modification to peripheral nerves to achieve feedback (Micera et al., 2010). The University of Chicago institution have developed a TMR interface and are offering its use to amputee patients who fall into a specified criterion (Chicago et al., 2013). The process involved surgical intervention to reassign nerves used to previously control limb movement to pectoral muscles in the chest. Although direct-neural stimulation technologies such as the ones proposed have shown to be an effective method in producing sensory feedback and in theory could be key in recovering all somatic sensory information, including tactility, temperature and proprioception, there are definite issues surrounding such procedures. These include technological limitations, for example, the lacking in ability to precisely stimulate afferent nerves, leading to inauthentic sensations (Johansson and Flanagan, 2009). Feasibility concerns, both in the cost to produce the neural interfaces as well as the surgical cost are also apparent. Amputee patients may also be reluctant in undergoing such invasive procedures, despite the potential benefits. Overall, direct-neural stimulation as a method of achieving sensory feedback is still far from being a viable solution at this moment in time.

Brain gate interface

Human brain has ability to process immeasurable amount of information. BrainGate's technology can help for a wide amount of this electrical activity data from the neurons in the brain to be transmitted to computers for analysis in real time with help of signal processing software algorithms that analyze the electrical activity of neurons and convert it into control signals, this technology can be used for several computer base application (Howard, 2015).

In 2008, US Defense Advanced Research Projects Agency's (DARPA) Revolutionary Prosthetics program implanted BrainGates into brains of monkeys, and wired it to robots arm, when monkeys was thinking about moving his own arm, his brain cells or neurons fire off electric signals the implanted sensors can pick up the signals send the comments to computer and robot arms, this way the monkey can control the robotic arm in three dimensions as well as griper (Telis, 2013). Within five years of this test, the team made a robotic hand with the same size and weight of average person hand with everything

inside, including computers and batteries. This hand can simulate everything a man can do with same strength. The 53 years old woman who was paralyzed as a result of genetic disease volunteered to connect this robot to her brain directly, two sensors was implanted in surface of her brain and sensors was wired to computer connections called pedestal. Five months of training after surgery needed for patient to control the arm with her thoughts as she was controlling her own. This way the team could restore the function for paralyzed patients. Next step, additional sensor added to previous one to restore the sensation. One of the problems with this method is, when the patient looks at the object directly, she cannot grab it, but as soon as the object removed, she can move the hand without the problem, the reason is still unknown. The infections, also the risks of brain surgery such as blood clot and death is major risk for patients (Orenstein, 2012).
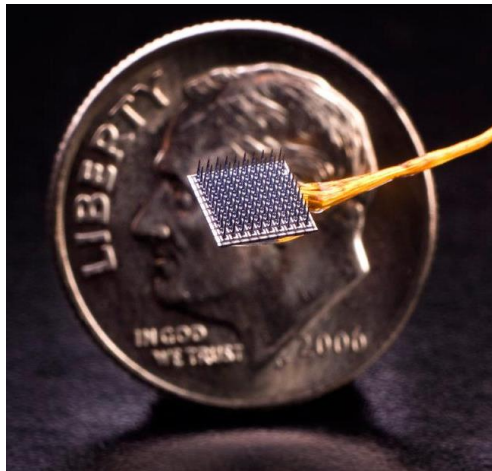
Figure 33: Electrode array, called BrainGate

Reads brain waves and sends them to a computer that translates them into commands (Orenstein, 2012)

Bionic arm with interface

In 2013, research at the Cleveland Veterans medical research centre (Gibbard, 2016) developed an interface that could develop various senses and feelings at over 20 spots in a prosthetic hand. The interface directly stimulates peripheral nerves, which are nerve bundles that exist in the arms of patients. The interface has a life of up to 18 months in spite of the degradations in performance that occur in electrical interfaces. In a test (Talbot, 2013), in which the prosthetic wearer was blindfolded and wears voice cancelling headphone, the interface allowed the force of the hand to be controlled, as it gripped with excessive force without the interface, crushing the cherries that were used as a test subject, whereas the interface allowed analysis of them. This was due to force detectors on the

digits that convey information to tiny nerve interfaces. Myoelectric interfaces are used to control the movement of the hand.

Figure 34: Bionic hands with interface

A cuff electrode is responsible for the control of the prosthetic. This electrode allows connection to the three nerve bundles in the arm (radial, median and ulnar), and holds them in "cuffs" that allows a larger surface area. They also avoid penetrating the protective layer of living cells, which can degrade signal and cause long term nerve damage.

Figure 35: A x-ray reveals the surgically implanted electro cuffs in forearm and the wires in upper arm that connect to an external computer (Tyler Lab/The Cleveland VA Medical Center)

3.4 Non-invasive sensory feedback solution

Adoption of the rubber hand illusion

Non-invasive techniques are also being implemented to achieve sensory feedback from prostheses. Studies undertaken in the application of the 'rubber hand illusion' have shown

promising results. The rubber hand illusion (Botvinick and Cohen, 1998) is a phenomenon that occurs when participants experience an illusory feeling of tactile sensory feedback from an artificial limb (rubber hand) when synchronous tactile stimuli are applied to the rubber hand and real hand of the participants simultaneously. The illusion occurs due to the brain interpreting conflicting visual-sensory information from the rubber hand with the tactile-sensory information from the skin of the real hand that is hidden from view. From a physiological standpoint, the process involves regions of the brain including premotor, parietal and cerebellar structures that correspond to multisensory processing. Further supporting the validity of phenomenon, is a study on the neural correlation of the rubber hand illusion, where researchers used a fMRI to show "for the first time that the same brain regions underlie ownership sensations of an artificial hand" (Schmalzl et al., 2013)
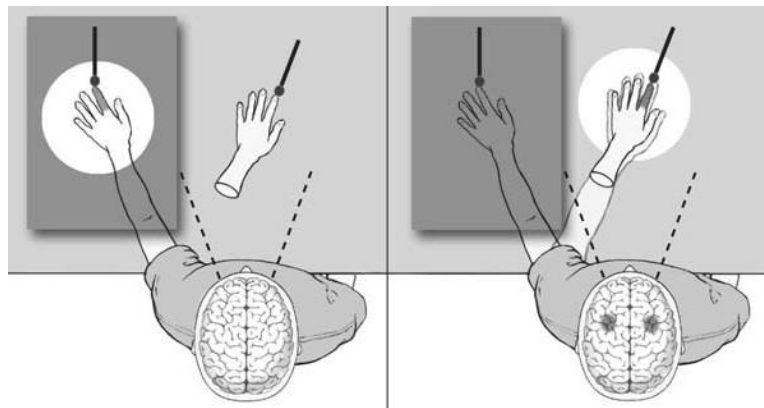
Figure 36: Schematic of the RHI.

Participant is in view of rubber hand only. After continuous stimulation, the illusion self-attribution towards the rubber hand is elicited (Orso, 2016)

In a study by Henrik Ehrsson -Department of Neuroscience Karolinska Institutet, Stockholm-, it was investigated if the methodology behind the RHI could successfully elicit a similar sensory illusion in 18 amputee patients (Ehrsson, 2008). In this study synchronous brushstrokes were applied to the skin of the participants' residual limb (i.e. the 'stump') along with the index finger of the rubber hand. In healthy participants the RHI would only occur if the same locations on the rubber and real hand are stimulated. However, Ehrsson hypothesized that stroking the stump of an amputee could produce the illusion. After amputation, the arise of substantial plasticity in the somatosensory cortex causing cortical zones representing body parts adjacent to the missing one to expand into this area (Yang et al., 1994 & Flor et al., 2006). Hence, by brushing the stump, tactile information reaches cortical tissue that used to process information from the missing

hand. This theory is also thought to be the cause behind the referred 'phantom limb' sensations often experienced by amputees. The experiment findings indeed show that tactile sensations were experienced local to the prosthetic hand of participants, rather than at the stump (i.e. proprioceptive drift had occurred). The results were obtained by both subjective means in the form of a questionnaire and also objective physiological measure of skin conductance test. Critical analysis of the literature shows that the illusion observed by the participants was much weaker than that observed in the traditional RHI. This is to be expected, given phantom sensations of the pre-existing hand experienced when touching the stump cannot fully-match the experience of feedback from a real hand. It is also imperative to note other factors such as the time since amputation also greatly affected the strength of the perceived illusion in the participants, as shown in the figure 37 (Ehrsson et al., 2008).
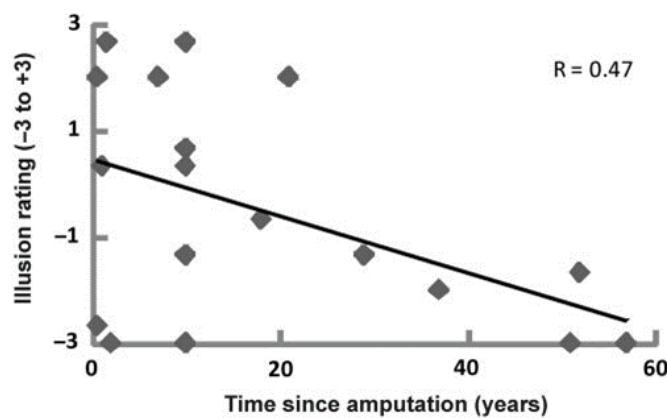
Figure 37: Graph obtained from Ehrsson's studys

Showing statical correlation between the time since amputation and vividness of the RHI induced in participants.

The study concluded that the process used could be adapted in the development of prostheses integrated with tactile stimulators on the stump region coupled with tactile sensors in the prostheses fingertips. The proposed device would likely incorporate mechanotactile stimulation techniques to produce modality-matched (i.e. the visual sensory input of touch on the prosthesis is felt as touch). The issue with incorporating modality-matched feedback use that the strategies required are subjected to technological limitation, (The BioRobotics Institute, Scuola Superiore Sant'Anna, Pontedera). Despite mechanotactile stimulation, devices being able to portray accurate haptic force feedback resembling the visual sensory input, current devices are heavy, power-consuming and expensive. An advanced haptic stimulator, with the ability to portray modality matched,

pressure, contact, vibration shear force, and temperature sensations currently in development (Kim et al., 2010) would unfortunately still extremely bulky and inconvenient for consumer use.

Closed-Looped control and timing aspect

In addition, to extend of time a user is exposed to the stimuli (as deemed by classical conditioning methods); the perception of timing of the sensory feedback is also of significant importance. A tactile stimulus in a healthy individual, reaches the cuneate nucleus within 14-28ms (Johansson and Flanagan, 2009). For an artificial sensory feedback system, e.g. one incorporating sensory substitution feedback, it recommended that this time is reduced even further (e.g. 3-5ms) (Antfolk et al., 2013). Thus, for sufficient sense of embodiment to be produced between the user and the prosthesis the latency between the sensory input and output stimulus must be kept to a minimal value as possible. The sensory feedback should also not be presented in continuous manner with little variation as this lead to stimulation adaption. As previously mentioned adoptive causes the feedback to become unrecognizable to user. This has been found to occur with prolonged exposure to electrotactile (further deliberate below) stimulation. Johnson and Edin (1993) suggested that stimulation should be provided in discrete sensory-event related fashion, i.e. when there is a sensory input present.

The implementation of closed-loop control in prostheses can be greatly beneficial for amputees, improving functionality and proprioception. Childress (1973) summarized the extent of sensory feedback in three pathway illustrated below in figure 38. 'Pathway A' is reliant on visual and auditory feedback, present in all body-powered and myoelectric prosthesis. 'Pathway B' demonstrate higher degree of feedback, with somatic signals producing a tactile sensory feedback using temperature, vibration etc. applied to skin of the residual limb (non-invasively) or directly the CNS (invasively). Finally 'Pathway C' incorporates closed-loop feedback in which sensors are imbedded in the prosthesis are used to automatically alter the response output intensity (e.g. the amount of force applied) to match the sensory input. In this way, the grip is automatically regulated. Pathway C would be the ideal mechanism to adopt as it is akin to control response in an unimpaired hand. In recent years, commercial hand prostheses have incorporated such sensors to automatically regulate functional grasping without the users effort.

Due to complexities of these sensors and programming capabilities required to implement them, this study opted on implementing the feedback mechanics of pathway B. Since the input stimulus does not vary for RHI experiments, active closed-loop feedback is not a requirement. It is of importance to note though, that stimulation intensities were altered depending on the stimulation condition.
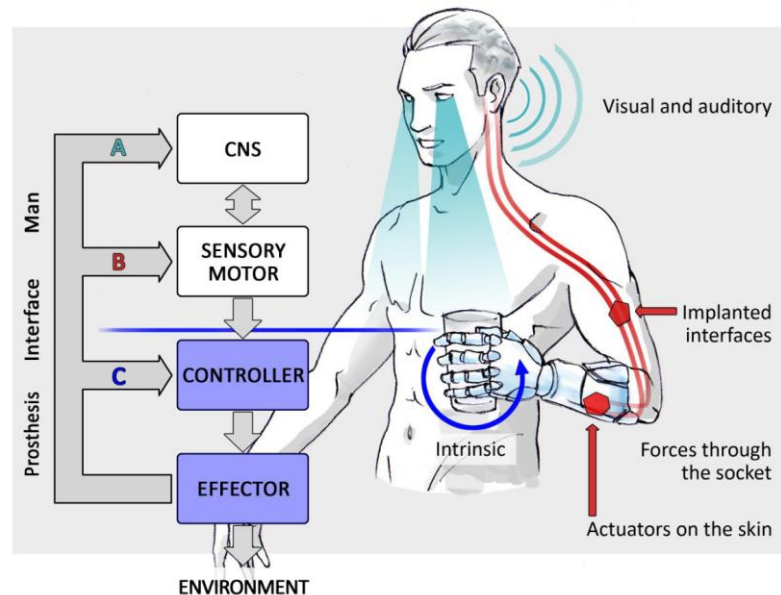
Figure 38: Demonstrating the three possible pathways of feedback in upper limb prosthesis control proposed by Childress (Antfolk et al., 2013)

Sensory substitution

An alternative non-invasive approach to provide tactile sensory feedback, also incorporating the RHI phenomena is using sensory substitution (modality-mismatched stimulation). Sensory substitution is a non-invasive technique in which sensory information from one form is substituted by a stimulus in a different sensory form (e.g. substituting physical contact with hearing) or in the same form but different modality (modality-mismatched stimulation, e.g. substituting the sensation of touch with vibration) (D'Alonzo and Cipriani, 2012). The two sensory substitution methods, which currently promote the best clinical viability in prosthesis use, are electrical surface stimulation (ESS) and mechanical surface stimulation (MSS).

The BioRobotics Institute (D'Alonzo and Cipriani, 2012), investigated the effectiveness of sensory-substitution devices in producing a sensory response similar to that elicited in the RHI experiment. This study specifically focused on mechanical surface stimulation (MSS), in which miniature vibratory motors were attached to the fingers of healthy participants, producing vibrio-tactile sensations on the skin when activated. In the classic

rubber-hand illusion experiment and also Erhsonn's modified versions of the experiment (Ehrsson, 2008), the visual-tactile stimuli were modality matched i.e. brushstrokes applied to the prosthesis and the corresponding real hand/stump in near perfect synchronous. Hence it was investigated if changing the output tactile stimulus on the skin to a different modality (vibrations) compared to the input visual stimulus (brushstrokes) would elicit a similar perceptual illusion and to what extent. The experiment conducted in a similar fashion to Ehrsonn's study with the three data measurements taken: questionnaire, proprioceptive drift test (pointing task), and skin conductance response (SCR) test. The key conditions that were investigated were: synchronous incongruent (modality-mismatched) brushstrokes and synchronous incongruent tapping which relates to grasping of an object.

The outcome of the study provided evidence that vibrio-tactile sensory substitution can indeed elicit a sensory illusion and sense of ownership akin to that perceived in the classical RHI experiment. The illusion was overall much stronger for the brushstroke condition than the tapping condition and there was no statistically relevant difference when compared asynchronous tapping. From the literature it was theorised that this may possibly be due the tapping action being quick, weak-pointed touch whereas brushstrokes on the skin provide a richer, longer-lasting sensory experience. Another, more anatomically hypothesis given for the weaker illusion in the tapping condition is regarding the stimulated nerve afferents. Tapping is mediated by quick-firing FA-*I* and SA-*I* mechatronic receptors whilst brushstrokes mainly evoke FA-*II* afferents that activate in a continuous fashion, proportional to the speed of the brushstroke (Vallbo and Johansson, 1984). FA-*II* receptors are known to respond to very high frequency vibrations which fall into the frequency range of the vibrio tactile stimulators used in this experiment. Therefore, both the vibrations and brushstrokes activate the same receptors, leading to a more vivid perceptual illusion. It was suggested that investigated lower frequency vibrators could help to enhance the illusion for the tapping condition and hence for functional grasping. Perhaps also, using other stimulation methods, such as electro-tactile stimulation (further discussed below) could produce different results.

Though successful in electing the RHI using modality-mismatched vibrotactile feedback, the study however found that the illusion induced in the participants was weaker additional RHI (Botvinick and Cohen, 1998) and similar studies. Even when modality -

matched feedback was used (brushstrokes applied to both rubber hand and real hand) the level proprioceptive drift towards the rubber hand was lower compared to prior studies. The proprioceptive drift is a measure of position at which the individual perceives the tactile stimulation relative to the real hand, hence the illusion is greater if the proprioceptive drift is larger. It was hypothesised the weaker illusion elicited in these experiments may due the shorter duration time of the tests (45 seconds per trial) compared to previous studies. The proprioceptive drift is proportional to the stimulation time as shown by Tsakiris and Haggard. Knowledge of classical/Pavlovian conditioning techniques, which play key significance in the RHI methodology, show that the time the stimulus is presented is crucial in eliciting a strong conditioned response.

It is important to note that the study above was undertaken on healthy participants and not amputees with referred phantom sensations. However, another investigation on sensory substitution feedback was undertaken by Pylatiuk (2006) whose study focused on development of a low-cost force feedback system for a myoelectric prosthesis. Five amputee patients were involved in this study which aimed to improve control over grasping force by means of closed-loop force feedback. It has been said that current myoelectric prostheses provide imprecise control to users, noting that grip force applied by the user is generally much greater than is required. The feedback system proposed here aimed to aid in improving the precision of the grasping force. The force was recorded by use of a hand dynamotor with different weights attached and it was investigated the force applied correlated with the weight increase. The force feedback system was incorporated into the prostheses and consisted of three main components:

- A force sensor connected to the palm of the prosthetic hand; used to measure pressure applied to the prosthesis
- A vibration motor attached to the skin of the residual limb to stimulate sensory feedback
- An integrated electronic circuit board which is used to connect the force sensor to the vibration motor, by converting resistances from the sensors to electric signals.
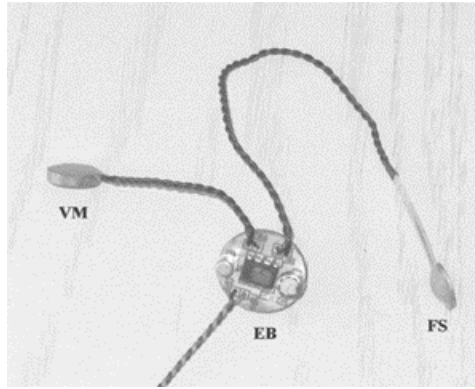
Figure 39: Feedback system

Consisting of a force sensor (FS), an electronic board (EB), and the vibration motor for stimulation (VM) (Pylatiuk et al., 2006)

One can give critical appraisal to the choice of these components because they are relatively low-cost and easily available, thus reproduction of similar feedback system is easily achievable. Results from the study showed that grasping force was significantly reduced when sensory feedback was applied (54% mean decrease across the participants). From the figure 40, it seen there is a clear distinction between the grip force applied compared to where no tactile feedback is presented and the highest linear correlation between force applied and object weight occurs when feedback was applied directly to the skin. Overall, this study has demonstrated that the implementation of sensory substitution feedback system is successful in providing more accurate prosthesis control in upper-limb amputees.
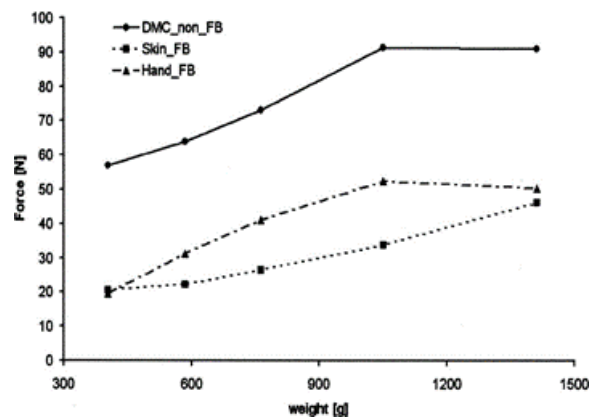
Figure 40: Results illustrate mean grasping force applied with and without feedback.

(Pylatiuk et al., 2006). Applied force is significantly less when feedback is in place

Comparison of sensory substitution technique

As stated earlier the two sensory substitution methods, which currently promote the best clinical viability in prosthesis use, are electrical surface stimulation (ESS) and mechanical surface stimulation (MSS). Discussed above were examples of MSS methods in the form

of modality-mismatched vibrotactile feedback. It has been demonstrated that this stimulation method can successfully elicit a sensory feedback response in amputees, similar to that in the classical RHI experiment. However, it is significant to compare different sensory substitution feedback techniques to determine the most practical system, considering design and performance.

Mechanical surface stimulation (MSS) – Vibrotactile feedback:

Vibrotactile stimulation device is likely the most viable method of sensory substitution feedback due to its compatibility with myoelectric control systems as well as having a greater psychological acceptance (Kaczmarek et al., 1991). As shown from analysis of the previous literature, such devices are low-cost and easily accessible (D'Alonzo and Cipriani, 2012 and Pylatiuk et al., 2006). Feedback involves high frequency vibrations to the skin surface that can range 10–500 Hz. Forces applied onto the prosthesis as well as the grasping force applied by the user can be distinguished in terms magnitude by varying the vibration intensity. A greater potential difference applied across the vibration motor, corresponds to a higher vibration frequency and amplitude. In this way, weaker forces/grip applied to the prosthesis correspond to lower vibration intensities, whereas with stronger forces the frequency is increased – hence a closed-loop feedback response can be executed.

Electrical surface stimulation (ESS) – Electrotactile feedback:

Electro-tactile (electro-cutaneous) stimulation involves the stimulation of afferent nerve endings within skin when a potential difference is applied between electrodes, emanating a local flow of current. Stimulation control over these devices is achieved by either regulating current or voltage. In current regulated ESS, the current is not affected by impedance between electrode-skin surfaces nor by variation in tissue density. Whereas using voltage-regulated devices reduces the chance of skin burns and irritation that can be associated with high current stimulation (Antfolk et al., 2013). A pulsating signal is used to avoid sensory adaption, which can occur when continuous application of the electrical signal causes the nervous system to become accustomed to the tactile feedback, and thus indistinguishable to the user (Guangzhi Wang et al., 2002). Conveying varying grip-strength or position is achieved through altering the 'intensity' of the tactile stimulus. This is accomplished through modulation of various signal parameters such as: amplitude, pulse rate or frequency modulation. Studies show that pulse rate modulation is less susceptible to response adaption; however, amplitude modulation (by means of

current variation) was better in conveying grip intensity (Kaczmarek et al., 1991). A considerable disadvantage of electrotactile stimulation is the interface that is sometimes caused with myoelectric prosthesis control. However, research has been undertaken to address this issue by using frequency-multiplexing techniques (Scott et al., 1980).

Table 9: MSS vs. ESS

Advantages (+) and disadvantages (-) of the leading two tactile sensory substitution techniques

MSS (Vibrotactile)	ESS (Electrotactile)
+ cost efficient	+ Low powered
+ Universal physiological acceptance (Kaczmarek et al., 1991)	+ Faster response time
+More comprehensive studies undertaken	+ Wide frequency range (from 1 Hz to 5 kHz) allows for more precise control
-Very limited range of stimulation intensity (10-500Hz)	- Prolonged stimulation is susceptible to response adaption
- Noise due to moving mechanical parts during vibration.	- Lack of comprehensive studies conducted possibly due to interface compatibility.
- Application of vibration motors to the skin is more cumbersome compared to electrode application which are also easily replaceable.	- The range of signal current between the detection threshold (1 mA) and pain threshold (2 mA) is narrow, and pain sensations are reported to be the major disadvantage of electrotactile stimulation.
	-Interference with myoelectric prosthesis control when the stimulation sites are close to the EMG electrodes; (Scott et al., 1980)

Constraints of the RHI

As shown, prior studies have gathered positive results in adapting the RHI methodology to sensory feedback mechanism in prostheses development. Returning to original notion of the rubber hand illusion, it is imperative to note the constraints surrounding the creation of this phenomenon and the factors that governs the strength of elicited sensory illusion. Altering different experiment variables including the prosthesis and the location of the applied stimulus to the skin, play the key role on the feedback responses. Studies shows that if the rubber hand/ prosthesis in an anatomically plausible position, like that of a real hand, then the illusion is diminished (Tsakiris and Haggard, 2005). This is proven also apply to amputees undergoing a modified version of the illusion when tactile stimulus is applied to the stump (Craik and Lockhart, 1972). The location at which the tactile

stimulus is applied to the skin also effects the illusion. From the study mentioned earlier conducted by BioRobotics Institute involving Vibrotactile stimulation on healthy individual, it was hypothesized that the weaker RHI experienced by participants in their experiments was because stimulation was applied to the inner side of the fingers (palms facing up), whereas in majority of previous studies the stimulus was applied to the no anterior side. It is suggested that the higher sensibility of fingertip compared to dorsal area of the finger makes it easier for participants to be aware of discrepancies between the visual-tactile stimuli.

3.5 Virtual sensation
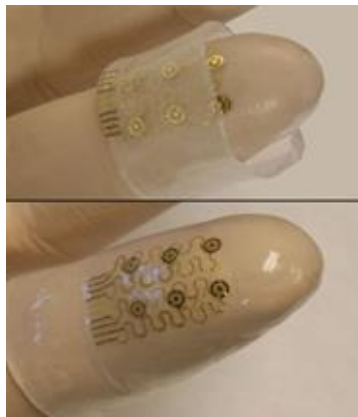
Figure 41: Electronic fingertips (Storr, 2012)

Electro tactile stimulation allows information to be presented through the skin as an artificial sensation of touch in the form of vibration or tingling. These feelings are created because cutaneous mechanoreceptors are excited due to passage of a modulated electrical current into the tissue. Feelings of motion or temperature can also be virtually produced. The device used to create this is flexible as it is made of silicone. This means it can conform to the fingers shape so the electronics in the tube are pressed in a natural, realistic way. The device relies on the action of capacitors. As the distance between the capacitor increases its value decreases. The distance is able to change due to flexible material the capacitor is mounted on. This change in capacitor value needs to be detected and related to a value of pressure in order to create a pressure sensor. As pressure increases the distance decreases and the capacitor value increases, so higher pressure can be correlated with higher capacitor value. The next step would be for this detection in pressure change to be converted into a value that can be interpreted by the brain (Nanowerk.com, 2012).

Chapter 4: Developed Design

In the following chapters, 4, 5 and 6, the first approach towards reaching the project goals will be described. The method that leads to results is explained. The results will be presented and in chapter 7 they will be analyzed and followed by a discussion about the methods benefits.

4.1 Choosing the replacement for touch

There are five basic senses in human and absence of each these senses can compromise the ones independent living. Basic senses are sight, hearing, smell, taste and touch; they are associating with sensing organs for sending information to brain to help with understanding and recognizing of the world.

As it mentioned before somatic sense is very important in human and especially amputee patients. Retrieving this sense can help the amputee to control the prosthetic better as it will help with feeling of ownership, and in this project focus is finding a way to manipulate the brain to understand sensation in other terms.

To attain the goal a device was designed to process the input as tactile perception and send output to brain to get feedback using other senses. From previous studies, it is already established that vision has a great impact on sensation as it can provide geometric information and pictures; however, this work is targeting both sighted and unsighted patients so the alternative should be applicable for either group. The initial idea was to use touch in a different form, like pressure or vibration. Both idea was studied and decided that they are unfit for this work due to their limitation.

Primary problem was identifying where the signal was coming from as touch was happening in skin, it is quite difficult and time consuming to train the brain to recognize the localization of the signals. Even though, human perception of vibration is between 0.04-500 Hz but they feel the vibration over 500 Hz more as textures. For pressure, it is largely depends on place of stimulation, the low threshold of body has higher resolution. Glabrous skin is generally more sensitive to vibration and pressure than hairy skin.

Moreover, perception of pressure will decreases as a function of age. Figure 42 shows the tactile perception for pressure and vibration:
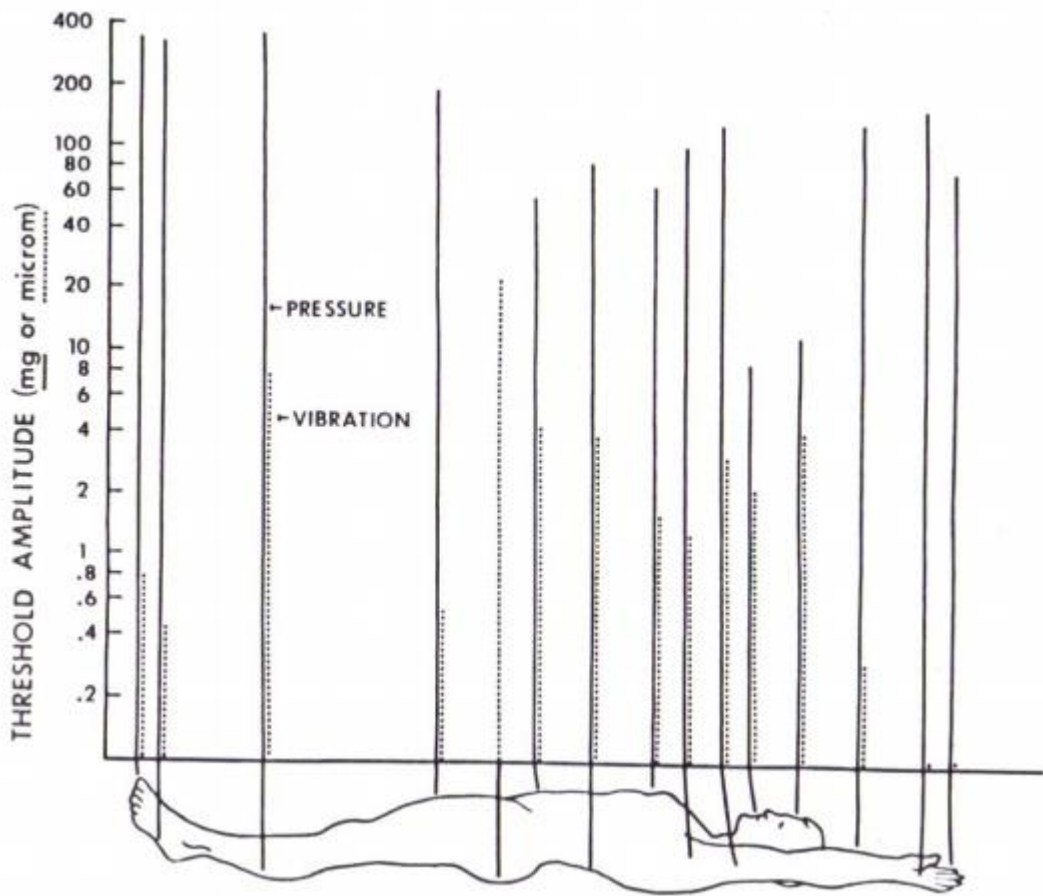
Figure 42: Tactile acuity for pressure and vibration (Rantala, n.d.)

The substitute chosen for final design was hearing, since human ear can hear noises in range of 12Hz to 28 kHz (in ideal lab condition), choosing a sound was a decent replacement. This device was used in healthy side of amputee to train the brain and store the memory of the feedback in patient's brain so it can react the same way when it is used on effected side.

4.2 Fabrication and testing sound generation system

Sound generation system (SGS) is equipped with an analogue temperature sensor with an accuracy of 0.5 °C and measuring the range of -55 to +150 °C, can create audio proportional to temperature, so that the frequency of sound produced depends on the temperature is measured. The acoustic signals generated connect to headphones or speakers by a 3.5 mm jack. Maximum power of output voice is up to 100 mW. The core of the system is ARM processor from family CORTEX-M4; it is a production of ST

Company. This Processor can process 168 million instructions per second, for this reason, test board was chosen from the same company. This board is power up with input USB that has embedded on the same board.

Selected board

STM324 DISCOVERY board, is one of the products of STMicroelectronics, to make this board work faster, STM32F407VGT6 chip used in its design also all the pins all moved outside the board. This board has built-in JTAG debugger called ST-Link will help accelerate the design process. Therefore, negate the need for an external debugger for planning and troubleshooting, it also has embedded digital microphone, two ST MEMS digital accelerometers, audio DAC with an integrated class D speaker driver, LEDs and push buttons and a USB OTG micro-AB connector (St.com, n.d.).

In Figure 44, components of this board are introduced and in Figure 45, PinOut for the STM32F4 Discovery Board is shown.
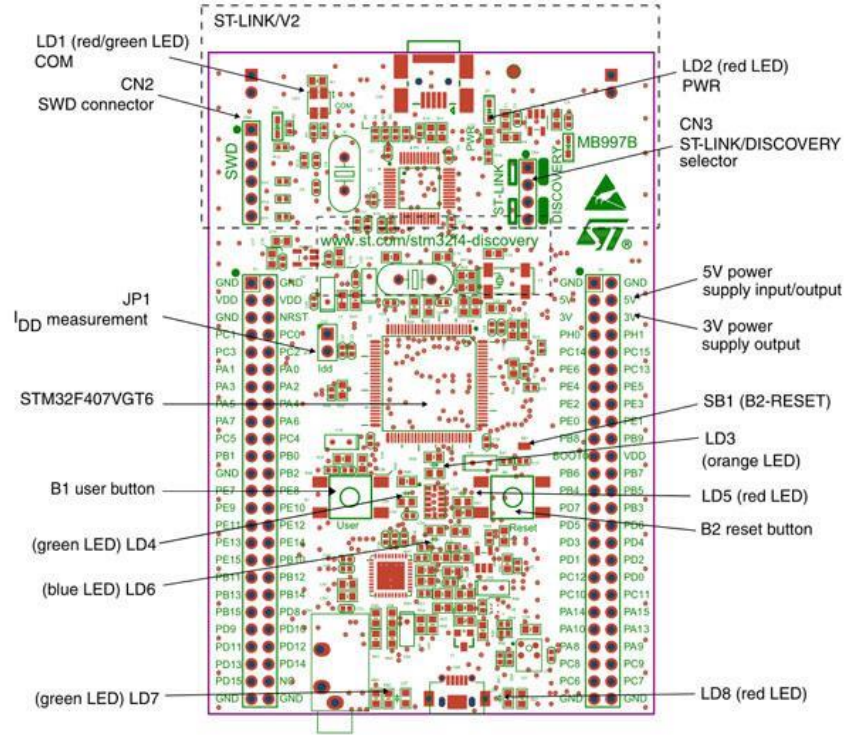
Figure 44: STM324 DISCOVERY board and its components (St.com, n.d.)
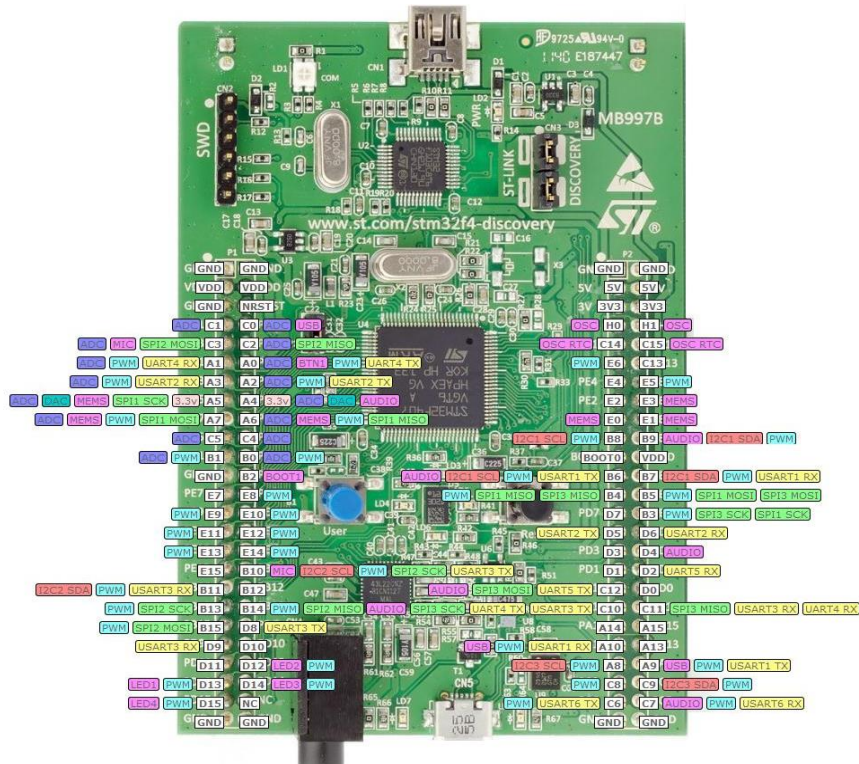
Figure 45: STM32F4 DISCOVERY pinout

Selected sensor

The LM35 is simple temperature sensor is accuracy integrated circuit (IC) with analogue output voltage (range between 4V-30V) proportional to the temperature in Celsius. This sensor can provide accuracies of $\pm 1/4\,°C$ at room temperature, and $\pm 3/4\,°C$ over a full range of temperature between $-55\,°C$ to $150\,°C$, without requiring any external calibration or trimming. The linear output is low impendence; exact fundamental adjustment of LM35 makes control circuitry and interfacing of readout easy. It has very low self-heating, less than 0.1°C in still air, as it draws only 60μA from the supply. The device is used with single power supplies, or with plus and minus supplies (LM35 Precision Centigrade Temperature Sensors, 2016). This micro-power circuit, like many others, has restricted capability to drive heavy capacitive loads and can drive 50 pF without special precautions.
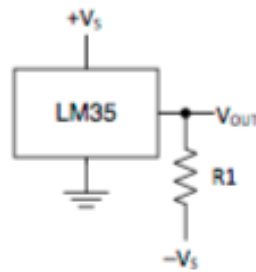
Figure 46: LM35 temperature sensor

$R_1 = -V_S / 50\ \mu A$

$V_{OUT} = 1500\ mV$ at $150\,°C$

$V_{OUT} = 250\ mV$ at $25\,°C$

$V_{OUT} = -550\ mV$ at $-55\,°C$
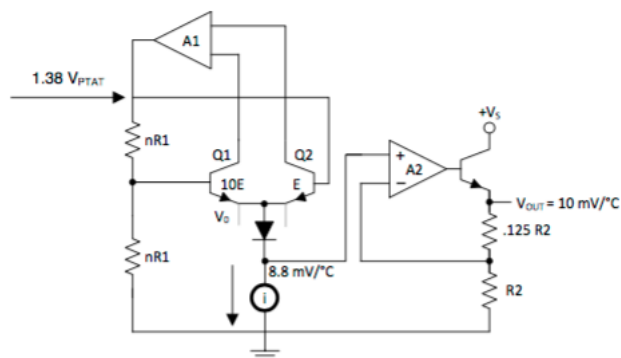
Figure 47: Functional block diagram

$V_{OUT} = 10\ mv/°C \times T$

Where

- V_{OUT} is the LM35 output voltage
- T is the temperature in °C

System components
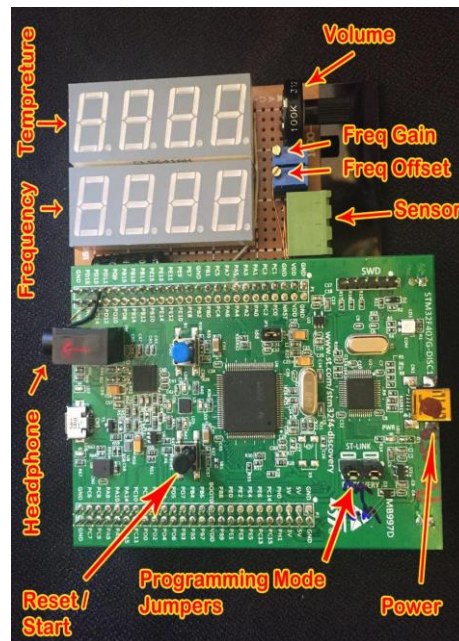
Figure 48: SGS components

Figure 48 shows the final design of sound generator system and arrows show the components of the system.

- **Power:** The embedded USB port on STM32F4DISCOVERY board, not only supply power to CPU, it also provides total power of the device including display and audio amplifier output, this USB input is the only one can power the device. Another USB input placed on the side of the output jack, this one cannot be used for powering this device.

- **Start/Reset bottom:** This key is used to start/reset the machine performance.

- **Headphone:** This is 3.5mm jack to connect the speaker, headphone or any other audio device. Maximum output power is 100mW and it uses MONO output.

- **Programming mode jumper:** If these two jumpers are connected, ST-Link Debugger is connected to the system, and the processor can be updated or troubleshooting. When using the system two jumpers need to be disconnected.

- **Volume:** It adjusts the intensity of the sound.

- **Frequency gain:** The potentiometer is used to adjust the output frequency to temperature. Gain-Frequency setting range is between 0.1Hz /^{0}C to 60Hz/^{0}C.

- **Frequency offset:** The potentiometer is used for adjusting the temperature attributed to the minimum frequency. By way of explanation, the minimum frequency can be generated by this system is 10 HZ and it defined by this potentiometer that in what

temperature this frequency is produced. The frequency offset adjustment range is between -50 to +50.

- **Sensor:** LM35 sensor connections port.
- **Temperature:** it displays the temperature read by the sensor at the time.
- **Frequency:** It displays the current frequency that is being produced.

When the value of potentiometers device is changing, temperature and frequency displays, temporary showing the setting values.

Schematic diagram
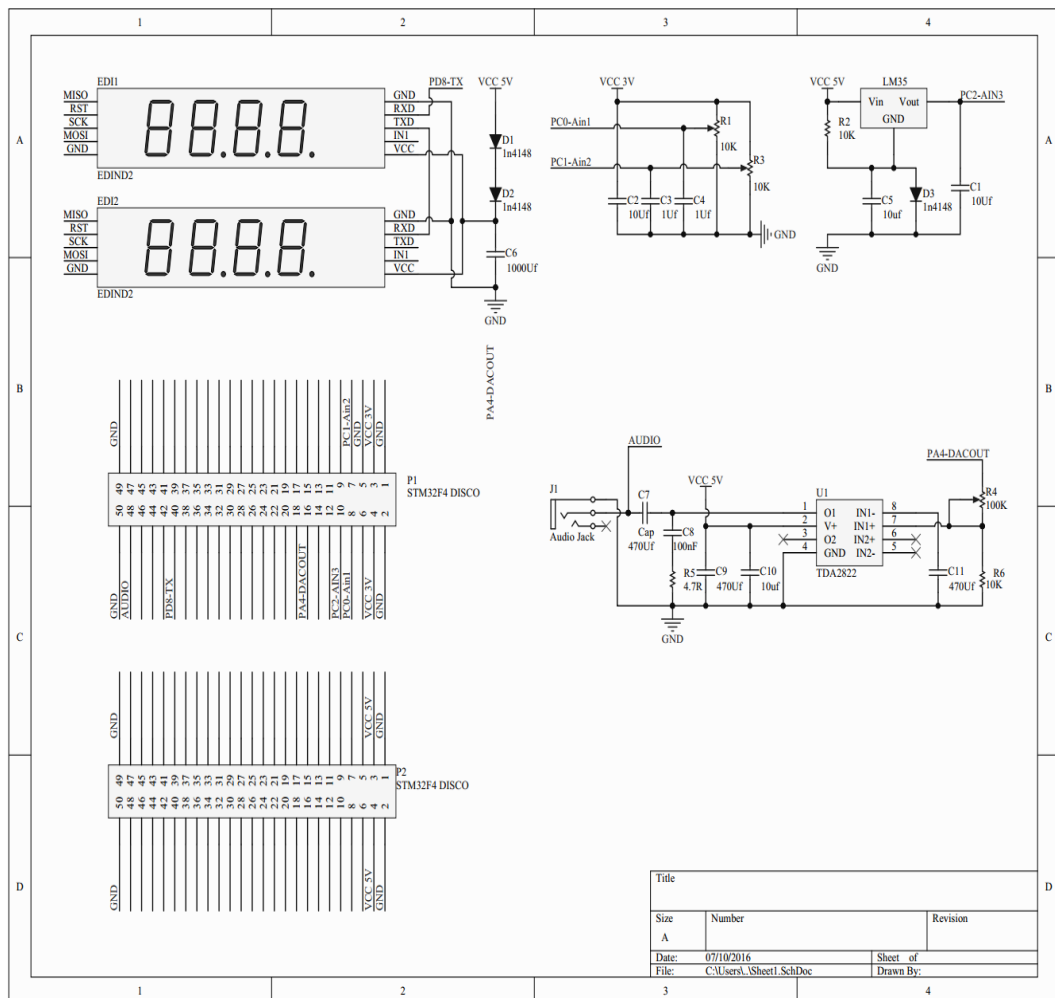
Figure 49: Schematic diagram of the system

Schematic diagram was designed using Altium designer/portal DXP software.

- P1 and P2 socket are consistent with the Board STM32F4 DISCOVERY.
- U1 is an amplifier, product of ST Company.
- EDI 1 and EDI 2 two numeric display module that receives data via serial port.
- R1 and R2 are potentiometers for adjusting the OFFSET and GAIN.
- R4 is the potentiometer to adjusting volume.

➕ J1 is audio output jack.

Software performance

Calculation of output frequency in accordance with input temperature

LM35 sensor output voltage and two potentiometers setting voltage have been connected to three analogue input pins of the STM32F407 processor. The processor will measure and calculate the average of these three inputs in real-time in 100,000 times per second. For this purpose, internal ADC microprocessor with 12-bit resolution has been used. Then, the measurement data is calibrated and placed in the original formula. The formula is as follows:

$$\text{Freq}_{OUT} = |\text{TEMP}_{avr} - \text{GAIN}_{avr}| * \text{OFFSET}_{avr} + 10$$

Equation 6: Output frequency

Moreover, values of TEMP$_{avr}$, GAIN$_{avr}$ and OFFSET$_{avr}$ are calculated with the following procedure:

$$\text{GAIN}_{avr} = \left(1 - \frac{\left(\sum_{k=0}^{400} (\text{ADC3DATA}_k - 4096)\right)}{400}/4096\right) * 60 + 0.1$$

Equation 7: Average gain

$$\text{OFFSET}_{avr} = \left(1 - \frac{\left(\sum_{k=0}^{400} (\text{ADC1DATA}_k - 4096)\right)}{400}/4096\right) * 100 - 50$$

Equation 8: Average offset

$$\text{TEMP}_{avr} = \left(\frac{\left(\sum_{k=0}^{400}(\text{ADC2DATA}_k - 4096)\right) - \left(\sum_{k=0}^{400}(\text{ADC4DATA}_k - 4096)\right) * 295}{400 * 4096}\right)$$

Equation 9: Average temperature

ADC4DATA and ADC1DATA values are converted 12-bit values from input analogue channels of 1 to 4 each. These values have been recorded in the memory RAM by DMA each time before the implementation of this formula. These values are collected at 100 thousand samples per second. Channel 1, is connected to the potentiometer for offset setting, channel 2 is attached to the LM35 sensor output, channel 3 is linked to GAIN setting potentiometer and to improve the accuracy of the measurement (differential measurement), channel 4 is connected to the negative line of the sensor.

Few examples of different frequency output proportional to the temperature input are shown below:
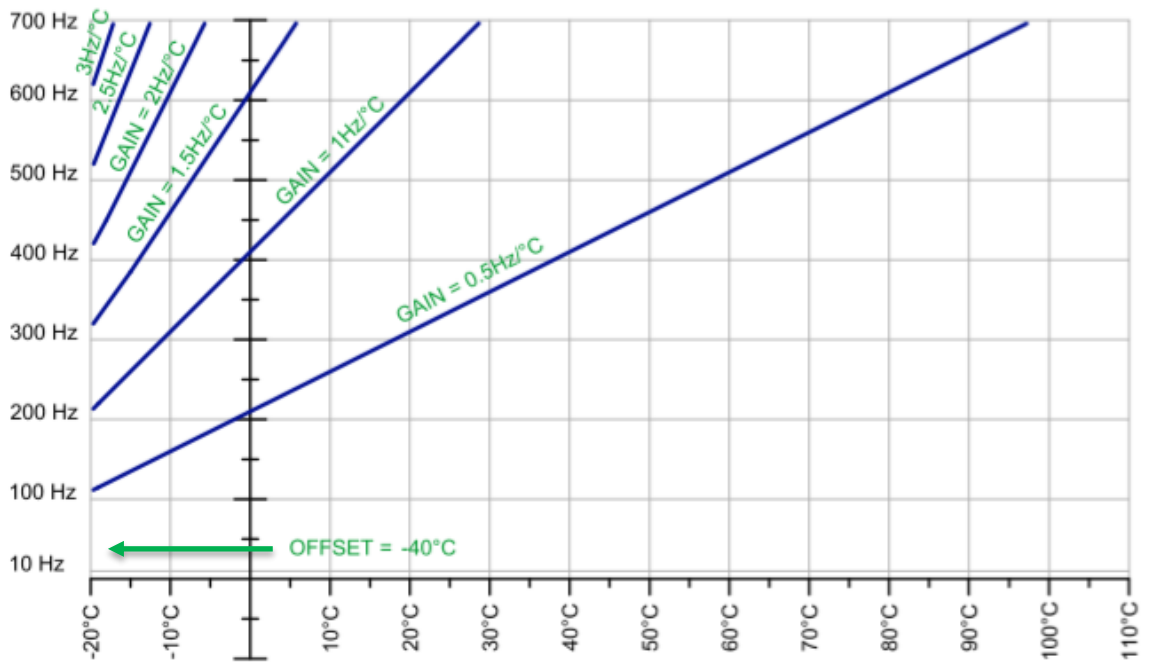
Figure 50: Gain range when offset is adjust to -40⁰C
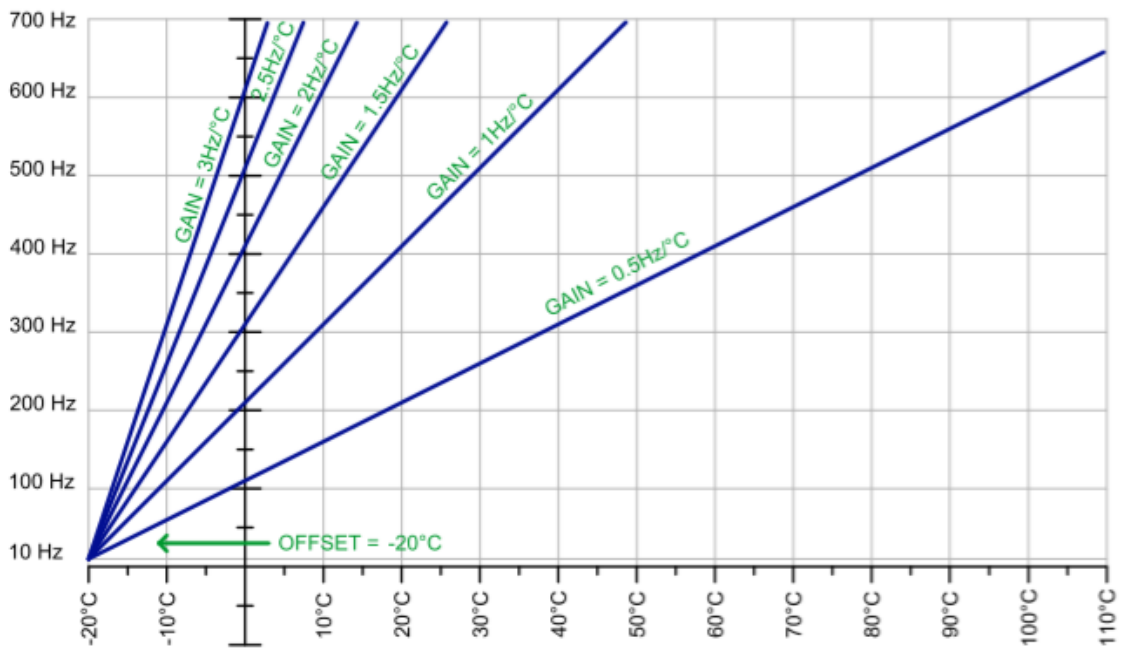
Figure 51: Gain range when offset is adjust to -20ºC
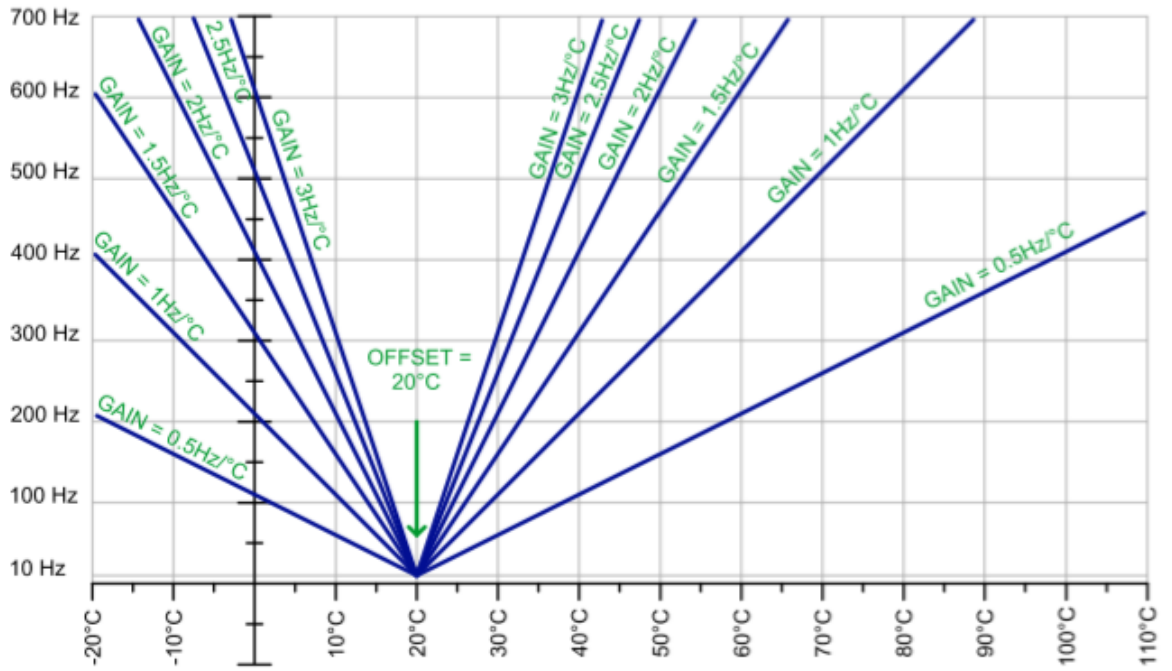
Figure 52: Gain range when offset is adjust to 20ºC
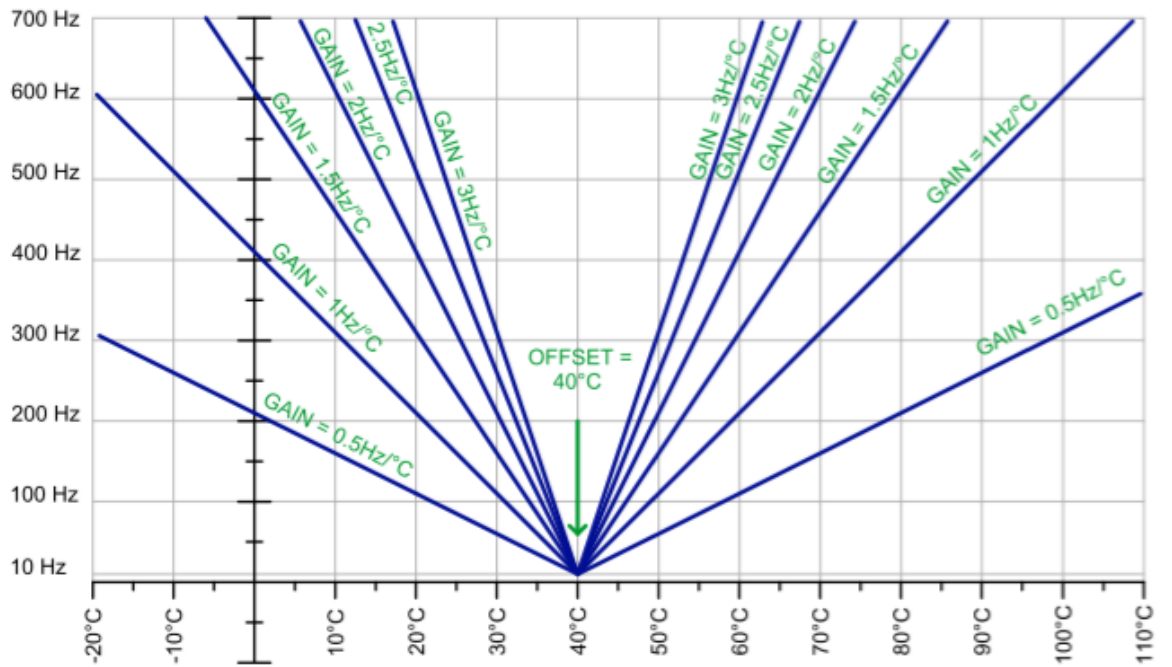
Figure 53: Gain range when offset is adjust to 40ºC

Create output frequency

To create the output frequency, a reference clock is used as well as TIMER6, DMA1_STR6_CH7 and DAC2. The output waveform is sine and flexible. For this purpose, after each change in frequency range 50 kHz to 200 kHz, one external trigger is created by TIMER6. DMA will pick up pre-built sin wave data from a table in RAM in form of synchronizing with timer 6, once activation happens and transferred them to DAC.

To have a better quality of sin wave, six separate lookup table has been used, each used for frequency range, 10Hz-100Hz, 100Hz-200Hz, 200Hz-400Hz, 400Hz-800Hz, 800Hz-1600Hz, 1600Hz-3200 and above Hz.

```
static uint16_t sine100[3205];
static uint16_t sine200[3205];
static uint16_t sine400[3205];
static uint16_t sine800[3205];
static uint16_t sine1600[3205];
static uint16_t sine3200[3205];
static uint16_t * sine=sine3200;
```

Figure 54: Lookup code

Six numbers of the will be computed after device is turn on for first the time.

```
double f=0;
int k;

for(f=0,k=0;f<6.2831853;f+=6.2831853/3200,k++)
    sine100[k]=(int)((sin(f*32)+1)*2000);
for(f=0,k=0;f<6.2831853;f+=6.2831853/3200,k++)
    sine200[k]=(int)((sin(f*16)+1)*2000);
for(f=0,k=0;f<6.2831853;f+=6.2831853/3200,k++)
    sine400[k]=(int)((sin(f*8)+1)*2000);
for(f=0,k=0;f<6.2831853;f+=6.2831853/3200,k++)
    sine800[k]=(int)((sin(f*4)+1)*2000);
for(f=0,k=0;f<6.2831853;f+=6.2831853/3200,k++)
    sine1600[k]=(int)((sin(f*2)+1)*2000);
for(f=0,k=0;f<6.2831853;f+=6.2831853/3200,k++)
    sine3200[k]=(int)((sin(f)+1)*2000);
```

Figure 55: Code to calculate sin wave value for the first time

Once the design of the device was completed and calculation was tested, the device was programmed using IAR embedded workbench ARM software. The full code for

programming the device is provided in **Appendix 2.** The code was tested and worked for this device and used to complete the experiments.

Figure 56: Testing SGS device

Device configuration

1. Connecting sensor to the system
2. Connecting headphone to the system (only one speaker will work if stereo headphones used also the system will not work if headset with microphone like mobile headphone used)
3. For power connection, USB to MiniUSB-B and mobile charger can be used.
4. By using small screwdriver change numbers in the potentiometer to reach favorable numbers. (The value of OFFSET, Volume and GAIN can be changed online)
5. By pressing the Reset / Start, system will start producing sound.

Chapter 5: Illusionary Experiments

This chapter describes the overall final system implementation. Some details are left for next chapters, 7 and 8, which were more relevant. Two set of experiments is to explore how the brain resolves conflicting multisensory evidence during perceptual interference.

5.1 Ethic statement

28 participants (aged 18- 57), SD ≈10.04 and μ≈28.61 , 7 right handed male, 7 left handed male, 7 right handed female and 7 left handed female took part in first set of experiments over course of six months, None had previously participated in a RHI study, and they were naïve as a requirement for the experiment. All contributors were recruited through word of mouth, were fully informed about the experimental procedure, and its potential risks and benefits and gave written consent prior to the beginning of the experiments. Participant demographics are found in Table 10. Both experiments and its recruitments procedure were reviewed and approved by Brunel University Institutional review board.

Table 10: Demography of participants

Subject number	Gender	Age	Left/right handed
1	F	23	R
2	F	26	R
3	F	26	R
4	F	57	R
5	F	32	R
6	F	41	R
7	F	22	R
8	M	23	R
9	M	23	R
10	M	22	R
11	M	26	R
12	M	33	R
13	M	21	R
14	M	30	R
15	F	21	L
16	F	48	L
17	F	25	L
18	F	30	L
19	F	30	L
20	F	26	L
21	F	29	L
22	M	35	L
23	M	26	L
24	M	28	L
25	M	24	L
26	M	29	L
27	M	24	L
28	M	21	L

5.2 Experiment one: Rubber hand illusion

Rubber hand illusion originally presented by Botvinick and Cohen in 1998. It involves plastic hand partially covered so it appears to be attached to volunteers' arms, real hand will be covered from the vision and in same position of artificial hand. By stroking real hand and artificial one simultaneously in same location, it feel like the sensation of stroking moves from real hand to artificial one.

Figure 57: RHI equipment

To capture brain activity and have better understanding of what is happening inside the brain ANT device was used during these illusionary experiments. The aim was to understand the level of interfering of vision with sensation and find a replacement for it. At the end of this series of experiments, participant was asked to complete the questionnaire (**Appendix 3**), which had mix statements related to feeling of ownership and sensations, these statements were adapted from existing questionnaire used in traditional RHI experiments (Botvinick and Cohen, 1998; Longo et al., 2008).

Seven consecutive experiments were conducted. All experiments involve similar settings and same equipment with minor changes. Each experiment was conducted once to avoid conditioning due to repetition rather than conditioning due to changes in experimental parameters, as one of the aims of the project is to determine the success of conditioning after modification of the experimental design. The subjects were asked to remove all rings and bracelets from their hands before the start of the experiment. This action was taken to keep the visual similarity with the rubber hand as accurate as possible. All subjects were allowed to make small changes in the posture of their arms on the table to make sure that they were sitting restfully and did not have to change their arms during

the experimental period. To measure the time, subjects would say stop as soon as they feel the rubber hand to stop the time.

The first experiment was the classical rubber hand illusion (RHI), in the second experiment the rubber hand was removed to see the effect of unobservable hand in the illusion, and then the opposite hand of participant was hidden from their sight to study whether the illusion will happen in reverse set up. For the same reasoning, set up number four was designed, in which participants was asked to turn their hand around. In experiment five, the box was removed and participant could see both of their hand and rubber hand while stroking was happening. The six experiment is the classical RHI but blindfolded the subject in order to study the effectiveness of the illusion with the absence of visual input. In final set up, moving hand, only one left-handed male participant was used for a month. The purpose was to determine the effect of time and distance in the illusion.
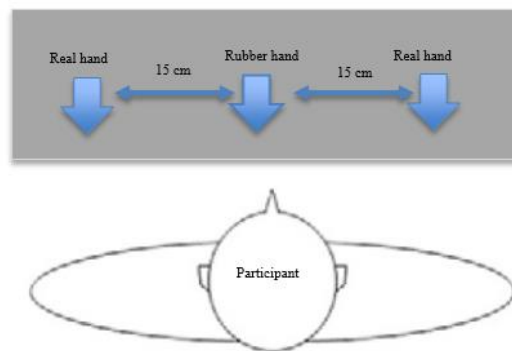
Figure 58: Dimensions of experimental set up

Each experiment is explained in detail in the following sections. All participants initially took part in the classical RHI experiment followed by six modified RHI experiments. In each experiment. The signals were processed and analysed using EEGLAB by MATLAB software, first by collecting the data, second pre-processing by filtering and remove the artefacts from the data. Last is post-processing by extracting the epochs and find the relevant graphs such as heat-maps, activity power spectrum and time-frequency component. In addition to EEG data, a questionnaire was administered to test the subjective experience of the participants after each experiment.

Classic

This is an experiment where a subject puts their hand in front of them nearby a realistic rubber hand, real hand will cover and put out of their sight and rubber hand is placed

where the volunteer can see it and then a series of touches are given to the rubber hand and real hand concurrently. The illusion works when the volunteer responds to threat applies to the rubber hand as if it were his/her own hand. To control brain activity, participants were asked to wear EEG headset, during this experiment. The sign of stress appears on software, which was used to map the brain when threat was applied to participants at the end of the experiment (Ferguson, 2011).

Figure 59: Classical RHI experiment setting

Invisible hand

Second experiment take place when real hand was hidden from participant's vision and in absence of rubber hand, real hand was stroke same time as empty space and EEG headset captured their brainwave. The illusion only appears if the stroking is the right size and direction of the real hand. In this experiment again, participant showed tension when they feel menace, which was captured in brain signal.

Figure 60: Invisible hand illusion experiments setting

Opposite hand

The hand opposite to rubber hand was used for this experiment. Same method as first two experiments was used. EEG headset captured brain signal during the experiments and again brain map was captured the sign of stress when threat was applied. For this experiment to see the illusion, period of stroking hands was longer than the first two experiments.

Figure 61: Opposite hand illusion experiment setting

Rotated hand

For this condition, volunteers was asked to rotate their hand and place it in a box out of their vision, rubber hand was place in front of participant in original condition and series of stroke and touches were applied simultaneously. It took longer than any other condition for illusion to appear for this set up.

Figure 62: Rotated hand illusion experiment setting

Conspicuous

In this experiment, volunteers was asked to place their hand next to the rubber hand, this time, real hand was not hidden from participant eyes and during stroke they could see

their hand and rubber hand at the same time, EEG headset captured the signals during the experiments and neural activity was obvious during the experiment.

Figure 63: Conspicuous hand illusion setting

Blindfolded

PLP in blind amputee is considered as unmanageable due to absence of visual input to the brain. PLP is a serious problem and greatly affects the quality of life of those affected. The aim of this experiment is to show that the presence of a prosthetic can be registered in the brain of blind limb amputees despite the loss of visual cues and that aids in the reduction of PLP

For this condition, participants were blindfolded and seated with their arms resting on a table and rubber hand was placed between participant's hands. Plastic gloves were used on both real hand and fake hand to make tactile surface as similar as possible. Rubber hand was stroke by participant left hand while right hand of participant was stroke by experimenter. Headset was used all time to check the effect of self-touch.

Figure 64: Blindfolded RHI setting

Moving Hand

This set up concentrates on the time influence on illusion, it also investigate the effect of vertical position on the illusion. For this reason, one of the participant was asked to return to the lab for seven days, with two days break, he returned to the lab for four continues days and again six continues days with three days break. A box with three different height (level to real hand, 4cm and 7cm above the real hand) was provided and classical RHI was repeated in three different position.

Figure 65: Moving hand position

5.3 Experiment three: Temperature illusion

During past two experiments, it established that vision has great interfere with sensation, the question is can visionary illusion bring back sensation to amputee patients?

Figure 66: Sound generator systems

Using the result for past two experiments, a device was designed and developed. The fabrication of this device was explained in previous chapter. Since the illusion will last only few second after the tests, classical conditioning was applied for this experiment to find out if there is a way to make illusion last longer or even permanent. Four subjects participated in this experiment over a course of one month. ANT headset was used to

control the brain activity during this time and after the final attempt questionnaire provided in **Appendix 4** was answered.

The subject was seated in comfortable chair with both hand and arm place in front of them. To start experiment, participant had to wear headphone, objects with different temperate (0^{0C}, 25^{0C}, 40^{0C}.) was applied to system and subject at same time, since the device will provide different audio for different temperature applying to it, a person could use vision, tactile and voice to identify different object. After 5-10 minutes, the experiment was repeated while the subject was blindfolded and in third attempted the objects was applied only on device. The purpose of this experiment is to determine if adding auditory input will consolidate the illusion, and to condition.

Figure 67: SGS experiment setting

Chapter 6:EEG Signal Processing

This chapter explains all the key information about concepts, theories and models needs for EEG signal processing and software used.

6.1 ANT neuro device

To capture brain activity and have better understanding of what is happening inside the brain, ANT device (figure 68) was used during these illusionary experiments.
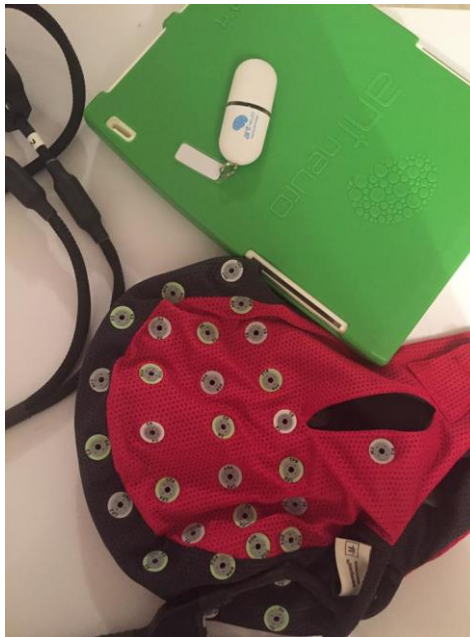
Figure 68: ANT neuron EEG headset

ANT Neuro is a cooperative technology company producing BCIs including EEG equipment involving Neuroheadsets and Software for medical and research purposes. The company was established in 1997 in University of Twente, Enschede, Netherlands.

The eego™ sports neuroheadset with research grade 64 Channel Mobile EEG as shown in Figure 69 was used for this study. This e-device is designed for cognitive neuroscience studies and advanced brain control interface (BCI) operations. Eego comes with post-processing software application, which is intuitive workflow steps, was used to process recorded signals. Recordings are stored in a server database called an MS-SQL, which allows access to user and archived through standardized interfaces.

ANT (Advanced Neuron Technology) is medical EEG headset and it is composed of high density WaveGuard cap system with 64 electrons with shielded wires and corresponding full-band DC amplifier that can reach a sampling rate of 2048 Hz. Electrons are positioned and categorised with respect to the international 10-20 system as mentioned previously in chapter 2 Based on the universal system (Ant-neuro.com, n.d.). The specification of the amplifier is presented in table

Figure 69: Waveguard 64 channel EEG cap
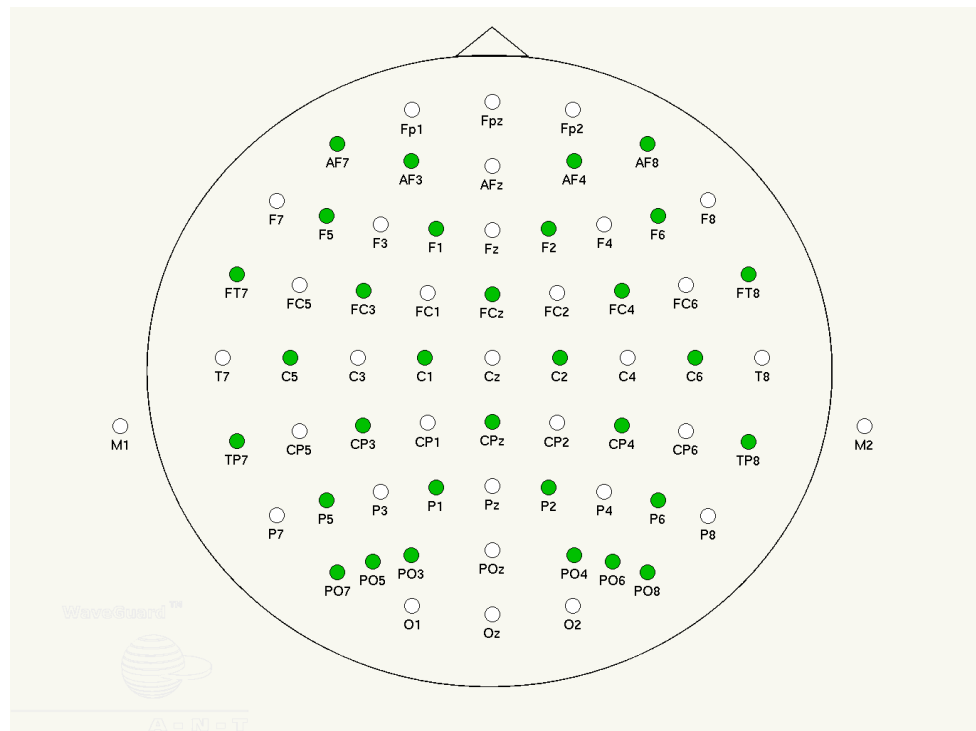
Figure 70: Illustration of the electrode position on the scalp

Dimensions (w x d x h)	160 x 205 x 22 mm
Weight	< 500 gram
Number of referential channels	32, 64
Number of bipolar channels	24 (pro version only)
Noise	< 1.0 uV rms
Referential input signal range	150 -1000 mV pp
Input Impedance	> 1GOhm
CMRR	> 100 dB
Max. sampling rate	2048 Hz
Resolution	24 bit
Bandwidth	DC (0Hz) – 0.26* Sampling Frequency
Trigger input	8-bit TTL
USB interface	USB 2, electrically separated
Battery	Integrated
Operation time	Up to 5 hrs

Preparing eego™ software

EEGo setup begins with adjusting the waveguard cap on participants scalp by measuring their head to choose a right size cap, if the cap is too big, the connection between the electrodes and the head will be compromised and if the cap is too small, the shielded wires inside the cap will be damaged. The position of the electrodes needs to be checked once the cap is on: the vertex electrodes, CZ, is position where the point at halfway between Nasion and Inion and the point at halfway between two pre-Auricular meets.
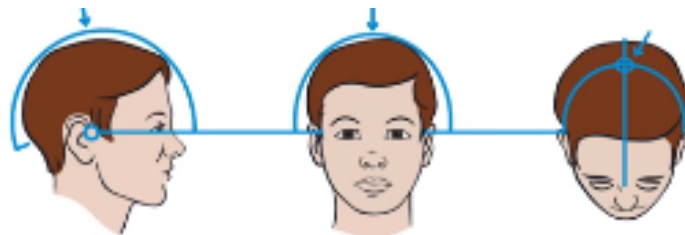
Figure 71: CZ position

The frontal electrodes FP1, FPz and FP2 is positioned 10% of the distance between Nasion and Inion and above the Nasion point.
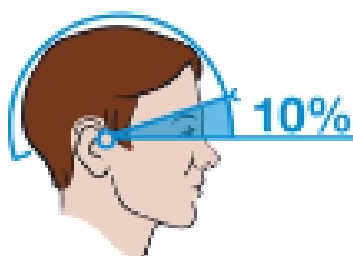
Figure 72: Frontal electrodes positions

Second step is connecting the cap to the amplifier and applying gel by dedicating syringes into the electrodes with circular movement to make excellent interaction with the brain. The connection of the amplifier and electrodes will be checked automatically.

Figure 73: Gel and syringes

6.2 EEGLAB MATLAB

EEGLAB software analysis used to investigate the recorded neurological signals, which allow interpretation of data channel positions, component information, and importing files in the form of EDF (Pfurtscheller et al., 2000).

In this project, MATLAB toolbox EEGLAB was utilised for signal processing analysis. Plotting relevant figures and graphs. The MATLAB version used in this project is MATLAB 6.1 along with Linux, EEGLAB keeps running on MATLAB versions 6 (R13) and 7 (R14) along with Linux or Unix, Windows (Delorme et al., 2006).

The EEGo [sport] neuro software uses RIFF-format to record and write brain signals, which can compile with the EEGLAB. In processing, recorded brain data was processed, and features were extracted. The process of cleaning the raw EEG data was conducted by

removing noise and artefacts using FIR filter, then Automatic Artefact Rejection (AAR), as well as Blind Source Separation (BSS), was implemented to the data, and lastly decomposing the data by running ICA. Then conducting post-processing extracting epochs and time and frequency domain features.

6.3 Data collection

EEG signal quality and accuracy of detecting the results mainly depends on proper placement and connection of the electrons on the cap. Eego™ software detect the connection of the electrode, amplifier and status automatically for all channels both prior to recording and when it is finished. Connection quality shown in figure 74 below:
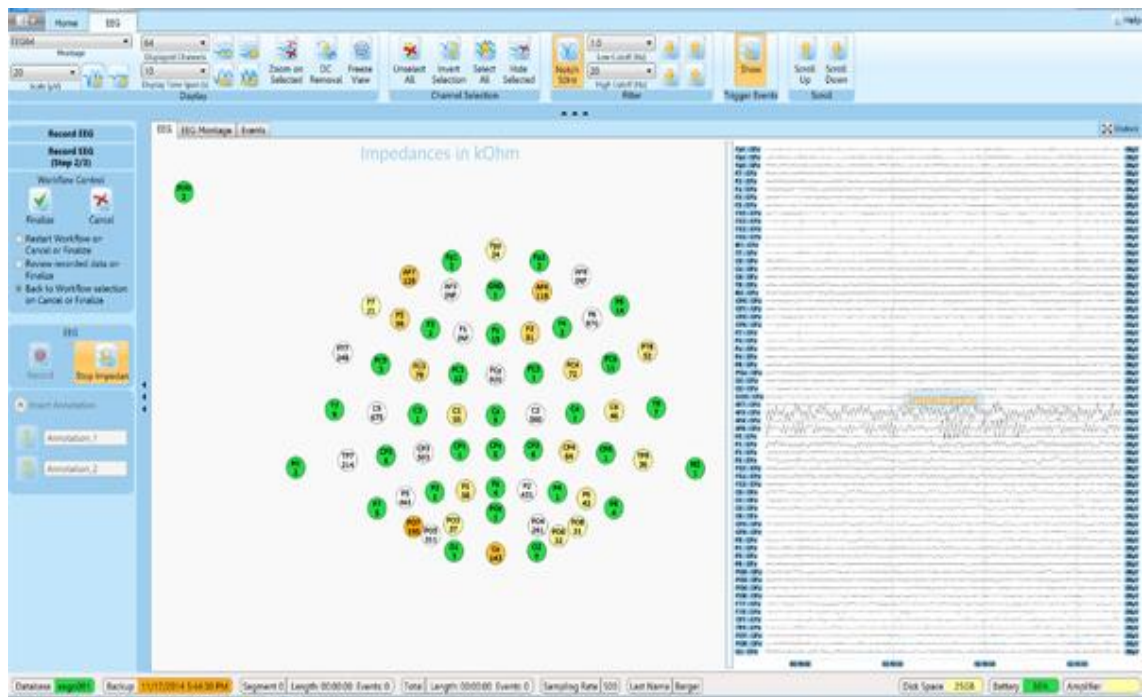
Figure 74: automatic electrode impedance-checking feature

Once the new recording is activated, the EEG panel section displays a sequence of oscillation graphs, representing the several channels' recognition of a subject's brain signals. The top graph shows particular brainwave signals; the signals will alternate concerning subject's experience. The graph shows Marker measures, and it is used when the experimenter needs to register significant signal periods to analyse.

Neural activity is recorded in the EEG Suite and displayed as real-time fluctuations of neural activity for the period of the experiment EEG displays brainwave signals of 64

channels. Here, channels are located in the left and right hemisphere of the brain were selected for analysis. A reference of the channels locations with the corresponding channel components is demonstrated in the Results chapter.
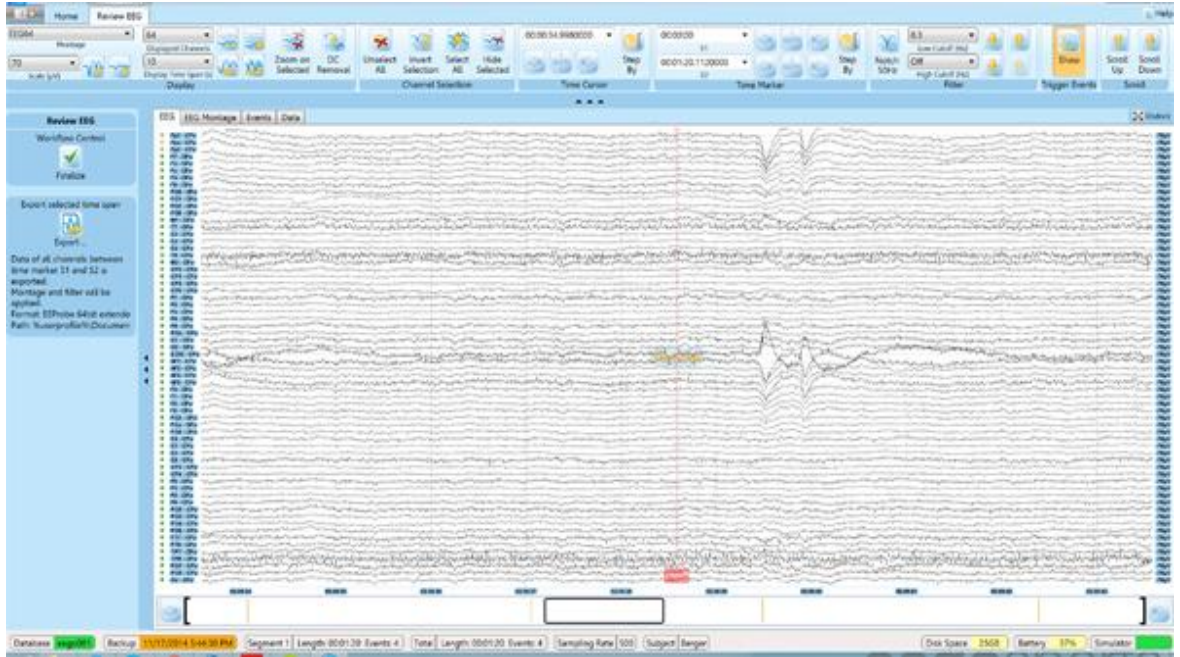
Figure 75: Software recording interface demonstrating EEG signal channel and recording in real time

Recordings are stored in a MS-SQL server database, which are compatible with EEGlab and can import in various versions, and those files are then imported into EEGLAB for signal processing (Figure 76). After selecting the relevant CNT file, the desired channel coordinates are loaded using predefined coding parameters. The files are now ready for signal processing in EEGLAB MATLAB. The theoretical part of EEG Signal processing analysis has been explained thoroughly in pervious chapters. Practically, the method used in this project to analyse the EEG data by using EEGLAB and MATLAB.

Table 12: Chosen channel for analysis

FP1	AF3	AF7	F3	F5	F7	FC3	FC5	FT7
FP2	AF4	AF8	F4	F6	F8	FC4	FC6	FT8
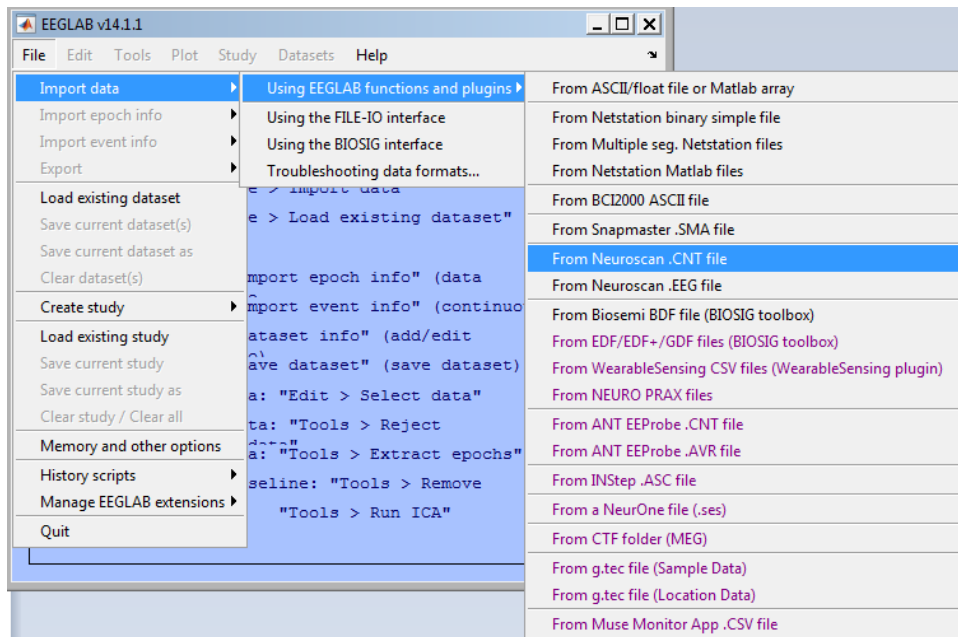
Figure 76: importing EDF files

The steps for importing CNT file by EEGLAB MATLAB (Delorme et al., 2006)

6.4 Pre-processing

Artefact elimination and FIR filtering

Basic FIR Filter, a band-pass filter, was initially used to eliminate any linearity trends in the data. This filtering step is important to clean the continuous EEG signals, before artefact elimination or epoching. The cut-off frequency limits in this project were set as 35 Hz for the upper cut-off frequency, and Lower cut-off frequency was 0.5 Hz.
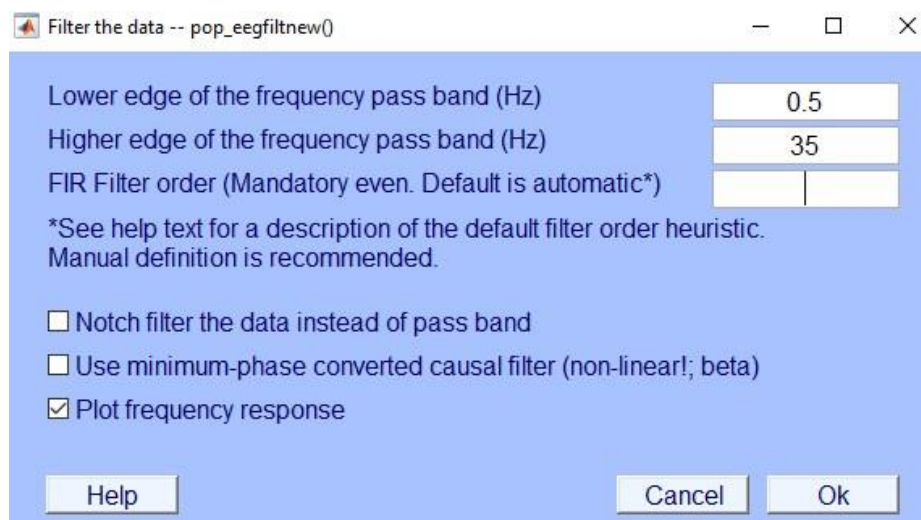
Figure 77: Print screen of applied FIR

Filter the data by using EEGLAB and MATLAB by specifying the upper and the cut-off frequencies in Hz as shown in the first two upper boxes.

Next, artefact removal was carried out using AAR and BSS to stop Electrooculography signal (EOG) spikes. The data is now ready to be decomposed by running ICA. Finally, baseline signals caused by poor contact of the electrodes, perspiration of the subject under the electrodes which may affect the electrode impedance and cause low-frequency artefacts, differences in temperature and damages in the equipment and amplifiers are removed. Baseline signals are undesirable and have to be eliminated prior to any signal post-processing, for appropriate investigation of the EEG signal.

6.5 Post-processing

Extracting Epoch and ERP

As specified in chapter 2, in EEG signals beta (13-30Hz) wave is a specific wave of interest in this project since the decrease of this wave is associated with illusion occurrence. EOG artefacts (blinking and eye movement) mostly appear beneath 4Hz, whereas ECG artefacts appear at 1.2Hz, and EMG (muscular extraction) artefacts appear over 30Hz. No human artefacts or noise regularly appear over 50Hz (Coburn & Moreno, 1988; Fatourechi et al., 2007). For this project the channels that located in frontal lobe of left and right hemisphere was selected. Based on their location in frontal lobe, they are the best exploring beta wave frequency patterns. Frontal lobe assumes an essential part in feeling and alertness experience. Likewise, the channels located in the frontal central area to detect the alertness once it usually starts on both or one side area of the brain and spreads toward to the frontal.

FFT post-processing was applied to extract beta wave frequency signals. Components heat maps and activity power spectrum plots were then generated. Following epochs and events can be imported in many formats where in this project epochs were extracted using event information from data channel.

FFT, time-frequency analysis with the changes event-related spectral power (ERSP) plot were produced. Sample of MATLAB code used to generate activity power spectrum plots is shown in Figure 78.

```
% Create surface
surface('Parent',axes1,'FaceColor','interp','EdgeColor','none',...
    'CData',CData1,...
    'ZData',ZData1,...
    'YData',YData1,...
    'XData',XData1);

% Create contour
contour(xdata2,ydata2,zdata2,'Parent',axes1,'LineColor',[0.2 0.2 0.2],...
    'LevelList',[-0.0342515411255264 1.55294077346749 3.14013308806051]);

% Create patch
patch('Parent',axes1,'ZData',ZData3,'YData',YData3,'XData',XData3,...
    'FaceColor',[0.93 0.96 1],...
    'EdgeColor','none');

% Create plot
plot(X1,Y1,'Parent',axes1,'LineWidth',2,'Color',[0 0 0]);

% Create plot3
plot3(X2,Y2,Z1,'Parent',axes1,'LineWidth',2,'Color',[0 0 0]);

% Create multiple lines using matrix input to plot3
plot3(XMatrix1,Y3,Z2,'Parent',axes1,'LineWidth',2,'Color',[0 0 0]);

% Create plot3
plot3(X3,Y4,Z3,'Parent',axes1,'MarkerSize',10,'Marker','.','LineWidth',1,...
    'LineStyle','none',...
    'Color',[0 0 0]);
```

Figure 78: MATLAB code

A part of EEGLAB by MATLAB code used to generate activity power spectrum plots (EEGLAB Toolbox, 2017).

A summary of the signal processing steps is shown in Figure 79.
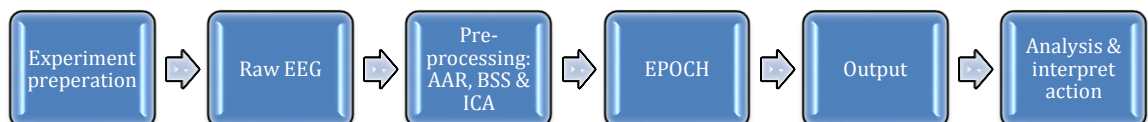
Figure 79: Signal processing steps summary

Chapter 7: Results, Validation and Discussion

This chapter will Focus on the results from experiments in chapter 5 and 6 and validate those results. It also talks about the contributions, which have been made, and their significance to the current knowledge are discussed. Some discussion

7.1 Statistical analysis of questionnaire data

First step of the experiment, participant information sheet was given to each subject and experiments was briefly explained to each of them, they asked to sign the consent form before the experiments can start. At the end of each task, subjects were asked to fill up the questionnaire that had statements of ownership, agency and sensation. All numerical assessments are based on prior hypotheses. Participants were exposed to several minutes of stimulation for each individual condition, after which they reported their subjective experience on a 5-point Liker scale ranging from "1" (totally disagree) to "5" (totally agree), with "3" indicating neither agreement nor disagreement ("uncertain"). Stimulation for each experiment continued until the participant marked they feel the illusion and sign of illusion appeared in EEG signals.

To analyze the questionnaire data, the average score of statement related to ownership and average score of statements related to agency for RHI and average score of statements related to sensation for SGS was calculated and compared. In each experiment several factors like gender differences, time and handedness were studied. In experiment 11, the most important parameter of study was time, the main focus was to find out whether or not the illusion can happen sooner and last longer over time.

The mean score of the questions in experiments 1- 5 are very similar. In experiment 6 the illusionary hand-ownership is not as strong as previous experiments. Furthermore, questions relating to proprioceptive drift were also greater in those experiments. The results are slightly increased in invisible and conspicuous which suggest that brain was pre-conditioned after first experiment. And decreased in opposite, rotated and blindfolded which shows changing position of hand and removing visual cues effecting the illusion.

Next phase, the participant divided into different group to investigate the effect of handedness and gender in appearing the illusion.
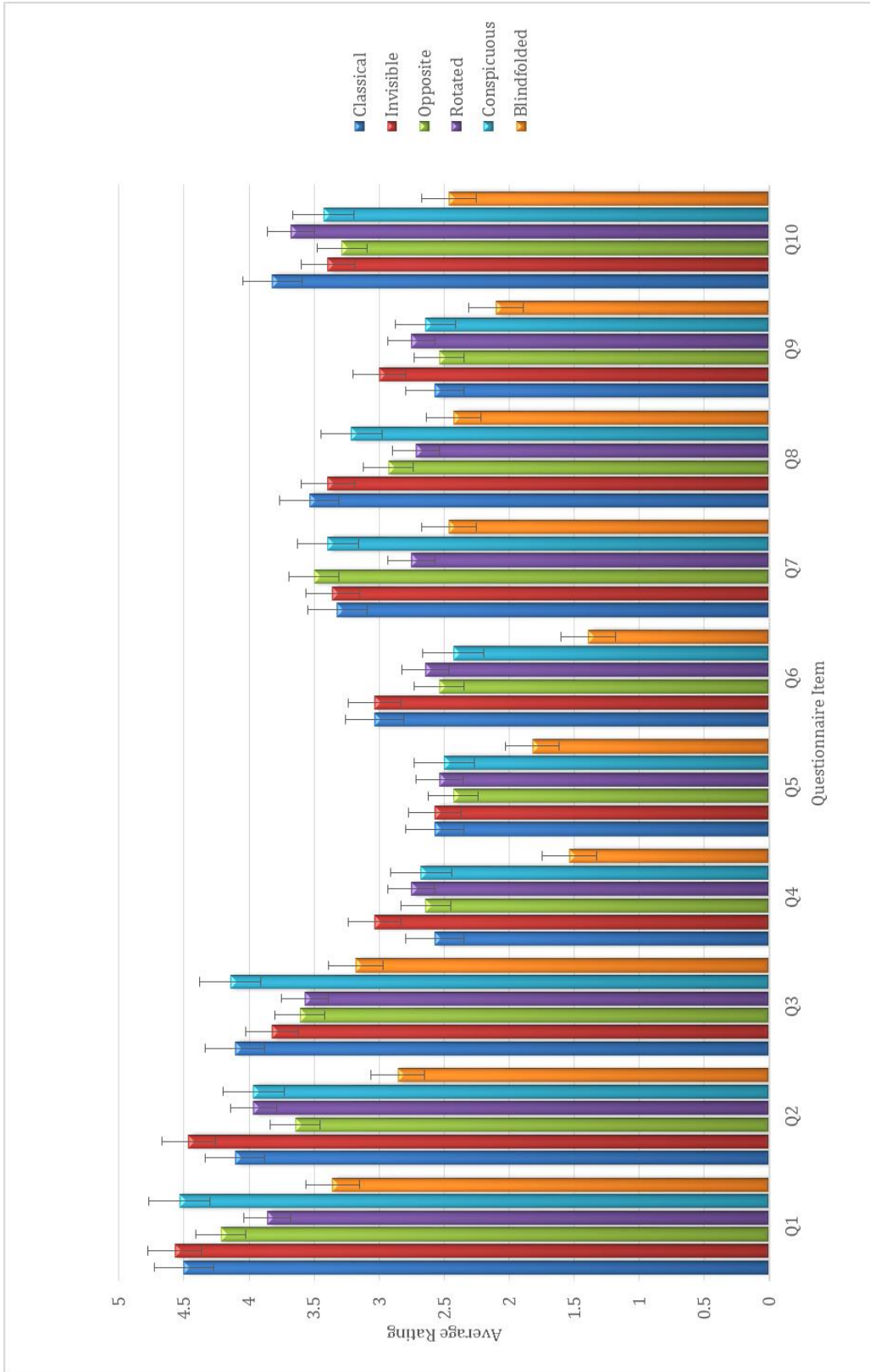
Figure 80: Mean for RHI questionnaire

Table 13: The mean of rated answer to questionnaire for RHIs experiments

	Classical	Invisible	Opposite	Rotated	Conspicuous	Blindfolded	Average
Q1	4.5	4.5	4.2	3.8	4.5	3.3	4.1
Q2	4.1	4.4	3.6	3.9	3.9	2.8	3.8
Q3	4.1	3.8	3.6	3.6	4.1	3.2	3.7
Q4	2.5	3.0	2.6	2.7	2.7	1.5	2.5
Q5	2.5	2.5	2.4	2.5	2.5	1.8	2.4
Q6	3.0	3.0	2.5	2.6	2.4	1.4	2.5
Q7	3.3	3.3	3.5	2.7	3.4	2.5	3.1
Q8	3.5	3.3	2.9	2.7	3.2	2.4	3.0
Q9	2.5	3.0	2.5	2.7	2.6	2.1	2.6
Q10	3.8	3.3	3.3	3.7	3.4	2.5	3.3

Table 13 shows the mean data calculated by all the participant for different experiments and figure 81 compares the average answer of each question in different experiment. Question 1, 2 and 3 are illusion related statement and they received the highest number.
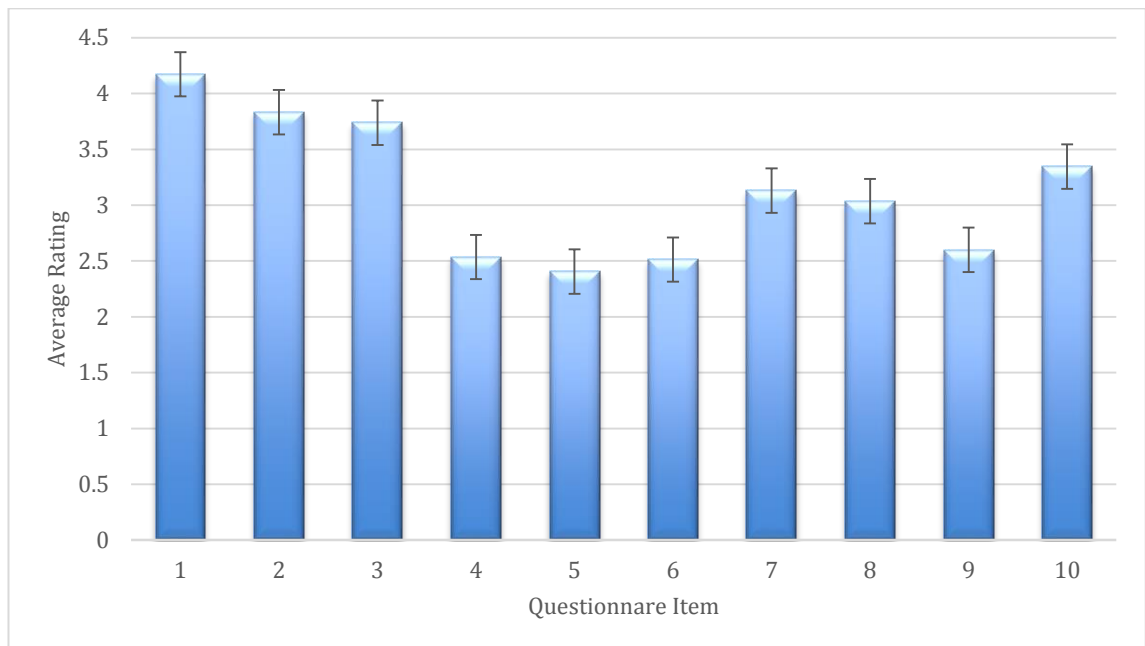
Figure 81: Mean of RHI and its modified version

Figure 82, compares the average rating of 28 participant for all 10 questions in different set up of the RHI. Except from blindfolded, all the other experiments have the similar rating.
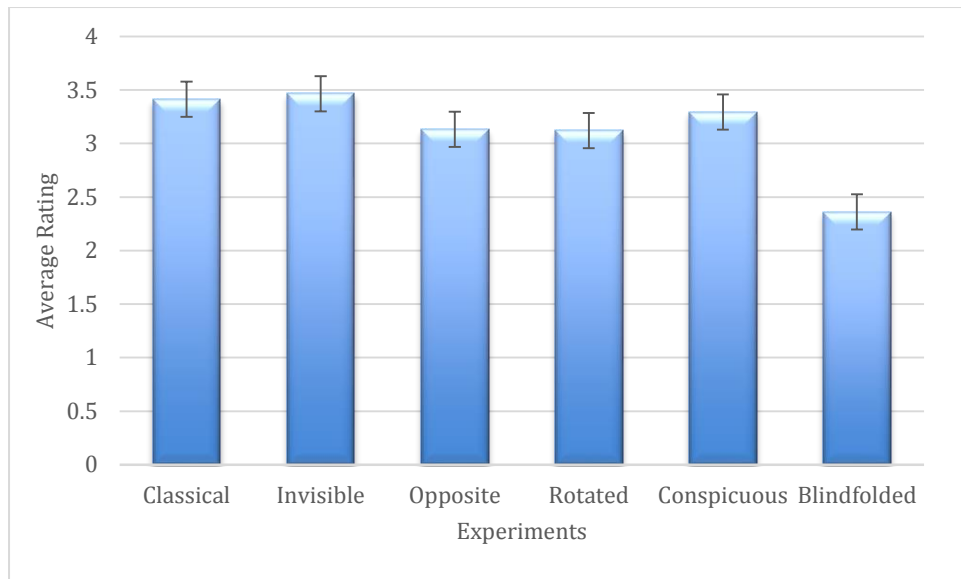
Figure 82: Average rating between different experiments

Illusion in male versus female

The graphs below comparison the gender differences in RHI experiments. The common outcome of these experiment is that female feel illusion more than male which indicates that female rely more on information received from vision and male and female do not participate visual signals and body sense in same way.

Table 14: The mean of rated answer to questionnaire for RHIs experiments by male and female group separately

		Classical	Invisible	Opposite	Rotated	Conspicuous	Blindfolded	average
Q1	Male	4.4	4.4	4.1	3.8	4.5	3.2	4.1
	Female	4.6	4.7	4.4	3.9	4.6	3.5	4.3
Q2	Male	4.0	4.3	3.5	3.6	3.6	2.4	3.6
	Female	4.2	4.6	3.8	4.3	4.3	3.3	4.1
Q3	Male	4.1	3.7	3.5	3.5	4.1	3.1	3.7
	Female	4.1	3.9	3.7	3.6	4.1	3.3	3.8
Q4	Male	2.3	2.9	2.7	2.9	2.5	1.5	2.5
	Female	2.9	3.1	2.6	2.6	2.9	1.6	2.6
Q5	Male	2.3	2.3	2.0	2.5	2.2	2.0	2.2
	Female	2.9	2.9	2.9	2.6	2.8	1.6	2.6
Q6	Male	3.1	2.9	2.7	2.4	2.4	1.5	2.5
	Female	2.9	3.1	2.4	2.9	2.5	1.3	2.5
Q7	Male	3.3	3.4	3.6	2.7	3.3	2.2	3.1
	Female	3.4	3.5	3.4	2.8	3.5	2.7	3.2
Q8	Male	3.5	3.4	2.6	2.4	3.5	2.5	3.0
	Female	3.6	3.4	3.2	3.0	2.9	2.4	3.1
Q9	Male	2.4	3.0	2.5	2.4	2.5	2.0	2.5
	Female	2.7	3.0	2.6	3.1	2.8	2.2	2.7
Q10	Male	3.7	3.4	3.1	3.2	3.2	2.1	3.1
	Female	3.9	3.4	3.4	4.1	3.6	2.8	3.5

Figure 83 compares the group of male and female, the average of each question in different experiment was calculated, and data is available in table 14. The average answer in female are higher than male in every question, which shows, that female can feel the illusion more than males. The red cells in table shows the exception that male gave higher rating to question.
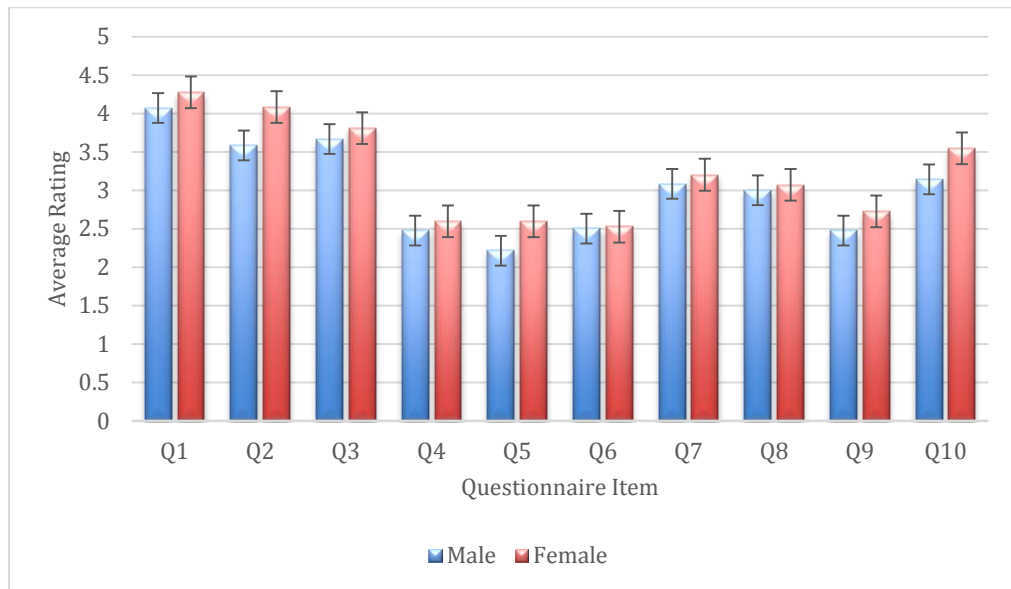
Figure 83: Comparison between male and female group by the average rate of questionnaire item

Figure 84, shows the gender difference for each experiment and each questions independently. In invisible hand experiment female gave the higher rate to questions compared to other experiments and males have higher rating in opposite hand and blindfolded compare to females. The lowest average for male is question 5 "it seemed as if the touch I was feeling came from somewhere between my own hand and the rubber hand", and for female is question 6 "It felt as if my hand were turning rubber" which both are control related statement. Also highest average is question 1 "It seemed as if I were feeling the touch of paintbrush in the location where I saw the rubber hand touched" which illusion related statement is.
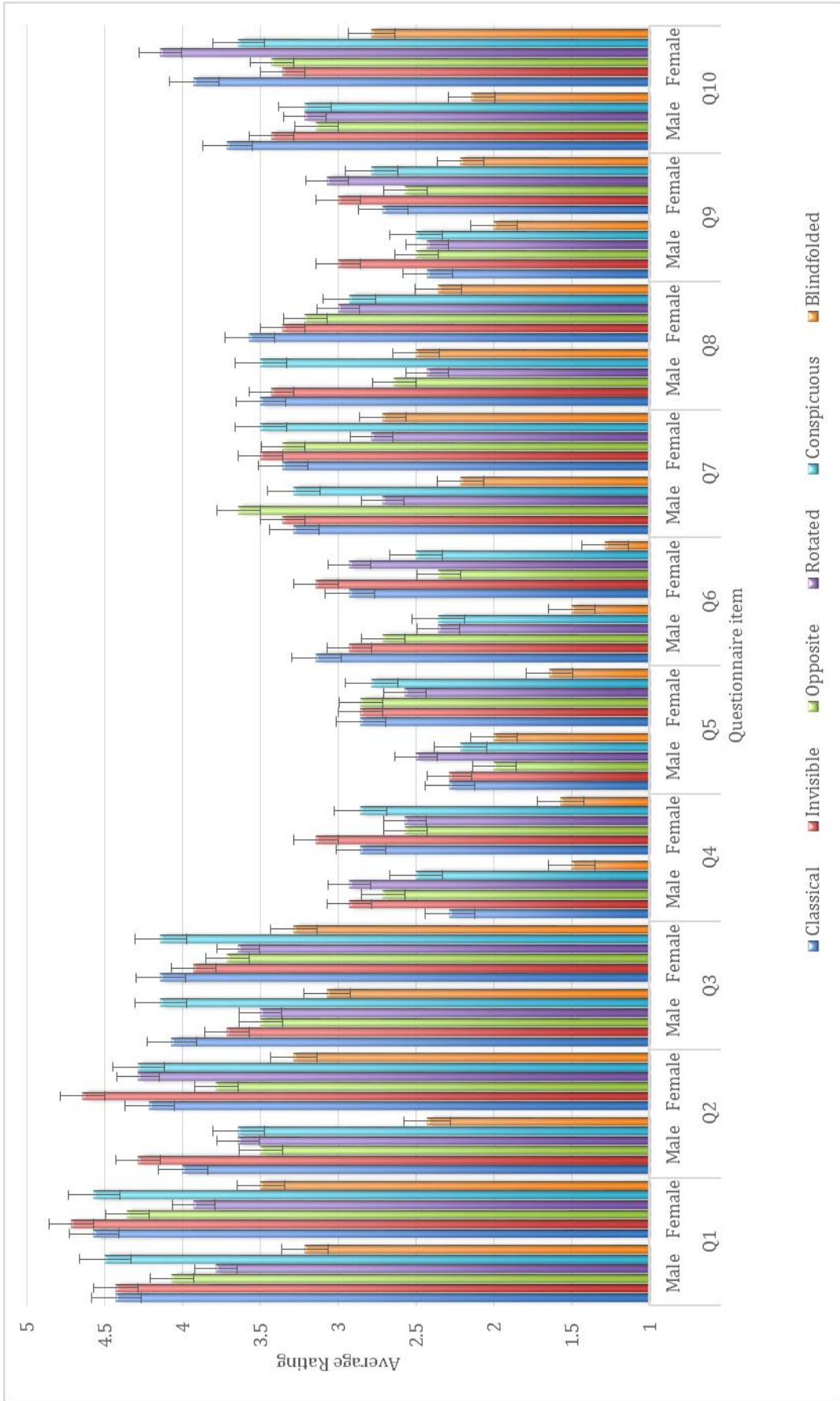
Figure 84: mean for gender difference in RHI questionnaire

Illusion in left-handed versus right handed

In this section, graphs are shows the difference between rights handed and left handed subjects in different experiments. The left handed group lean more on visual information than right handed group and sense the illusion more. Therefore, right-handed and left-handed process the visual information differently.

Table 15: The mean of rated answer to questionnaire for RHIs experiments by right handed and left handed group separately

		Classical	Invisible	Opposite	Rotated	Conspicuous	Blindfolded	Average
Q1	Left-handed	4.5	4.6	4.1	3.9	4.5	3.5	4.2
	Right-handed	4.5	4.6	4.3	3.8	4.6	3.2	4.2
Q2	Left-handed	4.2	4.6	3.8	4.2	4.1	3.4	4.0
	Right-handed	4.0	4.4	3.5	3.7	3.9	2.4	3.6
Q3	Left-handed	4.1	3.9	3.7	3.7	4.1	3.3	3.8
	Right-handed	4.1	3.7	3.5	3.4	4.1	3.1	3.7
Q4	Left-handed	2.9	3.1	2.8	2.8	3.0	1.8	2.7
	Right-handed	2.3	3.0	2.5	2.7	2.4	1.3	2.4
Q5	Left-handed	2.9	2.9	2.5	3.0	2.4	1.6	2.5
	Right-handed	2.3	2.3	2.4	2.1	2.6	2.0	2.3
Q6	Left-handed	3.1	3.1	2.7	2.7	2.6	1.4	2.6
	Right-handed	3.0	3.0	2.4	2.6	2.3	1.4	2.4
Q7	Left-handed	3.4	3.4	3.6	3.2	3.6	2.6	3.3
	Right-handed	3.3	3.3	3.4	2.3	3.2	2.4	3.0
Q8	Left-handed	3.6	3.4	3.1	3.4	3.3	2.5	3.2
	Right-handed	3.4	3.4	2.8	2.1	3.1	2.4	2.9
Q9	Left-handed	2.9	3.0	2.6	3.0	3.1	2.1	2.8
	Right-handed	2.3	3.0	2.4	2.5	2.1	2.1	2.4
Q10	Left-handed	3.7	3.4	3.6	3.9	3.4	2.5	3.4
	Right-handed	3.9	3.4	3.0	3.4	3.5	2.4	3.3

Figure 85 compares the left and right handed group, the average of each question in different experiment was calculated, and data is available in table 15. The average answer in left handed group are higher than right handed in every question which shows that left handed can feel the illusion more than right handed people. The red cells in table indicate the times right handed got higher average.

Both group has the highest rating for Invisible hand followed by second highest of classical RHI. The highest average for both group is question 1 "It seemed as if I were feeling the touch of paintbrush in the location where I saw the rubber hand touched" which is the illusion related statement and the lowest average for both group is question 5 "it seemed as if the touch I was feeling came from somewhere between my own hand and the rubber hand", which is control related statement.

Figure 87, shows the difference between the two group for each experiment and each questions separately.
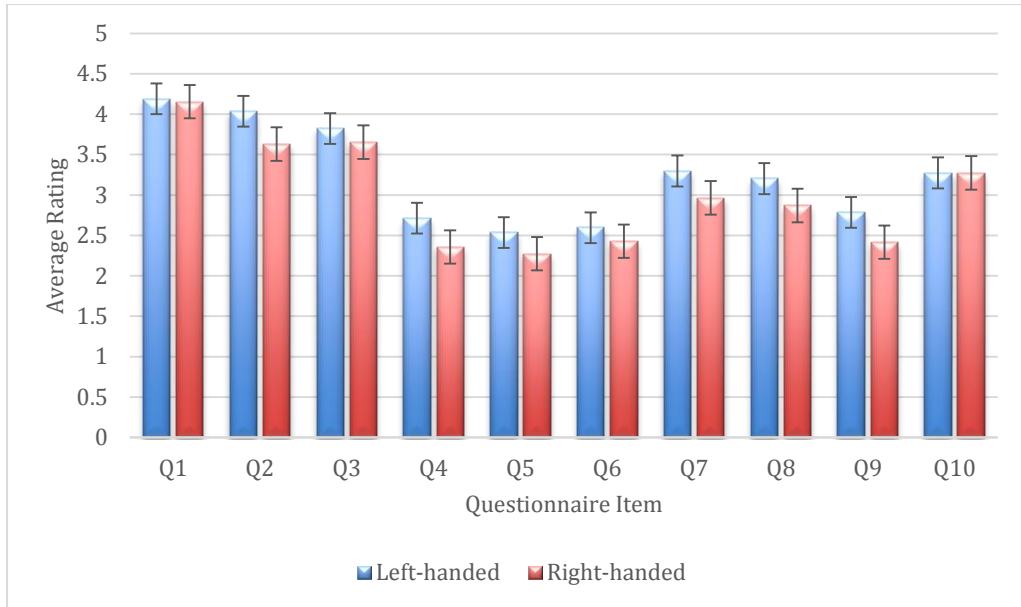
Figure 85: Comparison between right handed and left handed group by the average rate of questionnaire item

Figure 86, compared the total average of male, female, left handed and right handed group individually. According to this figure, female and left handed can feel the illusion more than the other two group.
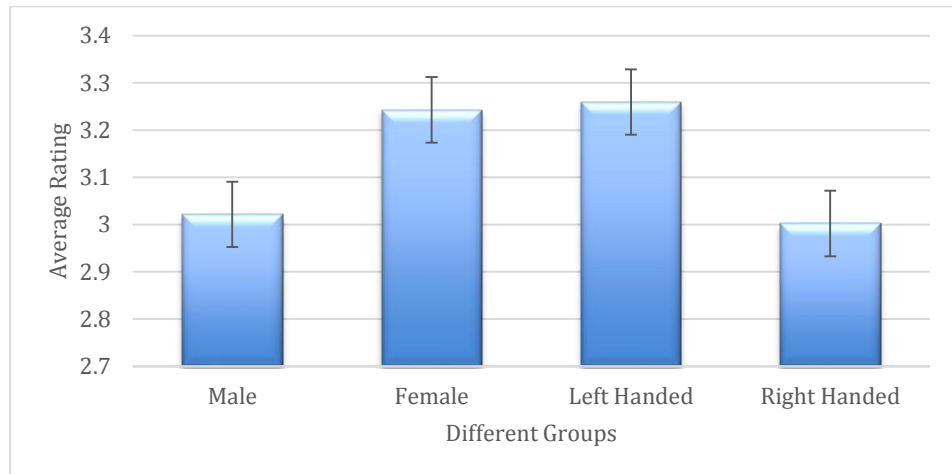
Figure 86: Difference between male and female, left handed and right handed
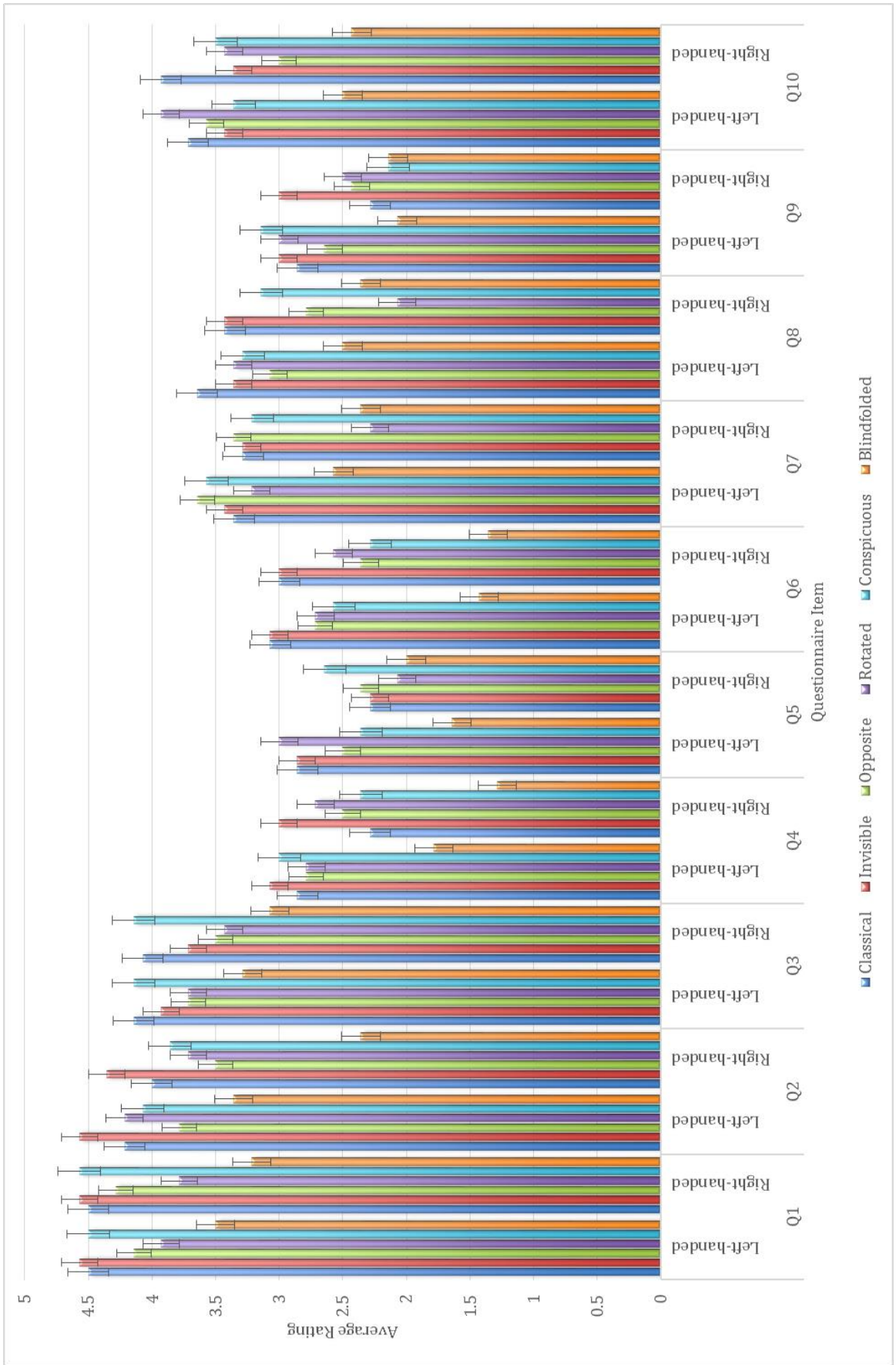
Figure 87: Mean for handedness in RHI questionnaire

Illusion across time

This section compares the time took for each subject to react to illusion, it will also compare this time for different gender and handedness.

condition	Classical	Invisible	Opposite	Rotated	Conspicuou:	Blindfolded
time	247.4	262.3	265.5	269.4	267.9	413.7

Although it is not much noticeable, the figure 88 shows male are faster to react to the illusion and left handed group need more time to recognize the rubber hand. In last experiment, blindfolded version, it took nearly as 1.5 times more for everyone to respond to the illusion, which is more visible in figure 89. Table 16 compares the average time for each illusion to happen in second.

Figure 88 shows right handed react fasted in classical conditioning, and took female longest to respond to blindfolded set up.
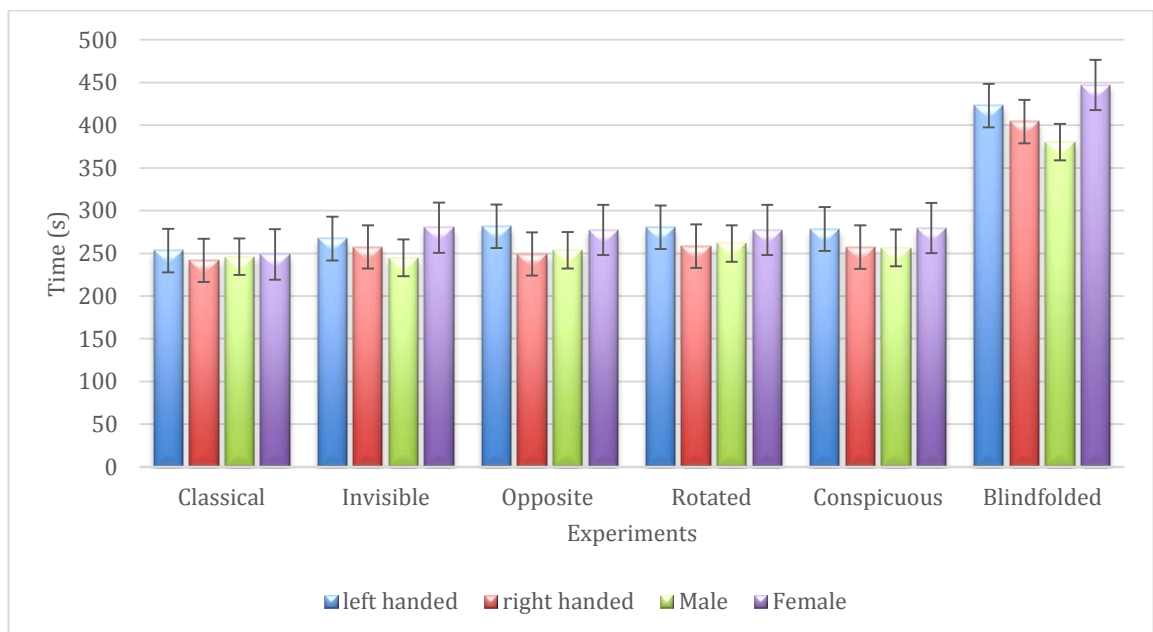
Figure 88: Average time in second for illusion to appear in different group and different condition of RHI
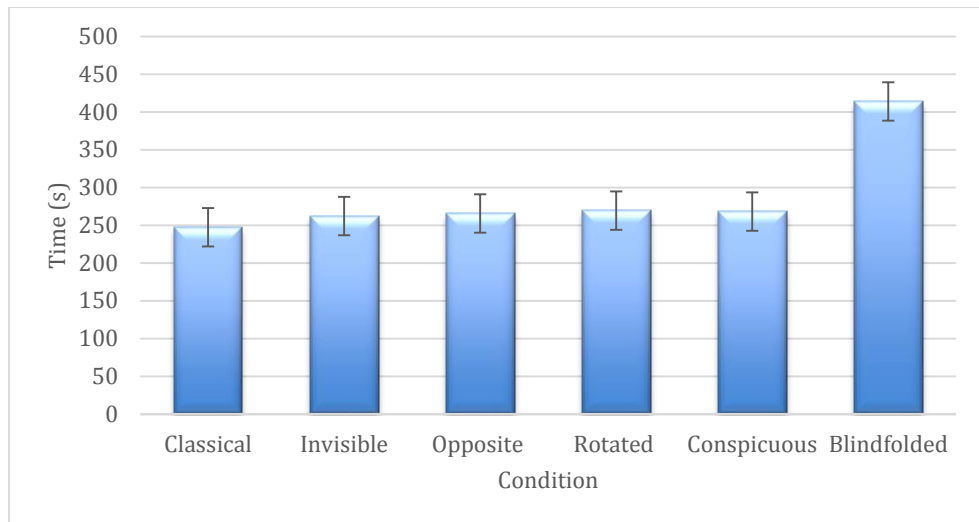
Figure 89: Average time in second for appearing illusion in each condition of RHI

Figure 90, uses the average rating of all experiments and shows the significant difference between the four groups. Male and right handed react much faster to illusion compare to the other group and illusion takes longest to appear in female.
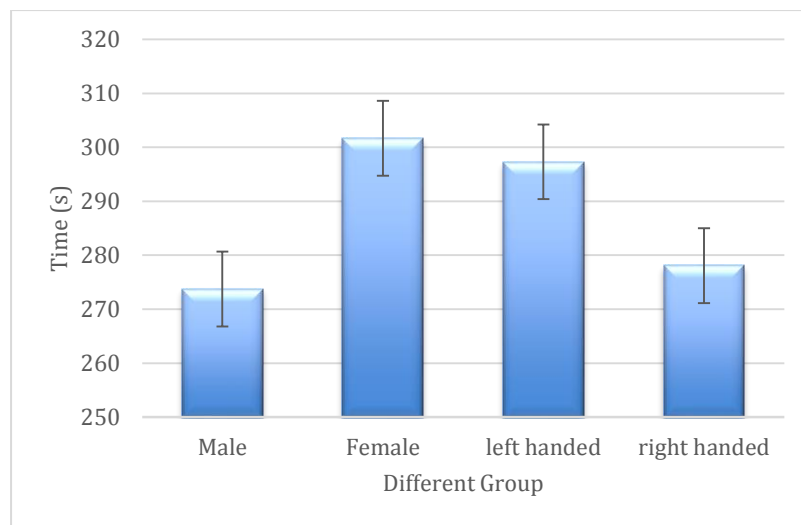
Figure 90: Significant difference between male and female, right handed and left handed for illusion time

Ownership across conditioning

One of the subjects was asked to return within one month and nine months breach for traditional RHI experiment for retraining and to prove the proposition that brain will store the memory of the illusion and it can appear faster after first attempt on subject. Below is the comparison of the result after each attempt and time for first event to happen. For first 4 questions and question 8 and 10, the results increased by third attempt. Question 5 and 6 remains the same and in question 9, second attempt got the highest rating.
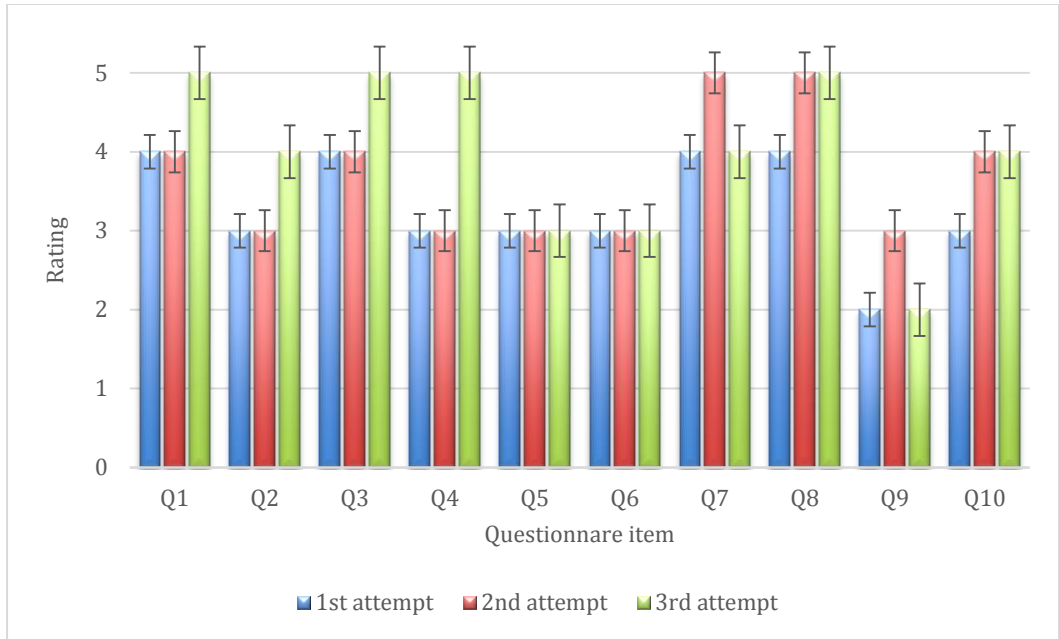
Figure 91: Ownership vs conditioning

Table 17 Time for illusion to happen for each attempt in one subject

Attempt	#1	#2	#3
Time	5:00:99	4:18:14	02:07:83

After comparing these results, moving hand experiment was designed for the same purpose of studying the ownership across conditioning. Graphs below shows the number of attempt with gap break for the subject.
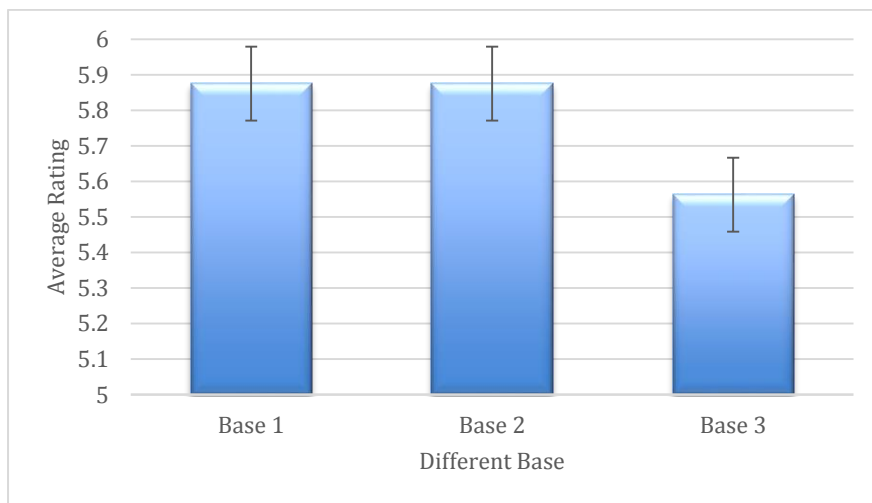
Figure 92: Average rating for three bases on 20 days experiments

Figure 92, represents the average rating of participant for placing hand in different height during the course of experiment. Base 1, represent the answer while the hand was on high base (7 cm), Base 2 is for middle base (4cm) and Base 3 is when both hands were placed in same height. The average answer for base 1 and 2 are exactly the same while base 3 has slightly lower rating. Figure 93, compares the average rating on different base for all the questions of questionnaire on each days. The average rating start increasing on day 3 with exception of Base 3 and has been improved towards the end with significant decrease on day 13 for base 1 and 3. After first gap, the result for Base 1 improved, Base 2 declined and Base 3 remained the same. After the second gap, the results for all Bases developed significantly.
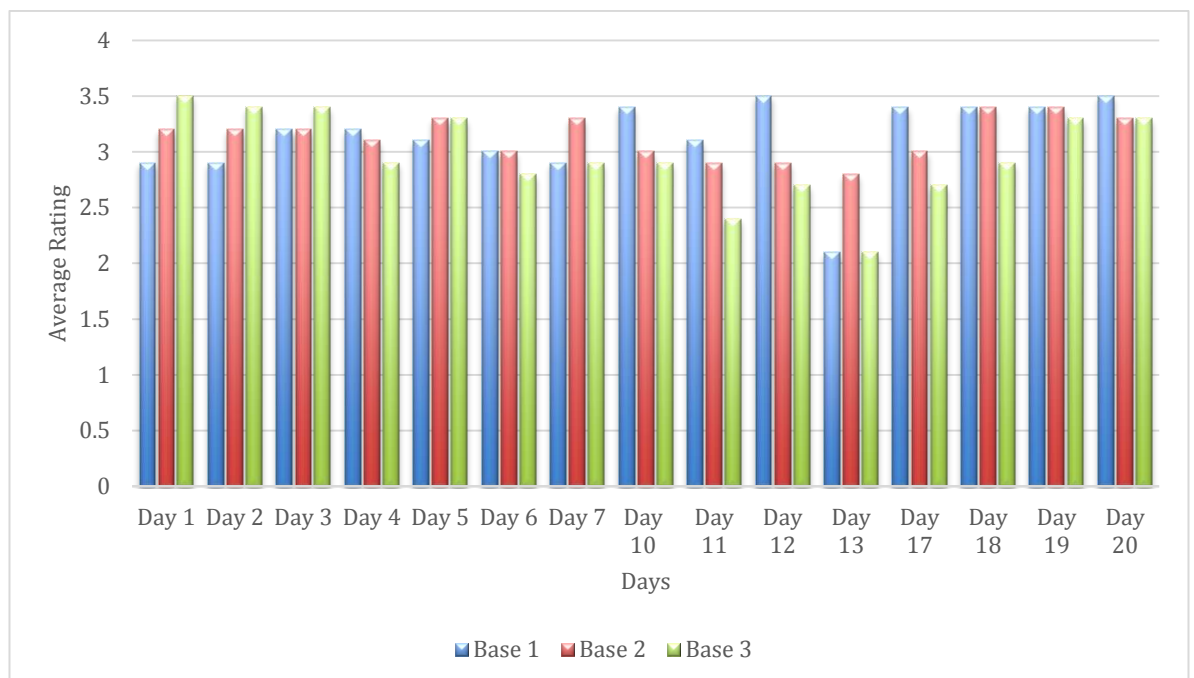
Figure 93: Average rating for each day on moving hand experiment

Figure 94, indications the average rating the participants gave to each item of questionnaire during the 20 days of experiments. The highest rating for all of the conditions is for question 1"It seemed as if I were feeling the touch of paintbrush in the location where I saw the rubber hand touched" which is the illusion related statement. And lowest rating are for question 5 "it seemed as if the touch I was feeling came from somewhere between my own hand and the rubber hand" and question 9 "It felt my real hand was drifting towards the rubber hand", both are control statements. Detailed figures related to each Base during 20 days of experiments are available in **Appendix 5**.
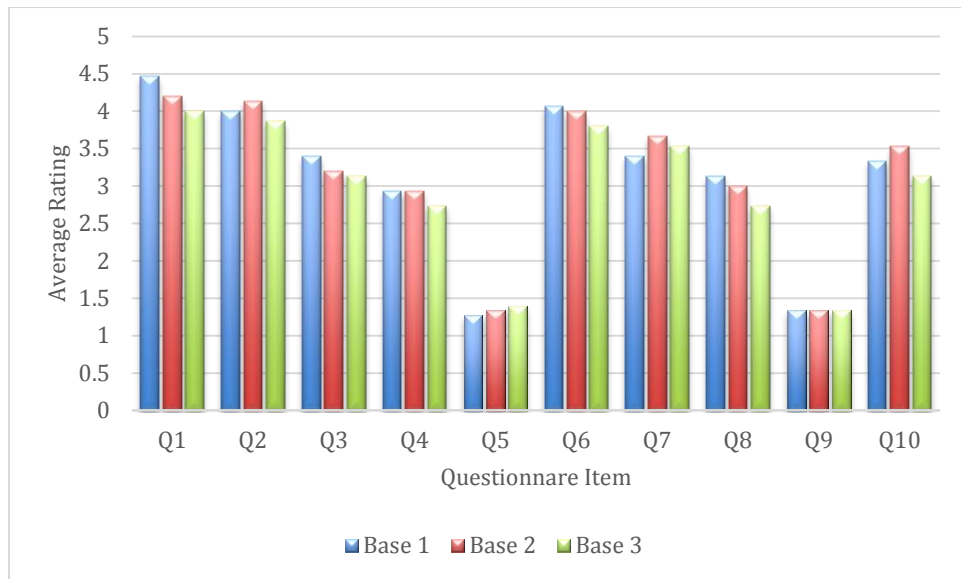
Figure 94: Mean for moving hand questionnaire

Figure 95 compares the timing for each base on moving hand set up during the course of study. The time for illusion to happen significantly decreased over time with exception on day 10. Illusion appeared faster when stroking was on same level, and took almost the same amount for Base 1 and 2. Base 1 has slightly less value than Base 2 as the brain was already conditioned.
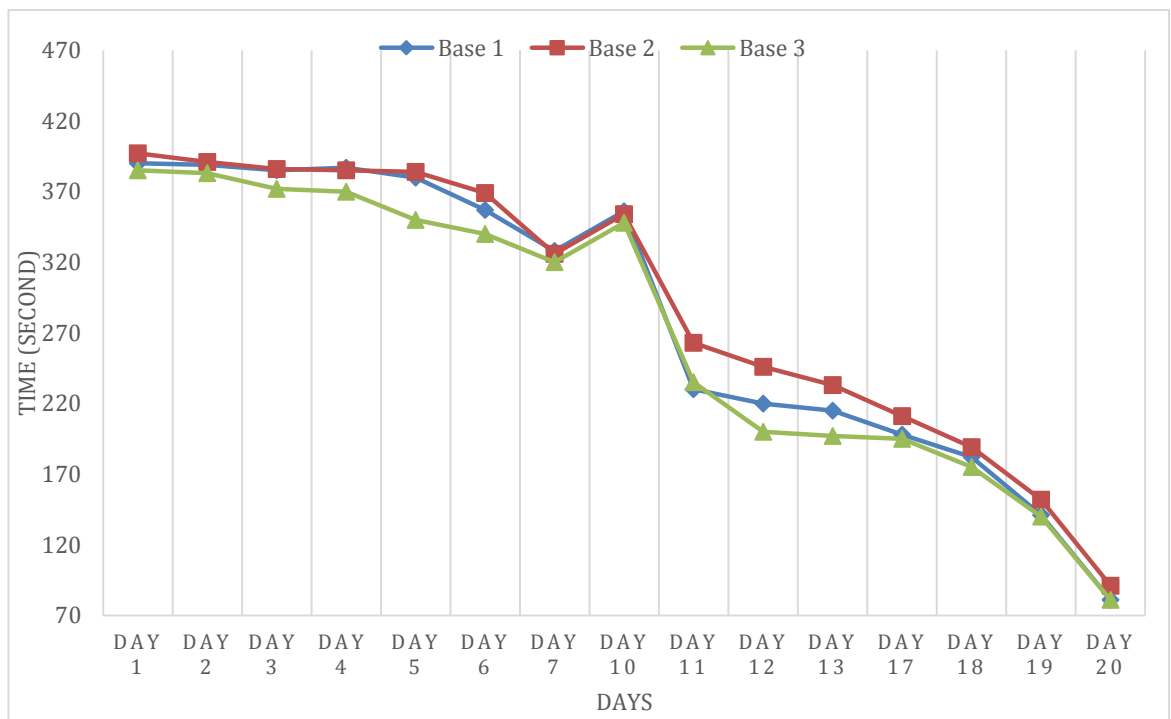
Figure 95: Time comparison between 3 bases of moving hand

This set of experiments reveals the divergence of visual and tactile senses and the results support the body ownership illusion. The present experiment reveals that self-recognition is a highly consistent process, which depends on available cues. The main finding was that, visual and auditory are the two main signals influenced self-recognition and sense of ownership. The results of RHI and its modified versions suggests that, the visual position of the hand with respect to the body and presence of movements can override other cues.

SGS results

It is worth mentioning the reason behind choosing auditory cues to compensate for the absence of the visual input. A recent study performed by Bauer et al. (2017) have the lead to demonstrate the differences in blind people's brain that does not appear in sighted people in terms of anatomical, structural and functional. These differences suggest that the high degree to which brains is "plastic" that it manages to compensate for the loss of any sensory information.

To shape the communication between an amputee and a prosthetic device, SGS was performed repeatedly to condition the brain and try to make this illusion last longer and check the possibility of making it permanent. This experiment carried out on four subjects, each subject attend the work place for a month. The graphs below present their answers to questionnaire during 30 days of experiment.

Figure 96, compares the average rating of each question during 30 days by participant in different group. In this graph, question 8 "How much attention did you paid to the sound at the end of the experiment" has the highest rating. This question was asked to target how brain will shift and adjust itself to the sound after 30 days. Participant gradually start giving the less score to this question towards the end of the experiment. Question 6 "I lost sensation from my hand" has the lowest rating, which is the control statement.
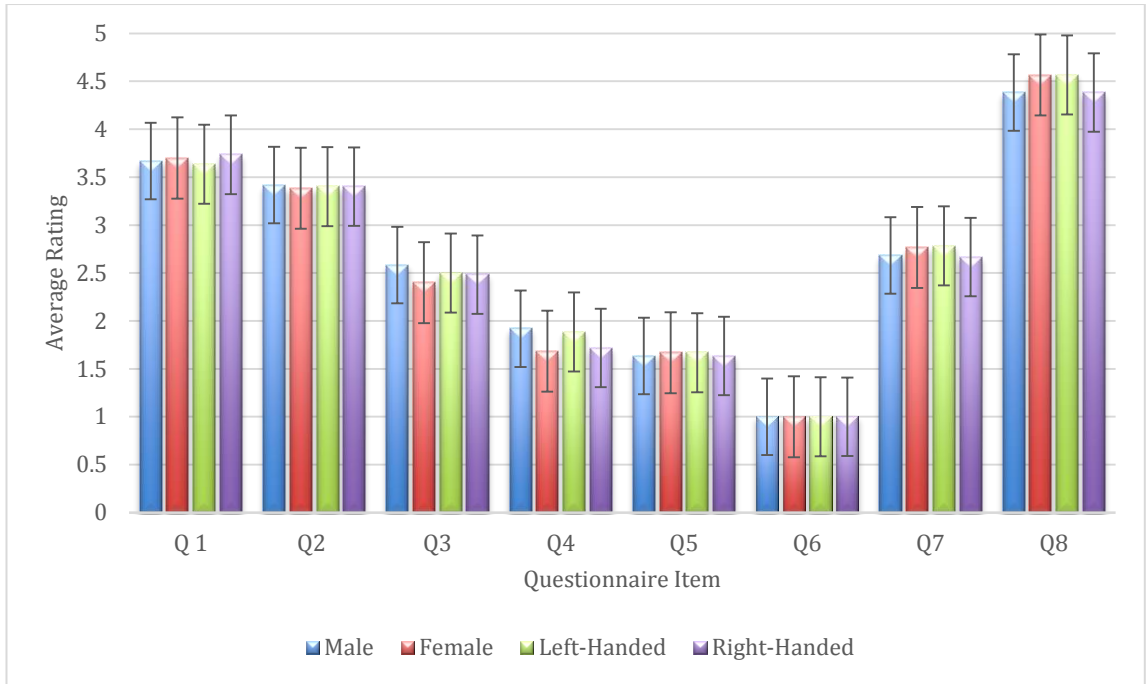
The rating was higher by female compare to male for questions 1,5,7 and 8 but the average rating for all the questions was higher for male. Left handed gave the higher ranking compare to right handed group in total. Figure 97, compares the total average rating of male, female, left handed and right handed group individually. Detailed figures for each participant during 30 days of experiments is available in **Appendix 5**.
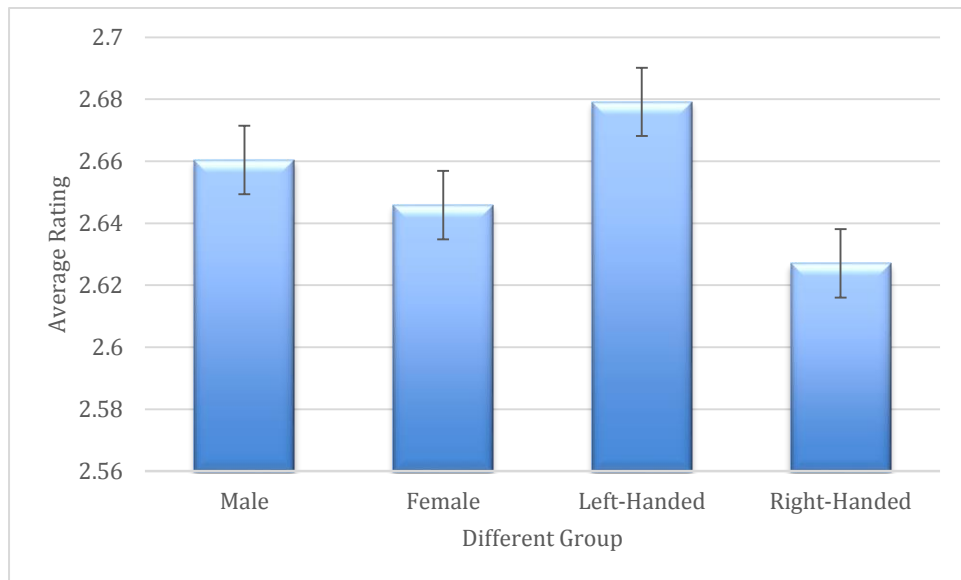
Figure 97: Comparison between the average ratings by each group

Figure 98 associates with the timing for each participant react to SGS during the course of study. The time for illusion to happen significantly decreased over time. Illusion

appeared faster much faster on day 30 compare to day 1 which proves that conditioning happened during the 30 days and memory of the illusion was stored in the brain.
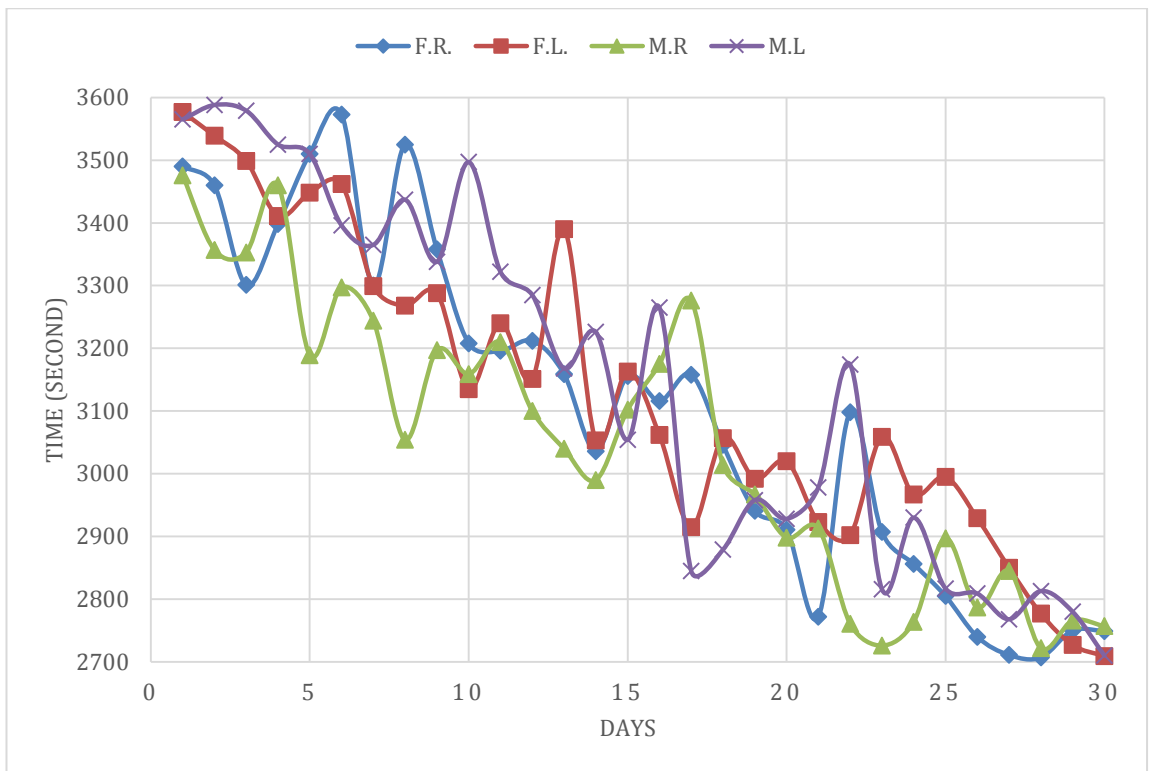
Figure 98: Average time in second for appearing illusion in each participant during 30 days of SGS

Figure 99 shows right handed are faster to respond to the illusion and female need more time to distinguish the illusion.
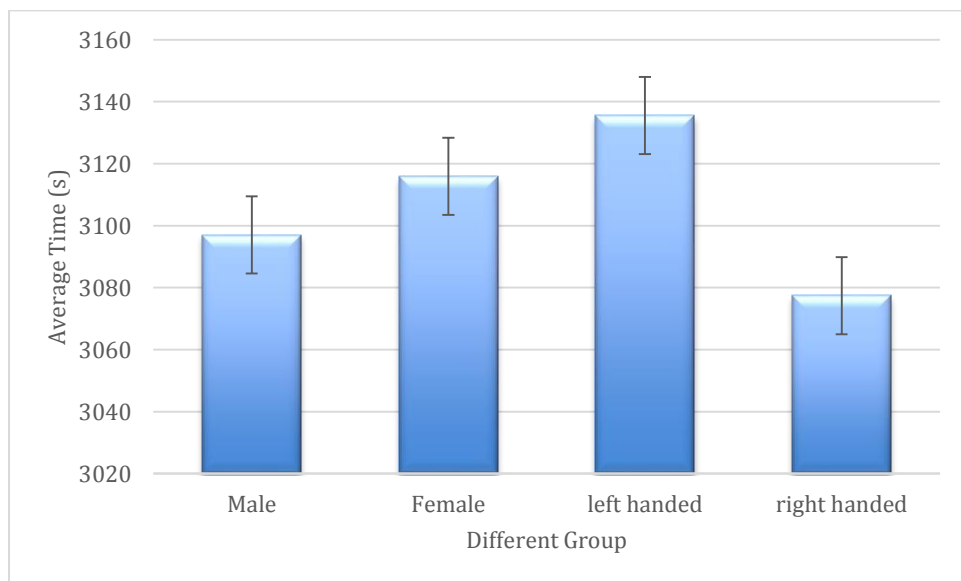
Figure 99: Significant difference between male and female, right handed and left handed for time of illusion to appear in SGS experiment during 30 days

7.2 EEG data acquisition and analysis

Relaying on questionnaire was not enough to confirm the results, so it was combined with data collected from EEG headset. Setting up the EEG took 30-45 minutes as each sensors had to be properly connected with scalp. As it was explained in chapter 6, wet electrodes was used to obtain better signals and increase subjects comfort. To check good signal from each electrode, signal bar for each electrodes was categorized by name. The EEG signals were collected using EEGo software from ANT Neuro and analyzed by EEGLAB. At the end of experiments, EEG cap was removed.

Raw EEG records cannot be processed. Therefore many methods of filtering techniques were used in this study such as FIR filter, BSS and ICA.

The spectral component heat maps

First of all the 2-D spectral Component heat Map was obtained for each subject to explain the neural activity (power) distribution over the scalp at specific frequency or component. Moreover, the spectral component heat map identifies the different areas of the brain where the increase and decrease of neural activity which may indicate the occurrence of an illusion. The plot's legend shows a range of colours starting from blue (negative) towards red (positive). Red colour indicates an increase in neural activity or power, which is the area of interest. After that, a computation of the activity power spectrum is conducted using a Fourier transform technique.

Activity Power Spectrum

Activity Power spectrum is simply the square of the magnitude of the Fourier transform of signals. It is utilised in this study to specify the amplitude of recurring neural activity in the signal as a function of frequency (Abhishek & Vali, 2016). In the Activity Power Spectrum plot, the X-axis denotes the frequency in Hertz and Y-axis denotes the intensity of power in (μV2/Hz). Decrease in power within the range of (8-30) Hz "alpha and beta wave" which is the area of interest (Rao & Kayser, 2017).

Component Time-Frequency Analysis of EEG data

Time-frequency analysis of the changes event-related spectral power (ERSP) is obtained to find the change in neural activity at different frequencies at a specific time. ERSP plots

mostly used to measure the total dynamic change in the degree of the EEG spectrum as a function of time in a specific event (Datta, 2016). This plot represents coloured clusters that express the strength of the neural activity of the subject with respect to time and frequency. These plots are generated after signal processing using FIR, ICA, BSS, baseline removal, epoch extraction and Component Time-Frequency Analysis of EEG data is shown in Figure 106. The plot's legend shows a range of colours starting from blue (negative) towards red (positive). Red colour indicates an increase in neural activity or power, which is the area of interest.

To better localise on the neural activity (illusion occurrences) and to ensure experiment consistency specified electrodes were chosen for inspection. Electrodes are FP1, AF3 AF7, F3, F5, F7, FC3, FC5 and FT7 which are located in the left hemisphere of the brain and FP2, AF4, AF8, F4, F6, F8, FC4, FC6 and FT8 on the right hemisphere of the brain. A reference to the channels locations with corresponding channel components is demonstrated in Figure 100 and 101. These electrode locations were chosen in accordance with published literature indicating that illusion occurs when there is increased levels of neural activity in the bilateral intraparietal cortex, bilateral dorsal premotor cortex, and supplementary motor area. Those areas are recognised to be involved in the processing of the feeling of ownership (Ehrsson et al., 2004).
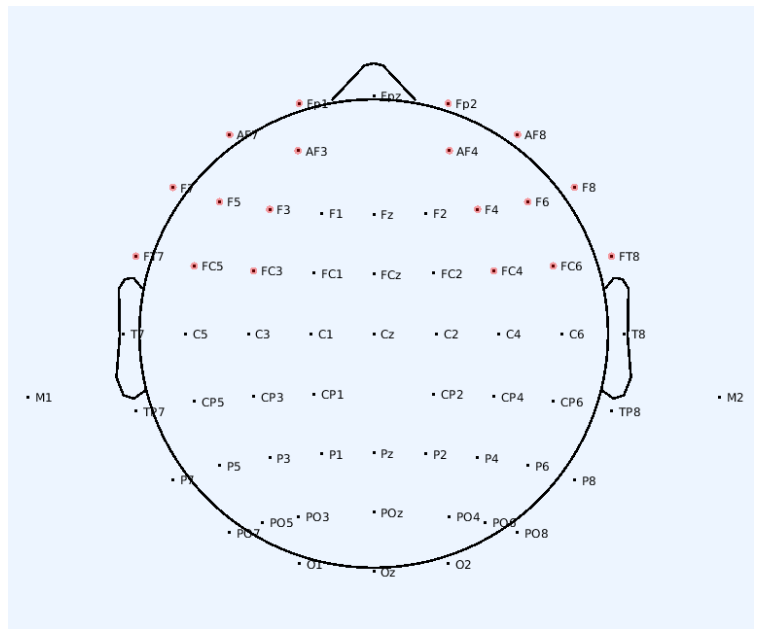
Figure 100: 2D EEGLAB channel locations plot and correspondent components by name

Channel choose for this study are highlighted in red.

EEG signal processing using EEG[rt] headset and EEGLAB by MATLAB software was used to determine the effect of each experiment in brain. The major challenge with this technique relate to aspects of both hardware and software. Accurate placement of electrons and appropriate conditions of the scalp (whether the participants used conditioner or not, sweat or wetness etc.), participant and testing environments are essential for registering clear and informative brain signals. Finding of body artifacts like bio-electrical signals generated from different body parts (heartbeat and muscular actions, eye squint and eyeball development) are also recorded in EEG (Reddy & Narava, 2013).

Furthermore, removal of artefacts and other interfering signals was carried out using appropriate filtration and signal processing parameters using EEGLAB and MATLAB. Data filtration step was a significant process in signal processing, as it involves cleaning the signal to produce a better signal of improved quality (Strang, 1999), especially that the Raw EEG signals are contaminated with artefacts and noise with utility frequency between 50-60 Hz. The techniques used to eliminate artefacts and to remove noise were (FIR and IIR filter, Blind Source Separation (BSS), independent component analysis (ICA).

Automatic Artefact Removal (AAR) where some of them are digital filters and algorithms (Gurumurthy et al., 2013). Considerable measures have been taken to ensure interference due to the above-mentioned factors was minimal. However, there is always some degree of interference which was taken into account while interpreting the results of the experiments.

Classical RHI

Classical RHI set up was set as a baseline against which the findings of rest of the modified versions of RHI experiments were compared. Neural activity profile of each experiment was determined from the Spectral component heat map, ERP and oscillatory signatures in addition to ERP and time-frequency signatures. As expected, there was significant neural activity starting from the temporal lobe moving to the frontal lobe.

The first step is to obtain the raw EEG channel data. Figure 102 represents an excerpt of subject's 24 EGG chart showing all channels on the y-axis and time seconds (s) on the x-axis. There is a notable upward spike at 38 s of the experiment in channel FP1, FPZ, FP2, F7, F3 and CP4 at 36s. All neural activity was observed in channels corresponding to the frontal cortex with noticeable background noise, blinking, and movement and baseline artefacts that need to be filtered in the signal processing step.
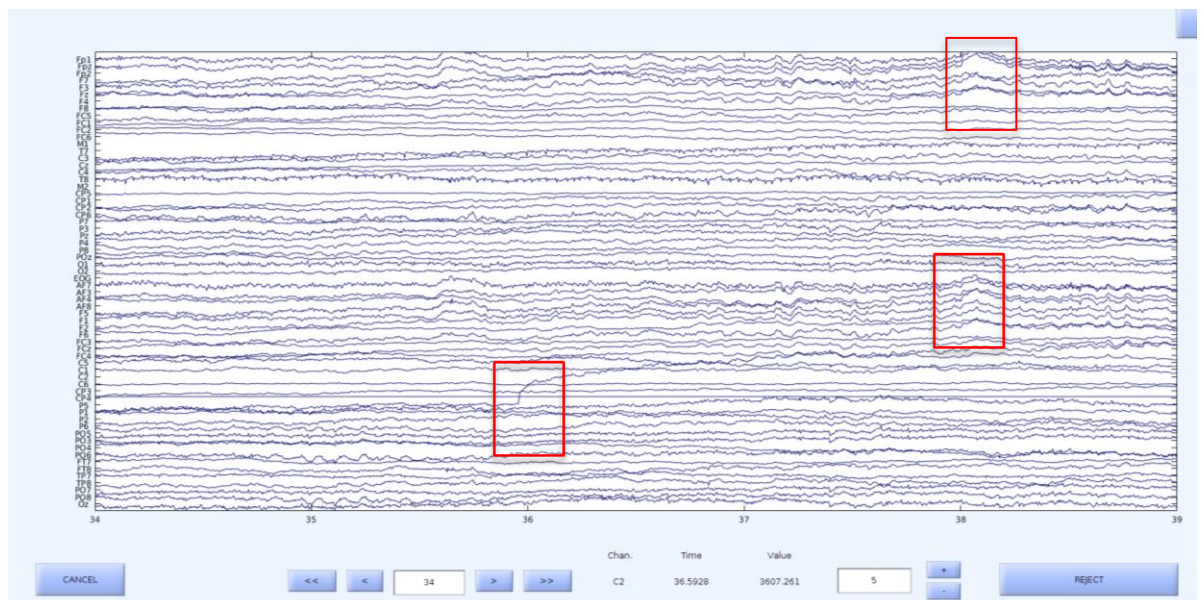
Figure 102: EEG chart.

This is an excerpt of subject 24, EGG chart showing all channels on the y-axis and time (sec) on the x-axis.

Figure 103 represents 2-D independent components maps that show readings of the brain about the different components as projected by each electrode. Electrodes are placed in a specific manner to reflect the activity in different brain regions – frontal, parietal, temporal and occipital. The strength of activity at each component and corresponding brain region is indicated by the colour of the heat map legend. Figure 103 is a demonstration of the first 100s of the 300s experiment time of subject 15. Components 13 and 19 are the counter and interpolated reference electrodes. Components 23, 55, 57 and 61 show an increase in power, whereas rest of the components show a decrease.
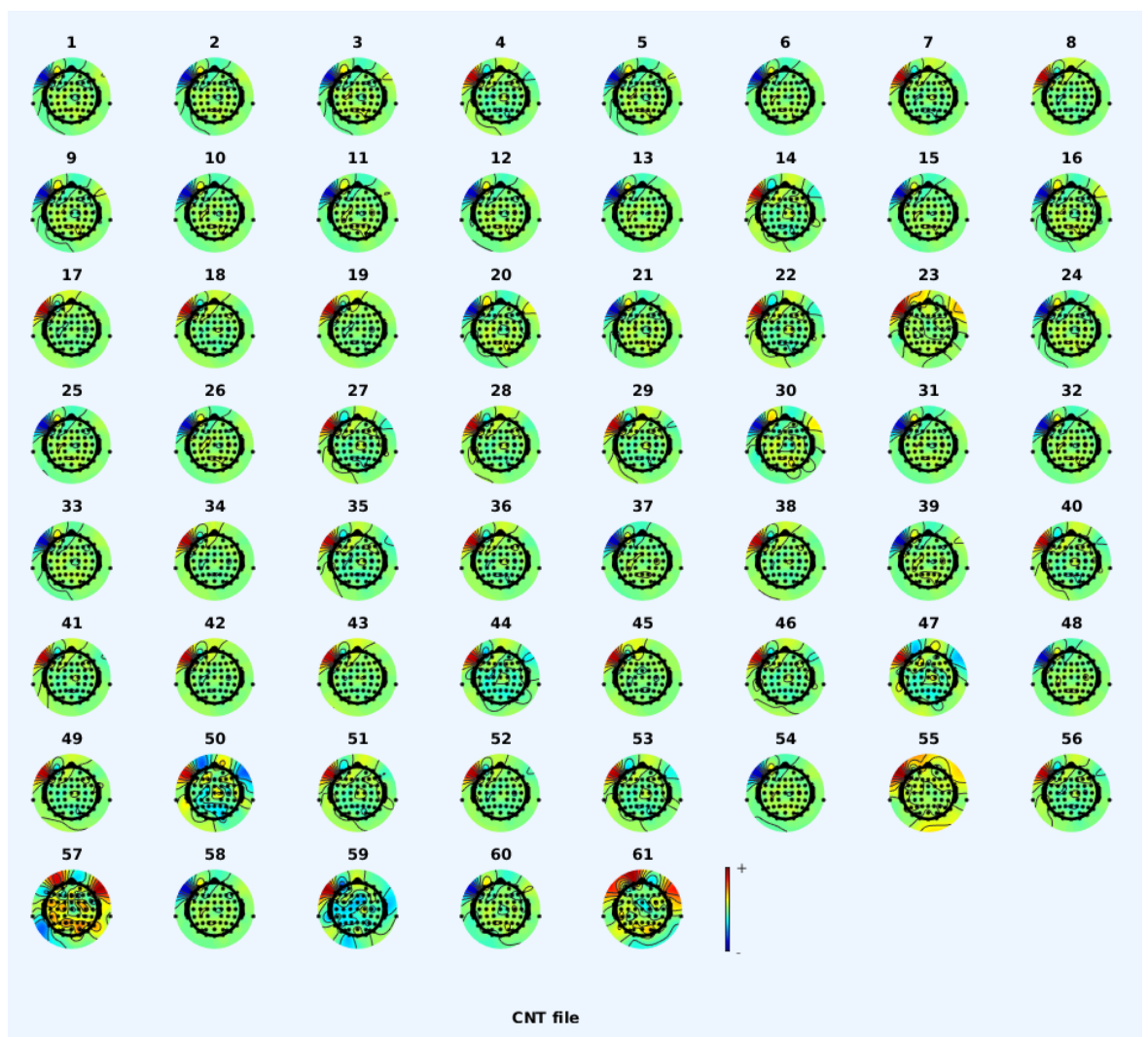
Figure 103: Spectral Components heat-map at the start of the experiment. The heat-map of subject-15 for the first 100 seconds for RHI experiment 1

Figure 104 represents independent spectral components maps show readings of the brain in relation to the different components as projected by each electrode. The above

components map is a representation of the last 100s of the 300s experiment of subject 15. It is notable that a significant change has occurred in the last 100s of the experiment Components 1, 3, 4, 7, 10, 33, 36, 37, 38, 39, 41, 42, 43 and 59 show an increase in power, whereas components 2, 5, 6, 9, 12, 15, 19, 22, 25, 27 and 57 show the greatest decrease.
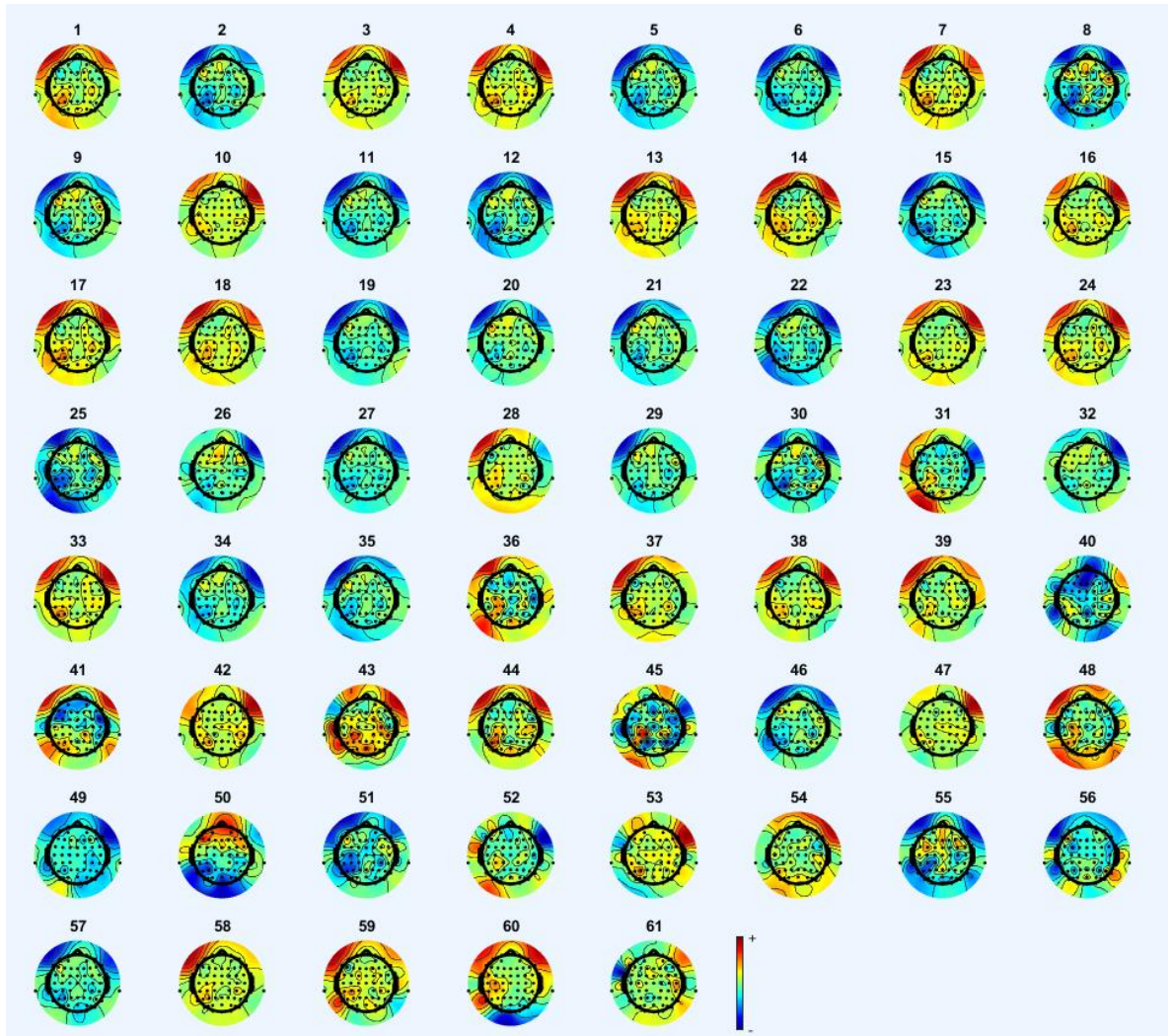
Figure 104 Spectral Components heat-map at the end of the experiment the heat-map of subject-15 for the last 100 seconds of RHI experiment 1.

Activity Power Spectrum

Figure 105 shows the brain heat map for component 7 for subject 23 that indicates high power throughout the brain but, concentrated especially at the right frontotemporal and bilateral temporal and occipital regions. This is reflected in the graph which shows a high-frequency fluctuations power spectrum. Remarkable is a strong downward spike which is reflected alpha and beta waves at frequencies 10.5 Hz and 38 Hz respectively.
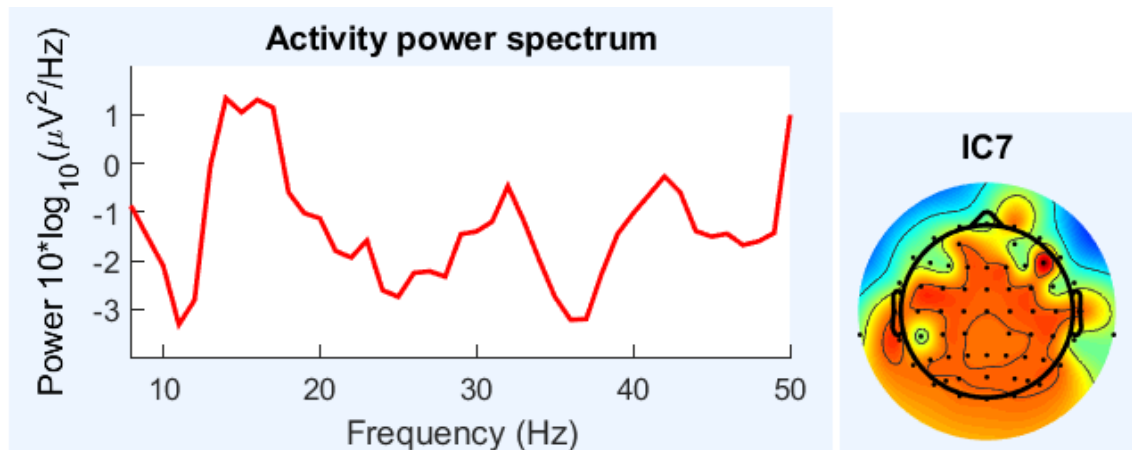
Figure 105: Activity power spectrum plot

Activity power spectrum corresponding to component 7 for subject 23 for RHI experiment 1.

Overall, all the subjects in first experiment experienced an increase in neural activity with differences in intensity and the initiation time except for subject 26 which has not experienced any increase in neural activity. This result was expected since human brain reacts differently towards brain manipulation technique depending on many factors such as (gender, authentic, and age) (Faivre et al., 2017).

Invisible hand

In invisible hand experiment the rubber hand was removed. Each subject was analysed using similar parameters, plots and graphs as shown in in the previous section. Neural activity experienced by subjects in this experiment was slightly less in intensity than the classical RHI, where two out of twenty eight subjects did not experience the change in neural activity. A sample of the main results is represented in this section.

2-D Spectral Component heat- Map

The graph plotted by EEGLAB was similar to first experiment in regards to change in all component, to make the comparison easier for the rest of the experiment only two component from right and left hemisphere was compared at the beginning and end of the experiments.

Figure 106 is a demonstration the spectral components heat-maps of subject 4 for the first and last 100 sec of the 300sec experiment time for Components 1 and 3. Figure 108-A and 108-B are showing decrease in power for the beginning of the experiment for

component 1 and 3, while they increase the power in last 100sec of experiment which is shown in figure 108-C and 108-D.
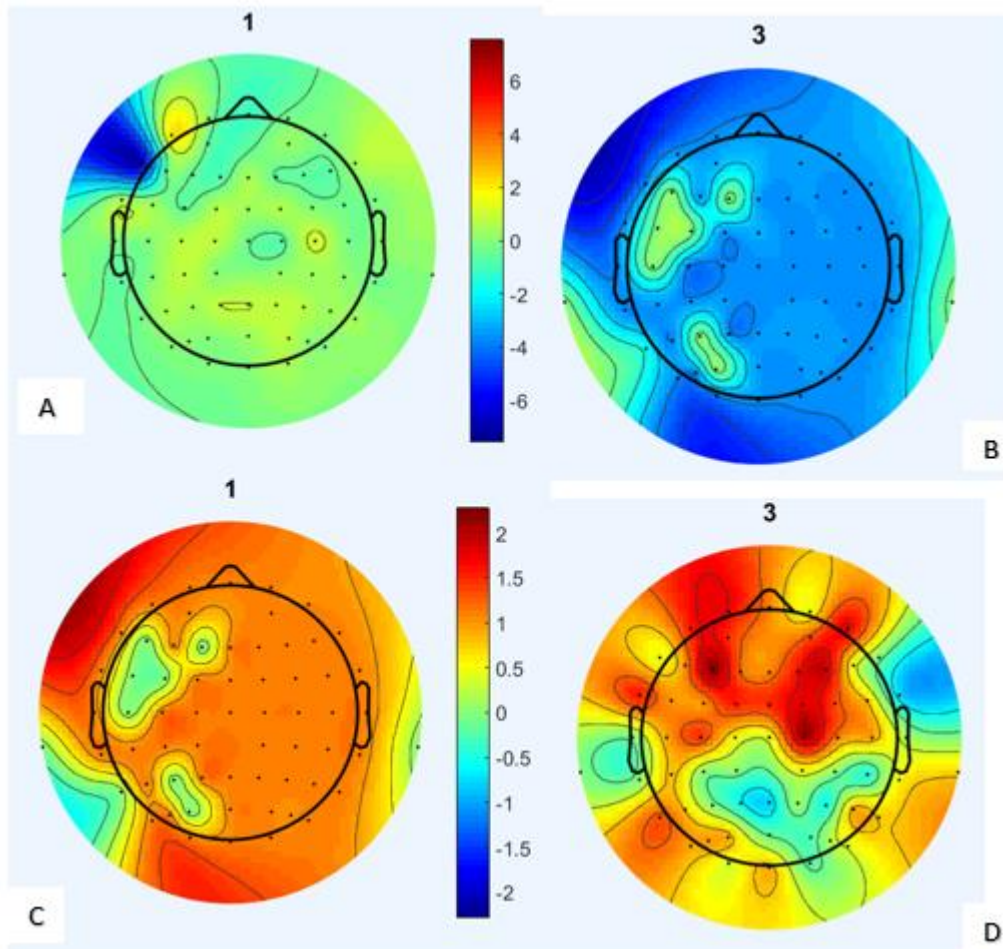
Figure 106: Spectral Components heat-map at the beginning and end of the invisible hand experiment.

The heat-map of subject-4. A and B for the first 100 second. C and D for last 100 seconds

For this experiment twenty-six out of twenty-eight subjects experienced an increase in neural activity with differences in intensity and the initiation time.

Opposite hand

Similar to the first two experiment, neural activity was analysed in opposite hand illusion for each subject. The main objective was to determine if the conditioning of previous experiments was successful. Neural activity experienced by subjects in this experiment was the same in intensity to invisible hand, where two out of twenty eight subjects did not experience the change in neural activity. A sample of the main results is represented in this section.

Demonstrated in Figure 107 (A) a spectral component heat-Map represents channel 34 (B) a spectral component heat-Map represents channel 35 over the first 100ms and (C) a spectral component heat-Map represents channel 34 (D) a spectral component heat-Map represents channel 35 over last 100ms of experiment for subject 20 which shows the increase in activity. This pattern of activity suggests that illusion did occur during the experiment.
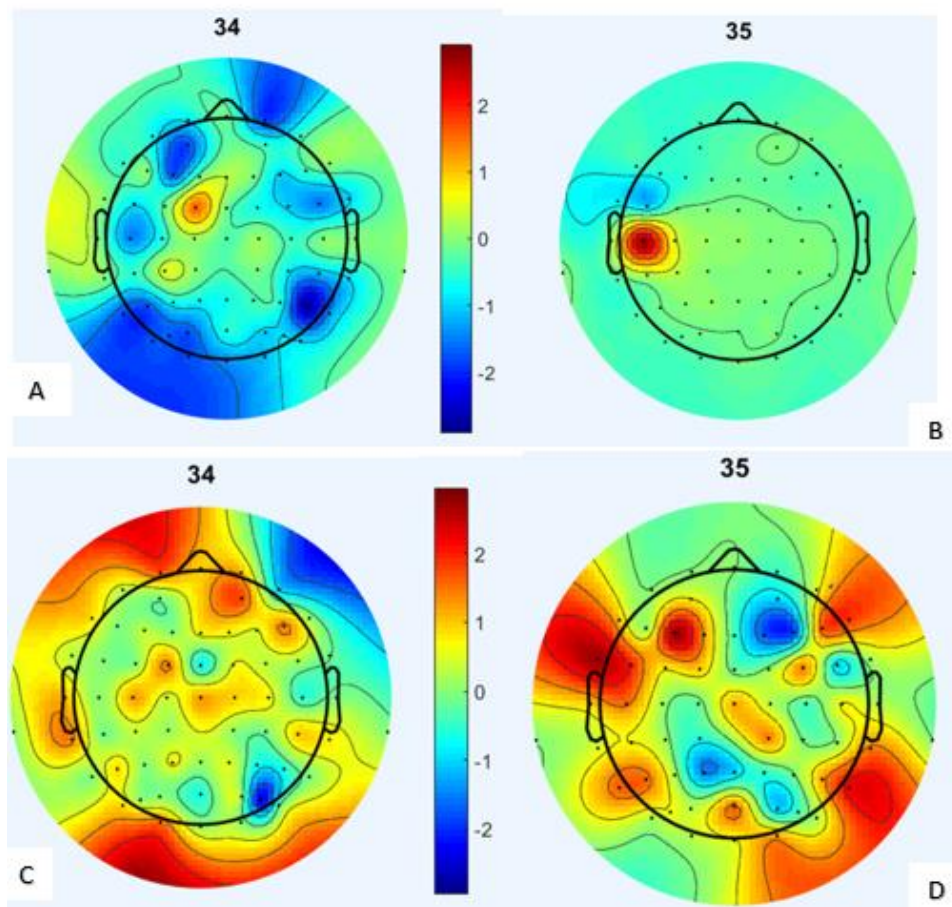
Figure 107: Spectral Components heat-map at the beginning and end of the Opposite hand experiment.

The heat-map of subject-20. A and B for the first 100 second. C and D for last 100 seconds

Overall, all the subjects in this test experienced an increase in neural activity with differences in intensity and the initiation time except for two who did not experience any increase in neural activity. The outcome of this experiment is comparable to that of the classical RHI.

Rotated hand

The main objective of rotated hand experiment is to determine if conditioning in previous experiments was successful and can work on different location of the hand by repeating the steps of classical experiment. Neural activity experienced by subjects in this experiment was less than previous experiments in intensity, where four out of twenty eight subjects did not experience the change in neural activity. A sample of the main results is represented in this section.

2-D Spectral Component heat- Map

Figure 108 indications the change in spectral heat-map for subject 22. (A) a spectral component heat-Map represents channel 5 (B) a spectral component heat-Map represents channel 7 over the first 100ms and (C) a spectral component heat-Map represents channel 5 (D) a spectral component heat-Map represents channel 7 over last 100ms of experiment demonstrate the increase in activity. This figures proves that illusion appears at the end of the test.
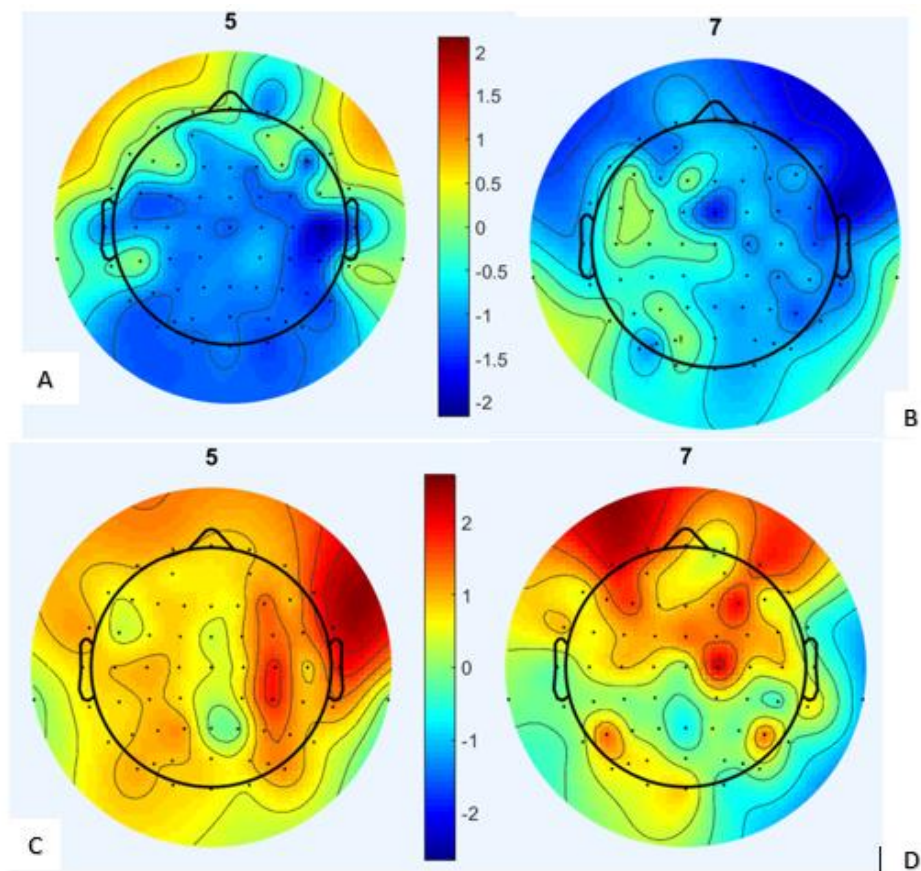
Figure 108: Spectral Components heat-map at the beginning and end of the Rotated hand experiment.

The heat-map of subject-22. A and B for the first 100 second. C and D for last 100 seconds

Total of twenty-four subjects showed neural activity during the experiment. This result is similar to that of the classical RHI.

Conspicuous hand

The main objective of conspicuous experiment is to investigate if three hand consolidate the effect of hand ownership. Neural activity experienced by subjects in this experiment was the same as classical rubber hand experiment in intensity, where one out of twenty eight subjects did not experience the change in neural activity. Representative results are presented in this section.

2-D Spectral Component heat- Map

Figure 109 (A) a spectral component heat-Map represents channel 37 (B) a spectral component heat-Map represents channel 40 over the first 100ms and (C) a spectral component heat-Map represents channel 37 (D) a spectral component heat-Map represents channel 40 over last 100ms of experiment demonstrate the increase in activity in participant 6. This records verifies that illusion appears at the end of this setting.
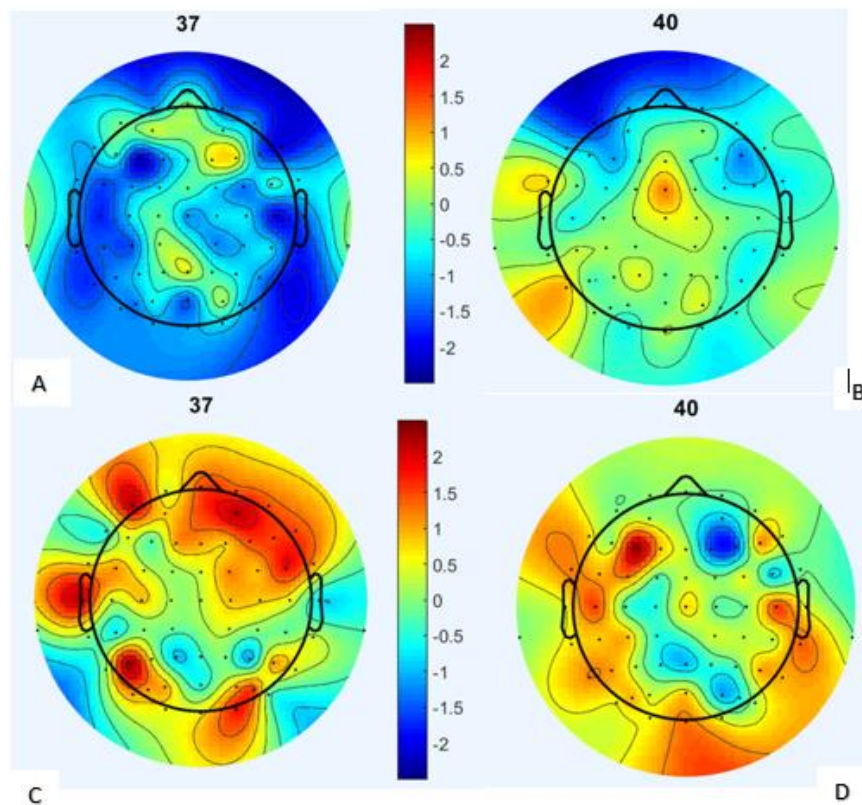
Figure 109: Spectral Components heat-map at the beginning and end of the conspicuous hand experiment.

The heat-map of subject-6. A and B for the first 100 second. C and D for last 100 seconds

Blindfolded

In blindfolded experiment, the main objective was to remove visual input by blindfolding the subject and relying on only tactile sensation. Each subject was analysed using similar parameters, plots and graphs as shown in in the previous sections. Neural activity experienced by subjects in this experiment was lowest in intensity compare to other experiments, where nineteen out of twenty-eight subjects experience the change in neural activity. A sample of the main results is represented in this section.

2-D Spectral Component heat- Map

The spectral components heat-maps of subject 28 as shown in Figure 110 indicates a slight increase in neural activity in components 33 and 36.
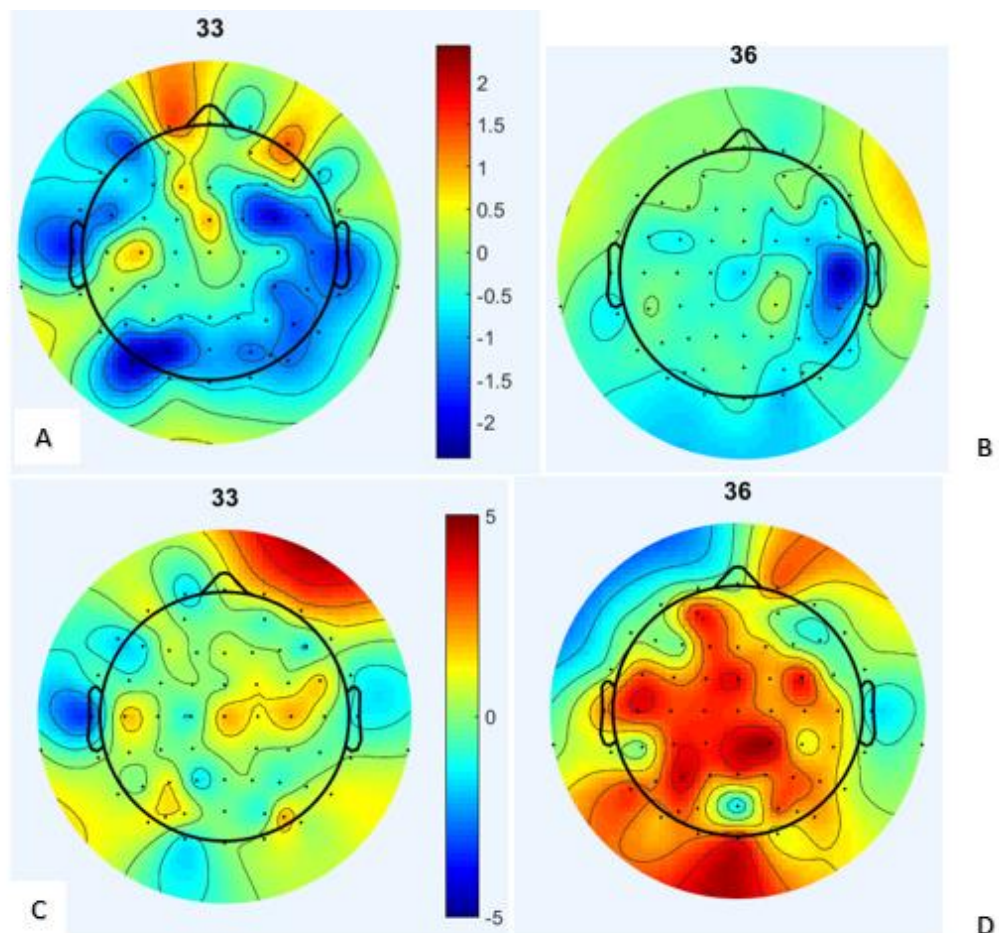
Figure 110: Spectral Components heat-map at the beginning and end of the conspicuous hand experiment.

The heat-map of subject-28. A and B for the first 100 second. C and D for last 100 seconds

The event-related spectral power (ERSP) plot of electrode 12 of subject 11 exhibited in Figure 111. After signal processing by using ICA, BSS, baseline removal, and FFT but without extracting the epochs. This time-frequency plot indicates dyssynchronous signals which translate to a reduction in power at a certain time in the given frequency range. The blue vertical patches refer to reduction in power (desynchronized) which can be related to the brush strokes. A decrease in power of alpha and beta waves at between 2000- 4000 ms and then slightly increased again after that point.
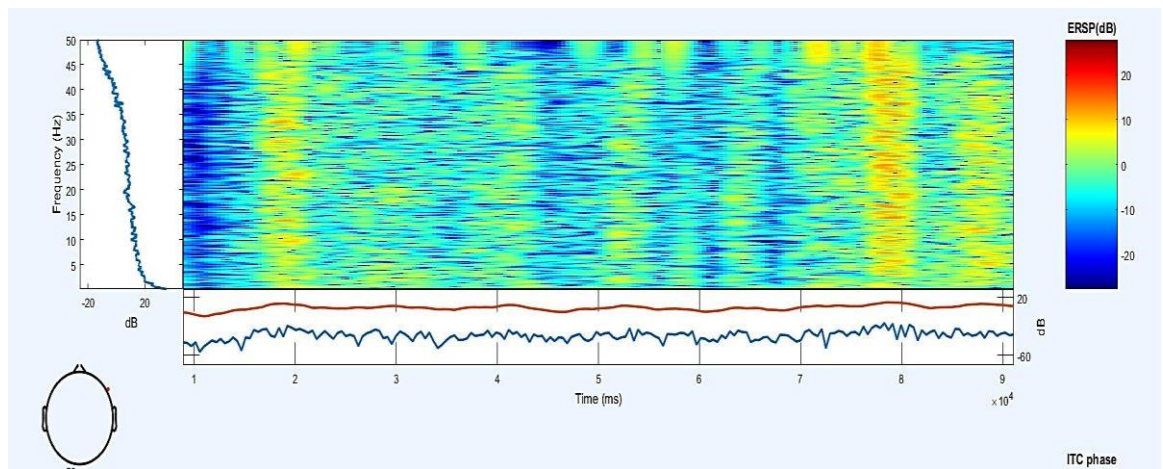
Figure 111: ERSP plot

An event-related spectral power (ERSP) plot of subject 11 in blindfolded experiment

Likewise, Figure 112 for subject 19 for same electrode position (component 12) in the frontal lobe showing similar neural behavior.
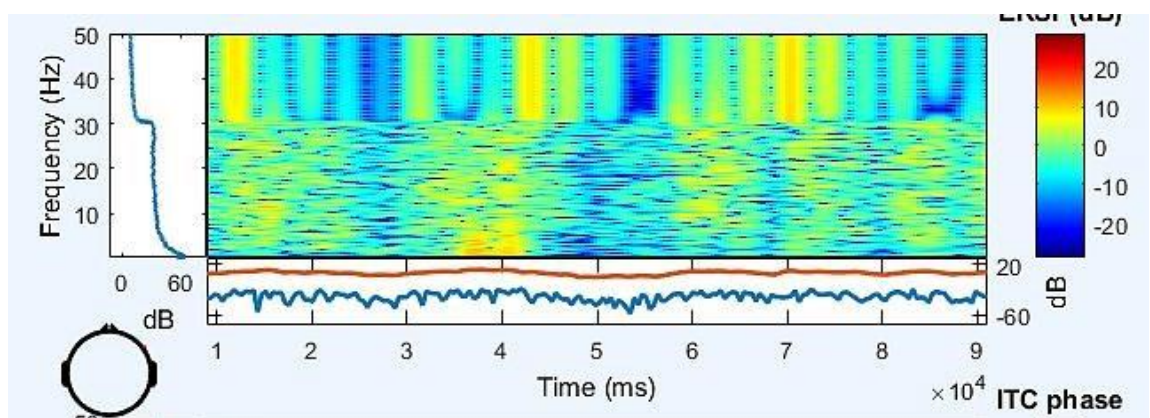
Figure 112: ERSP plot

An event-related spectral power (ERSP) plot of subject 19 in blindfolded experiment

When extracting the epochs the time-frequency analysis with event-related spectral power (ERSP) plot in Figure 113 for Subject 11 which shows an increase in neural activity in the gamma wave (greater than 35 Hz), theta and delta (less than 7 Hz) waves but no activity within the alpha and beta waves range, which are of particular interest for the purposes of this study. Unlike subject 11, subject 19 experienced an increase in the neural activity within alpha and beta waves at 400ms after the experiment started as shown in Figure 114.
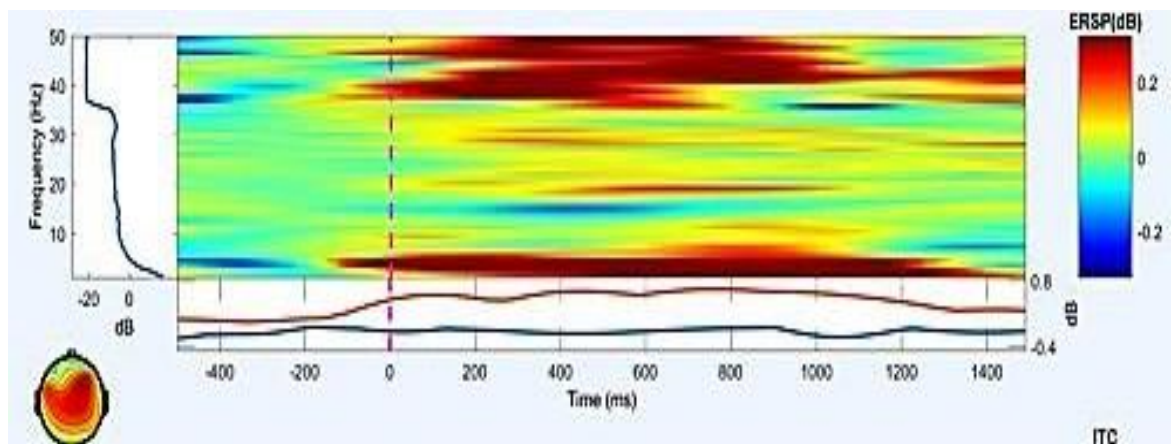
Figure 113: Time-frequency plot with ERSP

Time-frequency plot with ERSP for subject 19 by component 12 in blindfolded experiment
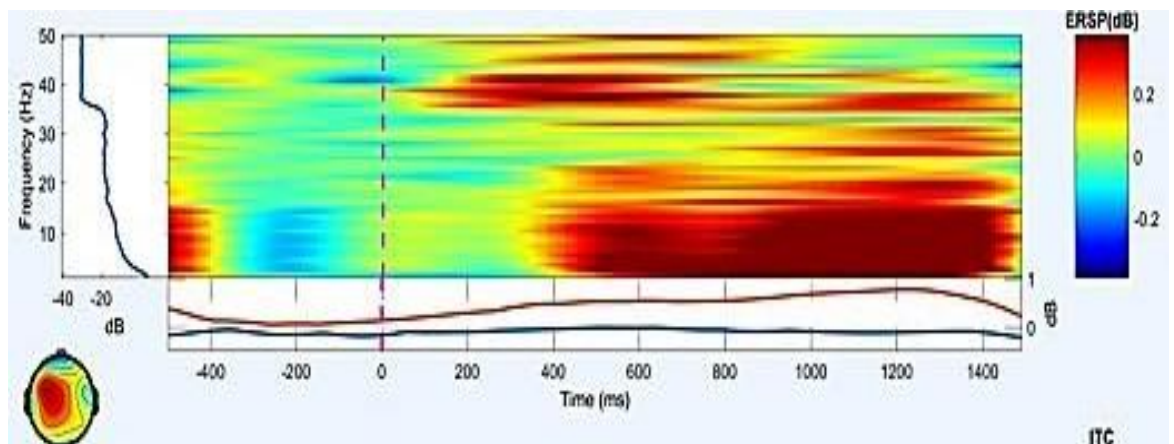
Figure 114: Time-frequency plot with ERSP

Time-frequency plot with (ERSP) for subject 11 by component 12 in blindfolded experiment

To sum up the results for this section, the number of subjects who experience an increase in neural activity in response to each experiment is shown in percentages in table 18.

Table 18: Number of subjects with neural activity in response to RHI set of experiments

Experiment	Neural activity (N=28)
Classical RHI	27 (96.42%)
Invisible Hand Illusion	26 (92.86%)
Opposite hand illusion	26 (92.86%)
Rotated hand illusion	24 (85.72%)
Conspicuous hand Illusion	27 (96.42%)
Blindfolded	19 (67.86%)

In the classical RHI and altered versions, change in Brain signal across temporal, parietal and frontal regions are similar to previous studies (Zeller et al. 2015; Rao & Kayser, 2017). The heat map at the beginning and end of the experiment indicate the evolution of change in brain response to the illusion as there was increased neural activity towards the end of the experiment whereas in premotor cortex cell's electrical activities lessened which indicated that brain stop seeing real hand as a part of the body, same reaction happens during brain damage, like brain stroke, that patients absolutely persuaded that limb is no longer belong to their body and it is someone else's body (Space, 2016) . These findings are incompatible with; the fMRI results found by Ehrsson et al. (2004) indicated three primary neural processing engaged with producing the RHI. Initially, coordination between the different types of sensory data that the subject is being given results in multisensory integration that happens in the parietal areas. In particular, the ventral premotor cortex, visual and somatosensory cortex and frontal motor area. Ultimately, the self-attribution of the rubber hand, at the core of the deception, goes on in the bilateral premotor cortex (Ehrsson et al., 2004).

Moreover, there was a reduction in alpha and beta oscillatory activity, and this has been shown to be a reliable marker for RHI (Rao & Kayser, 2017; Evansa & Blankea, 2015; Lenggenhager et al., 2011). Answers to the questionnaire reflect the experience of illusionary ownership by participants as was seen in the original study by (Botvinick &

Cohen, 1998). Furthermore, the results of the questionnaire corroborate that seen in EEG as there was a strong sense of hand-ownership.

Although the sign of illusion appeared in all set ups, invisible hand shows brain can be convinced there is unseen hand attached to the body, this set up is best set up to be used as a treatment of PLS, by stroking different size and shape of invisible hand. Using opposite hand and palm of the hand does not stop the brain to rearrange itself and respond to the third arm. Results from conspicuous set up is the evidence that body representation can be updated and it is possible to convince people they have three arms.

To investigate the effect of visual cues on brain, blindfolded experiment was designed. There are few studies in the literature pertaining to the RHI in the blind despite the suffering blind people with phantom limb pain (PLP) endure. It is therefore imperative to understand the effect of visuo-tactile stimulation on the brain to better aid the blind who suffer from PLP. RHI studies on blindfolded subjects act as a proxy to the blind and help to better inform us on possible therapeutic avenues.As in the classical RHI experiment, there was a reduction in alpha and beta oscillatory activity and sense of ownership experienced by the subjects in blindfolded experiment. It is important to note the presence of neural activity and self-attribution despite the loss of visual input, albeit of less strength than that seen in the classical RHI experiment and it took longer time than other experiment. Therefore, exclusion of visual input contributed to a decrease in the effect of RHI and may suggest that a comparable level of the neural activity seen in the classical RHI experiment may be reached given a longer stimulation period. Another important note is that results and recommendations from RHI experiments on the blindfolded may translate to those who lost their vision after the age of six (Sadato et al., 2002) or after the age of 12 (Büchel et al., 1998).

Moving hand

Moving hand performed in three bases as explained in previous section. The main aim of this experiment was to examine the conditioning idea. For each day of experiment data was analysed using similar parameters, plots and graphs as shown in RHI section. Classical RHI is used as baseline.

The spectral components heat-maps of subject on day 7 is shown in Figure 115. (A) spectral component heat-Map represents channel 4 Base 1 (C) spectral component heat-Map represents channel 4 Base 2 (E) spectral component heat-Map represents channel 4 Base 3 over the first 100ms and (B) a spectral component heat-Map represents channel 4 Base 1 (C) spectral component heat-Map represents channel 4 Base 2 (F) spectral component heat-Map represents channel 4 Base 3 over last 100ms of experiment demonstrate the increase in activity in participant during moving hand experiment.
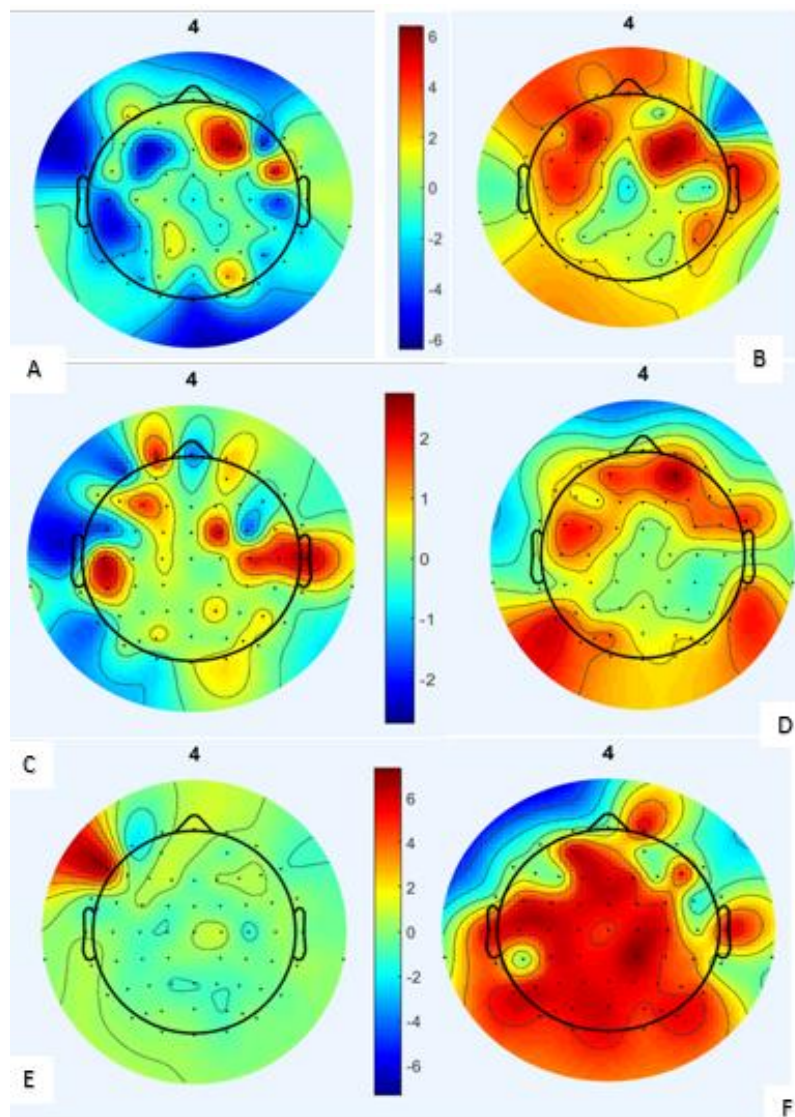
Figure 115: Spectral Components heat-map at the beginning and end of the moving hand experiment day 7

A, C and E are for the first 100 second. B, D and F for last 100 seconds

Changes of spectral power and event-related potential on day 10 are shown in Figure 116 for electrode 12. In the graph below, the red and blue regions refer to the spectral change in power. It shows that that the beta band power reduces at around 20 Hz which can be seen by the horizontal blue line. During the period of 200 to 1400ms, there is a slight reduction in alpha band power around 11-12Hz. This reduction remains low in intensity as compared to beta band power reduction (Rao & Kayser, 2017).
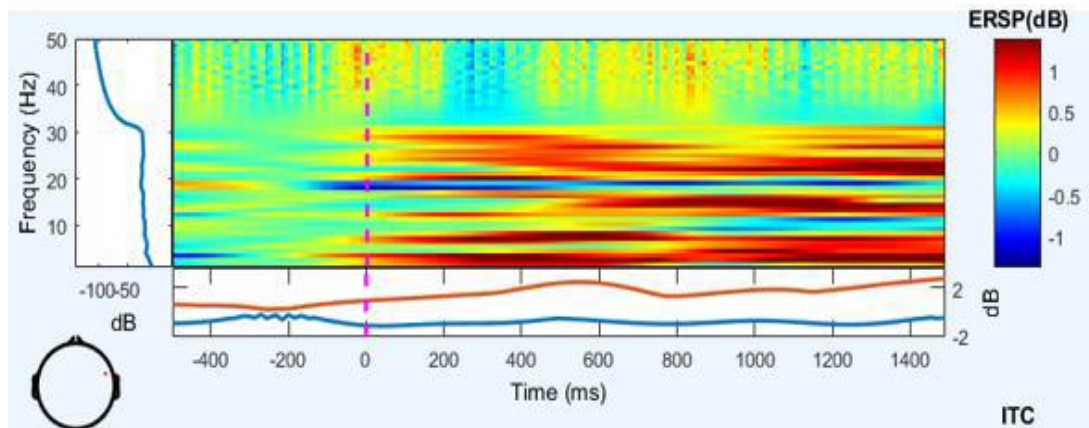
Figure 116: Time-frequency plot for ERSP

Time-frequency plot with ERSP for subject 9 in opposite hand experiment

To recap the moving hand effect, the number of days subject experience an increase in neural activity in response to the experiment is shown in tables 19.

Base	Neural activity (N=20)
Base 1	19 (95%)
Base 2	19 (95%)
Base 3	19 (95%)

Moving hand set up established two main finding, first the distance between the real hand and rubber hand effects the illusion also, conditioning will happen over the time as such the participant was reacting to illusion after each try and it will store in memory as the gaps in days did not interrupt the speed of experiment.

SGS

SGS experiment was performed during 30 days on four participants. Participant would go through three different settings as explained in chapter 5. For each day of experiment

data was analysed using similar parameters, plots and graphs as shown in RHI section. The main aim of this set up was to investigate the possibility of replacing vision with sound and also explore the prospective of retrieving sensation using other senses.

2-D Spectral Component heat- Map

The spectral components heat-maps of right handed female on day 1 component 8 is shown in Figure 117. (A) spectral component heat-Map represents for setting 1 (C) spectral component heat-Map represents setting 2 (E) spectral component heat-Map represents setting 3 over the first 100ms and (B) a spectral component heat-Map represents setting 1 (D) spectral component heat-Map represents setting 2 (F) spectral component heat-Map represents setting 3 over last 100ms of experiment demonstrate the increase in activity in participant during the experiments.
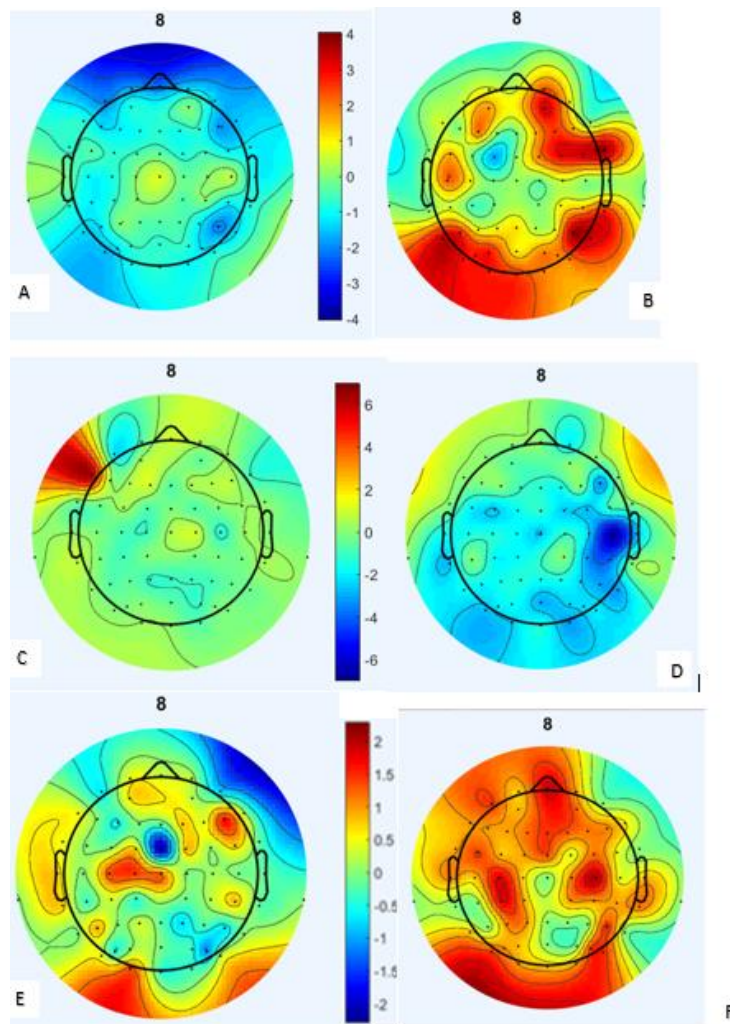
Figure 117: Spectral Components heat-map at the beginning and end of the SGS experiment day 1

A, C and E are for the first 100 second. B, D and F for last 100 seconds

The spectral components heat-maps of right handed female on day 30 component 9 is shown in Figure 118. (A) spectral component heat-Map represents for setting 1 (C) spectral component heat-Map represents setting 2 (E) spectral component heat-Map represents setting 3 over the first 100ms and (B) a spectral component heat-Map represents setting 1 (D) spectral component heat-Map represents setting 2 (F) spectral component heat-Map represents setting 3 over last 100ms of experiment demonstrate the increase in activity in participant during the experiments.
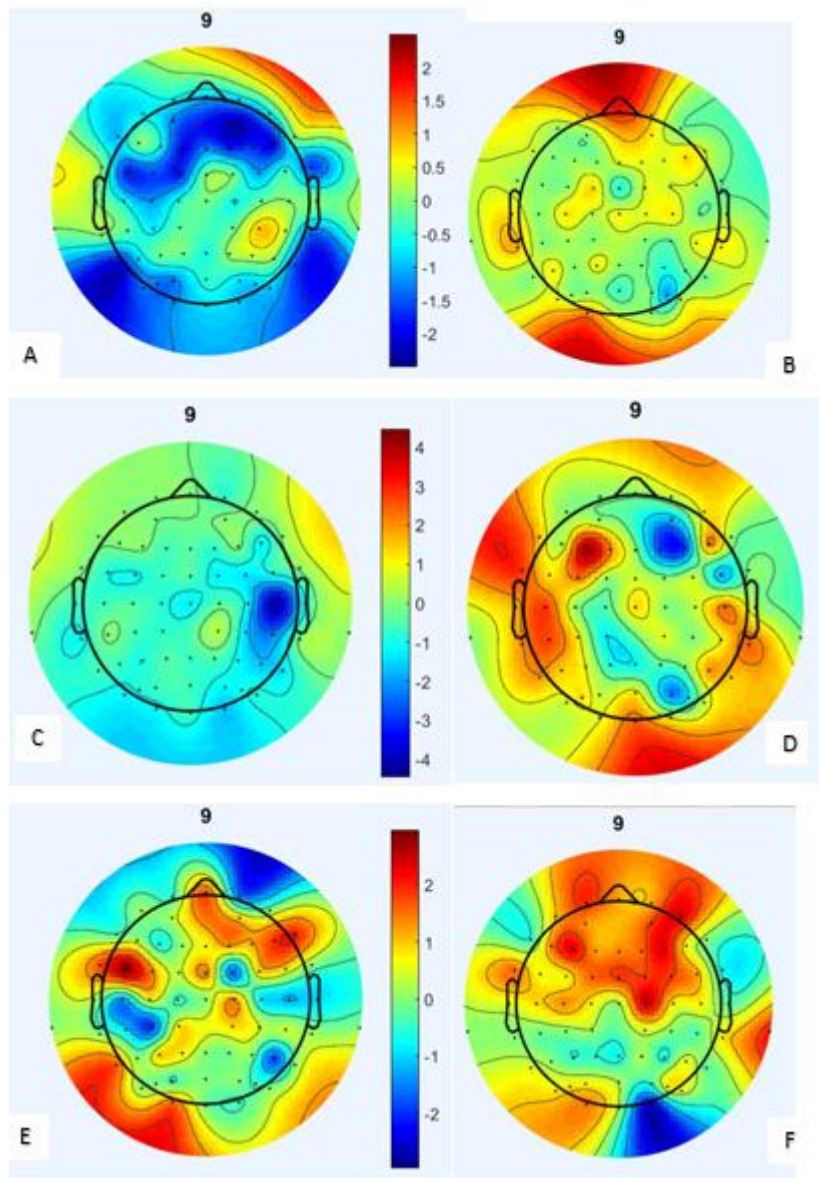
Figure 118: Spectral Components heat-map at the beginning and end of the SGS experiment day 30

A, C and E are for the first 100 second. B, D and F for last 100 seconds

Time-frequency analysis of the changes event-related spectral power (ERSP) plot is generated after signal processing using FIR, ICA, BSS, baseline removal, epoch extraction and FFT. Time plot where the zero-time mark indicates the time point at which object was introduced. This plot represents coloured cluster that expresses the strength of the neural activity with respect to time. In the graph, the X-axis denotes to time in Mille seconds (ms), and Y-axis denotes to the frequency in hertz (Hz), where the rectangle boxes lying on the both axis displays the variation in neural activity with respect to frequency and time.

Figure 119 shows a reduction of the time-frequency plot for right handed male on day 1 where the red and blue region that refers to the spectral change in power. The beta band power increases in a wave of alpha waves (7-13 Hz) and beta waves (13-35 Hz) starts after 1000ms after the stimulus was introduced (Kanayama et al., 2007). These changes were concentrated in the right and left fronto-parietal, temporal and frontal regions of the brain.

Unlike Day30 in Figure 120 the increase in activity initiating right after the stimulus was introduced and growing stronger towards the end of the experiment which may imply that the illusion has occurred. Then the activity get stronger towards the end of the experiment which may imply that the illusion was successful. These changes were concentrated in the central-temporal, region of the brain as shown in the same graph.
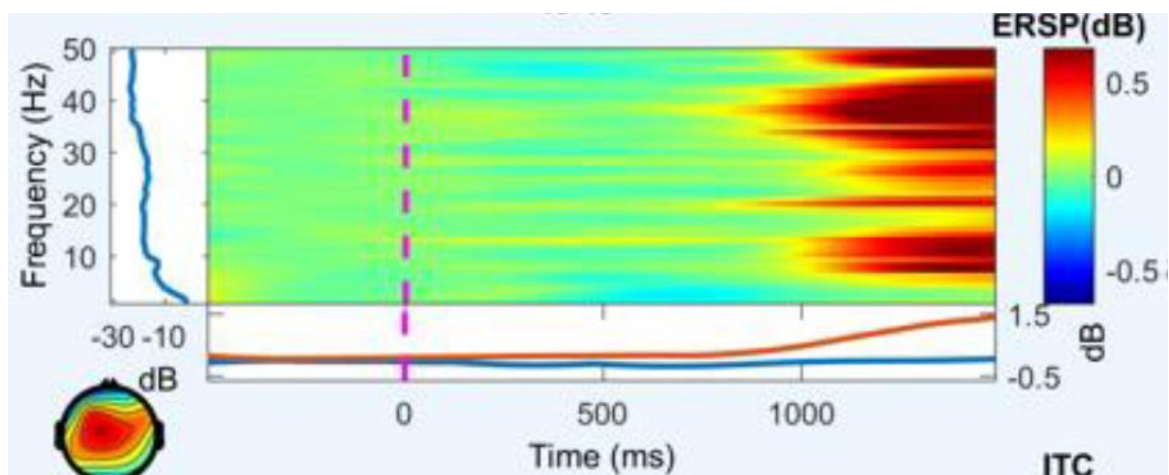
Figure 119: Time-frequency plot ERSP

Time-frequency plot with ERSP for Day 1 R.M.

To summarize the results for SGS, the number of days subjects experience an increase in neural activity in response to the experiment is shown in percentages in tables 20.

Table 19: Number of days subjects showing neural activity in response to SGS

Subjects	Neural activity (N=30)
Right-Handed Female	27 (90%)
Left-Handed Female	29 (96.6%)
Right-Handed Male	26 (86.6%)
Left-Handed Male	28 (93.3%)

The changes detected in the blind people's brain in terms of the functional and structural illustrate that the brain exclusively organises, transfer neural signals in a unique way that is not detected in sighted people. In particular, the decline in neural activity was detected in the occipital cortex (visual processing parts). Alternatively, an increase in neural activity was detected in brain cortices connected to movement, speech, and auditory, which possibly support the increase requirements located on these cortices in blind people. The occipital cortex in blind people is not damaged. However, it works differently when dealing with visual input (Burton et al., 2001). Recent studies confirm that blind people can utilise auditory input to detect the sources of sound also, sound-reflecting items (echolocation) (Nilsson & Schenkman, 2016). In the case of, Daniel Kish, (early blind) was capable of utilising echolocation to view the world (Gougoux et al., 2005).

Since the brain can adapt changes naturally when vision is missed, Blind people can detect sounds utilising both the occipital lobe and the auditory cortex, while, in sighted people, they utilise auditory cortex only (Kolarik et al., 2014).

The change in brain wave before, during and after the experiments propose that illusion can appear in form of the sound. The time is reduced significantly for this change to happen which suggest the conditioning in human brain. In day 29 and 30, participants claimed they could feel the temperature few minutes after training was stopped, this claim was supported by electrical wave of the brain.

All-encompassing

There have been numerous studies conducted over the past century on the subjective effects of body ownership illusion and its effects but very few studies examined whether this can be used for benefit of amputee patients.

When wearers have ability to feel through prosthetics, they can sees it as parts of their bodies and resumes more function. The main part and biggest challenge of this project was using illusion to replicate human feeling. The project has to mimic human sense of temperature as closely as possible, and must be as comfortable as possible.

Finding alternative way for person to recognize his/her own body rather than visional and tactile was another involvement. The outcomes of this report show similar responses in brain between both audio and visual feedback. The EEG results presented here provide understandings to mechanism of liable for body imaging. This finding can be used in future researches to reduce phantom sensation for blind patients as well as bringing them their sensation back in event of amputation.

In RHI experiments, the fundamental self-awareness question was answered. It also confirmed the statement of Ehrssonlab.se (2015) and showed how the brain characterizes the location, movement and force of limb. It also examined the awareness of acting self and how basic multisensory perception can be induced by mental imagery and how the brain differentiate between internally formed thoughts and real percepts produced by events in the external world

Chapter 8: Conclusions and Future work

This chapter conclude and review the finding of this project, following by list of contributions made in this work; it also makes suggestion for future work.

8.1 Conclusions

"When vision and touch conflicts, then vision is the dominant sense" (Rock and Victor, 1964).

The main question that was answered in this work was whether or not it is possible to make amputees feel through artificial limbs and make a connection between patients and the device using audio feedback. The SGS device met its purpose of bringing tactile feedback (temperature feedback) to the subjects. This illusionary feedback did not last long but it can create the habit in the brain by being repeated. EEG recorded presented an interesting reaction of the brain when subject was experiencing this tactile illusion. This system can be improved by using better and more sensitive sensor and needs to be tested in real patients to see it performance more clearly. EEG results in RHI and its modified versions are very comparable and it suggests that gender difference exist in perception of body transfer illusion. Visual input can be induced to trick the brain it also backed this theory the brain rearranges its sensory precision control so its attention allocation. Furthermore, the finding of blindfolded experiments implies that feeling of body ownership comes from multisensory signals rather than visual. Comparing the results between right-handed and left-handed individuals verify that left-handed can feel the illusion more than the right-handed.

Phantom limb pain (PLP) is a serious status and greatly affects the quality of life of amputees. Another aim of this study was to understand the effect of visual, tactile, proprioceptive and auditory input integration to aid amputees in registering the prosthetic as informed by the principles of body-ownership illusion.

In this study, EEG signal processing using EEGLAB and MATLAB in addition to questionnaires were used to determine the effect of Rubber Hand Illusion (RHI) on changes in brain signal and sense of ownership by participants. The findings of this study

highlight that despite excluding visual input, the capability of experiencing illusionary ownership in the blindfolded state persisted. The findings also suggest that addition of auditory cues to the trisensory visuo-tactile proprioceptive input of classical RHI may consolidate in changes of brain signal and ownership experienced.

The outcome of this study was conducted in the research lab, to carry it on real patients with PLP or blindness, further considerations need to be made.

8.2 Summary of contributions made in this work

This study yielded four main finding:

First, the results confirmed that the feeling of ownership and agency can be separated, proposing that these sensations represent independent process of the human brain.

Second, the outcome of the experiments shows that illusion happens in male and female differently. The collected brain signal as well as questionnaire data suggests that male will react faster than the female also the left handed group need more time to respond to the illusions.

Third findings of this study highlight that auditory signals may aid in registering a prosthetic in blind amputees by compensating for the loss of visual input. A challenge of body-ownership illusion in the blind is the loss of vision which complicates the registration of a prosthetic. This study points the usefulness of using blindfolded subjects as a proxy to inform on best practice methods and effective strategies in dealing with PLS in the blind.

Finally, proven that brain has ability to learn and capacity to remap itself and is response to the new signals. SGS experiment proved that illusion can appear faster and last long. Human senses can be retrieved using remaining senses and by rewiring brain map.

8.3 Further development and ideas for the future work

The findings of this study concur the importance of the integration of visual, tactile, proprioceptive and auditory input integration to the induction of body ownership illusion.

It is important, however, to repeat the experiments on a larger number of participants to ensure reproducibility of results and reliability of its outcomes. This study can then be carried forward by using the paradigms of RHI on blind amputees with the objective of improving their PLP and amputee for sense of touch. It is important to note that two groups of blind subjects – those who lost vision at birth and those who lost vision after being sighted – are included to explore differences in their capability to experience a sense of ownership.

The limited resources available affected the experiments and considerations would need to be made about how to allocate better funding for the model. A Main suggestion for further work proposed in this part is progresses in construct the sensitivity of the hand on the user.

The SGS device should be tested on both normal subjects and below the elbow hand amputee. More reliable temperature sensor should be used; they should be more sensitive to thermal and smaller so it can be attached to such a prosthetic hand, perhaps using multiple sensors can help faster the process of feedback but can conflict with right temperature, so programming needs to be more advanced.

Another consideration would be using verity of sensors such as pressure sensor, vibration sensor and etc. to replicate human feeling as closely as possible. As illusion method is used in this report, adding different input needs different type of output so brain can recognize and identify these inputs, therefore, using skin vibrator can be option, wider range of sound frequency can also be considered.

Computer feeds SGS system, and the size of this device is not right to be attached to designed hand, thus finding alternative charging way is recommended also smaller board can help connecting it to prosthetics like the one described here.

Extend the study to another illusionary condition using new technology like visual reality can speed up the process of learning and feedback training.

Bibliography

Aalborg University, (2013). *EU FUNDS 6 MILLION EURO FOR NEW TECH SOLUTIONS TO COMBAT PHANTOM LIMB PAIN.* [Online] Available at: http://www.en.aau.dk/news/show-news/eu-funds-6-million-euro-for-new-tech-solutions-to-combat-phantom-limb-pain.cid123977

Abhishek, P. & Vali, S. M. (2016). Implementation of a FFT using High Speed and Power Efficient Multiplier. *International Journal of Electronics & Communication Technology,* 7(1), pp. 28-32.

Agarwal, R., Gotman, J., Flanagan, D. and Rosenblatt, B. (1998). Automatic EEG analysis during long-term monitoring in the ICU. *Electroencephalography and Clinical Neurophysiology*, 107(1), pp.44-58.

Al-ani, T. & Trad, D. (2010). Signal Processing and Classification Approaches for Brain-Computer Interface. In: V. S. Somerset, ed. *Intelligent and Biosensors.* Cape Town: InTech, pp. 25-66.

Al-Fahoum, A. and Al-Fraihat, A. (2014). Methods of EEG Signal Features Extraction Using Linear Analysis in Frequency and Time-Frequency Domains. *ISRN Neuroscience*, 2014, pp.1-7.

Amputee Coalition. (2016). *Limb Loss Statistics - Amputee Coalition*. [online] Available at: http://www.amputee-coalition.org/limb-loss-resource-center/resources-by-topic/limb-loss-statistics/limb-loss-statistics/.

Andreassi, J. L. (2007). *Psychophysiology: Human Behaviour & Physiological Response.* 5th ed. New Jersey: Lawrence Erlbaum baum Associates.

Andrei, M. (2015). *First prosthetic arm that offers sensations*. [online] ZME Science. Available at: http://www.zmescience.com/medicine/mind-and-brain/paralyzed-man-darpa-prosthetic-15092015/.

Antfolk, C., D'Alonzo, M., Rosén, B., Lundborg, G., Sebelius, F. and Cipriani, C. (2013). Sensory feedback in upper limb prosthetics. *Expert Review of Medical Devices*, 10(1), pp.45-54.

✦ Ant-neuro.com. (n.d.). *ANT Neuro | inspiring technology for the human brain*. [online] Available at: https://www.ant-neuro.com/.

✦ Aofas.org. (2013). *Fewer Americans Undergoing Lower Limb Amputation*. [online] Available at: http://www.aofas.org/news-center/press-releases/Pages/2013-Press-Releases/Fewer-Americans-Undergoing-Lower-Limb-Amputation.aspx.

✦ Asghari Oskoei, M. and Hu, H. (2007). Myoelectric control systems—A survey. *Biomedical Signal Processing and Control*, 2(4), pp.275-294.

✦ Awang, S., Paulraj, M. and Yaacob, S. (2012). Analysis of EEG signals by eigenvector methods. *2012 IEEE-EMBS Conference on Biomedical Engineering and Sciences*, pp.778-783.

✦ Başar, E. (1998). *Brain Function and Oscillations.* Hermann Haken ed. s.l.:Springer.

✦ Bassareo, V. and Di Chiara, G. (1999). Modulation of feeding-induced activation of mesolimbic dopamine transmission by appetitive stimuli and its relation to motivational state. *European Journal of Neuroscience*, 11(12), pp.4389-4397.

✦ Bauer, C. M. et al. (2017). *Multimodal MR-imaging reveals large-scale structural and functional connectivity changes in profound early blindness*. PLOS ONE , Volume doi.org/10.1371/journal.pone.0173064 , pp. 1-26.

✦ Beauchamp, M., Nath, A. and Pasalar, S. (2010). fMRI-Guided Transcranial Magnetic Stimulation Reveals That the Superior Temporal Sulcus Is a Cortical Locus of the McGurk Effect. *Journal of Neuroscience*, 30(7), pp.2414-2417.

✦ Bebionic.com. (n.d.). *The bebionic 3 myoelectric hand product - features - bebionic*. [online] Available at: http://bebionic.com/the_hand/features.

✦ Bebionic.com. (n.d.). *The world's most advanced Prosthetic Hand - bebionic*. [online] Available at: http://bebionic.com/.

✦ Belter, J., Segil, J., Dollar, A. and Weir, R. (2013). Mechanical design and performance specifications of anthropomorphic prosthetic hands: A review. *The Journal of Rehabilitation Research and Development*, 50(5), p.599-618.

Biology. (2017). *Central Nervous System- Parts & Cells Involved | Neurons | Glia*. [online] Available at: https://byjus.com/biology/central-nervous-system/.

Bisawarna, I. (2013). *EEG electrode placement for motor imagery, Y01-M01-D10*. [online] Drhdrdro.blogspot.co.uk. Available at: http://drhdrdro.blogspot.co.uk/2013/09/eeg-electrode-placement-for-motor.html.

Blahut, R. E. (1985). *Fast Algorithms for Digital Signal Processing*. 1st ed. s.l.:Addison-Wesley.

Braverman ER, Blum K, Smayda S.J.-A. commentary on brain mapping in sixty substance abusers: Can the potential for drug abuse be predicted and prevented by treatment? Curr Ther Res, October 1990.

Bobele, G. (1990). Book Review: Fundamentals of EEG Technology. Volume II: Clinical Correlates, by F.S. Tyner, J.R. Knott, and W.B. Mayer, Jr. Published in 1989 by Raven Press, New York, *Journal of Child Neurology*, 5(1), pp.73-74.

Boos, N. and Aebi, M. (2008). *Spinal Disorders*. Dordrecht: Springer, p.319.

Bosanqueta, D. C. et al. (2015). Systematic Review and Meta-analysis of the Efficacy of Perineural Local Anaesthetic Catheters after Major Lower Limb Amputation. *European Journal of Vascular and Endovascular Surgery,* 50(2), pp. 241-249

Botvinick, M. and Cohen, J. (1998). Rubber hands 'feel' touch that eyes see. *Nature*, 391(6669), pp.756-756.

Braverman, E. (1990). *Brain Mapping: A Short Guide to Interpretation, Philosophy and Future*. [ebook] Journal of Orthomolecular Medicine. Available at:
https://pdfs.semanticscholar.org/0330/a4732a35fba8f5a1fa7b395e72b67357aaa0.pdf.

Bretherton, I. (1992). The origins of attachment theory: John Bowlby and Mary Ainsworth. *Developmental Psychology*, 28(5), pp.759-775

Bruce, V., Georgeson, M. A. & Green, P. R. (2003). *Visual Perception: Physiology, Psychology and Ecology*. 4th ed. s.l.: Psychology Press.

Büchel, C., Price, C. & Friston, K. (1998). *A multimodal language region in the ventral visual pathway*. Nature, 394(6690), pp. 274-277.

Burton, H. et al. (2001). *Adaptive Changes in Early and Late Blind: A fMRI Study of Braille Reading*. Journal of Neurophysiology, 87(1), p. 589–607.

Camdir, J. (2015). *Researchers develop prosthetic leg that you can control with your brain*. [online] Digital Trends. Available at: http://www.digitaltrends.com/cool-tech/emg-prosthetic-leg/.

Campisi, P., La Rocca, D. and Scarano, G. (2012). EEG for Automatic Person Recognition. *Computer*, 45(7), pp.87-89.

Carter, R. (2014). *The Brain book 2nd edition*. London: A Penguin Random House company.

Chang, B. S., Schomer, D. L. & Niedermeyer, E. (2007). Normal EEG and Sleep: Adults and Elderly. In: A. S. B. a. S. B. Rutkove, ed. *The Clinical Neurophysiology Primer.* Totowa, NJ: Humana Press Inc., pp. 57-71.

Childress, D. (1973). Powered Limb Prostheses: Their Clinical Significance. *IEEE Transactions on Biomedical Engineering*, BME-20(3), pp.200-207.

Thorndike, E. L. (1898). Animal intelligence: An experimental study of the associative processes in animals. *Psychological Monographs: General and Applied,* 2(4), i-109.

Cipriani, C., D'Alonzo, M. and Carrozza, M. (2012). A Miniature Vibrotactile Sensory Substitution Device for Multifingered Hand Prosthetics. *IEEE Transactions on Biomedical Engineering*, 59(2), pp.400-408.

Clements, I. (2008). *How Prosthetic Limbs Work*. [online] Available at: http://science.howstuffworks.com/prosthetic-limb1.htm.

Clifford, G. (2008). BLIND SOURCE SEPARATION: Principal & Independent Component Analysis. *Biomedical Signal and Image Processing,* pp. 1-47.

Clinicalgate, (2017). *Clinically Oriented Neuroanatomy.* [Online] Available at: https://clinicalgate.com/clinically-oriented-neuroanatomy-meridians-of-longitude-and-parallels-of-latitude/

Clippinger, F., Avery, R. and Titus, B. (1974). *A SENSORY FEEDBACK SYSTEM FOR AN UPPER-LIMB AMPUTATION PROSTHESIS*. Durham, North Carolina: Bull. Pros. Res.22, pp. 247–258.

Cohen, L. (1995). *Time-frequency analysis*. Englewood Cliffs, N.J: Prentice Hall PTR.

Conzelman, J., Ellis, H. and O'Brien, C. (1953). *Prosthetic device sensory attachment*. US Patent 2656545.

Cooley, J. W. & Tukey, J. W. (1965). An Algorithm for the Machine Calculation of Complex Fourier Series. *Mathematics of Computation,* Volume 19, pp. 297-301.

Cooljargon.com. (2016). *Anatomy and Physiology - Muscles of the Pectoral Girdle and Upper Limbs*. [online] Available at: https://cooljargon.com/ebooks/anatomy_and_physiology/m46495/index.cnxml.html

Correa, G., E. L. ,. D. P. & Valentinuzzi, M. E. (2009). *Artifact removal from EEG signals using adaptive filters in cascade.* s.l., Argentine Bioengineering Congress and the 5th Conference of Clinical Engineering, pp. 1-10.

Correa, M. A. G. & Leber, E. L. (2011). Noise Removal from EEG Signals in Polisomnographic Records Applying Adaptive Filters in Cascade. In: L. Garcia, ed. *Adaptive Filtering Applications.* s.l.: InTech, pp. 174-196.

Coxa, D. D. & Savoya, R. L. (2002). Functional magnetic resonance imaging (fMRI) "brain reading": detecting and classifying distributed patterns of fMRI activity in human visual cortex. *NeuroImage,* 19(2), pp. 261-270.

Craik, F. and Lockhart, R. (1972). Levels of processing: A framework for memory research. *Journal of Verbal Learning and Verbal Behavior*, 11(6), pp.671-684.

Cram, J. (2003). The History of Surface Electromyography. *Applied Psychophysiology and Biofeedback*, 28(2), pp.81-91.

Cutkosky, M. (1989). On grasp choice, grasp models, and the design of hands for manufacturing tasks. *IEEE Transactions on Robotics and Automation*, 5(3), pp.269-279.

Coburn, K. & Moreno, M., 1988. Facts and artifacts in brain electrical activity mapping. *Brain Topography,* 1(1), pp. 37-45.

Cvetkovic, D., Übeyli, E. and Cosic, I. (2008). Wavelet transform feature extraction from human PPG, ECG, and EEG signal responses to ELF PEMF exposures: A pilot study. *Digital Signal Processing*, 18(5), pp.861-874.

D'Alonzo, M. and Cipriani, C. (2012). Vibrotactile Sensory Substitution Elicits Feeling of Ownership of an Alien Hand. *PLoS ONE*, 7(11), p.e50756.

Daubechies, I. (1990). The wavelet transform, time-frequency localization and signal analysis. *IEEE Transactions on Information Theory*, 36(5), pp.961-1005.

Davalli, A., Sacchetti, R., Fanin, S., Avanzolini, G. and Urbano, E. (2000). *Biofeedback for upper limb myoelectric prostheses*. INAIL Prosthesis Centre, Vigorso di Budrio (Bologna), Italy | Dept. of Electronics, Information and System Technologies, Bologna University, Bologna, Italy: Technology and Disability, 13(3), pp.161-172.

Davies, E., Friz, B. and Clippinger, F. (1970). *Amputees and Their Prostheses | O&P Virtual Library*. 14(2) 19-48 [online] Oandplibrary.org. Available at: http://www.oandplibrary.org/al/1970_02_019.asp.

Delano, P. H. & Elgoyhen, A. B. (2016). Auditory Efferent System: New Insights from Cortex to Cochlea. *Frontiers in Systems Neuroscience,* Volume 10, pp. 4-5.

Delorme, A., Fernsler, T., Serby, H. & Makeig, S. (2006). *EEGLAB Tutorial.* California: University of San Diego.

Dhillon, G. and Horch, K. (2005). Direct Neural Sensory Feedback and Control of a Prosthetic Arm. *IEEE Transactions on Neural Systems and Rehabilitation Engineering*, 13(4), pp.468-472.

Dreamstime.com. (n.d.). *Structure of a typical neuron*. [online] Available at: https://www.dreamstime.com/royalty-free-stock-photos-structure-typical-

neuron-anatomy-human-axon-synapse-dendrite-mitochondrion-myelin-sheath-node-ranvier-schwann-cell-vector-image35116978

🔸 Ebeling, M. and Kotek, E. (2014). *Project Daniel - Not Impossible's 3D Printing Arms for Children of War-Torn Sudan*. [Online] not impossible. Available at: http://www.notimpossible.com/#thebook.

🔸 Ehrsson, H. (2011). The Concept of Body Ownership and Its Relation to Multisensory Integration. In: I. B. E. Stein, ed. Stein-The New Handbook of Multisensory Processes. Cambridge, UK: MIT Press, p. 775–792.

🔸 Ehrsson, H., Rosen, B., Stockselius, A., Ragno, C., Kohler, P. and Lundborg, G. (2008). Upper limb amputees can be induced to experience a rubber hand as their own. *Brain*, 131(12), pp.3443-3452.

🔸 Ehrsson, H., Spence, C. and Passingham, R. (2004). That's My Hand! Activity in Premotor Cortex Reflects Feeling of Ownership of a Limb. *Science*, 305(5685), pp.875-877.

🔸 Ehrssonlab.se. (2015). *Ehrsson lab - Karolinska Institutet*. [online] Available at: http://www.ehrssonlab.se/research.php

🔸 Evansa, N. & Blankea, b. O. (2015). Shared electrophysiology mechanisms of body ownership and motor imagery. Neuroimage , Volume 64, p. 216–228.

🔸 Faivre, N. et al., 2017. Self-Grounded Vision: Hand Ownership Modulates Visual Location through Cortical β and γ Oscillations. *Journal of Neuroscience,* 37(1), pp. 11-22.

🔸 Ferguson, B. (2011). *Rubber Hand Illusion*. [online] Billferguson.co.uk. Available at: http://www.billferguson.co.uk/rubber-hand-illusion.html.

🔸 Flor, H. (2002). Phantom-limb pain: characteristics, causes, and treatment. *The Lancet Neurology,* 1(3), pp. 182-189.

🔸 Flor, H., Nikolajsen, L. and Staehelin Jensen, T. (2006). Phantom limb pain: a case of maladaptive CNS plasticity?. *Nature Reviews Neuroscience*, 7(11), pp.873-881.

Florida Orthotics and Prosthetics Westcoast Brace & Limb. (n.d.). *Upper Extremity Prosthetics*. [online] Available at: http://www.wcbl.com/prosthetics-2/upper-extremity-prosthetic-services/.

Fonseca, L. C. et al. (2006). Quantitative EEG in children with learning disabilities: analysis of band power. *Arq Neuropsiquiatr,* 64 (2b), pp. 376-381.

Galambos, R., MAKE, S. & TALMACHOFF, P. J. (1981). A 40-Hz Auditory Potential Recorded from the Human Scalp. *Proceedings of the National Academy of Sciences of the United States of America,* 78(4), pp. 2643-2647.

Gaydecki, P. (2004). The Design and Implementation of Finite Impulse Response Filters. In: *Foundations of Digital Signal Processing: Theory, algorithms and hardware design.* Manchester: Institution of Engineering and Technology, pp. 68-98.

Gibbard, J. (2016). *Open Bionics - James Dyson Award*. [online] James Dyson Award. Available at: https://jamesdysonaward.org/projects/open-bionics/.

Giummarra, M., Georgiou-Karistianis, N., Nicholls, M., Gibson, S., Chou, M. and Bradshaw, J. (2010). Corporeal awareness and proprioceptive sense of the phantom. *British Journal of Psychology*, 101(4), pp.791-808.

Goodwin, A. and Wheat, H. (2004). SENSORY SIGNALS IN NEURAL POPULATIONS UNDERLYING TACTILE PERCEPTION AND MANIPULATION. *Annual Review of Neuroscience*, 27(1), pp.53-77.

Gougoux, F. et al. (2005). *A Functional Neuroimaging Study of Sound Localization: Visual Cortex Activity Predicts Performance in Early-Blind Individuals.* PLoS Biology, 3(2), pp. 0324-0333.

Graziano, M., Cooke, D. and Taylor, C. (2000). Coding the Location of the Arm by Sight. *Science*, 290(5497), pp.1782-1786.

Gregoire, C. (2015). *How our sense of touch affects everything we do*. [online] Available at: http://www.huffingtonpost.com/2015/01/20/neuroscience-touch_n_6489050.html.

Grill-Spector, K. & Malach, R. (2004). THE HUMAN VISUAL CORTEX. *Annu. Rev. Neurosci. 2004. 27:649–77,* Volume 27, p. 649–77.

Guangzhi Wang, Xiaoning Zhang, Jichuan Zhang and Gruver, W. (2002). Gripping force sensory feedback for a myoelectrically controlled forearm prosthesis. *1995 IEEE International Conference on Systems, Man and Cybernetics. Intelligent Systems for the 21st Century*.

Guerrero-Mosquera, C. and Vazquez, A. (2009). New approach in features extraction for EEG signal detection. *2009 Annual International Conference of the IEEE Engineering in Medicine and Biology Society*, pp.13-16.

Guger, C., Harkam, W., Hertnaes, C. and Pfurtscheller, G. (1999). Prosthetic Control by an EEG-based BrainComputer Interface (BCI). In: *AAATE 5th European Conference for the Advancement of Assistive Technology*. [online] Available at: https://www.researchgate.net/profile/Christoph_Guger/publication/220049412_ Prosthetic_Control_by_an_EEG-based_Brain- _Computer_Interface_BCI/links/0912f50618d04229f9000000.pdf.

Gurumurthy, S., Mahit, V. S. & Ghosh, R. (2013). Analysis and simulation of brain signal data by EEG signal processing technique using MATLAB. *International Journal of Engineering and Technology (IJET),* 5(3), pp. 2771-2776.

Hammond DC (2006). Quantitative EEG patterns associated with medical conditions. *Biofeedback*, 34(3), 87-94.

Hammond DC (2006). What is neurofeedback? *Journal of Neurotherapy*, 10(4), 25-36.

Hargrove, L., Simon, A., Young, A., Lipschutz, R., Finucane, S., Smith, D. and Kuiken, T. (2013). Robotic Leg Control with EMG Decoding in an Amputee with Nerve Transfers. *New England Journal of Medicine*, 369(13), pp.1237-1242.

Hassanien, E. & Azar, A. (2015). *Brain-Computer Interfaces: Current Trends and Applications*. Ella Hassanien; Aboul, Azar; Ahmad Taher ed. s.l.:Springer.

Hazarika, N., Chen, J., Tsoi, A. and Sergejew, A. (1997). Classification of EEG signals using the wavelet transform. *Proceedings of 13th International Conference on Digital Signal Processing*, pp.61-72.

Helm, P. A. v. d. (2017). *Peter A. van der Helm.* [Online] Available at: https://perswww.kuleuven.be/~u0084530/doc/architecture.html

Helm, P. A. v. d. (2017). *Peter A. van der Helm.* [Online] Available at: https://perswww.kuleuven.be/~u0084530/doc/architecture.html [Accessed 22 08 2017].

Hikosaka, O., Nakamura, K. and Nakahara, H. (2006). Basal Ganglia Orient Eyes to Reward. *Journal of Neurophysiology*, [online] 95(2), pp.567-584. Available at: http://jn.physiology.org/content/95/2/567.

Hill, A. (1999). Phantom limb pain: a review of the literature on attributes and potential mechanisms. *Pain Symptom Manage,* 17(2), pp. 125-142.

Horch, K., Meek, S., Taylor, T. and Hutchinson, D. (2011). Object Discrimination With an Artificial Hand Using Electrical Stimulation of Peripheral Tactile and Proprioceptive Pathways With Intrafascicular Electrodes. *IEEE Transactions on Neural Systems and Rehabilitation Engineering*, 19(5), pp.483-489.

Howard, A. (2015). *Paralyzed Man Can Feel Sense Of Touch Through Mind-Controlled Robotic Arm.* [online] HuffPost. Available at: http://www.huffingtonpost.com/entry/robotic-arm-darpa-revolutionizing-prosthetics_us_55f740f8e4b09ecde1d971d9.

Hu, X., Tong, K., Wei, X., Rong, W., Susanto, E. and Ho, S. (2013). The effects of post-stroke upper-limb training with an electromyography (EMG)-driven hand robot. *Journal of Electromyography and Kinesiology*, 23(5), pp.1065-1074.

Hubel, D. H. (1995). *Eye, Brain and Vision.* USA: Scientific American Library.

Humanbrainfacts.org. (2016). Human Brain Anatomy - Components of Human Brain with Images. [online] Available at: http://www.humanbrainfacts.org/human-brain-anatomy.php.

Idris, Z. et al. (2014). Principles, Anatomical Origin and Applications of Brainwaves: A Review, Our Experience and Hypothesis Related to Microgravity and the Question on Soul. *J. Biomedical Science and Engineering,* Volume 7, pp. 435-445.

IJsselsteijn, W. A., Kort, Y. A. W. d. & Haans, A. (2006). Is This My Hand I See Before Me? The Rubber Hand Illusion in Reality, Virtual Reality, and Mixed Reality. *the Massachusetts Institute of Technology,* 15(4), pp. 455-464.

iMotions, (2016). *EEG Pocket Guide.* [Online] Available at: https://imotions.com/blog/eeg-books/[Accessed 01 08 2017].

iMotions. (n.d.). *EEG (Electroencephalography): The Definitive Pocket Guide*. [online] Available at: https://imotions.com/blog/eeg/.

ITV News. (2015). *Amputations caused by diabetes reach all-time high*. [online] Available at: http://www.itv.com/news/2015-07-15/concern-over-public-health-as-amputations-caused-by-diabetes-reaches-all-time-high/.

Jensen, T. & Nikolajsen, L. (1999). Phantom pain and other phenomena after amputation. In: P. Wall & R. Melzack, eds. *Textbook of pain.* Churchill Livingstone, Edinburgh, UK: Churchill Livingstone, Edinburgh, UK, pp. 799-814.

Johansson, R. and Edin, B. (1993). Predictive feed-forward sensory control during grasping and manipulation in man. *Biomedical Research.* 14(4), pp.95-106.

Johansson, R. and Flanagan, J. (2009). Coding and use of tactile signals from the fingertips in object manipulation tasks. *Nature Reviews Neuroscience*, 10(5), pp.345-359.

Johansson, R. and Westling, G. (1987). Signals in tactile afferents from the fingers eliciting adaptive motor responses during precision grip. *Experimental Brain Research*, 66(1).

Jones, J. and Callan, D. (2003). Brain activity during audiovisual speech perception: An fMRI study of the McGurk effect. *NeuroReport*, 14(8), pp.1129-1133.

Jones, L. and Sarter, N. (2008). Tactile Displays: Guidance for Their Design and Application. *Human Factors: The Journal of the Human Factors and Ergonomics Society*, 50(1), pp.90-111.

Jones, O. (2016). *Muscles in the Anterior Compartment of the Forearm*. [online] TeachMeAnatomy. Available at: http://teachmeanatomy.info/upper-limb/muscles/anterior-forearm/.

Kabdebon, C. et al. (2014). Anatomical correlations of the international 10–20 sensor placement system in infants. *NeuroImage ,* Volume 99, p. 342–356.

Kaczmarek, K., Webster, J., Bach-y-Rita, P. and Tompkins, W. (1991). Electrotactile and vibrotactile displays for sensory substitution systems. *IEEE Transactions on Biomedical Engineering*, 38(1), pp.1-16.

Kaiser, D. (2005). Basic Principles of Quantitative EEG. *Journal of Adult Development*, 12(2-3), pp.99-104.

Kammers, M. P. M., Ham, I. J. M. v. d. & Dijkerman, H. C. (2006). Dissociating body representations in healthy individuals: Differential effects of a kinaesthetic illusion on perception and action. *Neuropsychologia,* 44(12), pp. 2430-2436.

Kanayama, N., Sato, A. & Ohira, H., 2007. Crossmodal effect with rubber hand illusion and gamma-band activity. *Psychophysiology,* Volume 44, p. 392–402.

Kandel, E., Schwartz, J., Jessell, T., Siegelbaum, S. and Hudspeth, A. (2013). *Principles of neural science*. New York: McGraw Hill.

Kaneko, W., Phillips, E., Riley, E. & Ehlers, C. (1996). EEG findings in fetal alcohol syndrome and Down syndrome children. *Electroencephalogr Clin Neurophysiol,* 98(1), pp. 20-28.

Kazamel, M., Province, P., Alsharabati, M. and Oh, S. (2013). *History of Electromyography (EMG) and Nerve Conduction Studies (NCS): A Tribute to the Founding Fathers (P05.259)*. [online] Neurology.org. Available at: http://www.neurology.org/content/80/7_Supplement/P05.259.

Keim, R. (n.d.). *Single-ended and Differential Amplifiers | Operational Amplifiers | Electronics Textbook*. [online] Allaboutcircuits.com. Available at: http://www.allaboutcircuits.com/textbook/semiconductors/chpt-8/single-ended-differential-amplifiers/.

Kelion, L. (2015). *Open Bionics robotic hand for amputees wins Dyson Award - BBC News*. [online] BBC News. Available at: http://www.bbc.co.uk/news/technology-34044453.

Kenhub. (2016). *Diagram / Pictures: Flexors of the Forearm (Anatomy) / Kenhub*. [online] Available at: https://www.kenhub.com/en/atlas/forearm-flexor-muscles.

Kim, K., Colgate, J., Santos-Munne, J., Makhlin, A. and Peshkin, M. (2010). On the Design of Miniature Haptic Devices for Upper Extremity Prosthetics. *IEEE/ASME Transactions on Mechatronics*, 15(1), pp.27-39.

Klem, G., Lüders, H., Jasper, H. & Elger, C. (1999). The ten-twenty electrode system of the International Federation. The International Federation of Clinical Neurophysiology. *Electroencephalogr Clin Neurophysiol Suppl. 1999;52:3-6,* Volume 52, pp. 3-6.

Knipe, H. (n.d.). *Anterior compartment of the forearm / Radiology Reference Article / Radiopaedia.org*. [online] Radiopaedia.org. Available at: http://radiopaedia.org/articles/anterior-compartment-of-the-forearm.

Kober, J., Bagnell, J. and Peters, J. (2013). Reinforcement learning in robotics: A survey. *The International Journal of Robotics Research*, 32(11), pp.1238-1274.

Kolarik, A. J., Cirstea, S., Pardhan, S. & Moore, B. C. (2014). *A summary of research investigating echolocation abilities of blind and sighted humans.* Hearing Research, Volume 310, pp. 60-68.

Kousarrizi, M., Ghanbari, A., Teshnehlab, M., Shorehdeli, M. and Gharaviri, A. (2009). Feature Extraction and Classification of EEG Signals Using Wavelet Transform, SVM and Artificial Neural Networks for Brain Computer Interfaces. *2009 International Joint Conference on Bioinformatics, Systems Biology and Intelligent Computing*, pp.352-355.

Krantz, J. (2012). *Experiencing Sensation and Perception*. Pearson Education (US).

Kratouni, D. (2015). *Electroencephalographic Electrodes, Channels, and Montages and How They Are Chosen*. [online] Clinical Gate. Available at:

http://clinicalgate.com/electroencephalographic-electrodes-channels-and-montages-and-how-they-are-chosen/.

Kritis, A., Stamoula, E., Paniskaki, K. and Vavilis, T. (2015). Researching glutamate – induced cytotoxicity in different cell lines: a comparative/collective analysis/study. *Frontiers in Cellular Neuroscience*, 9.

Kritis, A., Stamoula, E., Paniskaki, K. and Vavilis, T. (2015). Researching glutamate –induced cytotoxicity in different cell lines: a comparative/collective analysis/study. Frontiers in Cellular Neuroscience, 9.

Kropotov, J. (2009). *Quantitative EEG, event-related potentials and neurotherapy*. Amsterdam: Academic Press.

Kumar, D., Poosapadi Arjunan, S. and Singh, V. (2013). Towards identification of finger flexions using single channel surface electromyography – able bodied and amputee subjects. *Journal of NeuroEngineering and Rehabilitation*, 10(1), p.50.

Kumar, J. S. & Bhuvaneswarib, P. (2012). Analysis of Electroencephalography (EEG) Signals and Its Categorization–A Study. *Procedia Engineering,* Volume 38, pp. 2525-2536.

Kupers, R., Pietrini, P., Ricciardi, E. & Ptito, M. (2011). The nature of consciousness in the visually deprived brain. *Front Psychol,* pp. 2-19.

L. Nikolajsen, T. S. J. (2001). Phantom limb pain. *British Journal of Anaesthesia,* 87(1), pp. 107-116.

Ladegaard, J. (2002). Story of electromyography equipment. *Muscle & Nerve*, 999(S11), pp.S128-S133.

LeBlanc, M. (2008). *"Give Hope - Give a Hand" - The LN-4 Prosthetic Hand.* [ebook] Available at: https://web.stanford.edu/class/engr110/2011/LeBlanc-03a.pdf.

Lee, T. S., Mumford, D., Romero, R. & Lamme, V. A. (1998). The role of the primary visual cortex in higher level vision. *Vision Research,* p. 2429–2454.

Lenggenhager, B., Halje, P. & Blanke, O. (2011). α band oscillations correlate with illusory self-location induced by virtual reality. Eur. J. Neurosci. , Volume 33, pp. 1935-1943.

Leuthardt, E., Schalk, G., Roland, J., Rouse, A. and Moran, D. (2009). Evolution of brain-computer interfaces: going beyond classic motor physiology. *Neurosurgical Focus*, 27(1), p.E4.

Lévesque, J., Beauregard, M. and Mensour, B. (2006). Effect of neurofeedback training on the neural substrates of selective attention in children with attention-deficit/hyperactivity disorder: A functional magnetic resonance imaging study. *Neuroscience Letters*, 394(3), pp.216-221.

Liu, H., Yang, D., Fan, S. and Cai, H. (2016). On the development of intrinsically-actuated, multisensory dexterous robotic hands. *ROBOMECH Journal*, 3(1), pp.1-9.

Liu, H., Yang, D., Jiang, L., and Fan, S. (2014). Development of multi-DOF prosthetic hand with intrinsic actuation, intuitive control and sensory feedback. *Industrial Robot: An International Journal,* 41(4), pp.381-392.

Livingstone, C. et al (1987). *Anterior and Posterior Forearm muscles. In: Grays Anatomy*. 37th ed. pp.844–849.

LM35 Precision Centigrade Temperature Sensors. (2016). [ebook] Texas Instruments. Available at: http://www.ti.com/lit/ds/symlink/lm35.pdf.

Longo, M., Schüür, F., Kammers, M., Tsakiris, M. and Haggard, P. (2008). What is embodiment? A psychometric approach. *Cognition*, 107(3), pp.978-998.

Lundy, C. (2011). Radial nerve palsy in the newborn. *Canadian Medical Association Journal*, 183(12), pp.1348-1349.

Malhotra, A., Pinals, D., Weingartner, H., Sirocco, K., Missar, C., Pickar, D. and Breier, A. (1996). NMDA Receptor Function and Human Cognition: The Effects of Ketamine in Healthy Volunteers. *Neuropsychopharmacology*, 14(5), pp.301-307.

Marasco, P., Kim, K., Colgate, J., Peshkin, M. and Kuiken, T. (2011) 'Robotic touch shifts perception of embodiment to a prosthesis in targeted reinnervation amputees', Brain: a journal of neurology. 134, pp. 747–58.

Matthys, K., Smits, M., Van der Geest, J., Van der Lugt, A., Seurinck, R., Stam, H. and Selles, R. (2009). Mirror-Induced Visual Illusion of Hand Movements: A Functional Magnetic Resonance Imaging Study. *Archives of Physical Medicine and Rehabilitation*, 90(4), pp.675-681.

McLeod, S. (2007). *Edward Thorndike - Law of Effect | Simply Psychology*. [online] Simplypsychology.org. Available at: https://www.simplypsychology.org/edward-thorndike.html.

McLeod, S. (2008). *Classical Conditioning | Simply Psychology*. [online] Simplypsychology.org. Available at: http://www.simplypsychology.org/classical-conditioning.html.

Medved, V. (2001). *Measurement of human locomotion*. Boca Raton, Fla.: CRC Press, pp.170-174.

Mercer County Community College (n.d.) Structure and Function of the Hand.

Merletti, R. and Parker, P.A.(2004), Electromyography Physiology, Engineering, and Noninvasive Applications. A John Wiley & Sons Inc. 494.

Merzenich, M., Nelson, R., Stryker, M., Cynader, M., Schoppmann, A. and Zook, J. (1984). Somatosensory cortical map changes following digit amputation in adult monkeys. *The Journal of Comparative Neurology*, 224(4), pp.591-605.

Micera, S., Carpaneto, J. and Raspopovic, S. (2010). Control of Hand Prostheses Using Peripheral Information. *IEEE Reviews in Biomedical Engineering*, 3, pp.48-68.

Michel, C. et al. (2004). EEG source imaging. *Clin Neurophysiol,* 115(10), pp. 195-222.

Mihail, L. & Leon, D. (2013). Contributions to the Understanding of the Neural Bases of the Consciousness. In: T. Lichtor, ed. *Clinical Management and Evolving Novel Therapeutic Strategies for Patients with Brain Tumors.* s.l.:InTech, Morn Hill.

Mind Tricks Gallery. (2018). *The Rubber Hand Illusion – Is Seeing Believing?*. [online] Available at: http://mindtricksgallery.com/mindtricks/the-rubber-hand-illusion-is-seeing-believing/.

Morgan, w. (2015). *Phantom Limb Pain | Bethesda Spine*. [online] Bethesdaspineinstitute.com. Available at: http://bethesdaspineinstitute.com/?p=496.

Morris, R., Anderson, E., Lynch, G. and Baudry, M. (1986). Selective impairment of learning and blockade of long-term potentiation by an N-methyl-D-aspartate receptor antagonist, AP5. *Nature*, 319(6056), pp.774-776.

Muller-Putz, G. and Pfurtscheller, G. (2008). Control of an Electrical Prosthesis with an SSVEP-Based BCI. *IEEE Transactions on Biomedical Engineering*, 55(1), pp.361-364.

Nanowerk.com. (2012). *Electronic sensing with your fingertips*. [online] Available at: http://www.nanowerk.com/spotlight/spotid=26342.php.

Nature Reviews Neurology, (2016). *Brain–computer interfaces for communication and rehabilitation.* [Online] Available at: https://www.slideshare.net/nitish_kumar/bcippprsntn

Neil, M. (2015). Pain after amputation. BJA Education, 16(3), pp.107-112.

Nghiem, B., Sando, I., Gillespie, R., McLaughlin, B., Gerling, G., Langhals, N., Urbanchek, M. and Cederna, P. (2015). Providing a Sense of Touch to Prosthetic Hands. *Plastic and Reconstructive Surgery*, 135(6), pp.1652-1663.

Nghiem, B., Sando, I., Gillespie, R., McLaughlin, B., Gerling, G., Langhals, N., Urbanchek, M. and Cederna, P. (2015). Providing a Sense of Touch to Prosthetic Hands. *Plastic and Reconstructive Surgery*, 135(6), pp.1652-1663.

Nhs.uk. (2013). *Amputation - NHS Choices*. [online] Available at: http://www.nhs.uk/conditions/amputation/Pages/Introduction.aspx

Nilsson, M. E. & Schenkman, B. N. (2016). *Blind people are more sensitive than sighted people to binaural sound-location cues, particularly inter-aural level differences*. Hearing Research, Volume 332, pp. 223-232.

Norton, K. (2007). *A Brief History of Prosthetics - Amputee Coalition*. [online] Amputee Coalition. Available at: http://www.amputee-coalition.org/inmotion/nov_dec_07/history_prosthetics.html

Nowinski, W. L. (2011). Introduction to Brain Anatomy. In: K. Miller, ed. *Biomechanics of the Brain*. s.l.:Springer Science, pp. 5-40.

Nunez, P. L. & Srinivasan, R. (2006). *Electric Fields of the Brain: The Neurophysics of EEG.* 2nd ed. NewYork: Oxford University Press, Inc. . Ocak, H., 2009. Automatic detection of epileptic seizures in EEG using discrete wavelet transform and approximate entropy. *Expert Systems with Applications,* 36(2), pp. 2027-2036.

Nunez, P. L. (1981). *Electric Fields of the Brain: The Neurophysics of EEG.* Oxford: Oxford University Press.

Nunez, P. L. (1995). *Neocortical Dynamics and Human EEG Rhythms.* NewYork: Oxford University Press Inc.

O'Brien, M. (2010). *Aids to the examination of the peripheral nervous system*. 5th ed. Edinburgh: Saunders Elsevier.

Oostenvelda, R. & Praamstrac, P. (2001). The five percent electrode system for high-resolution EEG and ERP measurements. *Clinical Neurophysiology ,* Volume 112, pp. 713-719.

Open Bionics. (2015). *Wounded hero with 3D printed hand*. [online] Available at: https://www.openbionics.com/blog/wounded-hero-with-3d-printed-hand.

Open Bionics. (2016). *Blog*. [online] Available at: https://www.openbionics.com/about/

Orfanidis, S. (2010). *Introduction to signal processing*. Estados Unidos: Prentice Hall.

Orso, G. (2016). *The Rubber Hand Illusion*. [online] doppel. Available at: https://feeldoppel.com/blogs/news/the-rubber-hand-illusion.

Ott, K., Serlin, D. and Mihm, S. (2002). *Artificial parts, practical lives*. New York: New York University Press, p.122.

Ottobock.co.uk. (n.d.). *Above-elbow prosthesis with DynamicArm — Ottobock.* [online] Available at: http://www.ottobock.co.uk/prosthetics/upper_limbs_prosthetics/product-systems/above_elbow_prosthesis__featuring_dynamicarm_and_sensorhand_speed_hand/index.html

Ottobock.co.uk. (n.d.). *Arm prosthesis — Ottobock UK.* [online] Available at: http://www.ottobock.co.uk/prosthetics/upper_limbs_prosthetics/.

Parke, D., Ornstein, P., Rieser, J. and Zahn Waxler, C. (1994). *Century of development psychology.* Washington, DC: American Psychology Association, pp.431-471.

Patestas, M. A. & Gartner, L. P. (2016). *A Textbook of Neuroanatomy,* 2nd ed. s.l.: Wiley-Blackwell.

Peterson, D. A. et al. (2005). Feature Selection and Blind Source Separation in an EEG-Based Brain-Computer Interface. *EURASIP Journal on Applied Signal Processing ,* Volume 19, p. 3128–3140.

Petkova, V. I. & Ehrsson, H. H. (2008). If I Were You: Perceptual Illusion of Body Swapping. *PLoS ONE ,* 3(12), p. e3832.

Petkova, V., Zetterberg, H. & Ehrsson, H. (2012). Rubber Hands Feel Touch, but Not in Blind Individuals. *PLoS ONE,* 7(4), p. e35912.

Pfurtscheller, G. et al. (2000). Current trends in Graz Brain-Computer Interface (BCI) research. *IEEE transactions on rehabilitation engineering,* 8(2), pp. 216-219.

Pilarski, P., Dawson, M., Degris, T., Fahimi, F., Carey, J. and Sutton, R. (2011). Online human training of a myoelectric prosthesis controller via actor-critic reinforcement learning. *2011 IEEE International Conference on Rehabilitation Robotics.*

Pinterest, (2017). *pinterest.* [Online] Available at: https://www.pinterest.com/pin/342836590356494499/

Plettenburg, D. (2006). *Upper extremity prosthetics In: Upper Extremity Prosthetics.* Delft: VSSD, p.47, 48, 84.

Polak, M. and Kostov, A. (1998). Feature extraction in development of brain-computer interface: a case study. *Proceedings of the 20th Annual International Conference of the IEEE Engineering in Medicine and Biology Society. Vol.20 Biomedical Engineering Towards the Year 2000 and Beyond (Cat. No.98CH36286).* pp. 2058–2061.

Pons, T. P. et al. (1991). Massive Cortical Reorganization After Sensory Deafferentation in Adult Macaques. *Science, New Series,* 252(5014), pp. 1857-1860.

Press, W. H., Teukolsky, S. A., Vetterling, W. T. & Flannery, B. P. (1997). Fast Fourier Transform. In: *NUMERICAL RECIPES IN FORTRAN 77: THE ART OF SCIENTIFIC COMPUTING.* Newyork: Cambridge University Press, pp. 490-525.

Prochazka, A., Kukal, J. and Vysata, O. (2008). Wavelet transform use for feature extraction and EEG signal segments classification. *2008 3rd International Symposium on Communications, Control and Signal Processing*, pp.719-722.

Pylatiuk, C., Kargov, A. and Schulz, S. (2006). Design and Evaluation of a Low-Cost Force Feedback System for Myoelectric Prosthetic Hands. *JPO Journal of Prosthetics and Orthotics*, 18(2), pp.57-61.

Ramachandran, V. & Hirstein, W. (1998). The perception of phantom limbs. The D. O. Hebb lecture. *Brain*, 121(9), pp.1603-1630.

Ramachandran, V. and Rogers-Ramachandran, D. (1996). Synaesthesia in Phantom Limbs Induced with Mirrors. *Proceedings of the Royal Society B: Biological Sciences*, 263(1369), pp.377-386.

Ramchandran, V. & Hirstein, W. (1998). The perception of phantom limbs. *Brain,* 121 (9), p. 1603–1630.

Rangaswamy, M., Porjesz, B., Chorlian, D., Wang, K., Jones, K., Bauer, L., Rohrbaugh, J., O'Connor, S., Kuperman, S., Reich, T. and Begleiter, H. (2002). Beta power in the EEG of alcoholics. *Biological Psychiatry*, 52(8), pp.831-842.

Rantala, J. (n.d.). *The tactile senses & haptic perception*.

Rao, I. S. & Kayser, C. (2017). Neurophysiological Correlates of the Rubber Hand Illusion in Evoked and Oscillatory Brain Activity. *Frontiers in Human Neuroscience,* Volume 11, pp. 1-12.

Rechtschaffen, A. & Kales, A. (1968). *A manual of standardized terminology, techniques and scoring system for sleep stages of human subjects.* Los Angeles: U. S. National Institute of Neurological Diseases and Blindness.

Reddy, G. & Narava, S. (2013). Artifact Removal from EEG Signals. *International Journal of Computer Applications,* 77(13), pp. 17-19.

Riso, R. (1999). *Strategies for providing upper extremity amputees with tactile and hand position feedback – moving closer to the bionic arm*. Technology and Health Care 7(6), pp.401–409.

Rock I, Victor J (1964) Vision and touch: an experimentally created conflict between the two senses. Science 143:594–596

Rohde, M., Di Luca, M. and Ernst, M. (2011). The Rubber Hand Illusion: Feeling of Ownership and Proprioceptive Drift Do Not Go Hand in Hand. *PLoS ONE*, 6(6), p.e21659.

Rosén, B. and Lundborg, G. (2005). Training with a mirror in rehabilitation of the hand. *Scandinavian Journal of Plastic and Reconstructive Surgery and Hand Surgery*, 39(2), pp.104-108.

Rslsteeper.com. (n.d.). *Upper Limb - RSLSteeper*. [online] Available at: http://rslsteeper.com/products/prosthetics/products/upper_limb.

Rutkin, A. (2014). *Bionic arm gives cyborg drummer superhuman skills*. [online] New Scientist. Available at: https://www.newscientist.com/article/dn25142-bionic-arm-gives-cyborg-drummer-superhuman-skills/#.UxtMzuddWlo.

Sadato, N., Okada, T., Honda, M. & Yonekura, Y. (2002). Critical period for cross-modal plasticity in blind humans: *a functional MRI study. Neuroimage*, 16(2), pp. 389-400.

Salenius, S. et al. (1997). Modulation of human cortical rolandic rhythms during natural sensorimotor tasks. *Neuroimage,* 5(3), pp. 221-228.

Schmalzl, L., Kalckert, A., Ragnö, C. and Ehrsson, H. (2013). Neural correlates of the rubber hand illusion in amputees: A report of two cases. *Neurocase*, 20(4), pp.407-420.

Schwartz, A., Cui, X., Weber, D. and Moran, D. (2006). Brain-Controlled Interfaces: Movement Restoration with Neural Prosthetics. *Neuron*, 52(1), pp.205-220.

Sciencemuseum.org.uk. (n.d.). *Thalidomide*. [online] Available at: http://www.sciencemuseum.org.uk/broughttolife/themes/controversies/thalidomi de.aspx.

Scolaro, G. R., Azevedo, F. M. d., Boos, C. F. & Walz, R. (2013). Wavelet Filter to Attenuate the Background Activity and High Frequencies in EEG Signals Applied in the Automatic Identification of Epileptiform Events. In: A. O. Andrade, A. A. Pereira, E. L. M. Naves & A. B. Soares, eds. *Practical Applications in Biomedical Engineering.* s.l.:InTech, pp. 82-102.

Scott, R., Brittain, R., Caldwell, R., Cameron, A. and Dunfield, V. (1980). Sensory-feedback system compatible with myoelectric control. *Medical & Biological Engineering & Computing*, 18(1), pp.65-69.

Scott, S. K. & Johnsrude, I. S. (2003). The neuroanatomical and functional organization of speech perception. *TRENDS in Neurosciences,* 26(2), pp. 100-107.

Sekuler, R. and Erlebacher, A. (1971). The Two Illusions of Muller-Lyer: Confusion Theory Reexamined. *The American Journal of Psychology*, 84(4), p.477.

Sherman, R. A., Sherman, C. & Parker, L. (1984). Chronic phantom and stump pain among American veterans: Results of a survey. *The Journal of Pain,* Volume 18, p. 83–95.

Shimada, S., Fukuda, K. and Hiraki, K. (2009). Rubber Hand Illusion under Delayed Visual Feedback. *PLoS ONE*, 4(7), p.e6185.

Sinek, S. (2009). *Start with why*. New York: Portfolio/Penguin, p.41

Singh, L. & Priya, K. (2013). FIR Filter Design and IIR Filter Design. *IJCST ,* 4(1), pp. 108-109.

Singhi, P. D. & Bansa, D. (2004). Self induced photosensitive epilepsy. *The Indian Journal of Pediatrics,* 71(7), p. 649–651.

Sleepdata.org. (n.d.). Sleep Data - National Sleep Research Resource - NSRR. [online] Available at: https://sleepdata.org/datasets/cfs/pages/manuals/polysomnography/17-08-03-01-identify-landmarks.md.

Soltani, S. (2002). On the use of the wavelet decomposition for time series prediction. *Neurocomputing*, 48(1-4), pp.267-277.

Space (2016). *The rubber hand illusion | Earth Chronicles News*. [online] Earth-chronicles.com. Available at: https://earth-chronicles.com/science/the-rubber-hand-illusion.html.

Spector, D. (2014). *Artificial Limbs Have Gone Through An Amazing Evolution*. [online] Business Insider. Available at: http://www.businessinsider.com/the-evolution-of-prosthetic-technology-2014-8?IR=T

St.com. (n.d.). *STM32F4DISCOVERY - Discovery kit with STM32F407VG MCU * New order code STM32F407G-DISC1 (replaces STM32F4DISCOVERY) - STMicroelectronics*. [online] Available at: http://www.st.com/content/st_com/en/products/evaluation-tools/product-evaluation-tools/mcu-eval-tools/stm32-mcu-eval-tools/stm32-mcu-discovery-kits/stm32f4discovery.html.

Stoica, P. and Moses, R. (1997). *. Introduction to Spectral Analysis*. Upper Saddle River, NJ, USA: Prentice hall.

Storr, K. (2012). *'Smart Fingertips' Pave Way for Virtual Sensations*. [online] Science | AAAS. Available at: http://www.sciencemag.org/news/2012/08/smart-fingertips-pave-way-virtual-sensations

Strang, G. (1999). Signal Processing for Everyone. In: V. Capasso, H. Engl & J. Periaux, eds. *Computational Mathematics Driven by Industrial Problems.* Cambridge: Springer, pp. 366-412.

- Stromberg, J. (2015). *9 surprising facts about the sense of touch*. [online] Vox. Available at: http://www.vox.com/2015/1/28/7925737/touch-facts.

- Subasi, A., Kiymik, M., Alkan, A. and Koklukaya, E. (2005). Neural Network Classification of EEG Signals by Using AR with MLE Preprocessing for Epileptic Seizure Detection. *Mathematical and Computational Applications*, 10(3), pp.57-70.

- Subedi, B. & Grossberg, G. T. (2011). Phantom Limb Pain: Mechanisms and Treatment Approaches. *Pain Research and Treatment,* pp. 1-8.

- Sudarsan, S. and Sekaran, E. (2012). Design and Development of EMG Controlled Prosthetics Limb. *Procedia Engineering*, 38, pp.3547-3551.

- Sudarsan, S. and Sekaran, E. (2012). Design and Development of EMG Controlled Prosthetics Limb. *Procedia Engineering*, 38, pp.3547-3551.

- Sutton, R. and Barto, A. (1998). *Introduction to reinforcement learning*. Cambridge, Mass: MIT Press, p.322.

- Syuzev, V., Gouskov, A., and Galiamova, E. (2010), Human Skeletal Muscle - Mechanical and Mathematical Models, *1st International Conference on Applied Bionics and Biomechanics*. Venice, Italy.

- Szychowski, A., Sadler, J. and Thorsell, E. (2012). *The Jaipurknee Project I: Getting the need right*. [ebook] California: Global Health. Available at: https://www.gsb.stanford.edu/sites/gsb/files/publication-pdf/jaipurkneei-gettingtheneedright.pdf

- Taigang, H., Gari, C. & Lionel, T. (2005). Application of ICA in Removing Artefacts from the EGG. *Neural Computing & Applications,* 15(2), p. 105–116.

- Talbo, K. (2014). *Using Arduino to Design a Myoelectric Prosthetic*. PhD. College of Saint Benedict and Saint John's University.

- Talbot, D. (2013). *A Prosthetic Hand That Sends Feelings to Its Wearer*. [online] MIT Technology Review. Available at: https://www.technologyreview.com/s/522086/an-artificial-hand-with-real-feelings/.

Taplan, M. (2002). FUNDAMENTALS OF EEG MEASUREMENT. *MEASUREMENT SCIENCE REVIEW,* 2(2), pp. 1-11.

Tatum, W. O., Husain, A. M., Benbadis, S. R. & Kaplan, P. W. (2008). *Handbook of EEG Interpretation.* USA: Demos Medical Publishing, LLC. .

Telis, G. (2013) Paralyzed patients control robotic arm with their minds. Available at: http://www.sciencemag.org/news/2012/05/paralyzed-patients-control-robotic-arm-their-minds.

Teplan, M. (2002). FUNDAMENTALS OF EEG MEASUREMENT. *MEASUREMENT SCIENCE REVIEW,* 2(2), pp. 1-11.

Terjung, R. Darin-Smith, I (2011) Comprehensive physiology, The Sense of Touch: Performance and Peripheral Neural Processes. Edited by David M. Pollock. Bethesda, MD: John Wiley and Sons.

Thurston, A. J. (2007). Paré and prosthetics: the early history of artificial limbs. *ANZ Journal of Surgery,* 77(12), p. 1114–1119.

Tong, F. (2003). PRIMARY VISUAL CORTEX AND VISUAL AWARENESS. *NATURE REVIEWS | NEUROSCIENCE,* Volume 4, pp. 219-229.

Tong, S. & Thankor, N. V. (2009). *Quantitative EEG Analysis Methods and Applications (Engineering in Medicine & Biology).* 1st ed. s.l.:Artech House.

Tortora, G. and Derrickson, B. (2009). *Principles of anatomy and physiology.* 12th ed. Hoboken, N.J.: Wiley, p.642.

Tortora, G. and Derrickson, B. (2010). *Introduction to the Human Body: The Essentials of Anatomy and Physiology.* 8th ed. Hoboken, NJ: John Wiley & Sons, Inc.

Touchbionics.com. (2015). *New bionic hand from Touch Bionics controlled by simple gestures | Touch Bionics.* [online] Available at: http://www.touchbionics.com/news-events/news/new-bionic-hand-touch-bionics-controlled-simple-gestures

Touchbionics.com. (n.d.). *Touch Bionics: Leading Upper Limb Prosthetics Provider.* [online] Available at: http://www.touchbionics.com/.

🞣 Trans Cranial Technologies, (2012). *10/20 System Positioning Manual,* Wanchai: s.n.

🞣 Tri (n.d.). *The 5 Different Brainwave Frequencies and What They Mean*. [online] Examined Existence. Available at: http://examinedexistence.com/5-different-brainwave-frequencies-mean/

🞣 Troncossi, M. and Parenti-Castelli, V. (2007). Synthesis of Prosthesis Architectures and Design of Prosthetic Devices for Upper Limb Amputees. *Rehabilitation Robotics*.

🞣 Tsakiris, M. and Haggard, P. (2005). The Rubber Hand Illusion Revisited: Visuotactile Integration and Self-Attribution. *Journal of Experimental Psychology: Human Perception and Performance*, 31(1), pp.80-91.

🞣 Tudor, M., Tudor, L. & Tudor, K. I. (2005). Hans Berger (1873-1941)--the history of electroencephalography. *Acta Med Croatica,* 59(4), pp. 307-313.

🞣 Tyler, D. (2013). *Restoring Natural Human Sensation in Amputees*. [online] YouTube. Available at: https://www.youtube.com/watch?v=DIodb8qM9N0.

🞣 Übeyli, E. (2008). Analysis of EEG signals by combining eigenvector methods and multiclass support vector machines. *Computers in Biology and Medicine*, 38(1), pp.14-22.

🞣 Übeyli, E. (2009). Analysis of EEG signals by implementing eigenvector methods/recurrent neural networks. *Digital Signal Processing*, 19(1), pp.134-143.

🞣 Übeyli, E. (2009). Statistics over features: EEG signals analysis. Computers in Biology and Medicine, 39(8), pp.733-741.

🞣 Uellendahl, J. (1998). *inMotion: Materials Used in Prosthetics Part I*. [online] Amputee-coalition.org. Available at: http://www.amputee-coalition.org/inmotion/sep_oct_98/matinprs.html

🞣 Ungureanu, M., Bigan, C., Strungaru, R. & Lazarescu, V. (2004). Independent Component Analysis Applied in Biomedical Signal Processing. *MEASUREMENT SCIENCE REVIEW,* 4(2), pp. 1-8.

Vallabhaneni A., Wang T. and He B. (2005), Brain—computer interface, *Neural engineering*. Springer, pp.85-121.

Vallbo, Å. and Johansson, R. (1984). Properties of cutaneous mechanoreceptors in the human hand - related to touch sensation. *Human Neurobiol*, (3), pp.3-14.

Van den Bos, E. and Jeannerod, M. (2002). Sense of body and sense of action both contribute to self-recognition. *Cognition*, 85(2), pp.177-187.

Vaso, A. et al. (2014). Peripheral nervous system origin of phantom limb pain. *Pain,* 155(7), pp. 1384-1391.

Vernon, D. (2005). Can Neurofeedback Training Enhance Performance? An Evaluation of the Evidence with Implications for Future Research. *Applied Psychophysiology and Biofeedback*, 30(4), pp.347-364.

Wang, H. et al. (2013). The comparison of the extraction of beta wave from EEG between FFT and wavelet transform. *Sheng Wu Yi Xue Gong Cheng Xue Za Zhi,* 30(4), pp. 704-709.

Warren, R. (1970). Auditory Illusions and Confusions. *Scientific American*, 223(6), pp.30-37.

Watson, L., Ojo, O., Cumming, J., Cheese, F., Ozcan, E., Ward, D., Potter, L., Jobson, D., Sidhu, S., Wynter, S., Dann, A., McHugh, T., Dhir, T., Birtles, A., Fenn, J. and Elder, P. (2016). *Anatomy - Nerve Supply to the Upper Limb | Geeky Medics*. [online] Geeky Medics. Available at: http://geekymedics.com/nerve-supply-to-the-upper-limb/.

WebMD. (2014). *Nerves of the Arm*. [online] Available at: http://www.webmd.com/brain/nerves-of-the-arm.

Weir RF, Heckathorne CW, Childress DS (2001): Cineplasty as a control input for externally powered prosthetic components. *Journal of Rehabilitation Research & Development.*, 38: 357-363.

Weisstein, E.W. (2002) Standard deviation. Available from: http://mathworld.wolfram.com/StandardDeviation.html.

Wheelock, T. (2013). An Introduction To Human Neuroanatomy, Belmont: Harvard Brain Tissue Resource Center.

Widmann, A. & Schröger, E. (2012). Filter Effects and Filter Artifacts in the Analysis of Electrophysiological Data. *Front Psychol.,* Volume 3, pp. 1-5.

Woolsey, T. A., Hanaway, J. & Gado, M. H. (2003). *The Brain Atlas: A Visual Guide to the Human Central Nervous System*. 2nd ed. New Jeresy: John Wiley & Sons

Wolff, A., Vanduynhoven, E., van Kleef, M., Huygen, F., Pope, J. and Mekhail, N. (2011). 21. Phantom Pain. *Pain Practice*, 11(4), pp.403-413.

Yang, T., Gallen, C., Schwartz, B., Bloom, F., Ramachandran, V. and Cobb, S. (1994). Sensory maps in the human brain. *Nature*, 368(6472), pp.592-593.

Yong, X., Fatourechi, M., Ward, R. K. & Birch, G. E. (2012). Automatic artefact removal in a self-paced hybrid brain- computer interface system. *Journal of NeuroEngineering and Rehabilitation,* pp. 9-50.

Zachry, T. (2004). *Historical Perspective of EMG*. [online] Faculty.unlv.edu. Available at: https://faculty.unlv.edu/jmercer/Seminar%20presentation/History.ppt.

Zahoor, S. & Naseem, S. (2017). Design and implementation of an efficient FIR digital filter. *Cogent Engineering ,* Volume 4, pp. 1-12.

Zeller, D., Litvak, V., Friston, K. J. & Classen, J. (2015). Sensory Processing and the Rubber Hand Illusion—An Evoked Potentials Study. *Journal of Cognitive Neuroscience,* 27(3), pp. 573-582.

Zhang, L., He, W., Miao, X. and Yang, J. (2005). Dynamic EEG Analysis via the Variability of Band Relative Intensity Ratio: A Time-Frequency Method. *2005 IEEE Engineering in Medicine and Biology 27th Annual Conference*.

Zhang, Y., Chen, Y., Bressler, S. and Ding, M. (2008). Response preparation and inhibition: The role of the cortical sensorimotor beta rhythm. *Neuroscience*, 156(1), pp.238-246.

Appendices

1. Microprocessor specification

- Core: ARM® 32-bit Cortex® -M4 CPU with FPU, Adaptive real-time accelerator (ART AcceleratorTM) allowing 0-wait state execution from Flash memory, frequency up to 168 MHz, memory protection unit, 210 DMIPS/1.25 DMIPS/MHz (Dhrystone 2.1), and DSP instructions

- Memories
  - Up to 1 Mbyte of Flash memory
  - Up to 192+4 Kbytes of SRAM including 64-Kbyte of CCM (core coupled memory) data RAM
  - Flexible static memory controller supporting Compact Flash, SRAM, PSRAM, NOR and NAND memories

- Clock, reset and supply management
  - 1.8 V to 3.6 V application supply and I/Os
  - POR, PDR,PVDandBOR
  - 4-to-26 MHz crystal oscillator
  - Internal 16 MHz factory-trimmed RC (1% accuracy)
  - 32 kHz oscillator for RTC with calibration
  - Internal 32 kHz RC with calibration
  - Sleep, Stop and Standby modes
  - V_{BAT} supply for RTC, 20×32 bit backup registers + optional 4 KB backup SRAM

- 3x12-bit, 2.4 MSPS A/D converters: up to 24 channels and 7.2 MSPS in triple interleaved mode

- 2x12-bit converters

- General-purpose DMA: 16-stream DMA controller with FIFOs and burst support

- Up to 17 timers: up to twelve 16-bit and two 32-bit timers up to 168 MHz, each with up to 4 IC/OC/PWM or pulse counter and quadrature (incremental) encoder input
- Debug mode
  - Serial wire debug (SWD) & JTAG interfaces
  - Cortex-M4 Embedded Trace MacrocellTM
- Up to 140 I/O ports with interrupt capability
  - Up to 136 fast I/Os up to 84 MHz
  - Up to 138 5 V-tolerant I/Os
- Up to 15 communication interfaces
  - Up to $3 \times$ I2 C interfaces (SMBus/PMBus)
  - Up to 4 USARTs/2 UARTs (10.5 Mbit/s, ISO 7816 interface, LIN, IrDA, modem control)
  - Up to 3 SPIs (42 Mbits/s), 2 with muxed full-duplex I2S to achieve audio class accuracy via internal audio PLL or external clock
  - 2 x CAN interfaces (2.0B Active)
  - SDIO interface
- True random number generator
- CRC calculation unit
- 96-bit unique ID
- RTC: subsecond accuracy, hardware calendar

2. Final Code for Sound Generation System

```
/* Private function prototypes ----------------------------------------------*/


static struct cal_val_t{
        float offset[5];
        float     mul[5];
        unsigned long cs;
}CAL;


static struct WG_PAKAGE{
        short     guages[5];
        float     freg[5];
```

```
        unsigned long cs;
}OUT_DATA;



unsigned int cs_cal()
{
        unsigned int *p=(unsigned int *) &CAL;

        unsigned int sum=0;
        for(int i=((sizeof(CAL))/4)-1;i--;)
        {
                sum+=*p++;
        }
        return sum;
}
char load_cal();

void I2C_Configuration(void)
{

    I2C_InitTypeDef  I2C_InitStructure;
    GPIO_InitTypeDef  GPIO_InitStructure;

    RCC_APB1PeriphClockCmd(RCC_APB1Periph_I2C3,ENABLE);
    // RCC_APB2PeriphClockCmd( RCC_APB2Periph_AFIO , ENABLE);//

    /* Configure I2C1 pins: PA8->SCL and PC9->SDA */
    GPIO_InitStructure.GPIO_Pin =  GPIO_Pin_8 ;
    GPIO_InitStructure.GPIO_Speed = GPIO_Speed_50MHz;
    GPIO_InitStructure.GPIO_OType = GPIO_OType_OD;
            GPIO_InitStructure.GPIO_PuPd = GPIO_PuPd_UP;
            GPIO_InitStructure.GPIO_Mode = GPIO_Mode_AF;
    GPIO_Init(GPIOA, &GPIO_InitStructure);
    GPIO_InitStructure.GPIO_Pin =  GPIO_Pin_9 ;
    GPIO_InitStructure.GPIO_Speed = GPIO_Speed_50MHz;
    GPIO_InitStructure.GPIO_OType = GPIO_OType_OD;
            GPIO_InitStructure.GPIO_PuPd = GPIO_PuPd_UP;
            GPIO_InitStructure.GPIO_Mode = GPIO_Mode_AF;
    GPIO_Init(GPIOC, &GPIO_InitStructure);

            GPIO_PinAFConfig(GPIOA,8,GPIO_AF_I2C3);
            GPIO_PinAFConfig(GPIOC,9,GPIO_AF_I2C3);


    I2C_DeInit(I2C_EE);
    I2C_InitStructure.I2C_Mode = I2C_Mode_I2C;
    I2C_InitStructure.I2C_DutyCycle = I2C_DutyCycle_16_9;
    I2C_InitStructure.I2C_OwnAddress1 = 1;
    I2C_InitStructure.I2C_Ack = I2C_Ack_Enable;
    I2C_InitStructure.I2C_AcknowledgedAddress = I2C_AcknowledgedAddress_7bit;
    I2C_InitStructure.I2C_ClockSpeed = 100000;  /* 100kHz */

    I2C_Cmd(I2C_EE, ENABLE);
    I2C_Init(I2C_EE, &I2C_InitStructure);
    I2C_AcknowledgeConfig(I2C_EE, ENABLE);

}
```

```c
void I2C_EE_ByteWrite(uint8_t val, uint16_t WriteAddr)
{

    /* Send START condition */
    I2C_GenerateSTART(I2C_EE, ENABLE);

    /* Test on EV5 and clear it */
    while(!I2C_CheckEvent(I2C_EE, I2C_EVENT_MASTER_MODE_SELECT));

    /* Send EEPROM address for write */
    I2C_Send7bitAddress(I2C_EE, EEPROM_HW_ADDRESS, I2C_Direction_Transmitter);

    /* Test on EV6 and clear it */
    while(!I2C_CheckEvent(I2C_EE, I2C_EVENT_MASTER_TRANSMITTER_MODE_SELECTED));


    /* Send the EEPROM's internal address to write to : MSB of the address first */
    I2C_SendData(I2C_EE, (uint8_t)((WriteAddr & 0xFF00) >> 8));

    /* Test on EV8 and clear it */
    while(!I2C_CheckEvent(I2C_EE, I2C_EVENT_MASTER_BYTE_TRANSMITTED));



    /* Send the EEPROM's internal address to write to : LSB of the address */
    I2C_SendData(I2C_EE, (uint8_t)(WriteAddr & 0x00FF));

    /* Test on EV8 and clear it */
    while(! I2C_CheckEvent(I2C_EE, I2C_EVENT_MASTER_BYTE_TRANSMITTED));


    I2C_SendData(I2C_EE, val);

      /* Test on EV8 and clear it */
    while (!I2C_CheckEvent(I2C_EE, I2C_EVENT_MASTER_BYTE_TRANSMITTED));

    /* Send STOP condition */
    I2C_GenerateSTOP(I2C_EE, ENABLE);

    //delay between write and read...not less 4ms
    Delay_ms(5);
}
//*************************************************************************
uint8_t I2C_EE_ByteRead( uint16_t ReadAddr)
{
    uint8_t tmp;

      /* While the bus is busy */
    while(I2C_GetFlagStatus(I2C_EE, I2C_FLAG_BUSY));

    /* Send START condition */
    I2C_GenerateSTART(I2C_EE, ENABLE);

    /* Test on EV5 and clear it */
    while(!I2C_CheckEvent(I2C_EE, I2C_EVENT_MASTER_MODE_SELECT));

    /* Send EEPROM address for write */
    I2C_Send7bitAddress(I2C_EE, EEPROM_HW_ADDRESS, I2C_Direction_Transmitter);
```

```c
    /* Test on EV6 and clear it */
    while(!I2C_CheckEvent(I2C_EE, I2C_EVENT_MASTER_TRANSMITTER_MODE_SELECTED));


    /* Send the EEPROM's internal address to read from: MSB of the address first */
    I2C_SendData(I2C_EE, (uint8_t)((ReadAddr & 0xFF00) >> 8));

    /* Test on EV8 and clear it */
    while(!I2C_CheckEvent(I2C_EE, I2C_EVENT_MASTER_BYTE_TRANSMITTED));

    /* Send the EEPROM's internal address to read from: LSB of the address */
    I2C_SendData(I2C_EE, (uint8_t)(ReadAddr & 0x00FF));

    /* Test on EV8 and clear it */
    while(!I2C_CheckEvent(I2C_EE, I2C_EVENT_MASTER_BYTE_TRANSMITTED));


    /* Send STRAT condition a second time */
    I2C_GenerateSTART(I2C_EE, ENABLE);

    /* Test on EV5 and clear it */
    while(!I2C_CheckEvent(I2C_EE, I2C_EVENT_MASTER_MODE_SELECT));

    /* Send EEPROM address for read */
    I2C_Send7bitAddress(I2C_EE, EEPROM_HW_ADDRESS, I2C_Direction_Receiver);

    /* Test on EV6 and clear it */

while(!I2C_CheckEvent(I2C_EE,I2C_EVENT_MASTER_BYTE_RECEIVED));//I2C_EVENT_MAST
ER_RECEIVER_MODE_SELECTED));

    tmp=I2C_ReceiveData(I2C_EE);


    I2C_AcknowledgeConfig(I2C_EE, DISABLE);

    /* Send STOP Condition */
    I2C_GenerateSTOP(I2C_EE, ENABLE);

    return tmp;
    }
//****************************************************************************
void Delay_ms(uint32_t ms)
{
    volatile uint32_t nCount;
    RCC_ClocksTypeDef RCC_Clocks;
    RCC_GetClocksFreq (&RCC_Clocks);

    nCount=(RCC_Clocks.HCLK_Frequency/10000)*ms;
    for (; nCount!=0; nCount--);
}
//****************************************************************************

void reset_cal()
{
        /*CAL.offset[0]=2500;
        CAL.mul[0]=0.3;
        CAL.offset[1]=2500;
        CAL.mul[1]=0.3;
        CAL.offset[2]=2500;
```

```
        CAL.mul[2]=0.3;
        CAL.offset[3]=2500;
        CAL.mul[3]=0.3;
        CAL.offset[4]=2500;
        CAL.mul[4]=0.3;
        CAL.cs=cs_cal();*/
}


char load_cal()
{

        char * p=(char *)&CAL;
        for(int i=0;i<sizeof(CAL);i++)
        {
                *p++=I2C_EE_ByteRead(i);

                for(int i=10000;i--;);
        }

        if(CAL.cs==cs_cal())
                        return 1;

        return 0;



}

char save_cal()
{

                CAL.cs=cs_cal();
                char * p=(char *)&CAL;
                for(int i=0;i<sizeof(CAL);i++){
                        I2C_EE_ByteWrite(*p++,i);
                }


        return 1;
}




/* Private functions -------------------------------------------------------*/




// STM32 ADC Sample @ 1440.000 KHz (PC.1) STM32F4 Discovery - sourcer32@gmail.com

// Assumptions per system_stm32f4xx.c CPU @ 168 MHz, APB2 @ 84 MHz (/2), APB1 @ 42 MHz (/4)

#include "stm32f4_discovery.h"

/*****************************************************************************
**/
```

```c
void RCC_Configuration(void)
{
  RCC_APB1PeriphClockCmd(RCC_APB1Periph_DAC, ENABLE);
  RCC_AHB1PeriphClockCmd(RCC_AHB1Periph_DMA1, ENABLE);
  RCC_AHB1PeriphClockCmd(RCC_AHB1Periph_DMA2, ENABLE);
  RCC_AHB1PeriphClockCmd(RCC_AHB1Periph_GPIOC, ENABLE);
  RCC_AHB1PeriphClockCmd(RCC_AHB1Periph_GPIOA, ENABLE);
  RCC_AHB1PeriphClockCmd(RCC_AHB1Periph_GPIOD, ENABLE);
  RCC_APB2PeriphClockCmd(RCC_APB2Periph_ADC1, ENABLE);
  RCC_APB1PeriphClockCmd(RCC_APB1Periph_TIM2, ENABLE);
  RCC_APB1PeriphClockCmd(RCC_APB1Periph_TIM6, ENABLE);
}

/**************************************************************************
**/

void GPIO_Configuration(void)
{
  GPIO_InitTypeDef GPIO_InitStructure;

  // ADC Channel 11 -> PC1 12 -> PC2  13 -> PC3


  GPIO_InitStructure.GPIO_Pin = GPIO_Pin_0;
  GPIO_InitStructure.GPIO_Mode = GPIO_Mode_AN;
  GPIO_InitStructure.GPIO_PuPd = GPIO_PuPd_NOPULL ;
  GPIO_Init(GPIOC, &GPIO_InitStructure);

  GPIO_InitStructure.GPIO_Pin = GPIO_Pin_1;
  GPIO_InitStructure.GPIO_Mode = GPIO_Mode_AN;
  GPIO_InitStructure.GPIO_PuPd = GPIO_PuPd_NOPULL ;
  GPIO_Init(GPIOC, &GPIO_InitStructure);

  GPIO_InitStructure.GPIO_Pin = GPIO_Pin_2;
  GPIO_InitStructure.GPIO_Mode = GPIO_Mode_AN;
  GPIO_InitStructure.GPIO_PuPd = GPIO_PuPd_NOPULL ;
  GPIO_Init(GPIOC, &GPIO_InitStructure);

  GPIO_InitStructure.GPIO_Pin = GPIO_Pin_3;
  GPIO_InitStructure.GPIO_Mode = GPIO_Mode_AN;
  GPIO_InitStructure.GPIO_PuPd = GPIO_PuPd_NOPULL ;
  GPIO_Init(GPIOC, &GPIO_InitStructure);

  GPIO_InitStructure.GPIO_Pin = GPIO_Pin_4; //DAC1
  GPIO_InitStructure.GPIO_Mode = GPIO_Mode_AN;
  GPIO_InitStructure.GPIO_PuPd = GPIO_PuPd_NOPULL ;
  GPIO_Init(GPIOA, &GPIO_InitStructure);

  GPIO_InitStructure.GPIO_Pin = GPIO_Pin_5; //DAC2
  GPIO_InitStructure.GPIO_Mode = GPIO_Mode_AN;
  GPIO_InitStructure.GPIO_PuPd = GPIO_PuPd_NOPULL ;
  GPIO_Init(GPIOA, &GPIO_InitStructure);


  // LED  PA11


  GPIO_InitStructure.GPIO_Pin = GPIO_Pin_12; //green
  GPIO_InitStructure.GPIO_Mode = GPIO_Mode_OUT;
```

```
  GPIO_InitStructure.GPIO_OType = GPIO_OType_PP;
  GPIO_InitStructure.GPIO_PuPd = GPIO_PuPd_NOPULL ;
  GPIO_Init(GPIOD, &GPIO_InitStructure);

   GPIO_InitStructure.GPIO_Pin = GPIO_Pin_13;
  GPIO_InitStructure.GPIO_Mode = GPIO_Mode_OUT;
  GPIO_InitStructure.GPIO_OType = GPIO_OType_PP;
  GPIO_InitStructure.GPIO_PuPd = GPIO_PuPd_NOPULL ;
  GPIO_Init(GPIOD, &GPIO_InitStructure);

   GPIO_InitStructure.GPIO_Pin = GPIO_Pin_14;
  GPIO_InitStructure.GPIO_Mode = GPIO_Mode_OUT;
  GPIO_InitStructure.GPIO_OType = GPIO_OType_PP;
  GPIO_InitStructure.GPIO_PuPd = GPIO_PuPd_NOPULL ;
  GPIO_Init(GPIOD, &GPIO_InitStructure);

   GPIO_InitStructure.GPIO_Pin = GPIO_Pin_15;
  GPIO_InitStructure.GPIO_Mode = GPIO_Mode_OUT;
  GPIO_InitStructure.GPIO_OType = GPIO_OType_PP;
  GPIO_InitStructure.GPIO_PuPd = GPIO_PuPd_NOPULL ;
  GPIO_Init(GPIOD, &GPIO_InitStructure);

}

/******************************************************************************
**/

void ADC_Configuration(void)
{
  ADC_CommonInitTypeDef ADC_CommonInitStructure;
  ADC_InitTypeDef ADC_InitStructure;

  /* ADC Common Init */
  ADC_CommonInitStructure.ADC_Mode = ADC_Mode_Independent;
  ADC_CommonInitStructure.ADC_Prescaler = ADC_Prescaler_Div2;
  ADC_CommonInitStructure.ADC_DMAAccessMode = ADC_DMAAccessMode_Disabled;
  ADC_CommonInitStructure.ADC_TwoSamplingDelay = ADC_TwoSamplingDelay_5Cycles;
  ADC_CommonInit(&ADC_CommonInitStructure);

  ADC_InitStructure.ADC_Resolution = ADC_Resolution_12b;
  ADC_InitStructure.ADC_ScanConvMode = ENABLE; // 1 Channel
  ADC_InitStructure.ADC_ContinuousConvMode = DISABLE; // Conversions Triggered
  ADC_InitStructure.ADC_ExternalTrigConvEdge = ADC_ExternalTrigConvEdge_Rising;
  ADC_InitStructure.ADC_ExternalTrigConv = ADC_ExternalTrigConv_T2_TRGO;
  ADC_InitStructure.ADC_DataAlign = ADC_DataAlign_Right;
  ADC_InitStructure.ADC_NbrOfConversion = 4;
  ADC_Init(ADC1, &ADC_InitStructure);

  /* ADC1 regular channel 11 configuration */
        ADC_RegularChannelConfig(ADC1, ADC_Channel_10, 1, ADC_SampleTime_480Cycles); //
PA0
        ADC_RegularChannelConfig(ADC1, ADC_Channel_11, 2, ADC_SampleTime_480Cycles); //
PA1
        ADC_RegularChannelConfig(ADC1, ADC_Channel_12, 3, ADC_SampleTime_480Cycles); //
PA4
        ADC_RegularChannelConfig(ADC1, ADC_Channel_13, 4, ADC_SampleTime_480Cycles); //
PA5
        //ADC_RegularChannelConfig(ADC1, ADC_Channel_9, 5, ADC_SampleTime_15Cycles); //
PA7
```

```c
    /* Enable DMA request after last transfer (Single-ADC mode) */
    ADC_DMARequestAfterLastTransferCmd(ADC1, ENABLE);

    /* Enable ADC1 DMA */
    ADC_DMACmd(ADC1, ENABLE);

    /* Enable ADC1 */
    ADC_Cmd(ADC1, ENABLE);
}

/**********************************************************************************
**/


static void DMA_Configuration(void)
{
    DMA_InitTypeDef DMA_InitStructure;

    #define   OUT_FREQ        5000                // Output waveform frequency
    #define   SINE_RES        256                 // Waveform resolution
    #define   DAC_DHR12R1_ADDR  0x40007408              // DMA writes into this reg on every
    request
    #define   DAC_DHR12R2_ADDR  0x40007414              // DMA writes into this reg on every
    request
    #define   CNT_FREQ        42000000            // TIM6 counter clock (prescaled APB1)
    #define   TIM_PERIOD      ((CNT_FREQ)/((SINE_RES)*(OUT_FREQ))) // Autoreload reg value


    //ADC1
    DMA_InitStructure.DMA_Channel = DMA_Channel_0;
    DMA_InitStructure.DMA_Memory0BaseAddr = (uint32_t)&ADCConvertedValues[0];
    DMA_InitStructure.DMA_PeripheralBaseAddr = (uint32_t)&ADC1->DR;
    DMA_InitStructure.DMA_DIR = DMA_DIR_PeripheralToMemory;
    DMA_InitStructure.DMA_BufferSize = BUFFERSIZE; // Count of 16-bit words
    DMA_InitStructure.DMA_PeripheralInc = DMA_PeripheralInc_Disable;
    DMA_InitStructure.DMA_MemoryInc = DMA_MemoryInc_Enable;
    DMA_InitStructure.DMA_PeripheralDataSize = DMA_PeripheralDataSize_HalfWord;
    DMA_InitStructure.DMA_MemoryDataSize = DMA_MemoryDataSize_HalfWord;
    DMA_InitStructure.DMA_Mode = DMA_Mode_Circular;//DMA_Mode_Normal;
    DMA_InitStructure.DMA_Priority = DMA_Priority_High;
    DMA_InitStructure.DMA_FIFOMode = DMA_FIFOMode_Enable;
    DMA_InitStructure.DMA_FIFOThreshold = DMA_FIFOThreshold_HalfFull;
    DMA_InitStructure.DMA_MemoryBurst = DMA_MemoryBurst_Single;
    DMA_InitStructure.DMA_PeripheralBurst = DMA_PeripheralBurst_Single;
    DMA_Init(DMA2_Stream0, &DMA_InitStructure);

    /* Enable DMA Stream Half / Transfer Complete interrupt */
    DMA_ITConfig(DMA2_Stream0, DMA_IT_TC | DMA_IT_HT, ENABLE);

    /* DMA2_Stream0 enable */
    DMA_Cmd(DMA2_Stream0, ENABLE);



    DAC_InitTypeDef DAC_INIT;
    DMA_InitTypeDef DMA_INIT;

    DAC_INIT.DAC_Trigger       = DAC_Trigger_T6_TRGO;
    DAC_INIT.DAC_WaveGeneration = DAC_WaveGeneration_None;
```

```c
  DAC_INIT.DAC_OutputBuffer   = DAC_OutputBuffer_Enable;
  DAC_Init(DAC_Channel_2, &DAC_INIT);

  DMA_DeInit(DMA1_Stream6);
  DMA_INIT.DMA_Channel          = DMA_Channel_7;
  DMA_INIT.DMA_PeripheralBaseAddr = (uint32_t)DAC_DHR12R2_ADDR;
  DMA_INIT.DMA_Memory0BaseAddr   = (uint32_t)&sine200;
  DMA_INIT.DMA_DIR             = DMA_DIR_MemoryToPeripheral;
  DMA_INIT.DMA_BufferSize       = 3200;
  DMA_INIT.DMA_PeripheralInc     = DMA_PeripheralInc_Disable;
  DMA_INIT.DMA_MemoryInc        = DMA_MemoryInc_Enable;
  DMA_INIT.DMA_PeripheralDataSize = DMA_PeripheralDataSize_HalfWord;
  DMA_INIT.DMA_MemoryDataSize    = DMA_MemoryDataSize_HalfWord;
  DMA_INIT.DMA_Mode             = DMA_Mode_Normal;//DMA_Mode_Circular;
  DMA_INIT.DMA_Priority         = DMA_Priority_High;
  DMA_INIT.DMA_FIFOMode          = DMA_FIFOMode_Disable;
  DMA_INIT.DMA_FIFOThreshold     = DMA_FIFOThreshold_HalfFull;
  DMA_INIT.DMA_MemoryBurst       = DMA_MemoryBurst_Single;
  DMA_INIT.DMA_PeripheralBurst    = DMA_PeripheralBurst_Single;
  DMA_Init(DMA1_Stream6, &DMA_INIT);
  DMA_ITConfig(DMA1_Stream6,  DMA_IT_TC  |DMA_IT_TE  |DMA_IT_DME  |DMA_IT_FE/*|
DMA_IT_HT*/, ENABLE);




}

/*****************************************************************************
**/

void TIM2_Configuration(void)
{
  TIM_TimeBaseInitTypeDef TIM_TimeBaseStructure;

  /* Time base configuration */
  TIM_TimeBaseStructInit(&TIM_TimeBaseStructure);
  TIM_TimeBaseStructure.TIM_Period = (84000000 / 100000) - 1; // 100 KHz, from 84 MHz TIM2CLK
(ie APB1 = HCLK/4, TIM2CLK = HCLK/2)
  TIM_TimeBaseStructure.TIM_Prescaler = 0;
  TIM_TimeBaseStructure.TIM_ClockDivision = 0;
  TIM_TimeBaseStructure.TIM_CounterMode = TIM_CounterMode_Up;
  TIM_TimeBaseInit(TIM2, &TIM_TimeBaseStructure);

  /* TIM2 TRGO selection */
  TIM_SelectOutputTrigger(TIM2, TIM_TRGOSource_Update); // ADC_ExternalTrigConv_T2_TRGO

  /* TIM2 enable counter */
  TIM_Cmd(TIM2, ENABLE);


  /* Time base configuration */
  TIM_TimeBaseStructInit(&TIM_TimeBaseStructure);
  TIM_TimeBaseStructure.TIM_Period = (84000000 / 200000) - 1; // 100 KHz, from 84 MHz TIM2CLK
(ie APB1 = HCLK/4, TIM2CLK = HCLK/2)
  TIM_TimeBaseStructure.TIM_Prescaler = 0;
  TIM_TimeBaseStructure.TIM_ClockDivision = 0;
  TIM_TimeBaseStructure.TIM_CounterMode = TIM_CounterMode_Up;
  TIM_TimeBaseInit(TIM6, &TIM_TimeBaseStructure);

  /* TIM6 TRGO selection */
```

```
    TIM_SelectOutputTrigger(TIM6, TIM_TRGOSource_Update); // ADC_ExternalTrigConv_T2_TRGO

  /* TIM6 enable counter */
  TIM_Cmd(TIM6, ENABLE);

}
```

/***
**/

```
void NVIC_Configuration(void)
{
  NVIC_InitTypeDef NVIC_InitStructure;

  /* Enable the DMA Stream IRQ Channel */
  NVIC_InitStructure.NVIC_IRQChannel = DMA2_Stream0_IRQn;
  NVIC_InitStructure.NVIC_IRQChannelPreemptionPriority = 0;
  NVIC_InitStructure.NVIC_IRQChannelSubPriority = 0;
  NVIC_InitStructure.NVIC_IRQChannelCmd = ENABLE;
  NVIC_Init(&NVIC_InitStructure);

  NVIC_InitStructure.NVIC_IRQChannel = DMA1_Stream6_IRQn;
  NVIC_InitStructure.NVIC_IRQChannelPreemptionPriority = 0;
  NVIC_InitStructure.NVIC_IRQChannelSubPriority = 0;
  NVIC_InitStructure.NVIC_IRQChannelCmd = ENABLE;
  NVIC_Init(&NVIC_InitStructure);

}
```

/***
**/

```
/////////////////////////////////////
/////////////////////////////////////
/////////////////////////////////////
extern "C"{
/////////////////////////////////////
/////////////////////////////////////
/////////////////////////////////////


        void DMA1_Stream6_IRQHandler(void) // Called at 1 KHz for 200 KHz sample rate, LED
Toggles at 500 Hz
{

        LED2ON;

        /* Test on DMA Stream Transfer Complete interrupt */
        if(DMA_GetITStatus(DMA1_Stream6, DMA_IT_TCIF6))
        {
        /* Clear DMA Stream Transfer Complete interrupt pending bit */

        DMA_ClearITPendingBit(DMA1_Stream6,     DMA_IT_TCIF6     |     DMA_IT_FEIF6     |
DMA_IT_DMEIF6 | DMA_IT_TEIF6);
        }

        DMA1_Stream6->M0AR=(unsigned long) sine;
//      DMA_Cmd(DMA1_Stream6, ENABLE);
        TIM6->ARR=sine_period;
```

```c
        DMA1_Stream6->CR|=1;
        LED2OFF;
}


/////////////////////////////////////////////////////////////////////
/////////////////////////////////////////////////////////////////////
/////////////////////////////////////////////////////////////////////



void DMA2_Stream0_IRQHandler(void) // Called at 1 KHz for 200 KHz sample rate, LED Toggles at 500 Hz
{

        LEDON;
  int start_pos;
 /* Test on DMA Stream Half Transfer interrupt */
 if(DMA_GetITStatus(DMA2_Stream0, DMA_IT_HTIF0))
 {
   /* Clear DMA Stream Half Transfer interrupt pending bit */
   DMA_ClearITPendingBit(DMA2_Stream0, DMA_IT_HTIF0);
   start_pos=0;
 }

 /* Test on DMA Stream Transfer Complete interrupt */
 if(DMA_GetITStatus(DMA2_Stream0, DMA_IT_TCIF0))
 {
   /* Clear DMA Stream Transfer Complete interrupt pending bit */
   DMA_ClearITPendingBit(DMA2_Stream0, DMA_IT_TCIF0);
        start_pos=BUFFERSIZE/2;
 }

        LEDON;

        static float _average=2048;
          /*static float _dc=0;
        static double _ac=0;
        static long long sum;*/

        uint16_t  *p;
        p=&ADCConvertedValues[start_pos];



        static int sign_static=0,count_static=0,avr_static=2048;
        int avr=0/*avr_static*/,sign=sign_static,count=count_static;

        static int j=0;


        static unsigned long long avr2_static;
        unsigned long long avr2=avr2_static;
        unsigned long RMS_SQUARE_SUM=0;

        int RAW1=0,RAW2=0,RAW3=0,RAW4=0,c;

        for(int i=10;i--;)   //1 Cylce
        {
```

```c
//get and average 10 * 5ch samples // assumptive 30.000 KSMP
RAW1+=(*p++);
RAW2+=(*p++);
RAW3+=(*p++);
RAW4+=(*p++);

RAW1+=(*p++);
RAW2+=(*p++);
RAW3+=(*p++);
RAW4+=(*p++);

RAW1+=(*p++);
RAW2+=(*p++);
RAW3+=(*p++);
RAW4+=(*p++);

RAW1+=(*p++);
RAW2+=(*p++);
RAW3+=(*p++);
RAW4+=(*p++);


RAW1+=(*p++);
RAW2+=(*p++);
RAW3+=(*p++);
RAW4+=(*p++);

RAW1+=(*p++);
RAW2+=(*p++);
RAW3+=(*p++);
RAW4+=(*p++);

RAW1+=(*p++);
RAW2+=(*p++);
RAW3+=(*p++);
RAW4+=(*p++);

RAW1+=(*p++);
RAW2+=(*p++);
RAW3+=(*p++);
RAW4+=(*p++);

RAW1+=(*p++);
RAW2+=(*p++);
RAW3+=(*p++);
RAW4+=(*p++);

RAW1+=(*p++);
RAW2+=(*p++);
RAW3+=(*p++);
RAW4+=(*p++);

}


RAWV1+=(((float)RAW1/100)-RAWV1)/4;
RAWV2+=(((float)RAW2/100)-RAWV2)/4;
RAWV3+=(((float)RAW3/100)-RAWV3)/4;
RAWV4+=(((float)RAW4/100)-RAWV4)/4;
```

```
TEMP=((RAWV2/4096)-(RAWV4/4096))*295;//2.95 V
FL=((1-(RAWV3/4096))*100)-50;
FG=((1-RAWV1/4096)*60)+0.1;
float ff=fabs(TEMP-FL);
freq=(ff*FG)+10;
if(freq<10)freq=10;
if(freq>9999)freq=9999;
float f;
if(freq<100)
{
        //3200 step sine
        sine=sine3200;
        f=((84000000/3200)/freq);  // (84000000/12800)
        sine_period=(int)f;
}
else if(freq<200)
{
        //1600 step sine
        sine=sine1600;
        f=((84000000/1600)/freq);
        sine_period=(int)f;
}
else if(freq<400)
{
        //800 step sine
        sine=sine800;
        f=((84000000/800)/freq);
        sine_period=(int)f;
}
else if(freq<800)
{
        //400 step sine
        sine=sine400;
        f=((84000000/400)/freq);
        sine_period=(int)f;
}
else if(freq<1600)
{
        //200 step sine
        sine=sine200;
        f=((84000000/200)/freq);
        sine_period=(int)f;
}
else// if(freq<3200)
{
        //100 step sine
        sine=sine100;
        f=((84000000/100)/freq);
        sine_period=(int)f;
}

d_counter++;


LEDOFF;
}


////////////////////////////////////
```

```
///////////////////////////////
///////////////////////////////
}//extern "C"
///////////////////////////////
///////////////////////////////
///////////////////////////////

/*******************************************************************************
**/


/*
 struct TESLA_ANALOG_DAA{
         unsigned short AC;
         unsigned short DC;
         unsigned short ZERO;
         unsigned short CS;
};

static TESLA_ANALOG_DAA D;*/

unsigned short int D[10];
/*

if ( x < nmaxval )
{
        nscaledrootmean +( ( navgcoeff * x ) nrootmean ) - ( navgcoeff * nrootmean );
}
else
{
        nscaledrootmean +nAvgCoeff * ( ( xnrootmean ) - nrootmean );
}
*/

void execute_command(char * str){
        /////////////////////////////////////////
        if(str[0]=='~' && str[1]=='Z' && str[2]==';' )   // zeroing
        {
        /*      CAL.offset[0]=RAWV1;
                CAL.offset[1]=RAWV2;
                CAL.offset[2]=RAWV3;
                CAL.offset[3]=RAWV4;
                CAL.offset[4]=RAWV5;*/

        }
        /////////////////////////////////////////
        if(str[0]=='~' && str[1]=='S' && str[2]==';' )   // saving
        {

                /*if(save_cal())
                {
                        TM_USART_Puts(USART3, "~^d^o^n^E   ;");
                }
                else
                {
                        TM_USART_Puts(USART3, "~^E^r^r^   ;");
                }*/
        }
        /////////////////////////////////////////
        if(str[0]=='~' && str[1]=='C' && str[2]==':' )   // zeroing
```

```
            {
                    /*int input;
                    float real_val;
                    sscanf(str,"~C:%d;",&input);
                    real_val=input;

                    CAL.mul[4]=(RAWV5-CAL.offset[4])/real_val;
                    CAL.mul[3]=(RAWV4-CAL.offset[3])/real_val;
                    CAL.mul[2]=(RAWV3-CAL.offset[2])/real_val;
                    CAL.mul[1]=(RAWV2-CAL.offset[1])/real_val;
                    CAL.mul[0]=(RAWV1-CAL.offset[0])/real_val;*/

            }
            //////////////////////////////////////////
}


int main(void)
{
SystemInit();
  RCC_Configuration();
  GPIO_Configuration();

  for(int i=4;i--;){
            LEDON;
            LED4OFF;
            Delay_ms(70);
            LED2ON;
            LEDOFF;
            Delay_ms(70);
            LED3ON;
            LED2OFF;
            Delay_ms(70);
            LED4ON;
            LED3OFF;
            Delay_ms(70);
  }
  NVIC_Configuration();
  TIM2_Configuration();
  DMA_Configuration();
  ADC_Configuration();
  ADC_SoftwareStartConv(ADC1);
    // Initialize USART1 at 115200 baud, TX: PD8, RX: PD9
  TM_USART_Init(USART3, TM_USART_PinsPack_3, 38400);
      // Initialize USART1 at 115200 baud, TX: PD8, RX: PD9
// TM_USART_Init(USART2, TM_USART_PinsPack_1, 115200);

// TM_I2C_Init(I2C3, TM_I2C_PinsPack_1, 10000);
// I2C_Configuration();
            double f=0;
            int k;

            for(f=0,k=0;f<6.2831853;f+=6.2831853/3200,k++)
              sine100[k]=(int)((sin(f*32)+1)*2000);
            for(f=0,k=0;f<6.2831853;f+=6.2831853/3200,k++)
              sine200[k]=(int)((sin(f*16)+1)*2000);
            for(f=0,k=0;f<6.2831853;f+=6.2831853/3200,k++)
              sine400[k]=(int)((sin(f*8)+1)*2000);
            for(f=0,k=0;f<6.2831853;f+=6.2831853/3200,k++)
              sine800[k]=(int)((sin(f*4)+1)*2000);
```

```c
      for(f=0,k=0;f<6.2831853;f+=6.2831853/3200,k++)
        sine1600[k]=(int)((sin(f*2)+1)*2000);
      for(f=0,k=0;f<6.2831853;f+=6.2831853/3200,k++)
        sine3200[k]=(int)((sin(f)+1)*2000);
      static  char d=0, DISP_STR[40], * DS;
      static unsigned int last_d_counter=0;
      static char s[100];
      static char instr[100];
      char inlen=0;
      char inchar;

      DAC_Cmd(DAC_Channel_2, ENABLE);

      DMA_Cmd(DMA1_Stream6, ENABLE);
      DAC_DMACmd(DAC_Channel_2, ENABLE);
//  sprintf(s,";;~^L^o^a^d^-^-^-^-;");
//  TM_USART_Puts(USART3, s);
  Delay_ms(100);
  last_FL=FL;
  last_FG=FG;
  FL_change=0;
  FG_change=0;

  while(1)
  {


      if(!uncallibrated){
      static int disp_ch=0,disp_ch_counter=0;static int disp_prescaler=10;
              if(d>0)
              {

                      if(disp_prescaler<1)
                      {
                              TM_USART_Putc(USART3, *DS++);
                              d=d-1;
                              disp_prescaler=2;
                      }
              }
              else{
                      d=0;
                      disp_prescaler=0;
                      if(FL_change)
                      {
                              sprintf(DISP_STR,"~SEt0%2.1fc ;",FL);
                              d=strlen(DISP_STR);
                              DS=DISP_STR;
                              FL_change--;
                      }
                      else if(FG_change)
                      {
                              sprintf(DISP_STR,"~rAtE%2.2f ;",FG);
                              d=strlen(DISP_STR);
                              DS=DISP_STR;
                              FG_change--;
                      }
                      else
                      {
```

```c
                                if(TEMP<=0)
                                        sprintf(DISP_STR,"~%03dc%2.1f ;",(int)TEMP,freq);
                                else if(TEMP<10)
                                        sprintf(DISP_STR,"~%2.2fc%2.1f ;",TEMP,freq);
                                else if(TEMP<100)
                                        sprintf(DISP_STR,"~%3.1fc%2.1f ;",TEMP,freq);
                                else
                                        sprintf(DISP_STR,"~%3dc%2.1f                ;",(unsigned
int)TEMP,freq);
                                d=strlen(DISP_STR);
                                DS=DISP_STR;
                        }

                        if(fabs(last_FL-FL)>0.08){FL_change=30;last_FL=FL;}
                        if(fabs(last_FG-FG)>0.3){FG_change=30;last_FG=FG;}
                }
                if(d_counter>=last_d_counter+1)
                {
                        disp_prescaler--;
                        disp_ch_counter++;
                        last_d_counter=d_counter;
                }
        }


 }

}

#ifdef  USE_FULL_ASSERT

/**
  * @brief  Reports the name of the source file and the source line number
  *         where the assert_param error has occurred.
  * @param  file: pointer to the source file name
  * @param  line: assert_param error line source number
  * @retval None
  */
void assert_failed(uint8_t* file, uint32_t line)
{
  /* User can add his own implementation to report the file name and line number,
     ex: printf("Wrong parameters value: file %s on line %d\r\n", file, line) */

  /* Infinite loop */
  while (1)
  {
  }
}
#endif

/**
  * @}
  */

/**
  * @}
  */
```

3. Rubber Hand Illusion Questionnaire

Rubber Hand Illusion Questionnaire

Name:
Gender:
Age:
Do you have any health condition:

Please indicate your level of agreement or disagreement with each of these statements regarding RHI Experiment. Place an "X" mark in the box of your answer. 1 is strongly disagree and 5 is strongly agree.

	1	2	3	4	5
Q1: It seemed as if I were feeling the touch of paintbrush in the location where I saw the rubber hand touched					
Q2: It seemed as though the touch I felt was caused by the paintbrush touching the rubber hand					
Q3: I felt as if the rubber hand was my hand					
Q4: It seemed as if I might have more than one left hand/arm					
Q5: It seemed as if the touch I was feeling came from somewhere between my own hand and the rubber hand					
Q6: It felt as if my hand were turning "Rubber"					
Q7: I felt the touch of brush in both hands at the same time					
Q8: It no longer felt like my real hand belonged to my body					
Q9: It felt my real hand was drifting towards rubber hand					
Q10: I felt I can control the movement of the Rubber hand					

Further Comments:

Thank you for your time and cooperation

4. Sound Generator Questionnaire

Sound Generator System Questionnaire

Name:
Gender:
Age:
Do you have any health condition:

Please give mark to indicate your level of agreement or disagreement with each of these statements regarding SGS Experiment. Place an "X" mark in the box of your answer. 1 is lowest and 5 are highest.

	1	2	3	4	5
Q1: During SGS I could understand the temperature difference between objects					
Q2: I could understand the temperature difference with my closed eyes					
Q3: It felt like objects was applying to my body from two different places					
Q4: I was less aware of temperature from my own hand					
Q5: I was less aware of temperature from my ear					
Q6: I lost sensation from my hand					
Q7: How much you could identify each beeping sound during this experience?					
Q8: How much attention did you paid to the sound at the end of the experience?					

Further Comments:

Thank you for your time and cooperation

5. Detailed data on illusionary experiments

Table 20 Descriptive data on individual participants on RHI 1

Participant	Q1	Q2	Q3	Q4	Q5	Q6	Q7	Q8	Q9	Q10
NO 1	5	4	5	2	2	3	4	4	2	4
NO 2	4	3	4	1	1	2	2	2	3	3
NO 3	5	4	4	3	3	4	4	4	3	5
NO 4	4	3	3	3	3	2	4	3	3	3
NO 5	5	5	5	2	2	3	4	4	2	5
NO 6	4	4	4	2	2	3	3	3	2	4
NO 7	5	5	5	3	3	3	2	4	3	4
NO 8	5	5	4	3	3	4	3	4	1	5
NO 9	4	4	3	2	2	3	3	3	2	4
NO 10	4	3	4	2	2	3	4	3	2	3
NO 11	4	3	3	1	1	2	2	3	1	3
NO 12	5	4	4	3	3	3	4	4	3	4
NO 13	4	4	4	2	2	3	3	3	2	4
NO 14	5	5	5	3	3	4	4	4	3	4
NO 15	5	5	4	3	3	4	4	4	2	5
NO 16	3	3	4	3	3	3	3	3	3	3
NO 17	5	4	4	4	4	3	4	4	3	4
NO 18	5	5	3	3	3	3	3	4	3	4
NO 19	5	5	5	4	4	3	3	4	3	4
NO 20	5	5	4	4	4	2	3	4	4	4
NO 21	4	4	4	3	3	3	4	3	2	3
NO 22	5	5	4	2	2	3	3	4	3	4
NO 23	4	3	4	2	2	3	3	3	3	3
NO 24	5	4	4	3	3	3	3	4	3	4
NO 25	4	3	5	1	1	2	2	3	3	3
NO 26	4	4	5	3	3	4	4	4	3	3
NO 27	4	4	4	2	2	3	4	3	3	3
NO 28	5	5	4	3	3	4	4	4	2	5

Table 21 Descriptive data on individual participants on RHI 2

Participant	Q1	Q2	Q3	Q4	Q5	Q6	Q7	Q8	Q9	Q10
NO 1	5	4	5	4	2	4	3	4	3	3
NO 2	5	5	3	3	1	3	3	4	3	4
NO 3	5	4	4	3	3	3	4	3	4	3
NO 4	4	4	4	2	3	2	3	3	3	3
NO 5	5	4	4	3	2	3	4	4	3	3
NO 6	4	5	4	3	2	3	3	3	3	3
NO 7	5	5	3	4	3	4	4	4	3	3
NO 8	5	5	4	3	3	3	4	4	2	4
NO 9	4	4	3	2	2	2	3	3	4	4
NO 10	4	4	4	4	2	4	3	3	2	4
NO 11	4	4	3	2	1	2	3	3	3	3
NO 12	5	4	3	3	3	3	3	4	3	3
NO 13	4	5	3	3	2	3	3	3	3	3
NO 14	5	4	5	3	3	3	3	3	3	4
NO 15	5	4	4	3	3	3	3	3	3	4
NO 16	4	4	3	3	3	3	3	4	3	4
NO 17	5	5	5	3	4	3	4	3	3	3
NO 18	5	4	3	2	3	2	4	3	2	3
NO 19	5	4	5	4	4	4	4	3	3	4
NO 20	5	4	4	3	4	3	3	3	3	3
NO 21	4	5	4	4	3	4	4	3	3	4
NO 22	5	5	5	4	2	4	4	4	3	4
NO 23	4	5	4	3	2	3	3	4	2	3
NO 24	5	5	3	3	3	3	3	4	4	3
NO 25	4	4	3	3	1	3	3	3	3	3
NO 26	4	5	4	3	3	3	3	3	4	4
NO 27	4	5	4	2	2	2	4	3	4	3
NO 28	5	5	4	3	3	3	3	4	2	3

Table 22 Descriptive data on individual participants on RHI 3

Participant	Q1	Q2	Q3	Q4	Q5	Q6	Q7	Q8	Q9	Q10
NO 1	4	3	4	2	3	3	2	2	2	1
NO 2	4	3	3	2	5	3	2	3	3	3
NO 3	5	4	3	3	3	1	3	3	1	3
NO 4	5	4	4	2	3	2	5	4	1	2
NO 5	4	4	4	3	2	3	1	3	3	4
NO 6	4	1	2	1	1	1	4	3	3	4
NO 7	5	3	4	4	4	4	5	3	4	3
NO 8	5	5	3	3	1	1	2	1	1	5
NO 9	3	4	3	2	2	3	4	2	2	4
NO 10	4	4	5	4	1	2	4	3	1	2
NO 11	4	3	2	1	2	1	5	3	3	3
NO 12	5	4	4	2	1	2	5	3	3	2
NO 13	3	4	4	3	2	3	4	1	3	3
NO 14	5	3	4	3	3	4	1	5	4	3
NO 15	5	4	5	2	2	3	5	4	3	4
NO 16	4	5	4	2	2	2	4	3	3	4
NO 17	5	5	4	2	1	3	3	1	2	4
NO 18	4	5	5	5	5	1	4	4	3	5
NO 19	5	3	3	1	3	1	2	4	3	5
NO 20	3	4	4	2	3	2	5	4	1	2
NO 21	4	5	3	5	3	4	4	4	4	4
NO 22	4	2	2	2	2	2	5	2	1	3
NO 23	3	1	2	3	2	3	4	3	3	5
NO 24	4	4	4	4	1	5	4	2	3	4
NO 25	3	3	4	2	3	4	5	5	3	3
NO 26	5	5	4	3	3	3	2	2	3	2
NO 27	5	3	4	4	3	3	2	3	3	1
NO 28	4	4	4	2	2	2	2	2	2	4

Table 23 Descriptive data on individual participants on RHI 4

Participant	Q1	Q2	Q3	Q4	Q5	Q6	Q7	Q8	Q9	Q10
NO 1	3	4	3	2	1	3	4	3	4	5
NO 2	4	4	4	2	2	4	4	3	3	5
NO 3	4	5	4	2	1	2	1	3	3	4
NO 4	5	5	3	5	1	3	1	2	4	3
NO 5	3	3	2	4	4	2	1	3	3	3
NO 6	4	4	5	2	2	2	1	2	2	5
NO 7	4	4	4	1	3	4	3	1	1	3
NO 8	3	3	5	5	1	4	2	1	2	3
NO 9	3	3	4	4	3	4	3	3	3	2
NO 10	2	2	1	1	2	1	2	1	2	2
NO 11	5	4	2	2	3	1	1	1	2	1
NO 12	4	4	4	4	1	1	3	1	1	4
NO 13	5	3	3	3	3	2	3	3	2	4
NO 14	4	4	4	1	2	3	3	2	3	4
NO 15	3	3	4	3	3	3	5	3	1	4
NO 16	3	5	3	3	4	4	5	3	2	3
NO 17	5	5	5	5	2	1	2	3	4	4
NO 18	5	5	5	1	4	5	5	5	5	5
NO 19	4	4	2	3	3	2	4	5	5	5
NO 20	4	4	3	1	3	3	2	4	4	4
NO 21	4	5	4	2	3	3	1	2	2	5
NO 22	3	4	2	3	4	3	5	4	2	3
NO 23	5	5	4	2	5	1	3	2	1	4
NO 24	5	5	4	3	1	1	1	4	4	5
NO 25	4	4	4	3	2	2	1	3	3	4
NO 26	4	4	4	3	3	3	4	3	3	3
NO 27	3	3	4	3	2	3	4	3	3	3
NO 28	3	3	4	4	3	4	3	3	3	3

Table 24 Descriptive data on individual participants on RHI 5

Participant	Q1	Q2	Q3	Q4	Q5	Q6	Q7	Q8	Q9	Q10
NO 1	5	4	4	3	4	3	3	4	3	5
NO 2	5	4	4	1	2	1	4	2	1	3
NO 3	4	4	4	1	3	3	4	2	3	4
NO 4	5	5	5	4	2	1	3	1	1	4
NO 5	4	5	5	4	5	4	4	4	4	4
NO 6	5	4	5	2	2	3	3	2	2	5
NO 7	4	4	3	3	3	1	1	3	3	3
NO 8	5	3	5	1	2	4	4	3	2	3
NO 9	5	3	4	3	2	1	4	5	2	5
NO 10	5	4	5	2	1	3	2	5	1	3
NO 11	4	3	4	3	3	2	4	4	2	3
NO 12	5	4	3	1	2	1	3	2	3	2
NO 13	4	4	4	3	3	2	3	4	1	2
NO 14	4	3	3	2	3	3	3	3	2	3
NO 15	5	5	4	3	3	4	5	1	4	4
NO 16	4	5	4	4	3	3	3	4	3	3
NO 17	5	4	5	2	2	2	3	4	3	2
NO 18	4	5	4	4	2	3	4	4	2	3
NO 19	4	3	4	3	2	3	5	4	5	3
NO 20	5	4	4	3	5	3	3	3	2	4
NO 21	5	4	3	3	1	1	4	3	3	4
NO 22	4	3	5	4	2	1	3	3	1	4
NO 23	4	3	4	5	3	2	3	3	2	4
NO 24	4	5	4	1	2	3	2	3	4	3
NO 25	5	4	4	2	3	3	2	4	3	3
NO 26	5	5	4	3	2	3	4	4	5	3
NO 27	5	4	4	2	1	4	5	3	4	3
NO 28	4	3	5	3	2	1	4	3	3	4

Table 25 Descriptive data on individual participants on RHI 6

Participant	Q1	Q2	Q3	Q4	Q5	Q6	Q7	Q8	Q9	Q10
NO 1	2	1	2	1	2	1	3	1	2	2
NO 2	2	3	3	1	1	1	2	2	3	3
NO 3	5	3	4	2	1	2	2	3	1	4
NO 4	5	4	3	2	2	1	4	2	1	2
NO 5	4	3	4	2	1	1	3	3	3	2
NO 6	2	3	3	1	1	2	2	2	3	2
NO 7	4	4	3	1	4	1	2	1	4	4
NO 8	3	2	3	1	4	2	2	2	1	2
NO 9	4	2	4	1	3	2	1	3	2	3
NO 10	4	1	3	1	2	1	2	3	1	3
NO 11	5	2	4	2	2	1	2	3	3	1
NO 12	1	1	2	1	1	2	3	3	1	1
NO 13	2	2	2	1	3	1	2	2	2	3
NO 14	2	2	3	1	1	1	3	3	3	2
NO 15	5	1	3	2	1	2	3	1	2	5
NO 16	2	3	3	1	2	1	3	4	2	1
NO 17	5	4	4	3	1	1	3	3	1	2
NO 18	5	4	3	2	2	1	3	3	2	3
NO 19	2	5	4	2	2	1	2	3	3	3
NO 20	4	4	4	1	1	1	3	2	1	3
NO 21	2	4	3	1	2	2	3	3	3	3
NO 22	4	4	4	3	2	2	3	3	2	2
NO 23	2	3	3	2	1	1	3	3	2	1
NO 24	4	4	3	2	2	2	2	4	1	2
NO 25	4	2	3	1	1	2	2	2	2	2
NO 26	3	4	3	2	2	1	1	1	2	3
NO 27	3	3	3	2	2	2	2	1	3	2
NO 28	4	2	3	1	2	1	3	2	3	3

Table 26 Time (s) of effect of illusion in each participant in different experiments

Participants	RHI 1	RHI 2	RHI 3	RHI 4	RHI 5	RHI 6
NO 1	296	244	296	338	247	552
NO 2	194	276	275	204	297	431
NO 3	262	231	245	294	290	312
NO 4	218	270	214	260	214	276
NO 5	213	276	212	258	279	467
NO 6	243	262	259	275	259	549
NO 7	270	222	268	271	267	430
NO 8	215	251	223	297	191	358
NO 9	297	187	264	345	254	515
NO 10	274	257	237	195	237	358
NO 11	238	227	269	234	238	400
NO 12	209	198	310	203	223	345
NO 13	205	231	221	233	396	367
NO 14	250	294	197	210	211	300
NO 15	297	291	347	317	254	573
NO 16	236	307	328	219	269	451
NO 17	221	334	344	239	221	341
NO 18	292	222	283	243	381	575
NO 19	275	181	237	327	318	496
NO 20	205	311	332	292	334	336
NO 21	260	313	244	346	283	470
NO 22	295	284	250	237	186	439
NO 23	252	325	316	275	203	399
NO 24	295	246	204	197	299	298
NO 25	239	202	349	283	381	550
NO 26	222	334	263	312	221	318
NO 27	239	260	211	312	261	365
NO 28	215	309	236	327	288	312

Table 27: Descriptive data for moving hand 0cm height

	Q1	Q2	Q3	Q4	Q5	Q6	Q7	Q8	Q9	Q10	Time
Day 1	5	5	3	3	2	4	5	2	2	4	385
Day 2	5	5	3	3	2	4	4	3	2	3	383
Day 3	5	4	3	3	2	4	5	3	2	3	372
Day 4	3	3	3	2	2	4	4	3	2	3	370
Day 5	4	3	4	3	2	4	4	3	2	4	350
Day 6	3	3	3	3	2	4	3	3	1	3	340
Day 7	4	4	3	3	1	4	3	3	1	3	320
Day 8											
Day 9					GAP						
Day 10	4	4	3	3	1	4	3	3	1	3	348
Day 11	3	3	3	2	1	3	3	2	1	3	235
Day 12	4	3	3	3	1	4	3	2	1	3	200
Day 13	3	3	2	2	1	3	2	2	1	2	197
Day 14											
Day 15					GAP						
Day 16											
Day 17	4	4	3	2	1	3	3	3	1	3	195
Day 18	4	4	3	3	1	4	3	3	1	3	175
Day 19	4	5	4	3	1	4	4	3	1	4	140
Day 20	5	5	4	3	1	4	4	3	1	3	81

Table 28: Descriptive data for moving hand in 4cm height

	Q1	Q2	Q3	Q4	Q5	Q6	Q7	Q8	Q9	Q10	Time
Day 1	4	3	3	3	2	5	4	3	2	3	397
Day 2	4	3	3	3	2	5	4	3	2	3	391
Day 3	4	4	3	3	2	4	4	3	2	3	386
Day 4	4	4	3	3	2	3	4	3	2	3	385
Day 5	4	4	3	3	2	4	4	3	2	4	384
Day 6	4	4	3	3	1	4	4	3	1	3	369
Day 7	5	5	4	3	1	4	3	3	1	4	326
Day 8											
Day 9						GAP					
Day 10	4	4	3	3	1	4	4	3	1	3	354
Day 11	4	4	3	3	1	4	3	3	1	3	263
Day 12	4	4	3	2	1	4	3	3	1	4	246
Day 13	3	4	3	3	1	3	3	3	1	4	233
Day 14											
Day 15						GAP					
Day 16											
Day 17	4	4	3	3	1	4	3	3	1	4	211
Day 18	5	5	4	3	1	4	4	3	1	4	189
Day 19	5	5	4	3	1	4	4	3	1	4	152
Day 20	5	5	3	3	1	4	4	3	1	4	91

Table 29: Descriptive data for moving hand in 7cm height

	Q1	Q2	Q3	Q4	Q5	Q6	Q7	Q8	Q9	Q10	Time
Day 1	5	3	3	3	1	4	3	3	2	2	390
Day 2	4	3	3	3	2	4	3	3	2	2	389
Day 3	5	3	3	3	2	4	4	3	2	3	385
Day 4	4	4	3	3	2	4	4	3	2	3	387
Day 5	4	3	3	3	2	4	4	3	2	3	380
Day 6	4	4	3	3	1	4	3	3	1	4	357
Day 7	4	4	3	3	1	4	4	2	1	3	328
Day 8											
Day 9						GAP					
Day 10	5	5	4	3	1	4	4	3	1	4	356
Day 11	4	4	4	3	1	4	3	3	1	4	230
Day 12	5	5	4	3	1	5	3	4	1	4	220
Day 13	3	3	2	2	1	3	2	2	1	2	215
Day 14											
Day 15						GAP					
Day 16											
Day 17	5	5	4	3	1	4	4	3	1	4	198
Day 18	5	5	4	3	1	4	3	4	1	4	182
Day 19	5	5	4	3	1	4	3	4	1	4	141
Day 20	5	4	4	3	1	5	4	4	1	4	81

Table 30: Descriptive data on three attempt of RHI

	Q1	Q2	Q3	Q4	Q5	Q6	Q7	Q8	Q9	Q10	Time(s)
1St attempt	4	3	4	3	3	3	4	4	2	3	301
2nd attempt	4	3	4	3	3	3	5	5	3	4	90
3rd attempt	5	4	5	5	3	3	4	5	2	4	128

Table 31 Descriptive data on Right-handed male on SGS over 1 month

M, R, 22	Q1	Q2	Q3	Q4	Q5	Q6	Q7	Q8	Time
Day 1	3	2	1	1	2	1	3	5	3476
Day 2	3	3	1	1	2	1	3	5	3357
Day 3	3	3	1	1	1	1	2	5	3353
Day 4	4	3	2	1	1	1	2	5	3460
Day 5	4	3	2	2	1	1	2	5	3189
Day 6	4	2	2	2	1	1	2	5	3297
Day 7	4	2	2	2	2	1	3	5	3244
Day 8	4	3	2	2	2	1	3	5	3054
Day 9	4	3	2	1	1	1	2	4	3197
Day 10	4	3	3	1	1	1	2	5	3159
Day 11	4	4	3	1	2	1	3	5	3210
Day 12	4	3	3	2	2	1	3	4	3100
Day 13	4	4	2	1	1	1	2	4	3040
Day 14	4	4	4	2	1	1	2	5	2990
Day 15	4	3	4	2	3	1	4	5	3102
Day 16	4	4	4	3	1	1	2	4	3175
Day 17	4	4	4	2	2	1	3	4	3276
Day 18	5	4	2	2	2	1	3	4	3014
Day 19	5	3	2	3	3	1	4	3	2967
Day 20	4	5	3	1	3	1	4	5	2898
Day 21	4	4	4	1	1	1	2	3	2913
Day 22	3	4	3	2	1	1	2	5	2761
Day 23	4	3	3	3	2	1	3	5	2726
Day 24	4	4	3	3	1	1	2	4	2764
Day 25	3	5	2	1	3	1	4	3	2897
Day 26	4	4	2	2	3	1	4	3	2787
Day 27	3	3	3	1	1	1	2	4	2845
Day 28	3	4	4	1	2	1	3	5	2722
Day 29	4	4	4	2	1	1	2	3	2766
Day 30	4	3	4	2	1	1	2	3	2757

Table 32 Descriptive data on Right-handed female on SGS over 1 month

F, R, 29	Q1	Q2	Q3	Q4	Q5	Q6	Q7	Q8	Time
Day 1	2	3	1	1	1	1	2	5	3490
Day 2	2	4	1	1	1	1	2	5	3460
Day 3	2	4	2	1	1	1	2	5	3301
Day 4	3	4	1	2	1	1	2	5	3398
Day 5	3	4	2	2	1	1	2	4	3510
Day 6	2	3	2	2	2	1	3	4	3573
Day 7	3	3	2	2	1	1	2	5	3300
Day 8	3	3	1	2	1	1	2	5	3525
Day 9	2	3	1	2	2	1	3	5	3358
Day 10	3	4	2	3	2	1	3	5	3208
Day 11	4	4	2	2	2	1	3	5	3196
Day 12	3	3	2	2	1	1	2	5	3212
Day 13	3	3	2	1	1	1	2	4	3159
Day 14	4	3	2	1	1	1	2	5	3036
Day 15	4	3	3	1	2	1	3	5	3156
Day 16	4	3	3	2	2	1	3	4	3116
Day 17	3	4	3	2	1	1	2	5	3158
Day 18	5	3	2	1	2	1	3	4	3046
Day 19	4	3	2	1	2	1	3	4	2941
Day 20	5	4	2	1	1	1	2	3	2911
Day 21	5	3	3	2	2	1	3	4	2772
Day 22	4	3	2	3	3	1	4	3	3098
Day 23	4	4	3	3	3	1	4	5	2907
Day 24	4	3	3	3	1	1	2	5	2856
Day 25	5	4	2	1	2	1	3	3	2805
Day 26	5	3	2	1	2	1	3	5	2740
Day 27	5	3	3	2	1	1	2	5	2711
Day 28	4	3	4	2	3	1	4	3	2707
Day 29	4	4	4	1	1	1	3	4	2750
Day 30	5	3	4	2	2	1	4	4	2749

Table 33 Descriptive data on left-handed male on SGS over 1 month

M, L, 35	Q1	Q2	Q3	Q4	Q5	Q6	Q7	Q8	Time
Day 1	2	4	1	1	1	1	2	5	3565
Day 2	2	4	1	1	1	1	2	5	3588
Day 3	2	4	2	2	1	1	2	5	3579
Day 4	2	4	2	2	1	1	2	5	3525
Day 5	3	4	2	2	1	1	2	5	3510
Day 6	3	4	1	2	2	1	3	5	3396
Day 7	2	4	1	1	2	1	3	5	3365
Day 8	4	3	2	1	2	1	3	5	3437
Day 9	3	3	2	2	1	1	2	5	3338
Day 10	4	3	3	2	1	1	2	5	3497
Day 11	4	3	3	2	1	1	2	5	3322
Day 12	4	3	3	2	1	1	2	4	3285
Day 13	3	2	3	2	2	1	3	4	3168
Day 14	4	2	3	2	2	1	3	5	3226
Day 15	3	3	2	3	2	1	3	4	3054
Day 16	3	3	2	3	2	1	3	4	3265
Day 17	3	4	3	3	1	1	2	4	2845
Day 18	4	4	4	3	3	1	4	5	2879
Day 19	4	4	3	3	3	1	4	5	2958
Day 20	4	4	3	2	1	1	2	5	2928
Day 21	4	3	4	2	2	1	3	3	2978
Day 22	4	3	4	2	3	1	4	3	3174
Day 23	4	3	3	1	3	1	4	3	2816
Day 24	4	2	2	3	1	1	3	5	2930
Day 25	5	4	2	2	1	1	2	5	2817
Day 26	3	3	2	3	2	1	4	3	2809
Day 27	4	3	3	3	2	1	3	4	2768
Day 28	4	4	3	3	1	1	2	4	2813
Day 29	5	4	2	2	1	1	2	4	2780
Day 30	5	4	3	2	1	1	3	4	2710

Table 34 Descriptive data on Left-handed female on SGS over 1 month

| F, L, 49	Q1	Q2	Q3	Q4	Q5	Q6	Q7	Q8	Time
Day 1	3	3	2	1	1	1	3	5	3577
Day 2	3	3	3	1	1	1	3	5	3539
Day 3	3	3	3	2	1	1	2	5	3499
Day 4	3	3	2	2	1	1	2	5	3411
Day 5	2	2	2	2	1	1	2	5	3448
Day 6	3	2	2	2	1	1	2	4	3462
Day 7	3	2	3	2	1	1	2	5	3299
Day 8	3	3	2	1	1	1	2	4	3268
Day 9	4	2	2	1	1	1	3	4	3288
Day 10	4	3	3	1	2	1	3	4	3135
Day 11	4	4	2	1	2	1	3	4	3240
Day 12	3	4	3	1	1	1	3	5	3151
Day 13	4	4	2	1	2	1	2	5	3390
Day 14	5	4	2	1	2	1	3	5	3053
Day 15	5	3	2	1	1	1	2	5	3163
Day 16	3	3	2	1	2	1	3	5	3062
Day 17	3	4	3	2	1	1	2	5	2915
Day 18	5	3	3	2	1	1	2	4	3057
Day 19	5	3	3	1	2	1	3	4	2992
Day 20	3	4	3	1	3	1	4	4	3020
Day 21	4	4	2	2	3	1	4	5	2923
Day 22	4	4	2	2	2	1	4	5	2902
Day 23	5	5	2	2	3	1	4	5	3059
Day 24	4	5	3	2	3	1	4	5	2967
Day 25	5	3	3	1	2	1	3	5	2995
Day 26	3	5	3	3	2	1	3	4	2929
Day 27	3	3	3	2	2	1	3	5	2850
Day 28	5	3	3	3	1	1	2	5	2777
Day 29	5	4	3	3	3	1	4	5	2727
Day 30	4	4	3	2	3	1	4	5	2709
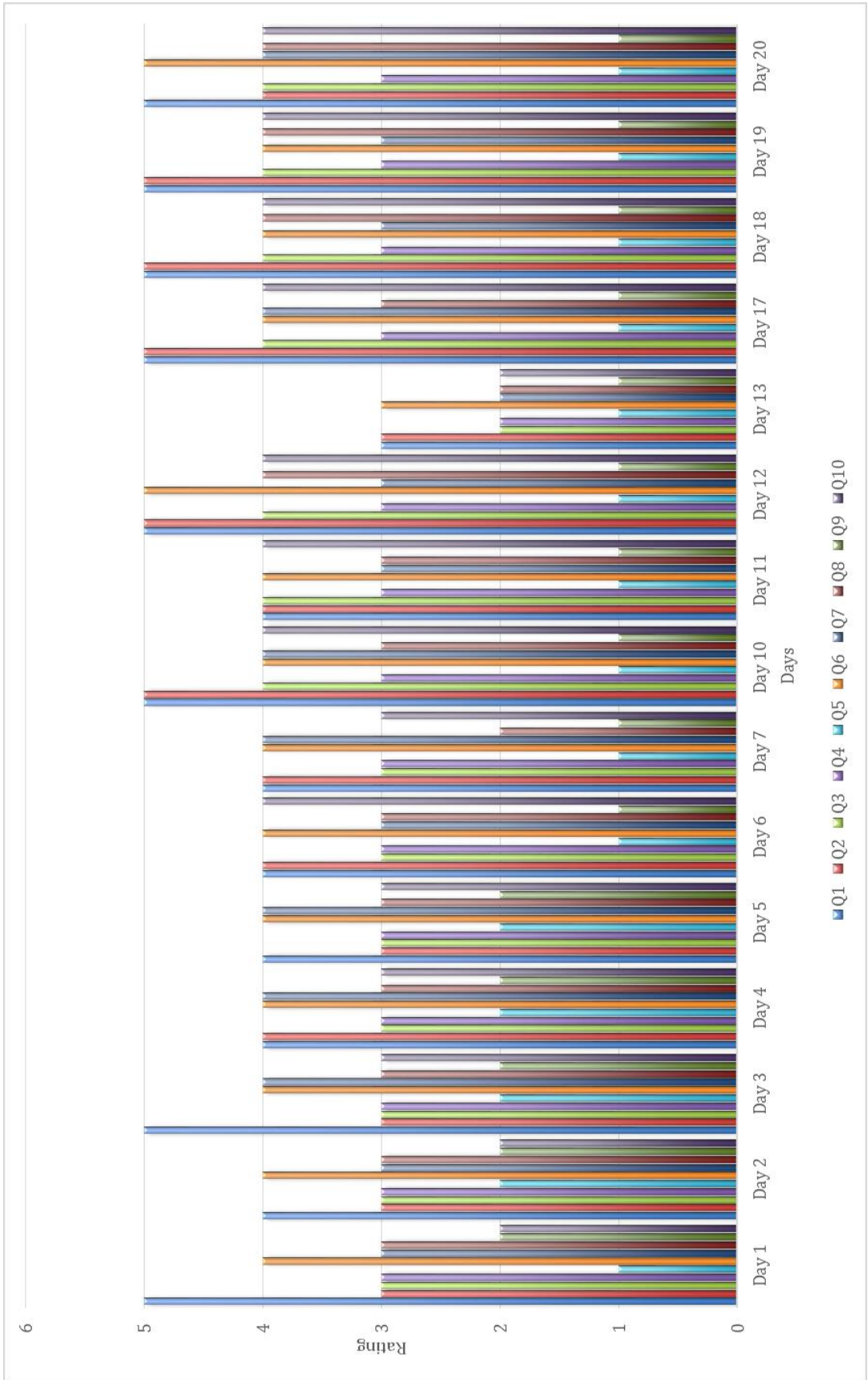
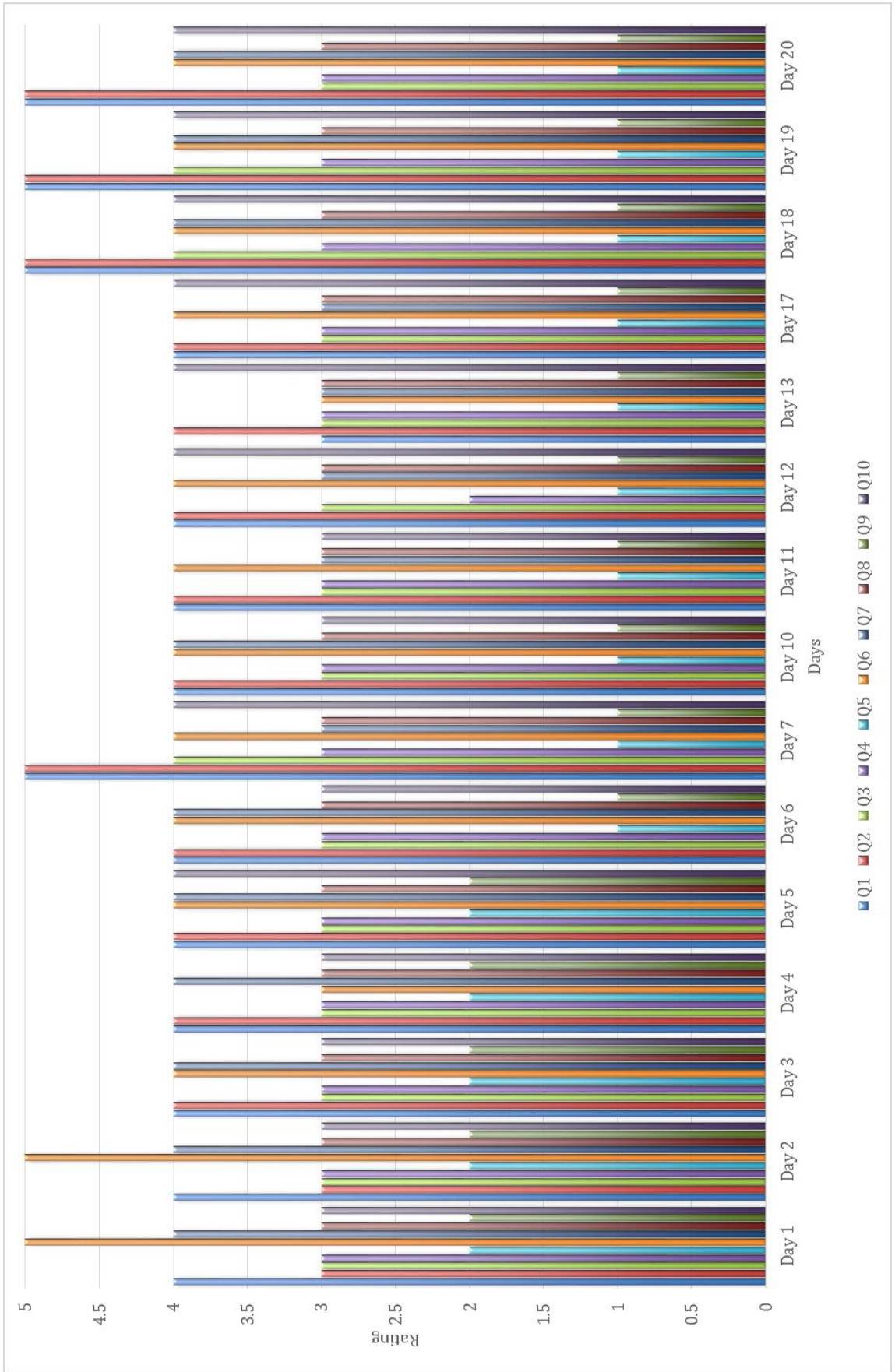**Figure 121: Detailed data for Base 1 (7cm) in moving hand**

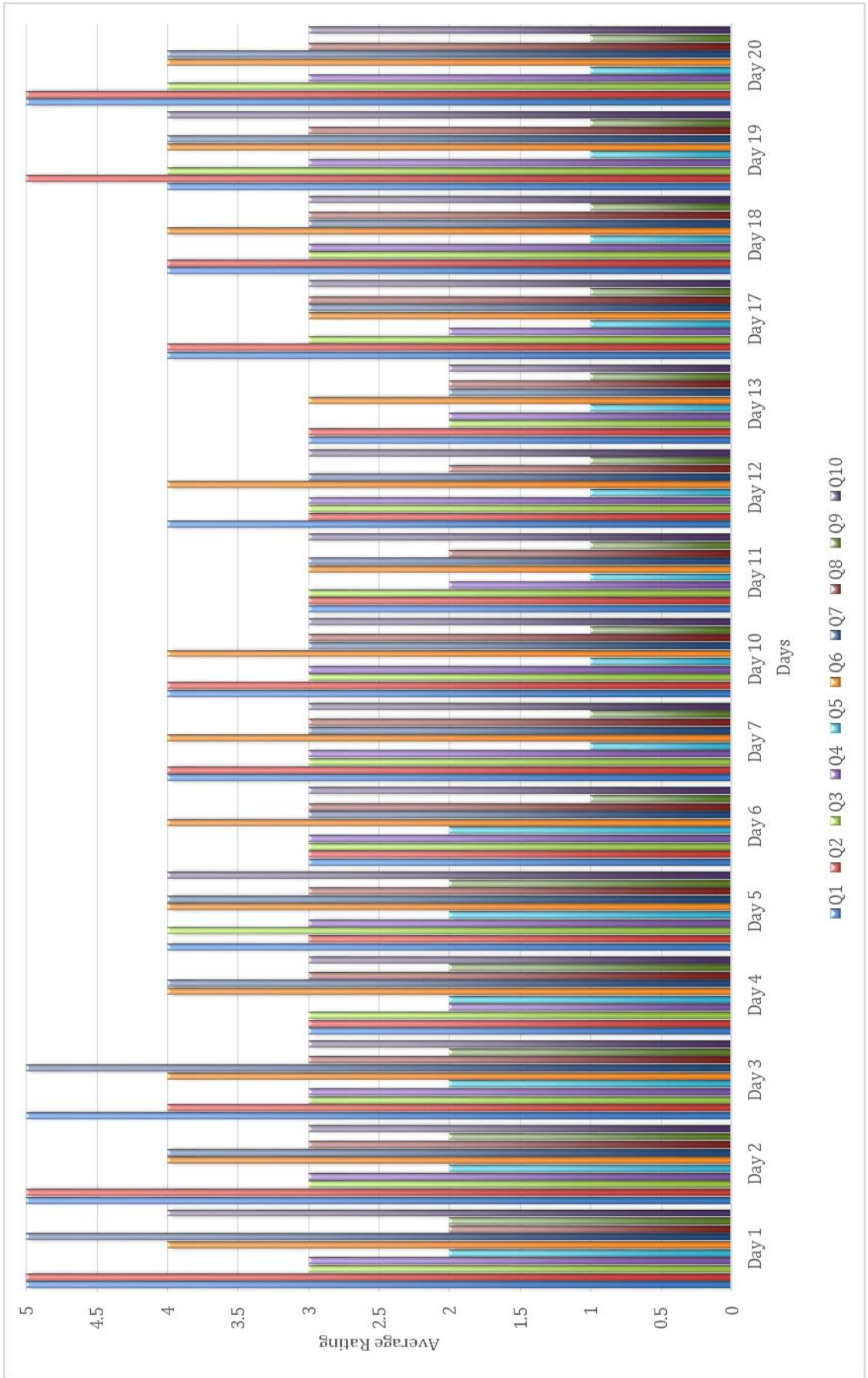**Figure 122: Detailed data for Base 2 (4cm) in moving hand**

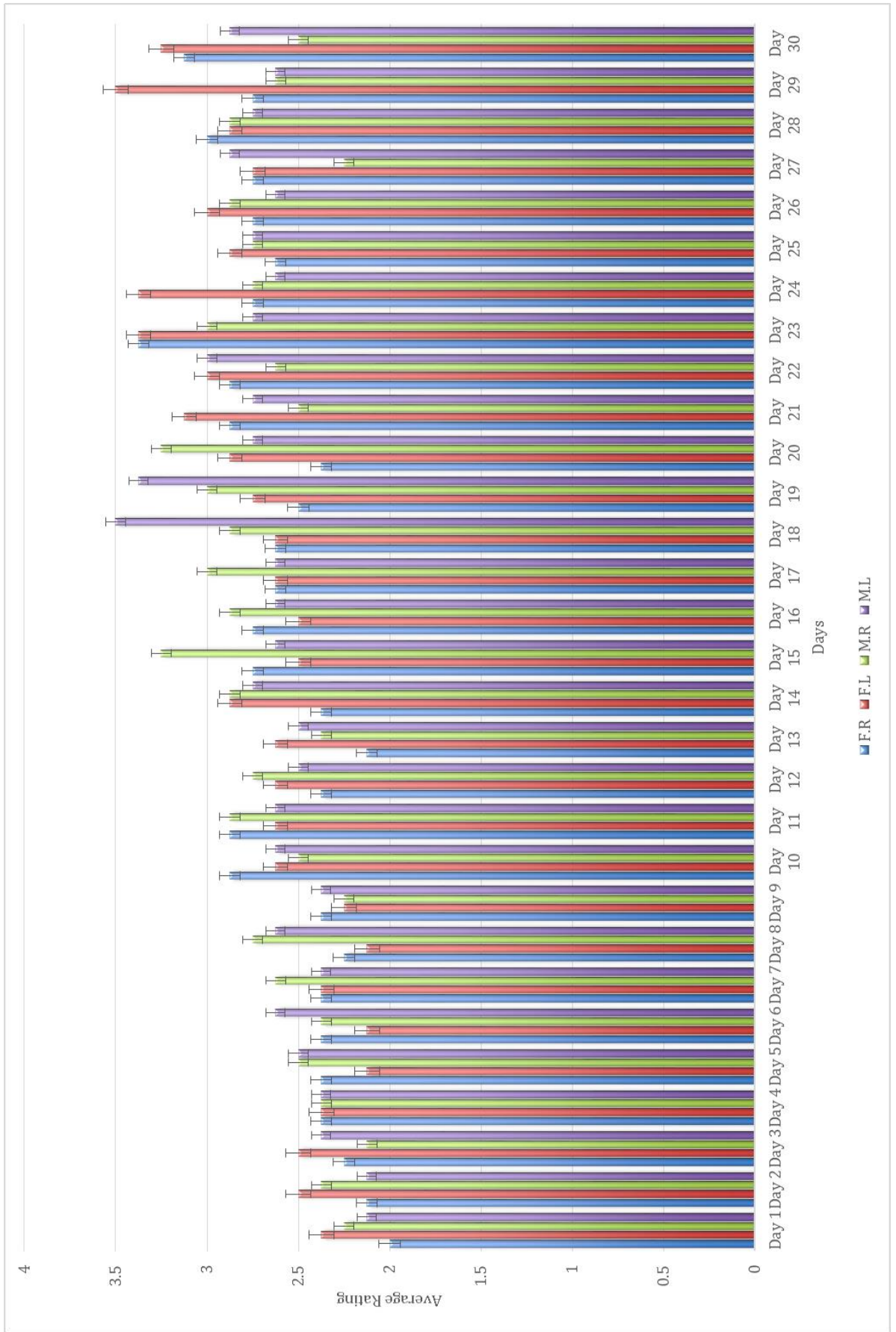**Figure 123: Detailed data for Base 3 in moving hand**

Figure 124: Detailed data for questionnaire average rating of each participant during 30 days of SGS experiment

6. Consent form for experiments

RHI:

Brunel
UNIVERSITY
L O N D O N

Consent Form

Researcher: Sheyda Shahriari, PhD Student, Sheyda.Shahriari@brunel.ac.uk

Project Supervisor: Prof, Ibrahim Esat, Ibrahim.Esat@brunel.ac.uk

Information for Participant:
Title of the study: EEG signal study from the effect of Rubber Hand Illusion

This study requires the volunteer participants to take part in the experiments including probing the brain signal using the Medical EEGo RT an electroencephalography headset. Participant will be asked to complete questionnaire after the experiment. Results are collected for the purpose of further analysis. The study will have no harm or risk to the participants. Participants in the study have the right to withdraw from the study at any stage during the research without any penalty. **The collected data from participants will be stored strictly confidentially and participants' identities will be secured**. **Data with participant's identity will be only accessed by the named researchers for further analysis**. Nameless data will also be analyzed. There will be no other use or access to the participants' data other than this study. **Participants are ensured that their personal information will be destroyed upon the completion of this study**. In the case of publication of the study's results the anonymity of the participants will be preserved.

	Yes	No
I have read the research Participant Information sheet.	☐	☐
I understand the content of the study	☐	☐
I have had the opportunity to ask questions about the study	☐	☐
I understand that I will remain anonymous in any publication of the result	☐	☐
I know that this study will not affect my assessment in the course	☐	☐
I agree willingly to take part in the study.	☐	☐

Signature of the participant
Name   Date:
For researcher's use:
I am satisfied that above person has given informed consent
Witnessed by: Date:

Brunel
UNIVERSITY
L O N D O N

Consent Form

Researcher: Sheyda Shahriari, Sheyda.shahriari@brunel.ac.uk

Project Supervisor: Prof. Ibrahim Esat, Ibrahim.Esat@brunel.ac.uk

Information for Participant:
Title of the study: EEG signal study from the effect of Sound generator system

This study requires the volunteer participants to take part in the experiments including probing the brain signal using the ANT RT Neuro, an electroencephalography headset. Participant will be asked how they feel after exposing to sound temperature experiment. Results are collected for the purpose of further analysis. The study will have no harm or risk to the participants. Participants in the study have the right to withdraw from the study at any stage during the research without any penalty. **The collected data from participants will be stored strictly confidentially and participants' identities will be secured**. **The named researchers for further analysis will, only access data with participant's identity**. Nameless data will also be analyzed. There will be no other use or access to the participants' data other than this study. **Participants are ensured that their personal information will be destroyed upon the completion of this study**. In the case of publication of the study's results the anonymity of the participants will be preserved.

	Yes	No
I have read the research Participant Information sheet.	☐	☐
I understand the content of the study	☐	☐
I have had the opportunity to ask questions about the study	☐	☐
I understand that I will remain anonymous in any publication of the result	☐	☐
I know that this study will not affect my assessment in the course	☐	☐
I agree willingly to take part in the study.	☐	☐

Signature of the participant
Name   Date:
For researcher's use:
I am satisfied that above person has given informed consent
Witnessed by: Date:

7. Participant information sheet

PARTICIPANT INFORMATION SHEET
Checklist
Study title: RHI, MBI, SGS
This information sheet will give to participant after the experiment

Invitation Paragraph
This study requires the volunteer participants to take part in the experiments including probing the brain signal using the ANT RT Neuro, an electroencephalography headset to study on how brain resolves conflicting multi-sensory evidence during perceptual interference.

What is the purpose of the study?
The purpose of the project is to show how the brain characterizes the location, movement and force of limb and using illusion to replicate human feeling and make connection between amputee and device.

Why have been invited to participate?
Because we feel that you might provide valuable input into the process of determining and assessing software metrics and that your views are valuable.

Do I have to take part?
No – you have the option to withdraw from the study at any point.

What will happen to me if I take part?
Your brain signal will be collected for the purpose of further analysis. You will be interviewed informally to develop ideas and be part of larger workshops to bring together those ideas.

What do I have to do?
The interviews will informal and will not intrude on your normal work.

What are the possible disadvantages and risks of taking part?
There are no disadvantages or risks in taking part other than a small amount of your time and effort.

What if something goes wrong?
The ethical guidelines and procedures put in place will ensure that there is very little that can go wrong and if it did would have minimal impact on any participant.

Will my taking part in this study be kept confidential?
The data will be anonymized – so that no individual is attributed to any particular view. The data will be aggregated and so it will be impossible to distinguish between participants. The collected data from participants will be stored strictly confidentially and participants' identities will be secured. The named researchers for further analysis will, only access data with participant's identity.

What will happen to the results of the research study?
These will be published and disseminated internally. Also, anonymised results will be published more widely as part of Conference and Journal papers.

Who has reviewed the study?
Two members of staff at Brunel University.
Researcher: Sheyda Shahriari, Sheyda.shahriari@brunel.ac.uk
Project Supervisor: Prof. Ibrahim Esat, Ibrahim.Esat@brunel.ac.uk

8. Ethics Approval RHI:

College of Engineering, Design and Physical Sciences Research Ethics Committee
Brunel University London
Kingston Lane
Uxbridge
UB8 3PH
United Kingdom

www.brunel.ac.uk

3 October 2016

LETTER OF APPROVAL

Applicant: miss sheyda shahriari

Project Title: rubber hand illusion 2

Reference: 3364-LR-Oct/2016- 4129-5

Dear miss sheyda shahriari

The Research Ethics Committee has considered the above application recently submitted by you.

The Chair, acting under delegated authority has agreed that there is no objection on ethical grounds to the proposed study. Approval is given on the understanding that the conditions of approval set out below are followed:

- The agreed protocol must be followed. Any changes to the protocol will require prior approval from the Committee by way of an application for an amendment.

Please note that:

- Research Participant Information Sheets and (where relevant) flyers, posters, and consent forms should include a clear statement that research ethics approval has been obtained from the relevant Research Ethics Committee.
- The Research Participant Information Sheets should include a clear statement that queries should be directed, in the first instance, to the Supervisor (where relevant), or the researcher. Complaints, on the other hand, should be directed, in the first instance, to the Chair of the relevant Research Ethics Committee.
- Approval to proceed with the study is granted subject to receipt by the Committee of satisfactory responses to any conditions that may appear above, in addition to any subsequent changes to the protocol.
- The Research Ethics Committee reserves the right to sample and review documentation, including raw data, relevant to the study.
- **[delete for staff applications]** You may not undertake any research activity if you are not a registered student of Brunel University or if you cease to become registered, including abeyance or temporary withdrawal. As a deregistered student you would not be insured to undertake research activity. Research activity includes the recruitment of participants, undertaking consent procedures and collection of data. Breach of this requirement constitutes research misconduct and is a disciplinary offence.

Professor Hua Zhao

Chair

College of Engineering, Design and Physical Sciences Research Ethics Committee
Brunel University London

Page 1 of 1

SGS:

29 September 2016

LETTER OF CONDITIONAL APPROVAL

Applicant: miss sheyda shahriari

Project Title: sensation illusion

Reference: 2947-MHR-Sep/2016- 4127-5

Dear miss sheyda shahriari

The Research Ethics Committee has considered the above application recently submitted by you.

The Chair, acting under delegated authority has agreed that there is no objection on ethical grounds to the proposed study. Approval is given on the understanding that the conditions of approval set out below are followed:

- **The agreed protocol must be followed. Any changes to the protocol will require prior approval from the Committee by way of an application for an amendment.**
- **Please ensure that the Participant Information Sheet is fully explained and that any participants have the right to withdraw once they are fully aware of the full implications of the tests(with no health risks).**
- **Please ensure that no data collected before this ethical approval is included in your research.**
- **Please ensure that all manufacturers guidelines are followed when using the headset.**

Please note that:

- Research Participant Information Sheets and (where relevant) flyers, posters, and consent forms should include a clear statement that research ethics approval has been obtained from the relevant Research Ethics Committee.
- The Research Participant Information Sheets should include a clear statement that queries should be directed, in the first instance, to the Supervisor (where relevant), or the researcher. Complaints, on the other hand, should be directed, in the first instance, to the Chair of the relevant Research Ethics Committee.
- Approval to proceed with the study is granted subject to receipt by the Committee of satisfactory responses to any conditions that may appear above, in addition to any subsequent changes to the protocol.
- The Research Ethics Committee reserves the right to sample and review documentation, including raw data, relevant to the study.
- **[delete for staff applications]** You may not undertake any research activity if you are not a registered student of Brunel University or if you cease to become registered, including abeyance or temporary withdrawal. As a deregistered student you would not be insured to undertake research activity. Research activity includes the recruitment of participants, undertaking consent procedures and collection of data. Breach of this requirement constitutes research misconduct and is a disciplinary offence.

Professor Hua Zhao

Chair

College of Engineering, Design and Physical Sciences Research Ethics Committee
Brunel University London

9. Publisher declaration of acceptance

Date: August 28, 2015
From: Murat M. Tanik, PhD; www.uab.edu/ece; SDPS board member and Process coordinator
Subject: 2015 SDPS conference invitation

To: Sheyda Shahriari, Department of Mechanical, Aerospace, and Civil Engineering, Brunel University, London, UK

Due to your contributions to the field especially taking into account your multidisciplinary activities, we would like to invite you to be a speaker in our 20th year celebrations of establishing SDPS.

The theme is Convergence developed by National Academy of Sciences (http://dels.nas.edu/resources/static-assets/materials-based-on-reports/reports-in-brief/convergence-brief-final.pdf) and the conference will be held first week of November, (1-5, November, 2015). Please remember, November 2nd Nobel Laureate, Father of Femtochemistry, Dr. Ahmed H. Zewail will give his talk.

Please do not delay your SDPS registration and reduced rate hotel reservations at http://sdpsnet.org/sdps2015 . Gala awards dinner will be Tuesday November 3, 2015. Advance program in PDF form (54 pages) can be downloaded at https://www.sdpsnet.org/sdps/documents/sdps-2015/SDPS_AdvanceProgram_1stEdition_email_2015_09_16.pdf

Please direct all questions and communications to Dr. Murat Tanik, www.uab.edu/ece, or Stan Gatchel, SDPS senior advisor.

Murat M. Tanik, PhD

Wallace R. Bunn Professor, SDPS Process coordinator and Executive Board Member

Dear sheyda shahriari,

On behalf of the 16th International Conference on Biomedical Engineering (ICBME 2016) Scientific Committee, we would like to inform that the below abstract has been propose to change to **Poster Presentation** instead.

Abstract Entry No.: D1-0003
Abstract title: Investigate Into Future Of Prosthetic With Sensation
Presentation type: Poster Presentation

Please let us know your acceptance, if you would like to present in poster and attend the conference, in order for the Scientific Committee to schedule your presentation. Appreciate if you can notify us via secretariat@icbme.org, by **2 September 2016**. We will let you know the presentation format once we hear from you.

To facilitate your attendance to the Conference, please take note of the below:

Registration
Authors are encourage to register before 2 Sep, to enjoy the Early Bird registration rates. More information can be found on our website:
http://www.icbme.org/registration.

Accommodation
Authors can book their accommodation through our list of official hotels. More information can be found on our website: http://www.icbme.org/accommodation.

Gala Dinner
The ICBME 2016 Gala Dinner will be held on Friday, 9 December 2016 at Novotel Singapore Clarke Quay. As admission is by Gala Dinner ticket only, please purchase your tickets through our website at http://www.icbme.org/gala-dinner.

Contact Us
You may visit us at our website http://www.icbme.org/ for the latest conference updates. If there is any further information you require, please contact us at secretariat@icbme.org.

Thank you.

Yours sincerely,
ICBME Secretariat
20 Kallang Avenue 2nd Floor Pico Creative Centre Singapore 339411
T +65 6393 0243 E secretariat@icbme.org F +65 6292 7577 W www.icbme.org